Characterisation of genomic islands in *Neisseria meningitidis*

Maria Chiara Erminia Catenazzi

A Thesis Submitted for the Degree

of Doctor of Philosophy (PhD)

University of York

Department of Biology

August 2013

Abstract

Neisseria meningitidis asymptomatically colonises the nasopharynx of about 10 % of the human population. This bacterium is an accidental pathogen, with *N. meningitidis* serogroup B being the main cause of meningitis and septicaemia in developed countries. Strain MC58 has a genome size of 2,272,360 bp and contains 2160 ORFs, more than half of which have already been assigned a function. Nine conserved genomic islands that are absent from the closely related commensal species *N. lactamica* were identified and comprise 38 genes. Of these, 14 still encode proteins of unknown function. Two of these islands (pathogenic islands 4 and 8) were investigated, and the genes crucial for two further islands (pathogenic islands 3 and 5) involved in polyamine biosynthesis were successfully knocked out in this work. Genomic island 4 contains six genes, which encode proteins that are involved in the 2-methylcitrate pathway; these genes are clustered together to form the *prp* operon. Several genes belonging to this pathway (*prpC*, *NMB0432* and *ackA-1*) were knocked out, and the resulting mutants were unable to utilise propionic acid, which is the substrate for the pathway being investigated. Saliva from over 300 healthy students was analysed for propionic acid content, and the data were compared to the meningococcal carriage status. No significant correlation, however, was found between the concentration of this fatty acid and the carriage status. Genomic island 8 contains coding sequences for the two hypothetical proteins NMB1048 and NMB1049. NMB1049 has been shown to regulate the expression of the divergently transcribed *NMB1048* but not *prpC*. NMB1049 is, in fact, a putative LysR-Type transcriptional regulator. Both genomic islands were also investigated for their involvement in *N. meningitidis* carriage or infection. Human blood samples from several healthy individuals were inoculated with *N. meningitidis* MC58, and results showed that only half of the blood samples had bactericidal effects. These results were independent of the strain used, as they were similar for the wild-type and the mutants in the *prpC* and *NMB1049* genes. The catabolism of propionic acid seems to give an advantage to *N. meningitidis* in colonising the adult nasopharynx.

Table of Contents

List of Figures

List of Tables

List of Abbreviations

APS = Ammonium persulfate

bp = base pair

BSA = Bovine Serum Albumin

CBA = Columbia Blood Agar Base

CDM = Chemically Defined Medium

cDNA = complementary DNA

CFU = Colony Forming Unit

Chl^R = Chloramphenicol resistance gene

DMSO = Dimethyl sulfoxide

DNA = deoxyribonucleic acid

dNTP = deoxyribonucleoside triphosphate

DTT = dithiothreitol

DUS = DNA uptake sequence

EDTA = ethylenediaminetetraacetic acid

EMSA = Electrophoretic Mobility Shift Assay

fHbp = factor H-binding protein

GC = Gas Chromatography

HGT = Horizontal Gene Transfer

Kan^R = Kanamycin resistance gene

kb = kilobase

kDa = kiloDalton

LB = Lysogeny Broth

LTTR = LysR-Type transcriptional regulator

Mbp = Mega base pair

MHB = Mueller Hinton Broth

NadA = *N. meningitidis* adhesion A

NCBI = National Centre for Biotechnology Information

NEB = New England Biolabs

NHBA = Neisserial Heparin Binding Antigen

NspA = Neisserial surface protein A

OD = Optical density

OMV = Outer membrane vesicle

Opc = Opacity protein

ORF = Open Reading Frame

PAGE = Polyacrylamide gel electrophoresis

PCR = Polymerase Chain Reaction

PorA = Porin A

PorB = Porin B

RNA = Ribonucleic acid

Rnase = ribonuclease

rpm = revolutions per minute

RT-PCR = quantitative Real-Time PCR

SBA = Serum Bactericidal Antibodies

SDS = Sodium dodecyl sulphate

SDS-PAGE = Sodium dodecyl sulphate-polyacrylamide gel electrophoresis

$Spec^R$ = Spectinomycin resistance gene

spp. = species

TBE = Tris / Borate / EDTA buffer

TCA = Tricarboxylic acid cycle

TEMED = tetramethylethylenediamine

Tet^R = Tetracycline resistance gene

TMHMM = transmembrane helices programme based on a hidden Markov model

Tris = Tris(hydroxymethyl)aminomethane

TSB = Transformation and Storage Buffer

Acknowledgements

Firstly, I would like to thank my supervisor Dr. James Moir for his guidance, support and supervision throughout my research.

I would also like to thank Dr. James Edwards for his precious advice throughout the project and both the Moir's lab and L1 for their help, friendship and discussions during the coffee breaks.

I also thank Dr. Marjan Van Der Woude and Dr. James Chong for being members of my training committee. Their guidance helped me to go forward.

My thanks go to Dr. Simon Breeden and Dr. Thomas Farmer for their technical advice when using the GC. I extend these thanks to all at Green Chemistry and to Dr. Gideon Grogan for letting me use their equipment.

Thanks also to Dr. Naveed Aziz and Celina Whalley at the University of York, for genomics training and to Mike Dunn for helping me with IT-related issues.

Many sincere thanks also go to the friends I made in York for their encouragement and interesting discussions.

I would finally like to thank my family for all their love and support over the years.

Author's Declaration

I declare that all of the work present in this thesis is my own, original work unless explicitly stated in the text.

Maria Chiara E. Catenazzi

York, 09.08.2013

Chapter 1 - General introduction

1.1 Microflora present in the oral cavity

Humans are always surrounded and inhabited by an enormous number of bacteria. It is estimated that an adult is permanently in contact with 10^{12} bacteria through skin contact, that 10^{10} bacteria inhabit the mouth and throat, and that an even greater number of bacteria, approaching the 10^{14} range, live in the gastro-intestinal tract (Tlaskalová-Hogenová *et al.*, 2004).

Measuring microbial biodiversity has always been very challenging. In the past, in fact, studies for identifying bacterial strains involved the cultivation of the bacteria. However, only a very small percentage of bacteria can be cultured in the laboratory, since more than 99 % of bacteria are not able to grow *in vitro* for lack of appropriate cultivation conditions or because specific culture methods are yet to be developed (Hugenholtz & Pace, 1996, Amann *et al.*, 1995). Bacteria present in the oral cavity, for example, can form polymicrobial communities, which then lead to biofilm formation. Some of the bacteria present in a specific biofilm will most likely depend on metabolites generated from other members of that community, and might therefore not be able to grow when cultured on their own *in vitro* (Jenkinson & Lamont, 2005). In order to overcome culturing single strains belonging to a community, more recent studies tested co-cultures of bacteria known to belong to the same community. One specific study included the inoculation of nine different organisms which are usually found in dental plaque, such as *Streptococci* spp. and *Veillonella*, in order to investigate biofilm formation. These studies confirmed that some bacteria, such as *Streptococcus sanguis* and *Neisseria* spp., needed to be

inoculated more than once, probably indicating that they could survive in this specific environment only when the other bacteria were already established in communities (McKee *et al.*, 1985).

Current developments include a more accurate estimate of bacterial populations present in a specific environment, as they do not rely on cultured bacteria. In fact, the microbiome can be studied more thoroughly by direct PCR amplification and pyrosequencing using universal primers. These primers are designed to be able to sequence the full 16S ribosomal DNA gene for drawing accurate phylogenetic trees for the new species discovered, or are designed to target the hypervariable regions within this highly conserved gene (Yang *et al.*, 2011, Chakravorty *et al.*, 2007).

Over 750 different bacterial species have been identified to date that compose the microflora of the oral cavity of healthy individuals, with the most predominant species detected being *Gemella*, *Granulicatella*, *Streptococcus* and *Veillonella* (Aas *et al.*, 2005). The nostrils are mainly composed of two phyla: *Firmicutes* and *Actinobacteria*, which have similarities to the distribution of bacteria in the skin, whereas the oropharynx comprises mainly the following three phyla, which are analogous to the ones present in the saliva: *Firmicutes*, *Proteobacteria* and *Bacteroidetes* (Lemon *et al.*, 2010). *Propionibacteria* spp. are also found as an important part of the oral flora (Bojar & Holland, 2004). All these bacteria are usually found colonising the host without causing any disease. Despite usually being innocuous, however, sometimes bacteria can take advantage of susceptible individuals such as elderly and immunocompromised people, and become therefore opportunistic pathogens: *Streptococcus pneumoniae*, *Neisseria meningitidis* and *Haemophilus influenzae* are just a few examples of microbes that can be found in the

mouth and that can give evidence of this change of behaviour (Schoen *et al.*, 2008, Hava & Camilli, 2002, Turk, 1984).

1.2 Bacteria and the role of propionic acid

1.2.1 Propionic acid abundance

Propionic acid is a compound that has anti-bacterial properties and strongly inhibits cellular growth of most microorganisms and fungi (Brock & Buckel, 2004, Matlho *et al.*, 1997, Salmond *et al.*, 1984). This in fact explains why propionic acid and its sodium, calcium and potassium salts are usually added in both animal feed and human food as a preservative agent (E280-E283). The legislation regarding food additives implemented by the European Commission allows propionic acid to be added into bread in amounts varying between 0.1 and 0.3 % of the food total weight, corresponding to a final concentration of between 13 and 40 mM (European Commission, 2011).

The concentration of propionic acid in human saliva is very variable, as it depends on many disparate factors, such as food intake, diet, oral hygiene, stimulation of saliva, sex, time and method used for collection of the samples, etc. In one particular study, propionic acid content was measured from the saliva of over 100 people, and gave a range of values starting from just above null to up to 600 μM (Takeda *et al.*, 2009). When gingival crevices were taken into consideration for studying the amount of this volatile fatty acid, however, it was concluded that the presence of propionic acid was directly dependent on the person's periodontal state: healthy gingival crevices had undetectable levels of propionic acid, whereas mild and severely diseased gingival

crevices could contain an average concentration of 0.5 and 10 mM propionic acid respectively (Niederman *et al.*, 1997).

1.2.2 Bacteria that synthesise propionic acid

The skin and pharynx of humans can host several species of microorganisms that use an alternative metabolic pathway, and produce propionic acid as the main end product. *Propionibacteria* spp. and *Veillonella* spp. are amongst these microorganisms, and are able to synthesise propionic acid thanks to genes coding for unusual transcarboxylase enzymes (Lewis & Yang, 1992, Distler & Kröncke, 1981).

Propionibacteria spp. are ubiquitous, slow growing, non-motile, anaerobic but aerotolerant Gram-positive bacteria that can synthesise propionic acid through fermentation of several carbon sources, such as lactate, glycerol and glucose (Liu *et al.*, 2011, Piveteau, 1999). These bacteria are most numerous in and around sweat and sebaceous glands, but can also be found on the skin, oral cavity and gastrointestinal tract of humans and animals. Propionibacteria are commensals, but can occasionally cause skin conditions, such as acne (Brüggemann *et al.*, 2004). The number of these bacteria remains almost constant on the skin and increases only slightly, whereas it significantly rises in the nostrils through aging. The increase in number of Propionibacteria in the nostrils is followed by an increase in number present in the throat (Mourelatos *et al.*, 2007).

Veillonella spp. are anaerobic, non-motile Gram-negative bacteria that can synthesise propionic acid through fermentation of lactate (Ng & Hamilton, 1971). They are present in the oral cavity and in the respiratory and intestinal tract of both humans

and animals as part of the normal flora, but can occasionally become pathogens leading to osteomyelitis and endocarditis (Singh & Victor, 1992, Rogosa, 1964).

The bacteria discussed in this section produce propionic acid as a by-product of fermentation. They usually inhabit the oral cavity and, as a consequence, this could indicate a rise in the concentration of propionic acid in the mouth and throat. The possibly higher concentration of propionic acid in the mouth would have a negative effect on many other bacteria which do not possess genes for catabolising this fatty acid. To overcome this noxious weak fatty acid, in fact, some bacteria have developed an alternative pathway that enables them to break propionic acid down to the final products succinate and pyruvate through the 2-methylcitrate pathway, as discussed in Section 1.7.2.

1.2.3 Pathways generating propionyl-CoA and propionic acid

Propionyl-CoA can be generated through several different routes. The most common route utilised by bacteria is the methylmalonyl-CoenzymeA pathway, which decarboxylates succinyl-CoA into propionyl-CoA with the help of specific enzymes (Figure 1.2.3-1). This pathway is used by several bacteria including *Propionibacteria* spp. and *Veillonella* spp., and in these bacteria it is responsible for catabolising 3 molecules of lactate into 2 molecules of propionate, 1 molecule of acetate, CO_2 and H_2O through fermentation (Seeliger *et al.*, 2002). This pathway is occasionally referred to as the succinate-propionate pathway, when succinate is produced by a reversal of the TCA cycle starting from oxaloacetate, or as the glyoxylate-methylmalonyl pathway when, in an anaerobic condition, succinate is formed with glyoxylate from isocitrate (Yagci *et al.*, 2003).

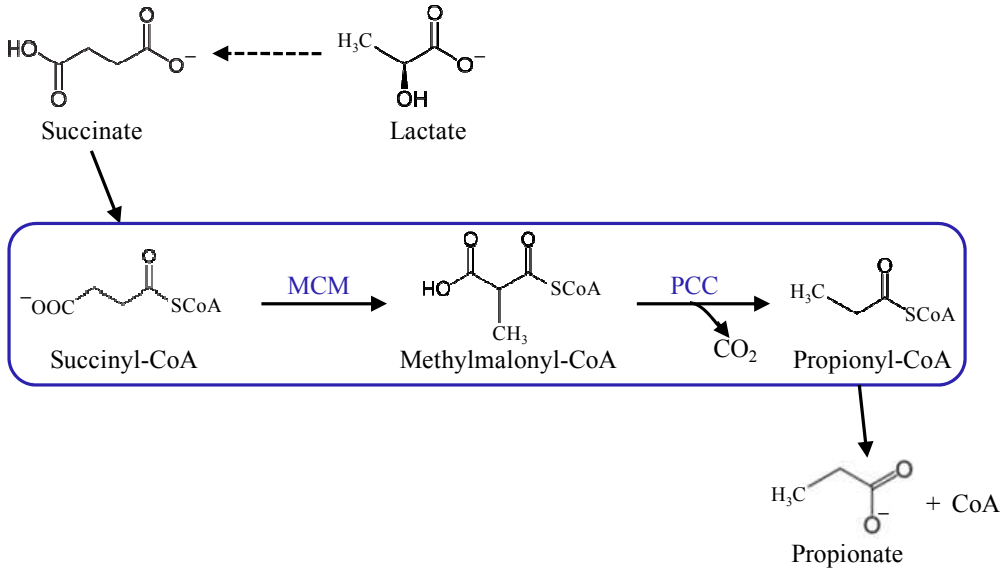

Figure 1.2.3-1: The Methylmalonyl-CoA pathway.
There are two specific genes that encode proteins involved in the methylmalonyl-CoA pathway. This pathway is involved in the formation of propionic acid. Abbreviation: MCM: methylmalonyl-CoA mutase. PCC: propionyl-CoA carboxylase (Figure adapted from Swick & Wood, 1960).

There are other metabolic pathways used by some bacteria to ferment lactate or other carbon sources into propionate. One example is the 3-hydroxypropionate cycle, also known as the acrylyl-CoA pathway, which converts 3-hydroxypropionate to propionyl-CoA through three specific reactions that include formation of the intermediate acrylyl-CoA (Alber & Fuchs, 2002, Seeliger *et al.*, 2002). Even catabolism of the amino acids isoleucine, methionine, valine and glutamate produces propionyl-CoA as an intermediate of succinyl-CoA (Maerker *et al.*, 2005, Plugge *et al.*, 2001).

Propionyl-CoA is thought to be highly cytotoxic, and accumulation of this compound is associated with the inhibition of coenzyme A-dependent enzymes, such as pyruvate dehydrogenase, succinyl-CoA synthetase and ATP citrate lyase (Brock & Buckel, 2004). Addition of acetate or sodium bicarbonate to the medium, however, has been shown to restore the bacterial growth rate, as acetate is a means of supplying acetyl-CoA needed for growth and bicarbonate ions stimulate degradation of propionyl-CoA to methylmalonyl-CoA via the propionyl-CoA carboxylase enzyme (Maruyama & Kitamura, 1985). A decrease of propionic acid, and therefore of propionyl-CoA, can also be achieved through a specific metabolic pathway which breaks propionic acid down, the 2-methylcitrate pathway (Brämer & Steinbüchel, 2001). This pathway is present in several bacteria and also in many *Neisseria* species.

1.3 Overview of the genus *Neisseria*

The genus *Neisseria* was named after Albert Neisser, a bacteriologist who discovered *Neisseria gonorrhoeae* in 1879 (Ligon, 2005). This genus belongs to the family of the *Neisseriaceae* and comprises all *Neisseria* species, which constitute a substantial part of the β-proteobacteria (Tønjum *et al.*, 2005).

The genus *Neisseria* is mainly composed of a group of closely related cocci with a diameter ranging between 0.6 and 1.9 μm. These cocci can be found as single cells, as pairs or as tetrads. However, there are a few bacteria belonging to this genus, such as *N. elongata* and *N. weaveri*, which are found as short rods 0.5 μm wide and are frequently arranged as diplobacilli or in chains (Garrity *et al.*, 2005).

Neisseria spp. are primarily commensal organisms of the normal flora in mammals. A growing number of species has been associated with animals, such as *N. canis* and *N. weaveri* (cats, dogs and humans' wounds caused by bites of both animals), *N. dentiae* (cows), *N. iguanae* (lizards), *N. macacae* (rhesus monkeys), *N. ovis* (sheep) to name a few (Allison & Clarridge., 2005, Sneath & Barrett, 1996, Barrett *et al.*, 1994, Andersen *et al.*, 1993, Vedros *et al.*, 1983, Lindqvist, 1960).

There are 14 *Neisseria* species that are currently known to exclusively colonise mucosal surfaces of humans (Feil *et al.*, 2001). Three amongst these are of outstanding clinical interest as two species, *Neisseria gonorrhoeae* and *Neisseria meningitidis*, are exclusive human pathogens which are most closely related to the third species, *Neisseria lactamica*, a common harmless human commensal (Snyder & Saunders, 2006).

Several strains belonging to *Neisseria gonorrhoeae*, *Neisseria meningitidis* and *Neisseria lactamica* have been fully sequenced, and all resulted in a comparable genome size of around 2.2 Mbp (Maiden, 2008). Three quarters of their genes, corresponding to about 1.7 Mbp, have been associated with the core neisserial genome, as they are present in all the *Neisseria*'s isolates so far sequenced. Less than 5 % of their genome has been defined pathogen-specific, as genes were only observed in *N. gonorrhoeae* and / or *N. meningitidis*. Less than 1 % of the genome was shared only between *N. meningitidis* and *N. lactamica* (Perrin *et al.*, 2002). As these three species strictly colonise humans, investigating them should constitute an advantage as there is no need to take into consideration other animals or the external environment. Their specific niche, however, makes it harder to study their mode of action during colonisation and pathogenicity, as animal models have failed to

harbour these bacteria so far. Recently, however, a new animal model involving monkeys has been successfully investigated. The rhesus macaque looks like a promising model, as this monkey has over 90 % sequence identity with humans and is anatomically and physiologically similar too. It can also be naturally colonised by two different species of *Neisseria* which are similar to human commensals, making it an ideal host for studying *Neisseria* – host interactions, colonisation, transmission and horizontal gene transfer (Weyand *et al.*, 2013).

Neisseria spp. are usually grown on Mueller-Hinton Agar or Chocolate Agar plates at 37 ºC in a CO_2 enriched atmosphere, and they are oxidase-positive. To isolate pathogenic *Neisseria*, bacteria can be grown on selective plates containing colistin. In this way, however, a few other commensal species such as *N. lactamica* and *N. subflava* are also able to grow. For this reason, colony morphology and a few further tests that measure acid production from various carbohydrates can be carried out to differentiate more carefully the various species (Knapp, 1988).

1.3.1 *Neisseria lactamica*

N. lactamica is a Gram-negative diplococcus that harmlessly colonises the human nasopharynx, and is carried especially by young children. Half of the children worldwide, in fact, will harbour this bacterium within the first two years of life, and its colonisation slowly decreases over time and reaches approximately 15 % in adolescents (Olsen *et al.*, 1991). This pattern of colonisation may be reflected by the fact that, when compared to other *Neisseria* species, *N. lactamica* is unique in its ability to ferment lactose, a sugar that is widely present in young children as they usually consume larger volumes of milk. *N. lactamica*, in fact, produces β-D-galactosidase (Knapp, 1988).

N. lactamica is the non-pathogenic species that is the most closely related to the two pathogenic *Neisseria* species that are described below. *N. lactamica* is of particular clinical relevance, as clear correlations have been found that show an inverse relationship between colonisation by *N. lactamica* and by *N. meningitidis*. Carriage of *N. lactamica*, in fact, is at its peak in young children, where *N. meningitidis* is generally not present. On the contrary, *N. meningitidis* peaks in adolescents and young adults, where the level of *N. lactamica* has already drastically dropped (Figure 1.3.1-1) (Bennett *et al.*, 2005). As a consequence, carriage of *N. lactamica* results in a decreased carriage of *N. meningitidis*, and this will therefore lower the incidence of invasive meningococcal disease in childhood. Protective immunity against *N. meningitidis* has also been demonstrated more recently by inoculating *N. lactamica* in healthy non-carriers (Evans *et al.*, 2011).

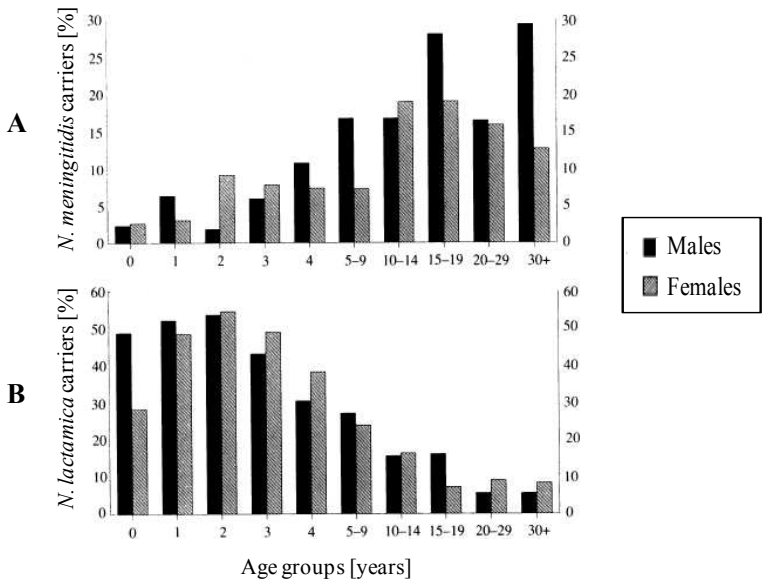

Figure 1.3.1-1: Carriage of *N. lactamica* and *N. meningitidis*.
These graphs show the carriage incidence of *N. meningitidis* (**A**) and *N. lactamica* (**B**) according to age and sex. The main difference in colonisation is highlighted by the age groups rather than the sex of the individuals (Figure adapted from Olsen *et al.*, 1991).

1.3.2 *Neisseria gonorrhoeae*

N. gonorrhoeae, also known as the gonococcus, is a Gram-negative diplococcus that is responsible for gonorrhoea, one of the major sexually transmitted diseases affecting both males and females equally in many countries worldwide. This bacterium colonises the urogenital tract, causing an infection that can be transmitted from one person to another through oral, vaginal or anal sexual relations. If left untreated, it may spread from the prostate or cervix throughout the body, ultimately affecting genitals, joints, vision and even heart valves (Ryan *et al.*, 2010). This pathogen is non-motile but possesses a type IV pilus that extends towards the host's cell surface and retracts upon contact, dragging the bacterium towards the host via the so-called "twitching motility" (Wolfgang *et al.*, 1998).

Signs of infection from *N. gonorrhoeae* can already appear after an incubation period of 2 to 10 days and, despite 30 to 60 % of the infected population showing none or very mild symptoms, it usually exhibits the first side effects 4 to 6 days after contraction (van Duynhoven, 1999). This species gives positive results to oxidase tests and can be differentiated from *N. lactamica* and *N. meningitidis* by hydroxyprolylaminopeptidase, as this enzyme is only produced by the gonococcus (Knapp, 1988).

N. gonorrhoeae has very high similarity to the other pathogen of this genus, *N. meningitidis*.

1.3.3 *Neisseria meningitidis*

N. meningitidis, also known as the meningococcus, is a Gram-negative diplococcus that was first identified as causative agent of bacterial meningitis by Anton

Weichselbaum in 1887 (Branham, 1940). This bacterium is a pathogen that usually colonises asymptomatically the human nasopharynx and oropharynx, but can be transmitted from one person to another through direct contact of nasal or oral secretions or through the inhalation of contaminated droplets (Caugant *et al.*, 2007).

The meningococcus is often carried asymptomatically, as people who harbour this bacterium rarely develop the disease. Its acquisition into the bloodstream, however, may result in an invasive disease, causing meningitis or septicaemia especially in susceptible people (Hill *et al.*, 2010). As an accidental pathogen, the meningococcus shows its often fatal effects between 1 to 14 days after contraction. However, it mostly only leads to a simple commensal asymptomatic colonisation, known as the carriage state (Stephens, 2007). This carriage state is thought to prevent the invasive form of the disease by inducing the human naturally acquired immunity against *N. meningitidis* (Goldschneider *et al.*, 1969).

N. meningitidis colonise approximately 10% of the total adult population at any given time, even though increased carriage rates have been observed during epidemics and close interactions (Caugant *et al.*, 1994). The highest incidence of meningococcal disease occurs amongst children under the age of four, when their immune system is still developing, or in teenagers and young adults, most likely as a result of an increased exposure to environmental risk factors, such as the number and closeness of contacts (Riesbeck *et al.*, 2000, Imrey *et al.*, 1995).

Like *N. gonorrhoeae*, this opportunistic pathogen is non-motile, possesses a type IV pilus and is oxidase-positive (Knapp, 1988).

1.4 Microbiology of *Neisseria meningitidis*

N. meningitidis is a heterotrophic and facultative anaerobic Gram-negative β-proteobacterium, which can occur as a single coccus or, more often, as a diplococcus with the adjacent sides flattened. It ranges between 0.6 to 1.9 μm in diameter and is an obligate human pathogen with optimal growth temperature of 35 - 37°C (Garrity *et al.*, 2005).

N. meningitidis possesses a typical Gram-negative cell envelope that is composed of two membranes, the inner- and outer- membranes, which surround the periplasm (Rosenstein *et al.*, 2001). The periplasm is formed of a peptidoglycan layer and a number of proteins. The inner membrane is made of a phospholipid bilayer containing proteins mainly implicated in the transport of nutrients and proteins through the inner membrane, whilst the asymmetrical outer membrane is primarily composed of lipopolysaccharides (LPS) on the outer leaflet and phospholipids on the inner leaflet. The outer membrane also includes various outer membrane proteins (OMPs), the most recurrent being Porin A (PorA), Porin B (PorB), opacity proteins (Opa, Opc), reduction-modifiable protein M (RmpM) and lactoferrin receptor proteins, all of which are mostly linked to meningococcal virulence (Ekins *et al.*, 2004, Massari *et al.*, 2003, Rosenstein *et al.*, 2001). *N. meningitidis* is often protected by a polysaccharide capsule that confers virulence. *N. lactamica* and *N. gonorrhoeae*, however, never have a capsule, and this suggests that the genes encoding the capsule might have been acquired by *N. meningitidis* from another virulent species by horizontal gene transfer (Schoen *et al.*, 2008, Claus *et al.*, 2002).

1.5 Carriage and pathogenicity of *Neisseria meningitidis*

Meningococci are obligate commensals of humans, and can colonise the mucosa of the upper tract of the respiratory system, usually without causing invasive disease. *N. meningitidis* can be passed between people, but this requires close contact, as the bacterium is very sensitive to dessication. Carriage rates are very variable amongst the population, and it is thought that almost everybody at some point in their life have been colonised by these bacteria. In fact, carriage rates can dramatically increase to nearly 100 % in closed or semi-closed environments, such as military training camps and schools (Caugant *et al.*, 1994, Caugant. *et al.*, 1992).

By a mechanism that is still unknown, and usually within less than ten days from first exposure, some *N. meningitidis* strains are able to cross the epithelial cells of the mucosa and consequently enter the bloodstream, from where they can start to reproduce and can cause a variety of mild clinical symptoms, such as chills, fever and muscle aches. Within hours of contraction, however, this state might rapidly degrade into life-threatening diseases such as septicaemia, if the bacteria cause a whole-body inflammation, or meningitis, if the bacteria manage to cross the blood-brain barrier (Van Deuren *et al.*, 2000). Depending on the strain and on the location, annual incidence rates during outbreaks could vary between 1 and 1,000 for every 100,000 people, killing on average about 10 % of the patients affected (Hill *et al.*, 2010). For this reason, understanding how *N. meningitidis* can be both a harmless commensal and a harmful human pathogen is still a challenge to date.

Nowadays, over half of the people affected by invasive meningococci can recover, if antibiotic treatments are followed promptly. In fact, the death rate can decrease to

about 10 % for the people affected by meningitis and to 30 % for the patients with sepsis (Brandtzaeg & van Deuren, 2012). Early antibiotic treatments, however, need to be administered as soon as possible once clinical diagnosis has confirmed meningococcal meningitis, since antibiotics can stop the propagation of *N. meningitidis* without delay. 5 – 20 % of the surviving patients, though, will suffer from severe permanent damage, such as amputation of limbs, mental retardation, and deafness (Van Deuren *et al.*, 2000).

Population predisposition for meningococcal survival and invasive infection is a key factor in the development of the disease. People with immunodeficiency problems, in fact, are an optimal target, as they lack circulating antibodies that protect them against these bacteria (D'amelio *et al.*, 1992). Other factors leading to predisposition involve respiratory tract infections, number and closeness of social contacts, age and active or passive smoking (MacLennan *et al.*, 2006). Carriage rates correspond to about 10 % of the total population, but it is not spread evenly worldwide. In Africa, for example, there is a more variable age distribution, whereas in Europe and North America carriage rates are low in the first years of life but suddenly increase in adolescents, with a peak at about 15 – 20 years of age (Trotter & Greenwood, 2007). Meningitis outbreaks still occur in clusters and localised epidemics around the world, and with particular extent in poorer countries (Moore, 1992).

The meningococcal invasive disease is believed to depend on the combination of several genes or genetic allelic variants, which may also exist in strains that are less invasive (Yazdankhah & Caugant, 2004). The genes that encode the capsule, for example, are considered a major virulence factor. However, despite conferring protection to the bacteria during infection, the real role of the capsule is still

ambiguous: its expression is considered necessary but not sufficient for illness, as only a few capsule variants do actually cause invasive diseases. Moreover, rare cases of virulence caused by non-capsulated *N. meningitidis* have been detected. In contrast with the strains that cause disease, half of the isolates derived from carriers do not express a capsule, and half amongst these do not even possess a gene that encodes it (Schoen *et al.*, 2008). Moreover, *N. meningitidis* comprises several other gene clusters, most of which have still unknown functions but are associated with virulence. These gene clusters are referred to as pathogenic islands (Stabler *et al.*, 2005, Tettelin *et al.*, 2000) and will be discussed in Section 1.7.2.

Meningococci are classified in thirteen different serogroups: serogroups A, B, C, D, 29E, H, I, K, L, Y, W-135, X and Z. These serogroups are based on differences in the structure of the polysaccharides that are present on the capsule, as polysaccharides are considered primary targets for mucosal humoral immunity (Yazdankhah & Caugant, 2004). However, only six serogroups, serogroups A, B, C, W135, X and Y, are accountable for the majority of the invasive diseases and are linked with endemics and epidemics (Boisier *et al.*, 2007, Yazdankhah & Caugant, 2004). These serogroups show regional distributions: serogroup A has disappeared from Europe and North America since World War II but is still predominant in the sub-Saharan belt, also referred to as the "Meningitis Belt" (Chippaux, 2008). Serogroup B is a primary concern in industrialised countries (Racloz & Luiz, 2010). Serogroup C outbreaks are observed worldwide, specifically targeting adolescents and young adults (Van Deuren *et al.*, 2000). Serogroups X, which has only recently revealed an epidemic potential, and W135 have both been accountable for epidemics in the sub-Saharan belt over the past ten years (Boisier *et al.*, 2007, Mueller *et al.*, 2006).

Serogroup Y has been a major cause of infection in North America in the last decade (Racoosin *et al.*, 1998).

Despite the absence of flagella, these virulent strains are usually protected not only by the capsules, but also by protruding fimbriae, called type IV pili. These fimbriae are filamentous proteins that play a number of fundamental roles in *N. meningitidis*, such as their natural capability for transformation and movement, the initial attachment to human host cells (Coureuil *et al.*, 2009, Rayner *et al.*, 1995) and biofilm formation (Yi *et al.*, 2004). Type IV pili, however, are not suitable as vaccine candidates despite being immunogenic, as they have a very high degree of antigenic variability (Nassif *et al.*, 1993).

1.6 Vaccine candidates for *Neisseria meningitidis*

Several vaccines against *N. meningitidis* have already been commercially available since the early 1970's and many others are still under development. These vaccines do not consist of killed or live but attenuated pathogens; instead, they are composed of purified protective components which directly target the polysaccharides present in the capsule of the virulent meningococci (Ulmer *et al.*, 2006). With this method there are fewer undesirable side-effects caused upon administration, compared to when the whole cell vaccines are used. Because they are composed of only capsular polysaccharides linked to protein carriers, vaccines are harmless and can be injected to infants that are just a few months old. Moreover, our immune system responds more effectively to proteins than sugars and, as a result, conjugate vaccines can trigger a long-lasting immune response. In this way, however, newborns need a vaccine boost a few years after first administration (Snape & Pollard, 2005).

The monovalent MenC conjugate vaccine is consistently used in all the industrialised countries, and has become routinely used for immunisation against serogroup C meningococci in Europe. Since its introduction just over a decade ago, meningitis caused by serogroup C has dramatically fallen and nowadays this strain accounts for less than 10 % of meningitis cases (Snape & Pollard, 2005).

The quadrivalent MenACWY conjugate vaccine has been developed more recently. The quadrivalent vaccine contains four of the six serogroups that are responsible for over 90 % of meningitis cases worldwide. In fact, it contains polysaccharides from the serogroups A, C, W135 and Y, which are major causes of meningitis outbreaks in developed countries. Several versions of this vaccine have been developed so far, where differences included the length of the meningococcal oligosaccharides used and the selection of the carrier protein and / or the chemistry of the conjugation (Pace *et al.*, 2009). Three quadrivalent MenACWY conjugate vaccines, which use different carriers such as diphtheria toxoid, diphtheria mutant toxin carrier protein (CRM_{197}) and tetanus toxoid, have just recently been licensed (Khatami *et al.*, 2012).

No successful vaccines against serogroup B meningococci have been made available yet, but several studies are under way. The capsular polysaccharide of *N. meningitidis* serogroup B cannot be used for the preparation of vaccines, as it contains polysialic acid residues, which could activate an autoimmune response in the human host (Holst, 2007). Polysialic acid is, in fact, a polysaccharide that is widely distributed in humans and that helps to protect autologous cells from complement attack (Horstmann, 1992). Other approaches for finding a suitable working vaccine are currently being explored. Outer membrane vesicle (OMV) vaccines have shown to be harmless and effective, as they induce strong protective

serum bactericidal antibodies (SBA) activity in humans. Porin A (PorA), which is the main component of the OMV, is the most expressed outer membrane protein of almost all meningococci. PorA, however, is hypervariable and therefore this protein potentially decreases the vaccine's efficacy (Granoff, 2010). For this reason, other outer membrane protein antigens such as porin B (PorB) (Urwin *et al.*, 2002), factor H-binding protein (fHbp, previously referred to as GNA1870) (Masignani *et al.*, 2003), opacity protein (Opc) (Jolley *et al.*, 2001), Neisserial surface protein A (NspA) and *N. meningitidis* adhesion A (NadA) (de Filippis, 2009) are being investigated as potential vaccine candidates.

Research is moving towards the study of recombinant protein vaccines, which could be administered either alone or mixed with other antigens. These vaccines are in late-stage clinical development and might work against most of the serogroup B strains. The new 4CMenB vaccine, for example, contains fHbp, NadA, Neisserial Heparin Binding Antigen (NHBA) and OMV. This vaccine was designed as a result of reverse vaccinology, where potential surface-exposed proteins were not determined from microbiology techniques, but from all the genomic data widely available to date. These specific proteins were chosen because they were present in all of the serogroup B strains analysed during the study, and they might therefore induce bactericidal antibodies in all bacteria tested (Figure 1.6-1). This vaccine is promising, as it results in an increase in serum bactericidal antibodies (SBA) indeed and is in the final stages of the trial (Caesar *et al.*, 2013, Serruto *et al.*, 2012).

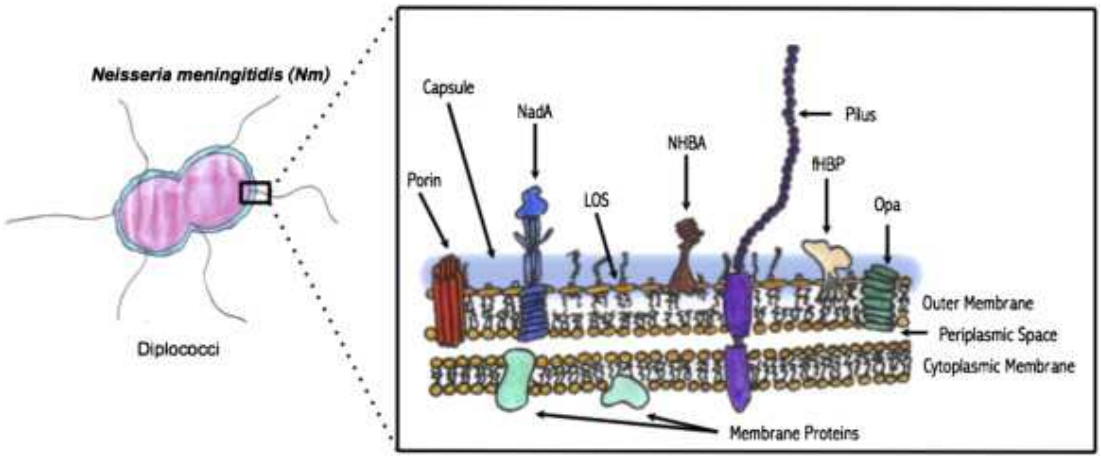

Figure 1.6-1: *N. meningitidis* surface virulence factors.
Schematic representation showing the main immunogenic protein antigens present on the cell surface of *N. meningitidis*. These surface virulence factors have major roles in conferring the ability to colonise and eventually infect the human host. Abbreviations used: NadA: *Neisseria* adhesin A. LOS: lipoologosaccharide. NHBA: Neisserial Heparin Binding Antigen. fHBP: factor H Binding Protein. Opa: opacity protein (Figure from Caesar *et al.*, 2013).

1.7 Genomic differences between *N. meningitidis* and the other bacteria

1.7.1 Genomic differences between *N. meningitidis* and *E. coli*

The genome size of *N. meningitidis* is fairly small, as it is approximately 2.2 – 2.3 Mb, and corresponds to about 2100 genes. The genome of *E. coli*, on the other hand, is much larger and is composed of 4.5 – 6 Mb, averaging about 5000 genes. One important aspect of this difference in the number of genes is given by the genome dynamics: *N. meningitidis* only inhabits the mucus layer that protects the naso- and

oropharynx of humans, hence this bacterium only needs a small number of regulatory proteins, whereas *E. coli* can colonise many environments between and within different hosts and therefore requires many more regulatory proteins in order to assist it with the diverse environmental conditions. The genome of *N. meningitidis* is hypervariable and continually undergoes mutational events. These mutations can be caused by horizontal gene transfer, by phase and antigenic variation, by recombination, etc. In fact, to help the bacterium survive in the hostile environment and evade the immune system, *N. meningitidis* contains approximately 100 genes that are involved in phase and antigenic variation, whereas the more stable *E. coli* genome contains less than 10 of those genes. Other probable differences in the survival strategy of *N. meningitidis* compared to *E. coli* involve a reduced DNA - repair capacity, and the presence of a very high number, approaching 2000, of the 10 bp DNA-uptake sequences (DUS) (Davidsen & Tønjum, 2006).

The bacterial strains that survive are those that are able to elude detection by the host immune system and its innate immune killing. For this reason, *N. meningitidis* possesses secretory proteins that are involved both in the adherence to host cells and in the suppression of the host's defence mechanisms. Site-specific proteases in *N. meningitidis*, for example, are responsible for cleaving several human proteins, such as immunoglobulin A1 (IgA1), a protein involved in the first line of defence in the mucosal membranes as it helps to prevent adhesion and colonisation of bacteria to the surface (Vitovski & Sayers, 2007).

1.7.2 Genomic differences between *N. lactamica*, *N. gonorrhoeae* and *N. meningitidis*

Studies of the genetic material have failed to identify consistent genomic differences amongst the *Neisseria* species. Most of the genome, in fact, is shared amongst *N. meningitidis*, *N. gonorrhoeae* and *N. lactamica*, despite their different relationship with the human host (Maiden, 2008). The genes that are communal between the commensal *N. lactamica* and the pathogenic *N. meningitidis*, for example, may be involved in the colonisation of the host's specific niche, whereas the genes that are only present in the meningococcus could possibly lead to the virulence of this bacterium (Snyder & Saunders, 2006).

Sequencing analysis of all three species resulted in the discovery of nine conserved genetic islands which are always present in *Neisseria meningitidis* and occasionally in *N. gonorrhoeae*, but are always absent from its closely related commensal *Neisseria lactamica* (Figure 1.7.2-1). As these nine genetic islands, composed of two or more genes, were only present in the pathogens, they can also be referred to as pathogenic islands. Several genes belonging to these 9 pathogenic islands still encode unknown proteins and therefore, to investigate their function, a BLAST analysis of all 38 genes and their proteins belonging to *N. meningitidis* strain MC58 was carried out. Most of these islands have been very likely acquired by horizontal gene transfer (HGT), as their flanking genes are found next to each other in *N. lactamica*.

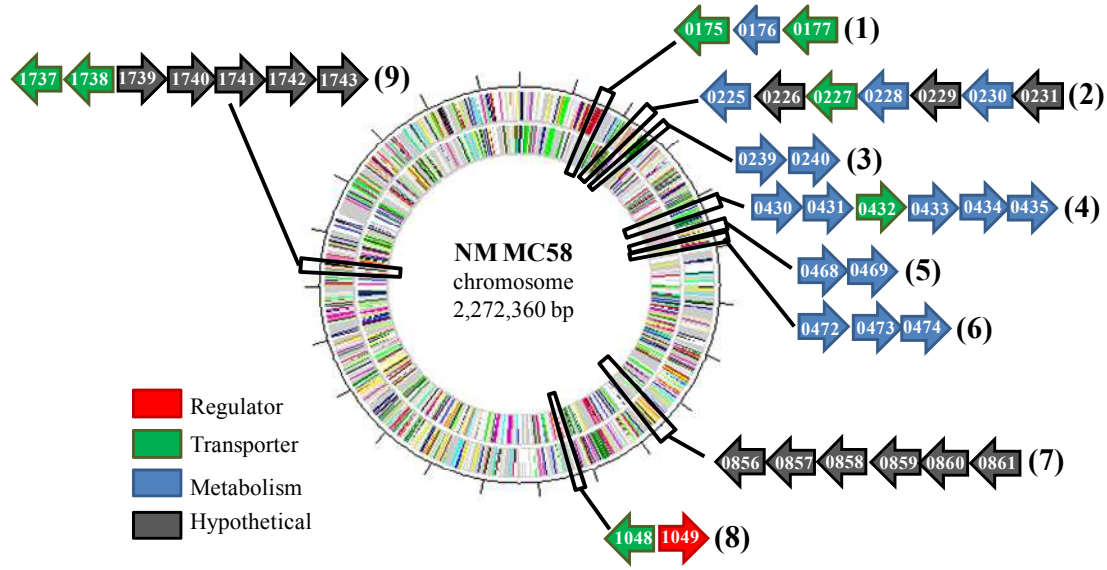

Figure 1.7.2-1: Genomic islands present in *N. meningitidis* and absent from *N. lactamica*.

This circular representation of the *N. meningitidis* strain MC58 genome shows the 9 genomic islands which are found in all *N. meningitidis* strains. Gene numbers correspond to the numbering given in the MC58 complete genome, where the number within each arrow is preceded by "NMB" (NCBI GenBank accession number AE002098.2) (Figure from James Moir).

All genes belonging to the nine pathogenic islands and their flanking genes from *N. meningitidis* strain MC58 (NCBI GenBank accession number AE002098.2) were compared to the genomes of *N. gonorrhoeae* strain FA 1090 (NCBI GenBank AE004969.1) and *N. lactamica* strain 020-06 (NCBI GenBank FN995097.1). Gene numbers in all the figures below correspond to the numbering given in the NCBI GenBank, where genes in **A** are preceded by "NMB0", in **B** are preceded by "NGO" and in **C** are preceded by "NLA_", unless stated otherwise.

The first pathogenic island, composed of three genes, is involved in the oxidation of D-amino acids with the help of the D-amino acid dehydrogenase enzyme (Figure 1.7.2-2).

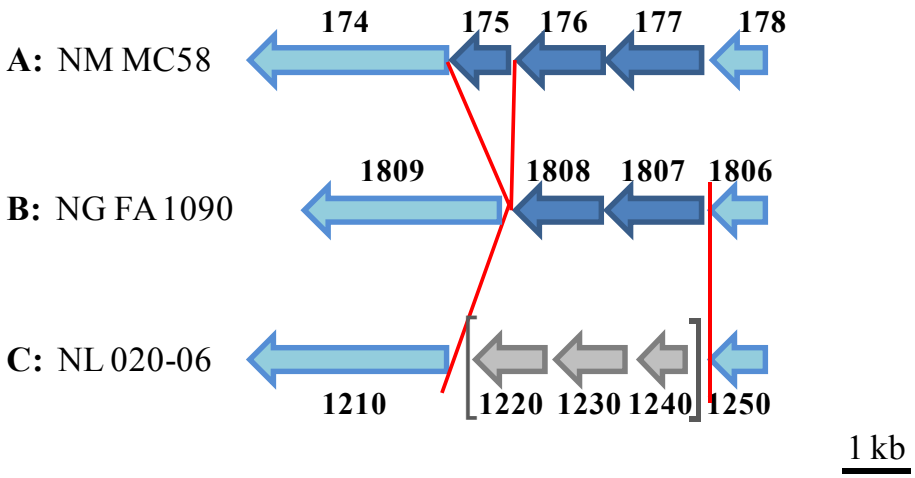

Figure 1.7.2-2: Genomic island 1 is involved in the oxidation of D-amino acids. BLAST analysis using the three genes from *N. meningitidis* as a query indicates that *N. gonorrhoeae* lacks the putative zinc transporter encoded by *NMB0175* and *N. lactamica* lacks all three genes. *N. lactamica*, however, contains three genes encoding hypothetical proteins which are absent from the genome of both pathogens. NMB0175: zinc transporter (ZupT) protein. NMB0176: D-amino acid dehydrogenase small sub-unit. NMB0177: putative sodium / alanine symporter.

The second pathogenic island is thought to be involved in the metabolism of urea and amino acids, and contains the allophanate hydrolase sub-units 1 and 2 (Figure 1.7.2-3).

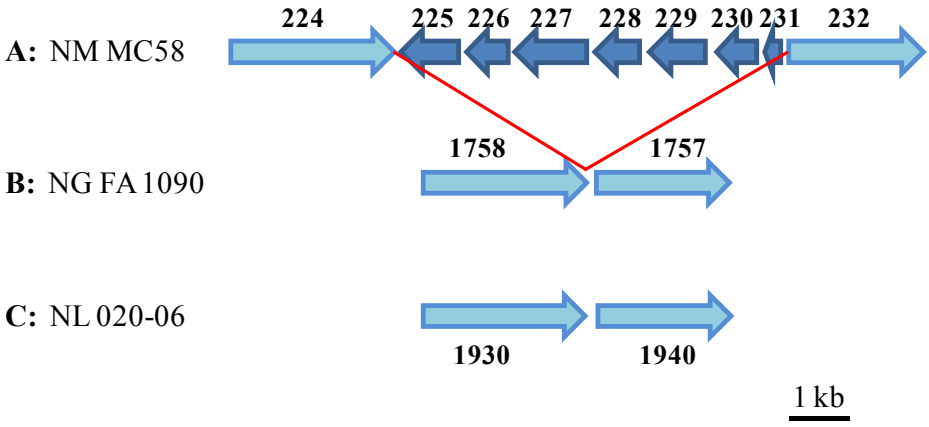

Figure 1.7.2-3: Genomic island 2 is involved in urea and amino acids metabolism.

BLAST analysis using the seven genes as a query indicates that this pathogenic island is exclusive to *N. meningitidis*, and several of the genes still encode hypothetical proteins. NMB0225: IS30 family transposase. NMB0226: hypothetical protein. NMB0227: transmembrane transport protein. NMB0228: LamB/Ycsf family protein. NMB0229: hypothetical protein. NMB0230: allophanate hydrolase sub-unit 1. NMB0231: hypothetical protein.

Pathogenic island 3 comprises two enzymes that are involved in polyamine biosynthesis, which are spermidine synthase and spermine synthase. This island and the knockout for *NMB0240* are referred in Appendix – A (Figure 1.7.2-4).

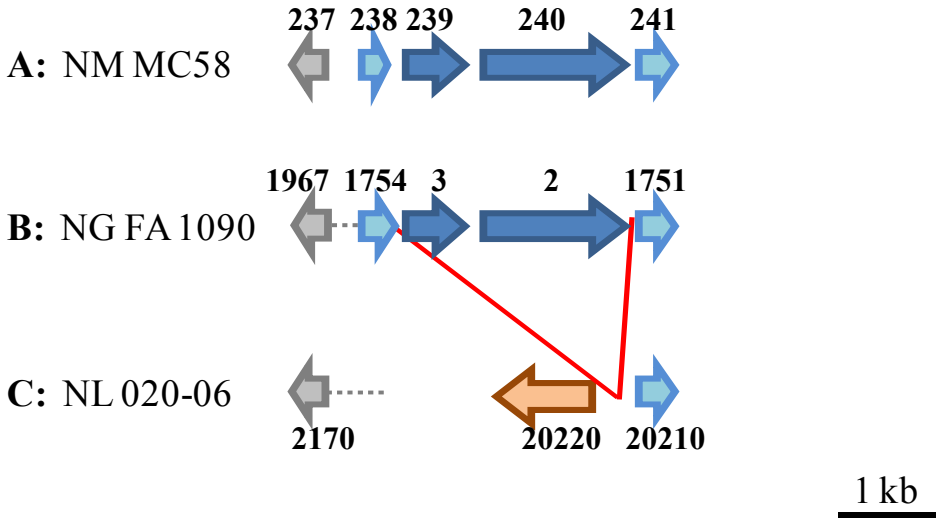

Figure 1.7.2-4: Genomic island 3 is involved in the synthesis of spermine.
This island is present in both pathogens and absent from *N. lactamica*. The flanking gene upstream of the island (*NMB0238*) is absent from *N. lactamica*, and a gene rearrangement occurred between these three species around the gene cluster, as *NMB0237* is found in different locations within the genome of both *N. gonorrhoeae* and *N. lactamica*. *NLA_20220* is present in both pathogens, and corresponds to *N. meningitidis NMB2127* and *N. gonorrhoeae NGO1963*. Abbreviations used: 3: 1753. 2: 1752. NMB0239: spermine synthase. NMB0240: spermidine synthase.

Genomic island 4, found in both *N. meningitidis* and *N. gonorrhoeae*, but absent from *N. lactamica*, is involved in the putative metabolic 2-methylcitrate pathway, a pathway that will be further discussed in Chapter 3. This pathogenic island is the largest amongst the nine that are found in all *N. meningitidis* strains, as it contains 9329 bp. This island has most likely been acquired by HGT in *N. meningitidis* or has followed selective gene loss in *N. lactamica*. In fact, both genes that are present in either side of the island in the two pathogens correspond to the same genes that are found flanking each other in *N. lactamica* (Figure 1.7.2-5).

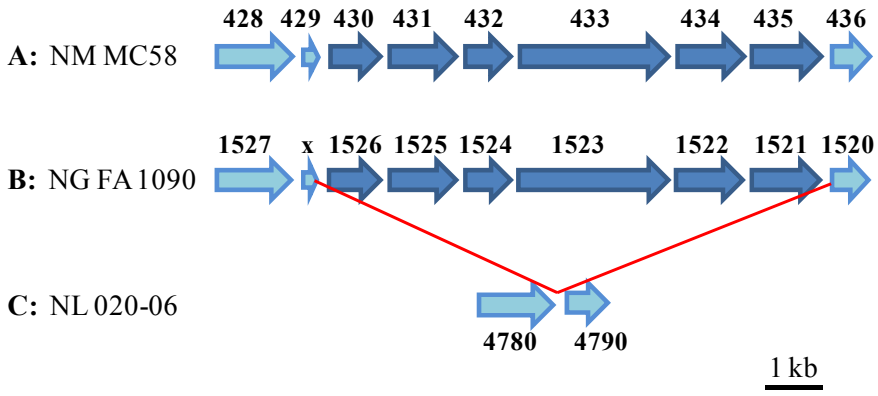

Figure 1.7.2-5: Genomic island 4 encodes genes for the 2-methylcitrate pathway. BLAST analysis using the six genes forming the 2-methylcitrate pathway and their flanking genes from the *N. meningitidis* strain MC58 genome reveals that all the genes are also present in *N. gonorrhoeae* but only the two flanking genes are found, adjacent to each other, in *N. lactamica*. NMB0430: 2-methylisocitrate lyase. NMB0431: 2-methylcitrate synthase. NMB0432: hypothetical membrane protein. NMB0433: Aconitate hydratase. NMB0434: AcnD - accessory protein PrpF. NMB0435: Propionate kinase (acetate kinase).

Pathogenic island 5 is thought to be involved in polyamine biosynthesis, as it catabolises L-arginine to putrescine. Putrescine is the substrate for pathogenic island 3. This island is absent from the commensal *N. lactamica* (Figure 1.7.2-6).

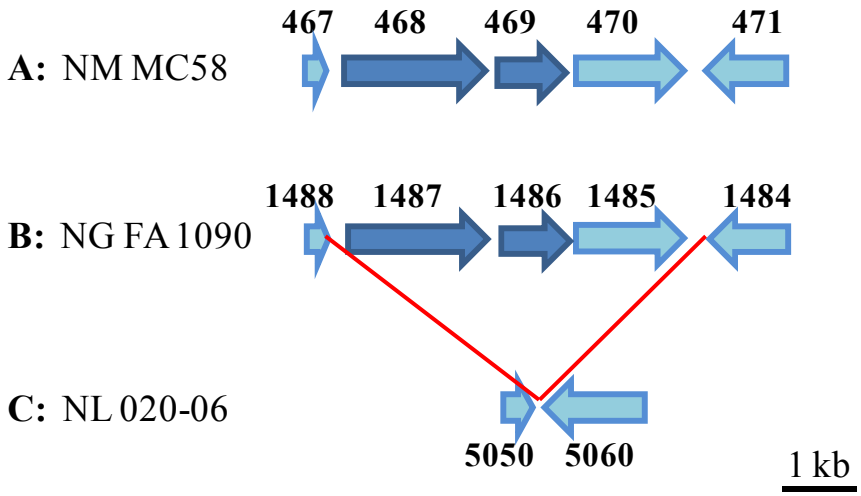

Figure 1.7.2-6: Genomic island 5 is involved in putrescine biosynthesis.
BLAST analysis using the two genes involved in polyamine biosynthesis and their flanking genes from the *N. meningitidis* strain MC58 genome reveals that all the genes are present in *N. gonorrhoeae* but only *NMB0467* and *NMB0471* are present, adjacent to each other, in *N. lactamica*. NMB0468: L-arginine decarboxylase. NMB0469 agmatinase. NMB0470: C_4-dicarboxylate transporter.

Pathogenic island 6 is involved in biotin synthesis. This island is absent from the commensal *N. lactamica* (Figure 1.7.2-7).

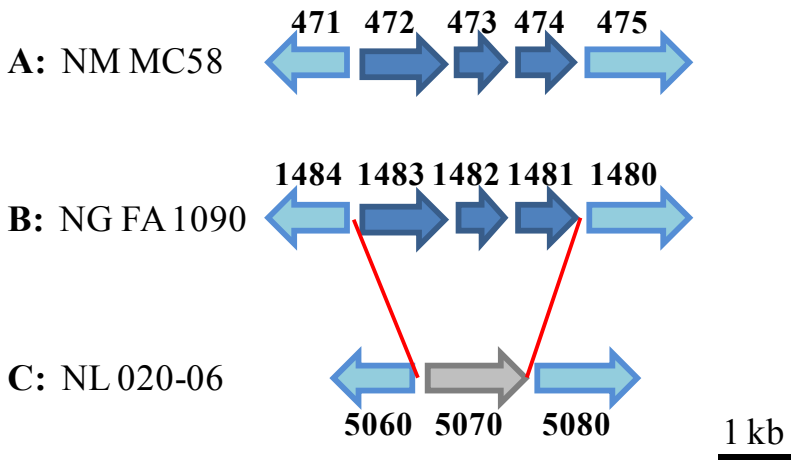

Figure 1.7.2-7: Genomic island 6 is involved in biotin synthesis.
BLAST analysis using the three genes involved in biotin synthesis and their flanking genes from the *N. meningitidis* strain MC58 genome reveals that all the genes are also present in *N. gonorrhoeae*. The two flanking genes are present in *N. lactamica* too, where they are separated by a 1359 bp gene that encodes a putative tRNA methyltransferase. The *NLA_5070* gene does not have similarities with any genes from *N. meningitidis* nor *N. gonorrhoeae* but it includes a 95 bp fragment that is present between *NMB0471* and *NMB0472*. NMB0472: 8-amino-7-oxononanoate synthase. NMB0473: hypothetical protein. NMB0474: putative biotin synthesis protein (BioC).

Pathogenic island 7 is composed of six genes, all of which have hypothetical functions (Figure 1.7.2-8).

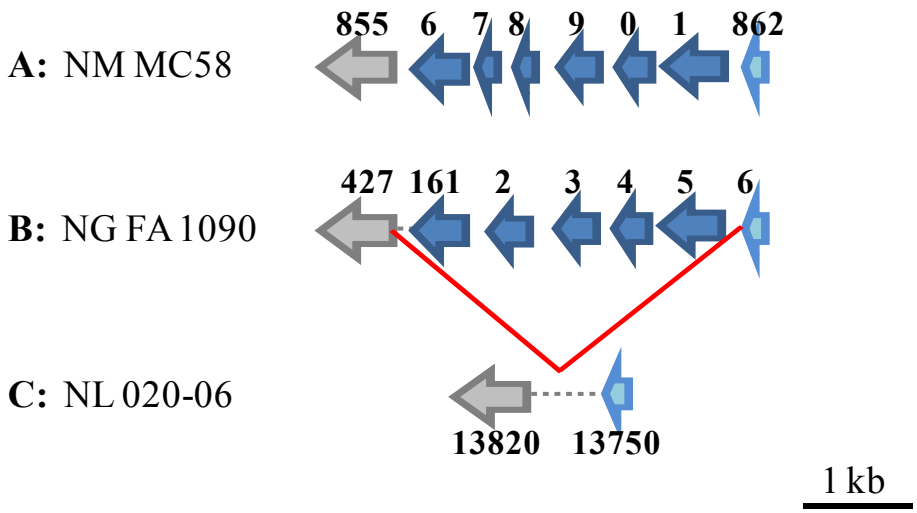

Figure 1.7.2-8: Genomic island 7 encodes five hypothetical proteins.
This island is present in both pathogens and absent from *N. lactamica*. The flanking genes are found in both *N. gonorrhoeae* and *N. lactamica*, even though there was a change of gene arrangement between species around these gene clusters. Abbreviations used: **A** - 6: 856. 7: 857. 8: 858. 9: 859. 0: 860. 1: 861. **B** – 2: 162. 3: 163. 4: 164. 5: 165. 6: 166. NMB0856: hypothetical protein. NMB0857: hypothetical protein. NMB0858: hypothetical protein. NMB0859: hypothetical protein. NMB0860: hypothetical protein. NMB0861: hypothetical membrane protein.

Pathogenic island 8, which is also found in *N. gonorrhoeae*, contains two genes that have hypothetical functions. Gene *NMB1049* encodes a hypothetical protein which has high sequence identity with LysR-type transcriptional regulator (LTTR). This genomic island and NMB1049 are further investigated in Chapter 4 and Chapter 5 (Figure 1.7.2-9).

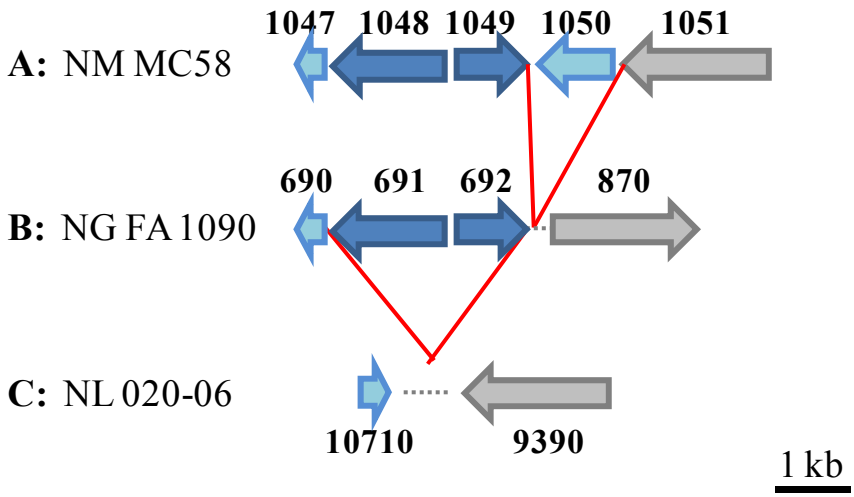

Figure 1.7.2-9: Genomic island 8 contains a putative LysR-Type transcriptional regulator.

This island is present in both pathogens and absent from *N. lactamica*. The flanking genes, with the exception of *NMB1050* which is only present in *N. meningitidis* strains, are found in both *N. gonorrhoeae* and *N. lactamica*. The island and the genes downstream appear to have been acquired by HGT in both pathogens, as both flanking genes are found in different locations within the genome of *N. lactamica*. NMB1048: putative membrane protein. NMB1049: putative LTTR protein.

Pathogenic island 9, the second largest acquisition in *N. meningitidis* genome, contains 5771 bp and comprises seven genes, the majority of which encode proteins with hypothetical functions. Two proteins have similarity to secretion proteins (Figure 1.7.2-10).

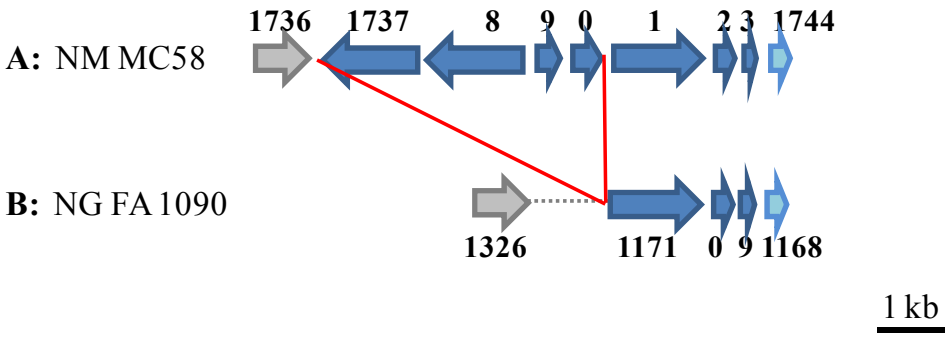

Figure 1.7.2-10: Genomic island 9 contains secretion proteins.
The complete island is found only in *N. meningitidis*. The three genes that are also present in *N. gonorrhoeae* encode proteins with hypothetical functions. There was a change in gene arrangement between the two pathogens around these gene clusters. The island and flanking genes are absent from *N. lactamica*. Abbreviations used: **A** – 8: 1738. 9: 1739. 0: 1740. 1: 1741. 2: 1742. 3: 1743. **B** – 0: 1170. 9: 1169. NMB1737: secretion protein. NMB1738: secretion protein. NMB1739: hypothetical protein. NMB1740: hypothetical protein. NMB1741: hypothetical protein. NMB1742: hypothetical protein. NMB1743: hypothetical protein.

1.8 Aims and objectives of this work

The nine genomic islands just described might be of major importance to the carriage and / or survival of *N. meningitidis* in their exclusive natural habitat, the human host. Genomic islands 4 and 8 have not yet been fully characterised and are the focus of the work presented in the following chapters.

This thesis aims to characterise a number of genes, homologues of which have already been characterised in other bacteria, but which are still only putatively involved in the 2-methylcitrate pathway in *N. meningitidis*. It also aims to identify and characterise new genes present in this pathway in the pathogenic *Neisseria* solely, as they are absent from all other microorganisms that have been sequenced so far. Studies of other genes belonging to a yet unknown pathway comprising a probable transcriptional regulator will be carried out, and potential genes regulated by this protein will also be identified. Finally, the mutants generated as part of this work will be used to examine their role in the survival of *N. meningitidis ex vivo*.

The work executed in this thesis aims to contribute to the understanding of the carriage and infection of *N. meningitidis*, so that new approaches could be taken into consideration for fighting against this pathogen.

Chapter 2 - Materials and Methods

2.1 Bacterial strains and plasmids used in this work

2.1.1 Bacterial strains used in this work

Strain	Genotype and Description	Source / Ref
Escherichia coli DH5α	General cloning strain carrying F^-ϕ80d*lacZ*ΔM15 Δ(*lac*ZYA-*arg*F)U169 *rec*A1 *end*A1 *hsd*R17(r_k^-, m_k^+) *pho*A *sup*E44 *thi*-1 *gyr*A96 *rel*A1 λ^-	Invitrogen™
Escherichia coli BL21 (DE3)	Cells for protein expression. General cloning strain carrying F^- *omp*T *hsd*S_B ($r_B^-m_B^-$) *gal dcm ara*B::T7RNAP-*tet*A	Invitrogen™
N. meningitidis MC58	Wild-type, clonal group ET-5, serogroup B	McGuinness *et al.*, 1991
N. meningitidis NMB0240::Spec^R	MC58 with disrupted genomic copy of *NMB0240* by insertion of spectinomycin resistance cassette	This work
N. meningitidis prpC::Spec^R	MC58 with disrupted genomic copy of *NMB0431* by insertion of spectinomycin resistance cassette	This work
N. meningitidis NMB0432::Spec^R	MC58 with disrupted genomic copy of *NMB0432* by insertion of spectinomycin resistance cassette	This work
N. meningitidis NMB0432::Tet^R	MC58 with disrupted genomic copy of *NMB0432* by insertion of tetracycline resistance cassette	This work
N. meningitidis ackA-1::Spec^R	MC58 with disrupted genomic copy of *NMB0435* by insertion of spectinomycin resistance cassette	This work
N. meningitidis NMB0468::Spec^R	MC58 with disrupted genomic copy of *NMB0468* by insertion of spectinomycin resistance cassette	This work
N. meningitidis NMB1048::Spec^R	MC58 with disrupted genomic copy of *NMB1048* by insertion of spectinomycin resistance cassette	This work
N. meningitidis NMB1049:: Chl^R	MC58 with disrupted genomic copy of *NMB1049* by insertion of chloramphenicol resistance cassette	This work
N. meningitidis NMB1049::Spec^R	MC58 with disrupted genomic copy of *NMB1049* by insertion of spectinomycin resistance cassette	This work
N. meningitidis NMB432:: Tet^R *1048:: Spec*^{R}	MC58 with disrupted genomic copy of *NMB0432* by insertion of tetracycline cassette and of *NMB01048* by insertion of spectinomycin cassette	This work
Veillonella spp.	*Veillonella* species isolated from mouth washes	S. Fergusson

2.1.2 Plasmids used in this work

Plasmid	Description	Source / Ref
pET-28b(+)-*NMV_1164*	Vector for expressing 6x His-tagged proteins containing a kanamycin resistance (Kan^R) cassette and a genomic copy of *NMV_1164* from *N. meningitidis* 8013	Dr V. Pelicic
pCR®-Blunt II-TOPO®	Linearised plasmid cloning vector containing a kanamycin resistance cassette, for blunt end cloning of PCR products	Invitrogen™
pCR®-Blunt II-TOPO®- *NMB0240*	Vector with a kanamycin cassette and a genomic copy of *NMB0240* from *N. meningitidis* MC58	This work
pCR®-Blunt II-TOPO®- *prpC*	Vector with a kanamycin cassette and a genomic copy of *NMB0431* from *N. meningitidis* MC58	This work
pCR®-Blunt II-TOPO®- *NMB0432*	Vector with a kanamycin cassette and a genomic copy of *NMB0432* from *N. meningitidis* MC58	This work
pCR®-Blunt II-TOPO®- *ackA-1*	Vector with a kanamycin cassette and a genomic copy of *NMB0435* from *N. meningitidis* MC58	This work
pCR®-Blunt II-TOPO®- *NMB0468*	Vector with a kanamycin cassette and a genomic copy of *NMB0468* from *N. meningitidis* MC58	This work
pCR®-Blunt II-TOPO®- *NMB1048*	Vector with a kanamycin cassette and a genomic copy of *NMB1048* from *N. meningitidis* MC58	This work
pCR®-Blunt II-TOPO®- *NMB1049*	Vector with a kanamycin cassette and a genomic copy of *NMB1049* from *N. meningitidis* MC58	This work
pHP45*Ω*	pHP45 plasmid containing spectinomycin resistance cassette, also called *Ω* cassette	Prentki & Krisch, 1984
pCMT18	Vector containing tetracycline resistance cassette	C. Tang
pST2	Vector containing chloramphenicol resistance cassette	S. Turner *et al*, 2003
pCR®-Blunt II-TOPO®- *NMB0240::Spec*^{R}	Vector with *Kan*^{R} cassette and disrupted genomic copy of *NMB0240* encasing a *Spec*^{R} cassette	This work
pCR®-Blunt II-TOPO®- *prpC::Spec*^{R}	Vector with *Kan*^{R} cassette and disrupted genomic copy of *NMB0431* encasing a *Spec*^{R} cassette	This work
pCR®-Blunt II-TOPO®- *NMB0240::Spec*^{R}	Vector with *Kan*^{R} cassette and disrupted genomic copy of *NMB0432* encasing a *Spec*^{R} cassette	This work
pCR®-Blunt II- TOPO®- *NMB0432::Tet*^{R}	Vector with *Kan*^{R} cassette and disrupted genomic copy of *NMB0432* encasing a *Tet*^{R} cassette	This work

Plasmid	Description	Source / Ref
pCR®-Blunt II- TOPO®-*ackA-1::Spec*^{R}	Vector with *Kan*^{R} cassette and disrupted genomic copy of *NMB0435* encasing a *Spec*^{R} cassette	This work
pCR®-Blunt II- TOPO®-*NMB0468::Spec*^{R}	Vector with *Kan*^{R} cassette and disrupted genomic copy of *NMB0468* encasing a *Spec*^{R} cassette	This work
pCR®-Blunt II- TOPO®-*NMB1048::Spec*^{R}	Vector with *Kan*^{R} cassette and disrupted genomic copy of *NMB1048* encasing a *Spec*^{R} cassette	This work
pCR®-Blunt II- TOPO®-*NMB1049::Spec*^{R}	Vector with *Kan*^{R} cassette and disrupted genomic copy of *NMB1049* encasing a *Spec*^{R} cassette	This work
pCR®-Blunt II- TOPO®-*NMB1049::Chl*^{R}	Vector with *Kan*^{R} cassette and disrupted genomic copy of *NMB1049* encasing a *Chl*^{R} cassette	This work

2.2 Growth of bacterial strains

2.2.1 Preparation of *Escherichia coli* DH5α and BL21 (DE3) competent cells

In this study, chemically competent *E. coli* DH5α cells were used to facilitate the uptake of the pCR®-Blunt II- TOPO® plasmid (Invitrogen™) containing the full gene of interest, and chemically competent *E. coli* BL21 (DE3) cells were used as a protein expression host to facilitate the uptake of pET-28b(+)-*NMV_1164* plasmid (Dr V. Pelicic). Both *E. coli* DH5α and *E. coli* BL21 (DE3) competent cells were prepared from original Invitrogen™ aliquots following the Hanahan method (Hanahan, 1983), and were stored as single use aliquots at -80 ºC.

Fresh colonies were grown on LB plates at 37 ºC overnight. A few colonies were then inoculated in 50 ml Lysogeny Broth (LB) medium and incubated at 37 ºC in an Innova 2300 Platform Shaker (New Brunswick Scientific) at 200 rpm for several hours, until the OD at 600 nm reached 0.3-0.6. Cells were harvested in a 50 ml cellstar® tube (greiner bio-one) at 4000 rpm at 4 ºC for 20 minutes using an

Allegra™ X-22R bench-top centrifuge (Beckman Coulter™). The pellet was resuspended in 15 ml of ice-cold RF1 Buffer (buffer composition described in Table 2.2.1-1) and centrifuged at 4000 rpm at 4 ºC for 10 further minutes. The cells were finally resuspended in 5 ml of ice-cold RF2 Buffer (Table 2.2.1-1) and incubated for 15 minutes on ice prior to being stored at -80 ºC as single use aliquots.

Table 2.2.1-1: Composition of Buffers RF1 and RF2 used for competent cells preparation.

Buffers were filtered and stored at 4 ºC.

RF1 Buffer	**Amount**	**Concentration (final)**
KCl (Fisher Scientific)	2.4 g	160.94 mM
$MgCl_2•6H_2O$ (Fisher Scientific)	2.4 g	59.02 mM
K acetate (Melford)	0.6 g	30.57 mM
$CaCl_2•2H_2O$ (Fisher Chemical)	0.3 g	10.20 mM
Glycerol (Fisher Chemical)	30 ml	15 % (w / v)
Deionised H_2O	Added to final 200 ml and to pH 5.8	
RF2 Buffer	**Amount**	**Concentration (final)**
0.5 M MOPS, pH 6.8 (Acros organics)	4 ml	2 % (w / v)
KCl (Fisher Scientific)	0.3 g	20.12 mM
$CaCl_2•2H_2O$ (Fisher Chemical)	2.2 g	74.82 mM
Glycerol (Fisher Chemical)	30 ml	15 % (w / v)
Deionised H_2O	Added to final 200 ml and to pH 5.8	

2.2.2 Growth of *Escherichia coli* DH5α

E. coli strain DH5α was used in this work as an intermediate host for overproducing plasmids containing the desired inserts or ligations.

E. coli bacteria from the -80 ºC stock or from the liquid cultures were grown on Lysogeny Broth (LB) agar plates at 37 ºC overnight. LB agar plates were prepared by pouring 20 ml of molten LB agar suspension (cooled to 50 ºC) into 85 mm diameter plastic Petri dishes (Sterilin®). *E. coli* was streaked or spread onto these plates once they had set.

E. coli bacteria for liquid cultures were grown aerobically in 8 ml Lysogeny Broth (LB) in 30 ml polystyrene universal tubes (Sterilin®). Cultures were incubated at 37 ºC overnight in an Innova 2000 shaker (New Brunswick Scientific Ltd.) at 220 rpm.

LB medium for agar plates and liquid growth was prepared as described in Table 2.2.2-1, and antibiotics to screen for mutant strains were eventually added during plate preparation or just prior to incubation in liquid growth.

Table 2.2.2-1: Composition of Lysogeny Broth (LB) medium and plates.

	LB Medium [g/L]	**LB Agar plates [g/L]**
Tryptone (Formedium™)	10g	10g
Yeast Extract (Formedium™)	5g	5g
NaCl (Fisher Scientific)	5g	5g
Agar Technical (Agar no. 3) (Oxoid)	-	15g
Deionised H_2O	Added to final 1L	Added to final 1L

2.2.3 Growth of *Escherichia coli* BL21 (DE3) for overexpression of the protein NMV_1164

E. coli strain BL21 (DE3) was used in this work as the host for the plasmid containing the *NMV_1164* gene. This transformed pET-28b(+) plasmid was kindly donated by Dr Vladimir Pelicic, Imperial College London. pET-28b(+), which contains a kanamycin resistance gene, is a vector that is generally used for expressing 6x His-tagged proteins.

E. coli was streaked onto LB agar plates once they had set and was incubated at 37 ºC overnight. LB agar plates were prepared by pouring 20 ml of molten LB agar suspension (cooled to 50 ºC) supplemented with 50 µg / ml kanamycin into 85 mm diameter plastic Petri dishes (Sterilin®). Starting liquid cultures of plated *E. coli* were grown aerobically the following day in 5 ml Lysogeny Broth (LB) with the addition of 50 µg / ml kanamycin at 37 ºC for several hours in 30 ml polystyrene universal tubes (Sterilin®), with shaking at 220 rpm in an Innova 2000 shaker (New Brunswick Scientific Ltd.). LB medium for both agar plates and liquid growth was prepared as described in Table 2.2.2-1.

Once the OD reached 0.8 – 1 at 600 nm, the 5 ml starting culture was transferred into a 2 L flask containing auto-induction medium (Table 2.2.3-1). All the solutions that were used for preparing the auto-induction medium are described in Table 2.2.3-2 and Table 2.2.3-3. The flask was then incubated at 30 ºC overnight, shaking at 180 rpm with a Lab-Shaker (Adolf Kühner AG Schweiz). The auto-induction medium was used for over expressing the putative protein NMV_1164, following the method of Studier *et al*. (Studier, 2005).

Table 2.2.3-1: Preparation of the auto-induction medium.

The auto-induction medium was prepared just prior to inoculation with *E. coli* BL21 (DE3) starter culture. Solutions 2-5 and the Trace Metals mixture 1000 x were added into the 2 L flask containing Solution 1.

Auto-Induction Medium (1 x)	**Stock concentration**	**Final concentration**
Solution 1 (ZY Medium 1 x)	590 ml	1 x
Solution 2 (NPS 20 x)	31 ml	1 x
Solution 3 (50x52 50 x)	12.5 ml	1 x
Solution 4 ($MgSO_4$ 1000 x)	630 µl	1 x
Trace Metals 1000 x	630 µl	1 x
Solution 5 (Kanamycin 1000 x)	630 µl	1 x

Table 2.2.3-2: Preparation of Solutions 1-5 for the auto-induction medium.
All stock solutions were stored at room temperature, except for the 50 mg / ml kanamycin solution (Solution 5), which was stored at -20 ºC.

	Chemicals used	Stock concentration	Final concentration
Solution 1 ZY Medium (1x)	Tryptone (Formedium™)	10 g / L	1 x
	Yeast Extract (Formedium™)	5 g / L	1 x
	Dissolved in 590 ml of deionised H_2O, stirred at room temperature for 10 minutes in 2 L flasks prior to autoclaving		
Solution 2 NPS (20x)	$(NH_4)_2SO_4$ (Fisher Scientific)	0.5 M	25 mM
	K_2HPO_4 (Fisher Chemical)	0.78 M	40 mM
	Dissolved in deionised H_2O, stirred at room temperature for 10 minutes prior to autoclaving		
Solution 3 50x52 (50x)	Glycerol (Fisher Chemical)	25 % (w / v)	0.5 % (w / v)
	Glucose (Fisher Scientific)	0.14 M	2.8 mM
	α-Lactose monohydrate (Sigma-Aldrich®)	0.28 M	5.6 mM
	Dissolved in deionised H_2O, stirred at room temperature for 10 minutes prior to autoclaving		
Solution 4 $MgSO_4$ (1000x)	$MgSO_4 \cdot 7H_2O$ (Sigma-Aldrich®)	1 M	1 mM
	Dissolved in deionised H_2O, stirred at room temperature for 10 minutes prior to autoclaving		
Solution 5 (1000x)	Kanamycin (Sigma-Aldrich®)	50 mg / ml	50 µg / ml
	Dissolved in deionised H_2O and stored at -20 ºC		

Table 2.2.3-3: Preparation of the Trace Metals mixture (1000 x).

Solution 2: the compound was dissolved in ~ 0.1 M HCl and filter sterilised. Solutions 3-11: each stock solution was prepared by dissolving the specific compound in deionised H_2O and then autoclaved. All solutions were stored at room temperature. The combined Trace Metals mixture 1000 x was prepared by adding the required volume of each solution in ascending order, to avoid precipitation, and was stored at room temperature.

	Chemicals used	**Volume**	**MW**	**1 x concentration**
1	deionised autoclaved H_2O	18 ml	-	-
2	0.1 M $FeCl_3$ (Sigma)	25 ml	162.21	50 µM Fe
3	1 M $CaCl_2 \cdot 2H_2O$ (Fisher Scientific)	1 ml	147.02	20 µM Ca
4	1 M $MnCl_2 \cdot 4H_2O$ (BDH Laboratory Supplies)	0.5 ml	197.91	10 µM Mn
5	1 M $ZnSO_4 \cdot 7H_2O$ (FSA Laboratory Supplies)	0.5 ml	287.56	10 µM Zn
6	0.2 M $CoCl_2 \cdot 6H_2O$ (Aldrich®)	0.5 ml	237.95	2 µM Co
7	0.1 M $CuCl_2 \cdot 2H_2O$ (Sigma)	1 ml	170.49	2 µM Cu
8	0.2 M $NiCl_2 \cdot 6H_2O$ (Sigma-Aldrich®)	0.5 ml	237.72	2 µM Ni
9	0.1 M $Na_2MoO_4 \cdot 2H_2O$ (Sigma-Aldrich®)	1 ml	241.98	2 µM Mo
10	0.1 M $Na_2SeO_3 \cdot 5H_2O$ (Fluka)	1 ml	263.03	2 µM Se
11	0.1 M H_3BO_3 (Fisher Scientific)	1 ml	61.83	2 µM B

2.2.4 Growth of *Neisseria meningitidis*

N. meningitidis strain MC58, which was kindly donated by Prof. Robert Read from the University of Sheffield, was used as wild-type control and as source of genomic DNA for mutant strain constructs. Its complete genome has been sequenced, published and annotated (Tettelin *et al.*, 2000).

MC58 *NMB0240::Spec^R*, *prpC::Spec^R*, *NMB0432::Spec^R*, *NMB0432::Tet^R*, *NMB0435::Spec^R*, *NMB0468::Spec^R*, *NMB1048::Spec^R*, *NMB1049::Chl^R* *NMB1049::Spec^R* gene knockout mutant strains and the double mutant *NMB0432::Tet^R-NMB1048::Spec^R* were generated in this study. All liquid handling steps were carried out inside a Category 2 flow hood to ensure aerosols of the bacteria were not released into the open air.

All *N. meningitidis* stocks, stored at -80 ºC, were streaked on Columbia Blood Agar Base plates (CBA) and incubated at 37 ºC overnight in a 5 % CO_2 atmosphere in order to enhance bacterial growth, as described by Heurlier (Heurlier *et al.*, 2008). CBA plates were prepared by adding 5 % Defibrinated Horse Blood (TCS biosciences) to cooled molten Columbia Agar Base (Oxoid) at 50 ºC. 20 ml of this suspension was poured into each 85 mm diameter plastic Petri dish (Sterilin®).

Liquid cultures of plated *N. meningitidis* were grown in Mueller Hinton Broth (MHB) (Oxoid) or in Chemically Defined Medium (CDM) modified from the method described by Catlin (Catlin & Schloer, 1962). MHB was prepared as recommended by the manufacturer and CDM was prepared as described in Table 2.2.4-1. Both media where supplemented with 10 mM $NaHCO_3$ prior to incubation. Liquid cultures were routinely grown from a starting OD reading of 0.05 at 600 nm.

Cultures were grown in triplicates in 30 ml polystyrene universal tubes (Sterilin®) under aerobic conditions in a total volume of 15 ml of medium, and were shaken at 200 rpm at 37 ºC in a microbial C25KC incubator shaker (New Brunswick Scientific Ltd.) over a 24h period. Growth in the presence of propionic acid was induced by the addition of propionic acid (Sigma-Aldrich®) to a final concentration of 5 mM into the 15 ml media prior to incubation.

Table 2.2.4-1: Composition of the Chemically Defined Medium (CDM).
All stock solutions were stored for up to one month at room temperature, except for solution 4b, which was stored for an indefinite period at 4 ºC. The final CDM solution was prepared by addition of stock solutions 1, 2, 3, 4a or 4b, and 5 to autoclaved deionised H_2O just prior to growth of liquid culture. The pH of the final medium was checked and eventually adjusted to be between 7 and 7.5. Solution 6 was only added to some of the cultures.

CDM	Chemicals used	Stock concentration	Final concentration
Solution 1 (Fe sol.) (40x)	$MgCl_2$ (Sigma-Aldrich®)	78 mM	1.95 mM
	$CaCl_2$ (Sigma-Aldrich®)	8.15 mM	0.20 mM
	Ferric citrate (Sigma-Aldrich®)	6.5 mM	0.15 mM
	Dissolved in deionised H_2O, stirred at 50 ºC for 3h approx., pH adjusted to 7 and filter sterilised		
Solution 2 (salts sol.) (20x)	NaCl (Sigma-Aldrich®)	2 M	100 mM
	K_2SO_4 (Sigma-Aldrich®)	114.8 mM	5.75 mM
	K_2HPO_4 (Sigma-Aldrich®)	460 mM	23 mM
	NH_4Cl (Sigma-Aldrich®)	360 mM	18 mM
	Dissolved in deionised H_2O, stirred at room temperature for 10 minutes prior to autoclaving		

CDM	Chemicals used	Stock concentration	Final concentration
Solution 3 (aa sol.) (20x)	Glycine (Sigma-Aldrich®)	75.6 mM	3.8 mM
	L-cystine (Sigma-Aldrich®)	8.3 mM	0.4 mM
	L-arginine (Sigma-Aldrich®)	14 mM	0.7 mM
	L-glutamine (Sigma-Aldrich®)	80 mM	4 mM
	L-serine (Sigma-Aldrich®)	95 mM	4.75 mM
	Dissolved in deionised H_2O with the addition of a few drops of NaOH, stirred at 40 ºC for 1 hour and filter sterilised		
Solution 4a (224x)	Glucose (Sigma-Aldrich®)	560 mM	2.5 mM
	Dissolved in deionised H_2O, stirred at room temperature for 10 minutes prior to autoclaving		
Solution 4b (40x)	Na pyruvate (Sigma-Aldrich®)	200 mM	5 mM
	Stirred at room temperature for 30 minutes and filter sterilised		
Solution 5 (100x)	$NaHCO_3$ (Sigma-Aldrich®)	1 M	10 mM
	Dissolved in deionised H_2O, vortexed until complete dissolution of sodium bicarbonate and filter sterilised		
Solution 6 (200x)	Propionic acid (Sigma-Aldrich®)	1 M	5 mM
	Dissolved in deionised H_2O, then adjusted to pH 7 prior to filter sterilisation		

Occasionally, liquid cultures of *N. meningitidis* MC58 were grown in an enriched medium. When this was case, bacteria were grown in MHB and CDM media as described above, but with the addition of amino acids or Vitox. The pH of each medium was adjusted to between 7 and 7.5 prior to the start of the growth. Amino acids stock solutions were prepared fresh on the day by dissolving each amino acid separately in deionised H_2O to 100 mM (making a 20 x stock), and then by filter

sterilising them with a 0.22 μm filter (Millipore). To help dissolving the amino acids, a few drops of concentrated HCl were usually needed. 2.5 ml of the desired amino acid stock solutions were added into the growth medium to obtain a final 5 mM (1 x) concentration, except for L-cysteine hydrochloride in all media and L-tyrosine in CDM medium, where only 0.5 ml were added to achieve a final 1 mM concentration. At 5 mM, in fact, *N. meningitidis*' growth with these two amino acids was severely impaired. Some amino acids were used together, whilst others were used singularly, as follows: 1: L-alanine, L-isoleucine, L-leucine, L-methionine, L-valine. 2: L-phenylalanine, L-tryptophan. 3: L-aspartic acid, L-glutamic acid. 4: L-lysine, L-proline. 5: L-asparagine. 6: L-cysteine hydrochloride. 7: L-threonine. 8: L-histidine. 9: L-tyrosine. std (standard amino acids solution): same amino acids and concentrations as in Solution 3 in the Table above. All amino acids were supplied from Sigma-Aldrich®.

Commercial Vitox (Oxoid) was used to enrich growth media at the concentration recommended by the supplier. It came into two separate vials, one containing a concentrate of essential lyophilised growth factors, whose final concentration in the growth medium is detailed in Table 2.2.4-2, and the other containing 0.55 M glucose dissolved in 10 ml of distilled water, which was needed to dissolve the lyophilised growth factors. Final concentration of glucose into the growth medium was 11.10 mM, as the commercial Vitox was made to supplement 500 ml of growth medium. The content of the two vials was mixed aseptically, and was ready for use on the day or was stored at – 20 ºC in single use aliquots. Laboratory Vitox was prepared by dissolving the 11 separate solutions in deionised water to a stock concentration of 100 x. Serial dilutions were occasionally made, but the stock concentration was always 100 x. 500 μl of each component were then added into a 50 ml final volume

of growth medium to give the desired 1 x concentration. The pH of the final medium was checked and eventually adjusted to be between 7 and 7.5.

Table 2.2.4-2: Composition of Vitox.

Commercial Vitox was aseptically diluted on the day of use with its hydration fluid (made of distilled water and 0.55 M glucose). Laboratory Vitox was prepared fresh on the day by dissolving the same components present in Vitox to 100 x with deionised H_2O and with the occasional addition of a few drops of concentrated HCl to help dissolution. Each solution was filter sterilised with a 0.22 μm filter (Millipore). All chemicals were from Sigma-Aldrich® except p-Aminobenzoic acid (ICN Biochemicals Inc) and commercial Vitox (Oxoid).

	Vitox Components	**Final concentration (1x)**
1	Vitamin B_{12}	0.148 nM
2	L-glutamine	1.37 mM
3	Adenine	150 nM
4	Guanine	3.97 nM
5	p-Aminobenzoic acid (PABA)	1.90 nM
6	L-cystine	91.55 nM
7	NAD (Coenzyme 1)	7.54 nM
8	Cocarboxylase	4.34 nM
9	Ferric nitrate	0.99 nM
10	Thiamine	0.20 nM
11	L-cysteine hydrochloride	3.29 mM

2.2.5 Growth of *Veillonella* spp. for co-culture with *Neisseria meningitidis*

Veillonella spp. isolated from mouth washes by Dr. Stacey Fergusson (James Moir's lab) was used for co-culture growth experiments with *N. meningitidis*. Bacterial stock stored at -80 ºC was streaked on Columbia Blood Agar Base plates (CBA) and incubated at 37 ºC overnight, in a 5 % CO_2 atmosphere. CBA plates were prepared as explained in Section 2.2.4.

Liquid cultures of plated *Veillonella* spp. were grown in Chemically Defined Medium (CDM) with the addition of 5 mM sodium L-lactate instead of Solutions 4a or 4b. CDM was prepared as described in Table 2.2.4-1 and 1 M sodium L-lactate (Sigma) stock was prepared by dissolving the compound in deionised H_2O, then adjusting it to pH 7 prior to filter sterilisation and storage at 4 ºC. Liquid cultures were grown from a starting OD reading of 0.05 at 600 nm. Cultures were grown in triplicates in 30 ml polystyrene universal tubes (Sterilin®) under aerobic conditions in a total volume of 20 ml of medium, and were shaken at 200 rpm at 37 ºC in a microbial C25KC incubator shaker (New Brunswick Scientific Ltd.) over a 32h period. Growth in the presence of *N. meningitidis* was achieved by mixing 10 ml of *Veillonella* spp. with an OD reading of 0.1 at 600 nm, with 10 ml of *N. meningitidis* strain MC58 with an OD of 0.1.

2.2.6 *Ex vivo* growth of *Neisseria meningitidis* in human whole blood

Human venous blood was collected from seven healthy adult volunteers (four females and three males) following Echenique-Rivera's studies (Echenique-Rivera *et al.*, 2011). An anti-coagulant agent, heparin, was instantly mixed in the blood at a concentration of 17 U / ml. Samples were obtained from Wayne Burrill, University

of Bradford, the morning subsequent to collection. *N. meningitidis* MC58 wild-type, *prpC::Spec*^{R} and *NMB1049::Spec*^{R} mutants were grown on CBA with 5 % Defibrinated Horse Blood (TCS biosciences) plates at 37 ºC overnight in a 5 % CO_2 atmosphere with the method described by Heurlier (Heurlier *et al.*, 2008). A few colonies for each strain were inoculated the following day into fresh MHB supplemented with 10 mM $NaHCO_3$ in 30 ml polystyrene universal tubes (Sterilin®), and grown under aerobic conditions in a total volume of 15 ml of medium. These were shaken at 200 rpm at 37 ºC in a microbial C25KC incubator shaker (New Brunswick Scientific Ltd.) for few hours until they reached an OD at 600 nm of about 0.3, which corresponded to approximately 3 x 10^8 bacteria / ml; this meant that the bacteria had entered the early log phase. Bacteria were consequently diluted to approximately 10^6 or 2 x 10^6 CFU / ml into fresh MHB containing 10 mM $NaHCO_3$ and 10 µl of these suspensions were inoculated in triplicates into 190 µl of 100 % human whole blood, resulting in a starting experimental concentration of between 50000 and 100000 CFU / ml. Whole blood infected with bacteria was then incubated over a period of two hours in a 96-Well Optical Reaction Plate (Applied Biosystems) at 37 ºC with shaking at about 110 rpm to avoid red blood cells sedimentation. At each predetermined time point (0, 30, 60, 90 and 120min), 20 µl of every sample were removed and spread onto CBA plates. The number of viable bacteria was determined by CFU counts by plating serial dilutions onto CBA plates and incubating at 37 ºC in a 5 % CO_2 atmosphere overnight, and was expressed as CFU / ml. Colony growth was checked again four days after incubation. Bacteria survival was determined by comparison of the viable count at the different time points with the control time 0, where survival rate corresponded to 100 %.

2.2.7 Bacterial growth curves

Neisseria meningitidis growth studies were conducted in MHB or CDM liquid media supplemented with 10 mM $NaHCO_3$, but without addition of the selective antibiotic, under aerobic conditions as described in Section 2.2.4. The cultures were incubated at 37 ºC in a microbial C25KC incubator shaker (New Brunswick Scientific Ltd.) at 200 rpm, and growth was monitored by measuring the increase in optical density at 600 nm in disposable 1.5 ml cuvettes (Kartell Labware) with a Jenway 6305 Spectrophotometer (Jenway). Samples were typically diluted two to four fold with the corresponding growth medium not to compromise the cultures' volume, as many measurements were taken by the end of each growth curve. Experiments were conducted in triplicate and repeated on several occasions.

2.2.8 Preparation of *E. coli* cell stocks

E. coli DH5α wild-type and mutant strains generated in this study were grown on standard or selective LB agar plates at 37 ºC overnight. Liquid cultures were grown in LB liquid medium containing the relative antibiotics at 37 ºC overnight, shaking at 220 rpm in an Innova 2000 shaker (New Brunswick Scientific Ltd.). The cells were then harvested for stocks preparation: 500 µl growth cultures were mixed with 500 µl 50 % LB / 50 % glycerol solution into sterile 1.5 ml Eppendorf tubes (Sarstedt), and the 1 ml bacterial stock aliquots were stored at -80 ºC. 10 µl were subsequently taken from each newly prepared -80 ºC stock solution and spread on LB +/- antibiotics plates to check for purity or contaminations prior to further use.

2.2.9 Preparation of wild-type and mutant *N. meningitidis* cell stocks

All *N. meningitidis* strains were grown on CBA plates without addition of antibiotics at 37 ºC overnight, in a 5 % CO_2 atmosphere. Liquid cultures were then grown at 37 ºC for several hours to late exponential phase in MHB supplemented with 10 mM $NaHCO_3$ and the corresponding antibiotic, shaking at 200 rpm in a microbial C25KC incubator shaker (New Brunswick Scientific Ltd.). 1 ml bacterial stock aliquots were then prepared by mixing 500 µl of growth cultures to 500 µl of 50 % MHB / 50 % glycerol solution into sterile 1.5 ml Eppendorf tubes (Sarstedt), and were stored at -80 ºC. 20 µl were subsequently taken from each newly prepared -80 ºC stock solution and spread on CBA +/- antibiotics plates to check for purity, bacterial health or contaminations prior to further use.

2.2.10 Preparation of antibiotic selective media

For preparing selective media, antibiotics were directly added into cooled molten agars (at 50 ºC) or into liquid media. The final concentration of antibiotics used for *E. coli* and *N. meningitidis* is shown in Table 2.2.10-1.

Table 2.2.10-1: Antibiotic concentrations used in this work.

Antibiotic	*E. coli*	*N. meningitidis*
Chloramphenicol (Chl)	25 µg / ml	2 µg / ml
Tetracycline (Tet)	20 µg / ml	2.5 µg / ml
Kanamycin (Kan)	50 µg / ml	50 µg / ml
Spectinomycin (Spec)	50 µg / ml	50 µg / ml

2.3 Molecular techniques

2.3.1 Polymerase chain reaction (PCR)

The polymerase chain reaction (PCR) was used throughout this work for amplifying desired DNA fragments and for screening constructs.

Primers used for amplification and their relative nucleotide position within the *N. meningitidi*s MC58 genome following the annotated GenBank accession number AE002098.2 from NCBI (Tettelin *et al.*, 2000) are shown in Table 2.3.1-1. Primers were synthesised by Eurofins MWG Operon. Template DNA was obtained from *N. meningitidis* MC58 genomic DNA stock or from plasmid DNA, which were stored at -20 ºC. Colony DNA was obtained by slightly dipping a 10 µl micropipette tip into a single bacterial colony, and suspending it directly into the reaction mix.

A standard PCR mix was prepared with GoTaq® Flexi DNA Polymerase kit (Promega) and 10 mM dNTPs (Fermentas) as shown in Table 2.3.1-2. The PCR amplification was carried out using a Techne TC-3000 Thermal Cycler (Techne) and the program described in Table 2.3.1-3. Occasionally, the annealing temperature and extension time were changed depending on the primers used and PCR products length expected. When these changes occurred, they were annotated next to the specific experimental description. PCR products were then separated using agarose gel electrophoresis to check for amplification of correct fragment sizes (Section 2.3.7) and were eventually purified using the QIAquick PCR Purification Kit (QIAGEN) and a Sigma 1-13 microcentrifuge (Sigma), following the manufacturer's instructions.

Table 2.3.1-1: Primers designed for PCR amplification.

Primers labelling and nucleotide position refer to the annotated genome and the primer's relative position in the *N. meningitidis* MC58 (AE002098.2). bis: primers used only for colony pick PCR of the *prpC::Spec*^{R} mutant strain. prot: primers used for NMV_1164 protein work. Underlined red characters correspond to mismatches. Abbreviations used: for: forward; rev: reverse.

PCR Primer	Primer Sequence (5' → 3')	Nucleotide position
NMB0240-for	CAGAAAGGATGGATATAGTGAAC	244652-244674
NMB0240-rev	ACCCTTTCAGACGGCTAAATCCC	246167-246145
NMB0240bis-for	CTGTTTGATTTCTGCTGCTG	245187-245206
NMB0240bis-rev	CAGATAGGCACGTTCGATG	245481-245463
NMB0430prot-for	CCTTGTTTTCTTCTTGTCTG	440212-440231
NMB0430prot-rev	TCGGGCATCCCAATCCAATC	440341-440322
NMB0431-for	CCAAGCTTGTGTCGAAGCC	440942-440960
NMB0431-rev	TTTCAGACGGCCTTTCCAATAAGG	442631-442608
NMB0431bis-for	GCAACGATTTGAGCTATCGC	441488-441507
NMB0431bis-rev	GCATACAGAATCAGTGAAACG	441965-441945
NMB0432-for	TTCTCTGCCGTTTCCTACCAA	442351-442371
NMB0432-rev	ATGTCGGTTCTCCTGTGGAT	443559-443540
NMB0435-for	TTGACGTAGCATGGGTTTGC	448138-448157
NMB0435-rev	ACGCCCGAAATTCAAAATCC	450072-450053
NMB0468-for	CTTTTCAACACGACAGACGG	488122-488141
NMB0468-rev	GCTTCAGACGGCATATCCGATG	490079-490058
NMB1048-for	TTGAATATCCGGTTGAAGCC	1064359-1064378
NMB1048-rev	TGTTTGTATTGCAGCAGGGA	1066439-1066420
NMB1048prot-for	CCATTATGTTTTTCCATAAC	1065941-1065960
NMB1048prot-rev	GTTTTATTGCCTGTTTGGGC	1066070-1066051
NMB1049-for	AAACCGCAATCGAAATGCC	1065528-1065546
NMB1049-rev	CCGAATCCAAGATGCTTTGA	1067570-1067551
NMB1049prot-for	GCCCAAACAGGCAATAAAAC	1066051-1066070
NMB1049prot-rev	TGTGCAATCGAAATCTTTTAG	1066180-1066160

Table 2.3.1-2: PCR reactions used for template DNA and colony pick DNA.
Concentration of starting DNA was variable and depended on plasmid concentration or amount of colony picked. For template DNA 0.5 µl were always sufficient.

Reagent	Final concentration	Amount
5 x Green GoTaq® Flexi Buffer	0.5 x	5 µl
25 mM $MgCl_2$	1.5 mM	3 µl
10 mM dNTPs (each)	200 µM (each)	1 µl
sterile deionised H_2O	-	38 µl
100 µM Forward primer	2 µM	1 µl
100 µM Reverse primer	2 µM	1 µl
Template DNA (or colony pick from a plate)	-	0.5 µl (or tip dipped into the colony)
GoTaq® DNA polymerase	5 U / µl	0.5 µl
Final volume	-	50 µl

Table 2.3.1-3: Standard PCR thermal cycler program used in this work.
The standard program was run with the details entered in this table. The annealing temperature (*) and extension time (**) were occasionally changed depending on the primers used and PCR products length expected. The annealing temperature was derived from the oligonucleotides' melting temperature (T_m) and the extension length was approximated to 1 minute per kb of DNA to be amplified.

Thermal cycler step #	Thermal cycler program		Thermal cycler program
Step 1	Initial denaturation		95 ºC – 5min
Step 2	35 cycles	Denaturation	95 ºC – 30sec
		Annealing*	58 ºC – 30sec
		Extension**	72 ºC – 4min
Step 3	Final extension		72 ºC – 8min
End	Storage		16 ºC – ∞

2.3.2 pCR® -Blunt II- TOPO® cloning and transformation

Zero Blunt® TOPO® PCR Cloning Kit (Invitrogen™) was used for cloning the genes under study into the pCR®-Blunt II-TOPO® vector, which contains a kanamycin resistance cassette. The orientation of the inserted genes was not certain, as the procedure consisted of blunt end cloning, but was checked by sequencing.

Each cloning reaction, which was set up in a 1.5 ml Eppendorf tube (Sarstedt), was prepared by mixing 3.5 µl sterile deionised H_2O, 1 µl Salt solution, 1 µl Control PCR Product or purified PCR product, and 0.5 µl pCR®-Blunt II-TOPO® vector. This mixture was then incubated for 5 minutes at room temperature to allow ligation and was subsequently kept on ice until further use. Plasmid maps illustrating the possible expected ligations with the gene being investigated is shown in Figure 2.3.2-1. As the ligations were blunt ended, there was a 50 % chance that the gene was inserted in the opposite direction, but this would not affect my studies.

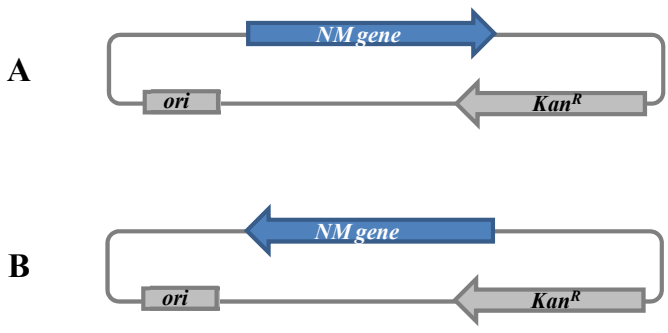

Figure 2.3.2-1: Plasmid map of the pCR®-Blunt II-TOPO® ligated with the gene being studied.
Plasmid map of the 3519 bp long pCR®-Blunt II-TOPO® vector (in gray) is shown with its relevant features (gray box and gray arrow) and with successful ligation of the gene under study (blue arrow). **A-B:** show the possible orientation of the inserted genes under investigation. *ori*: origin of replication. Kan^R: kanamycin resistance gene.

2.3.3 Transformation of *E. coli* strain DH5α

To introduce plasmid DNA into competent *E. coli* DH5α cells, an aliquot containing 50 µl of competent cells was quickly thawed on ice and added to the 6 µl cloning reaction prepared in Section 2.3.2. The reaction was then incubated on ice for 30 minutes, heat shocked at 42 ºC for 90 seconds and, finally, cooled on ice for 2 further minutes. After addition of 800 µl of LB liquid medium, the reaction was incubated at 37 ºC for 1 hour, shaking at 200 rpm in a SSL1 shaker (Stuart®). At this stage, the reaction was centrifuged at 13000 rpm for 60 seconds, and the harvested pellet was resuspended in 100 µl of fresh LB liquid medium, prior to plating on LB + 50 µg / ml kanamycin agar plates. Plates were then incubated at 37 ºC overnight. Only colonies with the newly acquired vector, containing the kanamycin resistance gene, were able to grow.

2.3.4 Isolation of plasmid DNA

In order to isolate plasmid DNA, transformed *E. coli* DH5α colonies were picked from the selective plate and grown in 8 ml of LB liquid medium in 30 ml polystyrene universal tubes (Sterilin®). Selective antibiotics were added into the growth medium to allow selection of cells containing the desired plasmid. Mini-preparations were grown aerobically with shaking at 220 rpm in an Innova 2000 shaker (New Brunswick Scientific Ltd.) at 37 ºC overnight. Cells were then harvested at 4500 rpm at 4 ºC for 10 minutes in an Allegra™ X-22R centrifuge (Beckman Coulter™), and plasmid DNA was extracted and purified using the QIApreparation Spin Miniprep Kit (QIAGEN) with a Sigma 1-13 microcentrifuge (Sigma), following the manufacturer's instructions. Purified plasmids were stored at -20 ºC until further use.

2.3.5 Preparation of pHP45Ω, tetracycline and chloramphenicol cassettes

pHP45Ω cassette from Prentki and Krisch (Prentki & Krisch, 1984), which conferred spectinomycin resistance, was prepared by plating 5 µl of the -80 ºC frozen stock of *E. coli* DH5α containing pHP45Ω on LB agar plates with 50 µg / ml spectinomycin. Plates were incubated at 37 ºC overnight, and mini-preps and plasmid purification were then carried out as explained in Section 2.3.4. The purified plasmid was digested with SmaI, as restriction sites for this enzyme were present at both ends of the 2 kb spectinomycin resistance cassette, as described in the next section.

Preparation of tetracycline resistance cassette, which conferred tetracycline resistance, was carried out by plating 5 µl of the -80 ºC frozen stock of *E. coli* DH5α containing the pCMT18 plasmid from Professor Christoph Tang, Imperial College London, on LB agar plates with 20 µg / ml tetracycline. This plasmid was obtained by Dr Karin Heurlier (Moir's lab). Plates were incubated at 37 ºC overnight, and mini-preps and plasmid purification were then carried out as explained in Section 2.3.4. The purified plasmid was digested with EcoRV, following Heurlier's method (Heurlier *et al.*, 2008), as restriction sites for this enzyme were present at both ends of the 2.5 kb tetracycline resistance cassette. Restriction digest is described in the next section.

Preparation of chloramphenicol resistance cassette, which conferred chloramphenicol resistance, was carried out by plating 5 µl of the -80 ºC frozen stock of *E. coli* DH5α containing the pST2 plasmid generated from Susan Turner (Turner *et al.*, 2003) on LB agar plates with 25 µg / ml chloramphenicol. Plates were incubated at 37 ºC overnight, and mini-preps and plasmid purification were then carried out as explained in Section 2.3.4. The purified plasmid followed standard PCR preparation

and amplification, as described in Section 2.3.1. The primers used were Chloram-for (AAGAATTGGAGCCAATCAATTC) and Chloram-rev (TACACTAAATCAGTA AGTTGGC), and were synthesised by Eurofins MWG Operon. The 2 kb chloramphenicol resistance cassette was excised from the gel, was purified, and was ready for ligation.

2.3.6 Endonuclease restriction digestion of DNA

Restriction enzymes were carefully chosen so that their restriction sites were present only in the genes investigated, and not in the pCR®-Blunt II-TOPO® plasmid to which they were ligated. All restriction digests were performed under the conditions recommended by the manufacturers' instructions. Standard restriction reactions were set up in a 0.5 ml Eppendorf tube (Sarstedt) and were prepared by mixing 12 µl sterile deionised H_2O, 5 µl purified plasmid DNA, 2 µl 10 x Restriction Buffer specific for the enzyme used, and 1 µl restriction enzyme. In a few occasions, when recommended by the manufacturer, 0.2 µl BSA 100 x (NEB) were added to the digests. Reactions were then usually incubated at 37 ºC for 2 hours, unless otherwise specified in the results chapters. When digests resulted in sticky end products, and needed filling of 5' overhangs to form blunt end DNA, 0.5 µl DNA polymerase I (Klenow) (NEB) and 0.5 µl dNTP 10 mM (each) (Fermentas) were added 30 minutes before the end of the incubation period. Double digests were carried out using the same standard restriction reactions just described, but with the additional 1 µl of the second restriction enzyme and in the NEB restriction buffer that gave the highest activity for both enzymes combined. Restriction enzymes and buffers used were from Promega and New England Biolabs®.

2.3.7 Agarose gel electrophoresis and DNA gel extraction

Agarose gel electrophoresis was used to estimate the size of DNA fragments following PCR (Section 2.3.1) or restriction digests (Section 2.3.6).

0.8 % agarose gel was routinely prepared by fully dissolving 0.48 g of agarose (Molecular Biology Grade, Melford) in 60 ml of 0.5 x TBE buffer in a microwave at full power for 1 minute. 0.5 x TBE buffer, also known as Tris / Borate / EDTA buffer, was prepared as shown in Table 2.3.7-1.

Table 2.3.7-1: Preparation of 0.5 x TBE buffer.
The medium was dissolved and stored at room temperature for several months.

Reagent	Final concentration	Amount
UltraPureTM Tris (Invitrogen™)	45 mM	54.5 g
Boric acid (Fisher Scientific)	45 mM	27 g
EDTA (Fisher Chemical)	1 mM	3.72 g
deionised H_2O	-	5 L

The molten agarose was cooled down at room temperature for a few minutes, then 7 µl SYBR® Safe DNA gel stain 10,000 x concentrate (Invitrogen™) were added, resulting in a final 1 x concentration of 1 mg / L which corresponds to 50 µg. The solution was mixed gently in order to avoid introducing too many air bubbles, and was immediately poured into a 10 cm wide and 11 cm long gel casting tray with a

comb. The tray was left to cool at room temperature for approximately 30 minutes, time needed for the gel to set. The gel tray was then placed into an electrophoresis tank and covered with 0.5 x TBE buffer. At this stage, 5 µl of each PCR sample was loaded directly onto the gel, as the 5 x Green GoTaq® Flexi Buffer used during the PCR already contained blue and yellow DNA loading dyes. The 20 µl DNA samples from the restriction digests, however, were mixed with 5 µl of the 5 x DNA loading buffer (YORBIO), before loading the full amount onto the agarose gel. One lane of 6 µl Q-Step 4 Quantitative DNA ladder (YORBIO) was also loaded on each gel to compare DNA band sizes. The gel was run at 100 V at room temperature for 60 to 90 minutes with a Power Pac 300 apparatus (BIO-RAD), then the DNA was visualised by UV illumination using the GeneGenius Bio Imaging System apparatus (Syngene) and the GeneSnap software. A digital picture was saved as a JPEG file.

Desired DNA fragments visualised on the agarose gel were excised from the gel using a clean scalpel and were placed into 1.5 ml Eppendorf tubes (Sarstedt). The DNA was then extracted using the QIAquick Gel Extraction Kit (QIAGEN), following the manufacturer's instructions.

2.3.8 Ligation of DNA fragments

Reactions for ligating the plasmids containing the genes under investigation with the chosen antibiotic resistance cassette were prepared by mixing together 5 µl gel extracted antibiotic resistance gene, 3 µl linearised gel extracted plasmid DNA, 1 µl T4 DNA Ligase Buffer 10 x (Promega) and 1 µl T4 DNA Ligase (Promega). Ligation reactions were incubated at room temperature overnight, and were then transformed into 50 µl *E. coli* DH5α competent cells by heat shock in the same way as described in Section 2.3.3. This time, however, each sample was plated onto LB

agar plates that contained both kanamycin and the antibiotic for the resistance cassette that has just been ligated to a final concentration described in Table 2.2.10-1. Ligations were incubated at 37 ºC overnight, then colonies were picked, mini-preparations were grown overnight, and plasmid DNA was purified as described in Section 2.3.4. Possible plasmid maps resulting from positive ligations are shown in Figure 2.3.8-1.

To check if the ligations worked, restriction digests with BamHI were performed by mixing 12 µl sterile dH_2O, 5 µl of the transformed plasmid, 2 µl Restriction buffer E 10 x (Promega) and 1 µl BamHI (Promega). The reactions were incubated at 37 ºC for 1 hour and then run on an agarose gel with also a control lane composed of 1.5 µl of the corresponding uncut plasmid. If the expected DNA fragment sizes were seen, the purified samples were sent for sequencing.

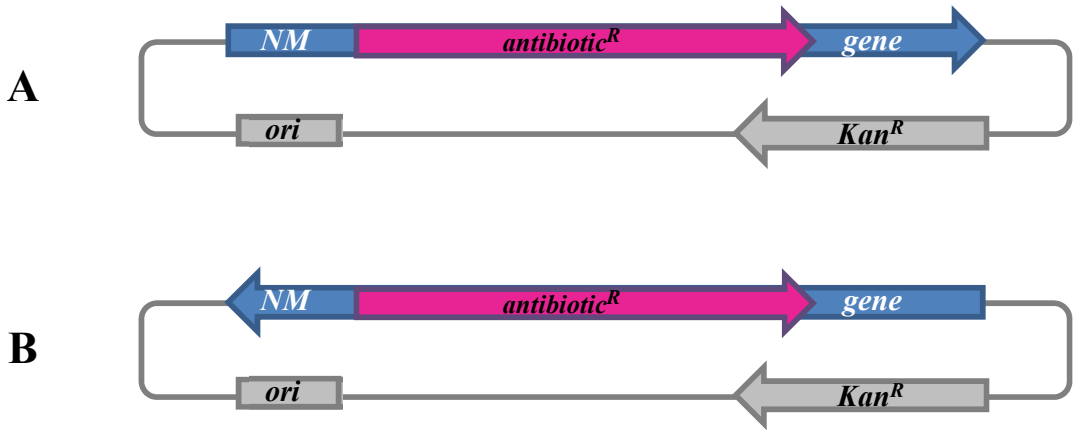

Figure 2.3.8-1: Plasmid map of the pCR®-Blunt II-TOPO® vector containing the gene under study disrupted with an antibiotic resistance cassette.
A-B: show the possible orientation of the inserted gene under investigation. The TOPO plasmid (gray) containing the gene under study (blue) was disrupted with an antibiotic resistance cassette (pink). The transformed plasmid contained cassettes for kanamycin and for the new antibiotic gene. *ori*: origin of replication. Kan^R: kanamycin resistance gene.

2.3.9 TSB transformation of *N. meningitidis* strain MC58

N. meningitidis MC58 is a naturally competent cell that actively uptakes DNA which is followed by homologous recombination with its own chromosome.

N. meningitidis MC58 wild-type was grown from -80 ºC frozen stocks on CBA plates at 37 ºC overnight in an atmosphere containing 5 % CO_2. Several colonies were used to inoculate an aerobic culture to a starting OD reading of 0.05 at 600 nm in 7.5 ml of MHB medium supplemented with 10 mM $NaHCO_3$ in a 30 ml polystyrene universal tube (Sterilin®). Cultures were grown at 37 ºC shaking at 200 rpm for approximately 5 hours, until they reached an OD reading of approximately 0.5 at 600 nm. Once reached the desired density, 2 ml of culture per transformation and for the control were harvested at 8000 rpm for 5 minutes in 2 ml Eppendorf tubes (Sarstedt) with a Sigma 1-13 microcentrifuge (Sigma). Cell pellets were subsequently resuspended in 200 µl ice cold Transformation and Storage Buffer (TSB) following Dr Melanie Thomson's protocol (which was adapted from Dr Willa Huston's method, personal communication, 2004), and were incubated on ice for 10 minutes. TSB was composed of MHB with 10 % PEG 4000, 10 mM $MgCl_2$, 10 mM $MgSO_4$, 5 % DMSO at a final pH of 6.5. This solution was filter sterilised with a 0.22 µm filter (Millipore) and stored in 1 ml single use aliquots at -80 ºC.

After the 10 minutes incubation, 10 µl of the purified plasmid DNA containing the disrupted copy of the gene under study was added into the cell suspension and was incubated on ice for 50 minutes in order to allow transformation into *N. meningitidis* MC58; for the control, no plasmid was added. For each transformation, 1.5 ml MHB medium with 10 mM NaHCO3 was pre-warmed into a 30 ml polystyrene universal tube (Sterilin®) for a few minutes. The transformation reaction then transferred into

the pre-warmed medium and cultured for 1.5 hours at 200 rpm at 37 ºC. Cells were harvested by centrifugation at 8000 rpm for 5 minutes and pellets resuspended in 100 µl fresh MHB medium, before being plated on CBA plates containing the antibiotic disrupting the gene under study. The control was split in half and plated on CBA plates with and without the selective antibiotic. Plates were incubated at 37 ºC overnight in an atmosphere containing 5 % CO_2. Mutant colonies were picked for both colony PCR and re-plating for overnight incubation on CBA plates containing the selective antibiotic. Several colonies per transformation were checked by PCR as described in Section 2.3.1. Re-plating was carried out because a double band, one for wild-type and one for the mutant, was often seen during PCR from the transformation plate. This was due to dead wild-type bacteria in the plate background. With re-plating the wild-type band disappeared from the agarose gel. If the PCR from the second plate resulted in the expected DNA fragment size, a stock solution was prepared and stored at -80 ºC.

2.3.10 Determination of DNA or RNA concentration

The concentration of the nucleic acids was measured using a NanoDrop® ND-1000 Spectrophotometer (Thermo Scientific), and was based on the absorbance at 260 nm, on the selected wavelength-dependent extinction coefficient for the nucleic acids and on a baseline correction at 340 nm. The extinction coefficients used were derived from a modified Beer-Lambert equation, resulting in 50 ng-cm / µl for double-stranded DNA (DNA-50) or 40 ng-cm / µl for RNA (RNA-40). After blanking the instrument with 1.2 µl Nuclease-Free dH_2O (Ambion®), 1.2 µl of the DNA or RNA sample was pipetted onto the spectrophotometer. The absorbance was then measured

and automatically converted into the final DNA or RNA concentration by the ND-1000 v3.7.1 software.

2.3.11 DNA sequencing and data analysis

The plasmid DNA to be sequenced was diluted to approximately 100 ng / µl with dH_2O and was then handed to the Technology Facility at the University of York for sequencing with an ABI3130xl Genetic Analyzer with a 16-capillary electrophoresis instrument and with the 3130xl Data Collection Software. Data was then analysed with the Sequencing Analysis version 5.2 software (Applied Biosystems). Data was finally exported to a word document with the Chromas version 1.41 Software, and was ready for analysis by BLAST.

Primers used for sequencing the full or disrupted genes transformed in the pCR®-Blunt II-TOPO® vector came with the cloning kit and were SP6: CGATTTAGGTGACACTATAG (forward primer) and T7: TAATACGACTCAC TATAGGG (reverse primer).

2.3.12 Preparation and purification of total RNA from *N. meningitidis*

Total RNA from wild-type and mutant strains of *N. meningitidis* MC58 was extracted for quantitative real-time PCR (RT-PCR) experiments.

Bacteria were incubated on CBA plates overnight, and then cultures were grown in MHB or CDM media for up to 12 hours. 1 ml of each sample was collected into a 1.5 ml Eppendorf tube (Sarstedt) at different time points and centrifuged for 5 minutes at 12000 rpm with a Sigma 1-13 microcentrifuge (Sigma). Due to the instability of

bacterial RNA, the pellet was stored immediately at -80 ºC, until the last sample was collected.

The following stock solutions were prepared prior to starting total RNA purification: Tris-EDTA Buffer 100 x (Sigma-Aldrich®) was diluted to 1 x with Nuclease-Free dH_2O (Ambion®) and stored at room temperature indefinitely. 10 mg / ml lysozyme stock solution was prepared by dissolving and filtering lysozyme Ultrapure (nuclease free) (usb®) kept at – 20 ºC in Nuclease-Free dH_2O (Ambion®), and was stored at – 20 ºC for several months. A stock solution of Buffer RLT / β-mercaptoethanol was prepared by mixing 10 µl of β-mercaptoethanol (Sigma-Aldrich®) per 1 ml of Buffer RLT (QIAGEN) and was stable for up to a month at room temperature.

From this point onwards, all steps of the procedure were performed at room temperature without interruption. The protocol followed for the next few steps was an adaptation of Protocol 1 (Enzymatic Lysis of Bacteria version 12/2005) (QIAGEN): frozen pellets were resuspended in 1 ml RNAprotect® Bacteria Reagent (QIAGEN) and incubated at room temperature for 10 minutes. During the incubation time, each sample was vortexed for 10 seconds every 2 minutes. The samples were then centrifuged for 5 minutes at 13000 rpm and the pellet was resuspended in 180 µl Tris-EDTA Buffer 1 x before adding 1 mg / ml lysozyme. At this stage, samples were incubated at room temperature for another 10 minutes and were vortexed for 10 seconds every 2 minutes again, after which 700 µl Buffer RLT / β-mercaptoethanol solution were added. The samples were vortexed briefly and, if a particulate material was visible, were centrifuged at 13000 rpm for 2 minutes and only the supernatant used. 500 µl ethanol 100 % were added to the lysed cells and mixed gently by pipetting, prior to transferring the lysate onto the spin-column provided with the

RNeasy® Mini Kit (QIAGEN). Total RNA was subsequently purified using the manufacturer's instructions for Protocol 7 (Purification of Total RNA from Bacterial Lysate Using the RNeasy Mini Kit version 12/2005) (QIAGEN) and with the optional on-column DNase digestion from Appendix B (Optional On-Column DNase Digestion Using the RNase-Free DNase Set version 12/2005) (QIAGEN).

The purified total RNA of each sample was quantified using a Nanodrop spectrophotometer as described in Section 2.3.10, and was then stored at -80 ºC, with the exception of the few µl that were needed to synthesise cDNA.

2.3.13 Preparation of cDNA

A cDNA copy of the total RNA was synthesised with the SuperScript™ II Reverse Transcriptase kit (Invitrogen™) according to the manufacturer's instructions. Each reaction was set up in a 1.5 ml RNase-free Eppendorf tube (Sarstedt) using 1 µl Random Primers (500 µg / ml) (Promega), 1 µl 10 mM dNTP Mix PCR Grade (Invitrogen™) and 10 µl total RNA. On a few occasions the total RNA added was diluted with Nuclease-Free dH_2O (Ambion®), because its concentration was higher than the recommended concentration range of 1 ng - 5 µg. At this point, the reactions were incubated at 65 ºC for 5 minutes, and then quickly chilled on ice for 1 minute, prior to adding 4 µl of 5 x First-Strand Buffer, 2 µl 0.1 M DTT and 1 µl RNaseOUT™ Recombinant Ribonuclease Inhibitor (40 units / µl) (Invitrogen™). The reactions were incubated at 30 ºC for 2 minutes and, after addition of 1 µl SuperScript™ II RT (200 units), were incubated at 30 ºC for 10 further minutes, before increasing the temperature to 42 ºC and incubating for 1 hour and 50 minutes. At the end, the enzyme was inactivated by heating the reactions at 70 ºC for 15 minutes.

To remove RNA complementary to the cDNA, 0.5 µl RNase H (5000 units / ml) (New England Biolabs®) were added into these 20 µl reactions. cDNA was incubated at 37 ºC for 20 minutes, and RNase H was inactivated by heating the samples at 65 ºC for 20 minutes. The cDNA was finally stored at -20 ºC.

2.3.14 Quantitative Real-Time PCR (RT-PCR) and analysis of gene expression

Transcript levels of the target genes were measured by RT-PCR. The chosen target genes were those involved in the 2-methylcitrate pathway: *prpC* (*NMB0431*), a gene encoding a hypothetical protein (*NMB0432*), *acnD* (*NMB0433*), and *prpF* (*NMB0434*). A control gene involved in the citrate pathway (*gltA*) and two further putative genes (*NMB1048* and *NMB1049*) were also analysed. *metK (NMB1799)*, which encodes S-adenosylmethionine synthetase, was selected as an endogenous housekeeping gene because it is always expressed at the same level, independently of the different conditions in which wild-type or mutant *N. meningitidis* MC58 were grown. Differences in gene expression could therefore be compared between the different samples, and were not influenced by the amount of starting cDNA in the reactions.

Reactions for each well were prepared by mixing 12.5 µl *Power* SYBR® Green Mix 2 x (Applied Biosystems), 5.5 µl Nuclease-Free dH_2O (Ambion®), 5 µl diluted cDNA sample (0.1 x) and 2 µl primer pair mix (10 µM each). Primers for the desired target genes were designed using the Primer Express® Software for Real-Time PCR version 3.0 (Applied Biosystems) and were synthesised by Eurofins MWG Operon. Primers are listed in Table 2.3.14-1.

Table 2.3.14-1: Primers designed for RT-PCR amplification.

Nucleotide position refers to the primer's relative position in the *N. meningitidis* MC58 genome (AE002098.2). Abbreviations used: for: forward; rev: reverse. *: primers used only for PCR amplification of the intergenic region between two adjacent genes, and not for RT-PCR.

RT-PCR Primer	Primer Sequence (5' → 3')	Nucleotide position
RT-NMB0428-for*	GCCCGCCCTGCTTTATGT	439543-439560
RT-NMB0428-rev*	CGTCATATCGTCCCAATCAATATC	439612-439589
RT-NMB0430-for*	GCCGTGAAAGAATCGAATCC	440460-440479
RT-NMB0430-rev*	TGGCCAATCGTGCAAAATAA	440526-440507
RT-NMB0431-for	GCCATGCACGTTTCACTGAT	441937-441956
RT-NMB0431-rev	CGCGGGCGGTAAAGGTA	442003-441987
RT-NMB0432-for	TGCAATCTTGGTTCGCTATCG	443247-443267
RT-NMB0432-rev	CCATCGTTGCCGCAATC	443316-443300
RT-NMB0433-for	CGCCCGTCGTCCAAGTC	444114-444130
NMB0433b-for*	AGGCTTCGAGCGTATCCAC	445870-445888
RT-NMB0433-rev	TGAGTCAGTACCGACGCAGGTA	444175-444154
RT-NMB0434-for	AGCTCGACGGCGTAACGT	447445-447462
RT-NMB0434-rev	CGTCGGCTGGATCAAGAAAT	447507-447488
RT-NMB0435-for*	CGCATGATTATTGCCCACTTAG	449150-449171
RT-NMB0435-rev*	GACGGATTTGCCGTTTTTGA	449215-449196
RT-NMB0436-for*	GAAGACGGCGAACCATTGA	450552-450570
RT-NMB0436-rev*	TCGACGGCGTGTTCCAA	450613-450597
RT-NMB0954-for	GCACGAGATGATTAGCGATCCT	967362-967383
RT-NMB0954-rev	GCGTTCCGAACCGGTATAAAG	967431-967411
RT-NMB1048-for	ACCCATCGCCACACACAAG	1064548-1064566
RT-NMB1048-rev	CAGTGCGCAATTAGGTTTCG	1064623-1064604
RT-NMB1049-for	GAAGCACCTGCACCAGTTTTG	1066812-1066832
RT-NMB1049-rev	GGGTAGTCGCACAAGATCTGTTT	1066880-1066858
RT-NMB1799-for	GCCTGCCAATACGCACAAG	1888530-1888548
RT-NMB1799-rev	GCGCAAGACCCAAAAGCA	1888598-1888581

Several 96-Well Optical Reaction Plates (Applied Biosystems) were run in an ABI 7000 Sequence Detection System Analyser (Applied Biosystems) for relative quantification, according to the manufacturer's instructions. Each sample was run in triplicates to avoid errors, and transcript levels were quantified using the ABI 7000 System Sequence Detection Software version 1.2.3. The software worked by quantifying the transcript levels of the cDNA using the threshold Cycle (C_T) method relative to the expression of the *metK* housekeeping gene.

2.3.15 Collection and handling of human saliva

Saliva fluid samples were collected from over 300 students by Professor Robert Read's group at the University of Sheffield. Participants rubbed their bottom gums with a sponge for 1 minute. The sponge was subsequently centrifuged at 1000 rpm for 5 minutes in order to collect the saliva sample. 100 µl of each supernatant was placed into a new Eppendorf tube and stored at - 80 ºC. Once all the samples were collected, they were promptly sent to me in dry ice thanks to Dr. Alice Deasy. These samples were stored at - 80 ºC upon receipt.

Once defrosted, all the samples were spun down for 1 minute at 13000 rpm in a Sigma 1-13 centrifuge (Sigma Laborzentrifugen GmbH) in order to get rid of any particulate present in the saliva, as this would ruin the gas chromatography column.

20 µl of the supernatant were mixed with 80 µl of 132 mM potassium phosphate (pH 3) in a 200 µl VerexTM Crimp-Top Vial (Phenomenex). At this point the samples were ready for being injected into the 6890 N Network GC system gas chromatograph (Agilent Technologies) for propionic acid measurements, as explained in Section 2.4.1.

2.4 Analytic chemistry techniques

2.4.1 Gas chromatography (GC)

Gas chromatography was used for separating the volatile propionic acid compound from the growth medium, so that the total concentration of propionic acid in the culture could be measured at any given time.

Bacteria were incubated on CBA plates overnight, and liquid cultures were grown as described in Section 2.2.4. 500 µl of each sample were collected at different time points over a period of 24 hours, centrifuged at 12000 rpm for 5 minutes with a Sigma 1-13 microcentrifuge (Sigma) and the supernatant was stored at -80 ºC until the last sample was collected. Each sample to be analysed was then mixed with 132 mM potassium phosphate (pH 3) as described in Section 2.3.15.

At this point, 0.5 µl of freshly acidified samples were sucked into a syringe, the syringe needle was positioned into a hot injector port of the 6890 N Network GC system gas chromatograph (Agilent Technologies), and the sample was injected. The injector was previously set to a temperature of 250 ºC, which corresponded to a higher temperature than the component's boiling point of 141 ºC, allowing it to be transformed into its gaseous phase inside the injector. Helium, a carrier gas, was then flowed through the injector at a constant flow of 2.2 ml / min in order to push all the components of the growth medium that were transformed into vapours onto the 150 ºC GC column (Alltech® AT-1000 Capillary Column), where partitioning of the components occurred. The detector was reached at different times, and this was due to variations in the separation between stationary and mobile phases. Signals were recorded with the GC ChemStation Rev. A.09.03 [1417] software (Agilent

Technologies) and resulted in peaks, whose area was relative to the number of molecules that were producing the signal. Graphs showing the area of propionic acid present in the samples measured at different time points were automatically drawn by the software. The area measured by the software was then converted to the actual concentration of propionic acid with the help of a standard curve.

A standard curve was established by comparing the areas of propionic acid measured by gas chromatography to the known amounts of propionic acid that had been previously added to each control sample. A $y = \alpha x + \beta$ equation was obtained, where α slope and β y-intercept values were automatically extrapolated by the excel software. The chromatograph values obtained for the area of propionic acid for each saliva sample were then applied to the graph's equation as the y values. The unknown x values, corresponding to the concentration of propionic acid in the sample, were derived from the equation and plotted in excel.

2.5 Protein techniques

2.5.1 Disruption of cells and preparation of soluble extract

After growing bacteria in auto-induction medium at 30 ºC in a Lab-Shaker (Adolf Kühner AG Schweiz) overnight, cells were harvested by centrifugation at 4500 rpm for 15 minutes at 4 ºC using a Sorvall 6000 (Sorvall® Evolution$_{RC}$, Kendro Laboratory Product) and then were resuspended in 30 ml HEPES Buffer A (Table 2.5.2-1). At this stage the cells could be stored at -20 ºC. After thoroughly thawing them, cells were sonicated for 2 minutes using a 10 seconds on/off cycle with a power output of approximately 70W using a Sonicator®3000 (Misonix), until the solution became homogenous. The solution was then transferred in a 35 ml

centrifuge tube and centrifuged at 48000 g at 4 ºC for 20 minutes using a Rotor JA-25.50 and an Avanti® J-26 XP Centrifuge (Beckman Coulter®). The supernatant was transferred in a 50 ml cellstar® tube (greiner bio-one) and was ready for protein purification.

2.5.2 Protein purification

Protein purification was achieved with a HisTrap HP 1 ml column (GE Healthcare), which was prepacked with the affinity medium Nickel Sepharose 6 Fast Flow, and an ÄKTAprime plus apparatus (Amersham Biosciences) and was performed at room temperature. Graphs were automatically plotted by the PrimeView™ 5.0 Software (GE Healthcare). Before connecting the 1 ml HisTrap column, the ÄKTAprime plus apparatus was carefully washed with water. The column was then primed with HEPES Buffer A binding buffer (Line 1) at a flow rate of 1 ml per minute for about 20-30 minutes until it was stabilised, then the 30 ml soluble fraction protein suspension prepared in Section 2.5.1 was run through the column (Line 8), and was followed by running HEPES Buffer A for about 25 minutes until the column was stable to elute non-specifically bound proteins. In order to elute the protein, an increasing gradient of HEPES Buffer B elution buffer (Line 2) was passed through the column until the final concentration of imidazole reached 1 M (corresponding to 100 % HEPES Buffer B). HEPES Buffer B was prepared as described in Table 2.5.2-1. The flow rate passing through the column was of 1 ml per minute for all the solutions, and the gradient was manually set as follows: set length = 40 ml; set target B (HEPES Buffer B) = 100 %; Fraction size = 5 ml; Buffer valve position left to Line A. 5 ml fractions containing the protein of interest, which were visualised with

a graph automatically plotted by the PrimeView 5.0 software, were collected and run on a 15 % SDS gel to verify that the protein of interest was there.

Table 2.5.2-1: Preparation of HEPES Buffer A and HEPES Buffer B.
The solutions were prepared fresh on the day and were filter sterilised. HEPES Buffer A was dissolved in 500 ml of deionised H_2O, whilst HEPES Buffer B was dissolved in 200 ml of deionised H_2O. The solutions were stirred at room temperature for 10 minutes prior to filter sterilising.

Chemicals used	HEPES Buffer A Final concentration	HEPES Buffer B Final concentration
HEPES, Free acid (Melford), pH 8.3	20 mM	20 mM
Imidazole (Sigma)	15 mM	1 M
β-Mercaptoethanol (Sigma)	3 mM	3 mM
NaCl (Fisher Scientific)	1 M	1 M
Glycerol (Fisher Chemical)	1 % (w / v)	1 % (w / v)

2.5.3 SDS-PAGE

To check that the correct protein was collected, a 15 % SDS-PAGE gel was run in 1 x SDS Buffer. The SDS-PAGE was prepared as described in Table 2.5.3-1. The Resolving gel Buffer was prepared by dissolving 1.5 M UltraPure™ Tris (Invitrogen™) at pH 8.8 and 0.4 % (w/v) SDS. The Stacking gel Buffer was made by mixing 0.5 M UltraPure™ Tris (Invitrogen™) at pH 6.8 and 0.4 % (w/v) SDS. The gel size was 6 cm long from the bottom of the wells, 8 cm wide and 1.0 mm thick,

and was cast between two Mini-Protean® System Glass Plates (BIO RAD). The 1 x SDS Buffer was composed of 25 mM UltraPure™ Tris (Invitrogen™), 125 mM Glycine (Fisher Chemical) and 1.75 mM SDS (Melford). Protein samples to be run were set up by mixing 10 µl of each elution of interest and the soluble fraction protein control with 5 µl 2 x SDS Loading Buffer containing 5 mM β-mercaptoethanol. Samples were heated for 5 minutes at 95 ºC in order to denature the protein and were then run with a lane containing 5 µl PageRuler™ Plus Prestained Protein Ladder (Thermo Scientific) on a 15 % SDS-PAGE using a Power PAC 300 (BIO RAD) at 30 A for 60 minutes at room temperature.

Table 2.5.3-1: Preparation of the 15 % SDS-PAGE gel.

The gel was usually prepared fresh on the day, but could be stored at 4 ºC for two days. Both Resolving gel and Stacking gel were mixed gently in order to avoid air bubbles slowing acrylamide polymerisation, and were prepared with an interval of 30 minutes to allow the Resolving gel to have fully polymerised in the gel plates before adding the Stacking gel.

Chemicals used	Resolving gel	Stacking gel
Deionised H_2O	2.4 ml	3.2 ml
Resolving gel buffer	2.5 ml	-
Stacking gel buffer	-	1.3 ml
Ultra Pure ProtoGel® 30 % (w / v) Acrylamide / 0.8 % (w / v) Bis-acrylamide stock solution (37.5 : 1) (National Diagnostics)	5 ml	0.5 ml
10% (w/v) APS (Sigma)	50 µl	25 µl
TEMED (Fluka)	8 µl	8 µl

2.5.4 Coomassie Staining of SDS gels

SDS gels were stained for about 40 minutes to 1 hour with Coomassie Brilliant Blue, then were quickly rinsed with water and destained for 1 to 2 hours until the protein bands were visible. During this process, the gels were rocking at 15 rpm with a Gyro-Rocker® STR 9 (BIBBY Stuart). Once the background was removed, the gel was quickly rinsed with water and the protein bands were visualised using the GeneGenius Bio Imaging System apparatus (Syngene) and a digital picture was saved as a JPEG file. Coomassie Brilliant Blue Stain was prepared by mixing 20 % Methanol (Sigma-Aldrich®) and 10 % Glacial Acetic acid (Fisher Scientific) in deionised water and then by adding 0.1 % (w/v) Coomassie Blue R350, following the method from Maniatis (Maniatis, 1989). SDS Destain solution was prepared by mixing 10 % Ethanol (Fisher Scientific) and 10 % Glacial Acetic acid (Fisher Scientific) in deionised water, and the solution was stored at room temperature for an indefinite time.

2.5.5 PD-10 Buffer exchange

A PD-10 Desalting Column (GE Healthcare) was used to buffer exchange the fractions that showed the presence of the correct protein band in the SDS gel, in order to prevent or delay precipitation of the protein of interest. In case of protein precipitation, the fractions were centrifuged at 4500 rpm at 4 ºC for 15 minutes using an Allegra™ X-22R (Beckman Coulter™) centrifuge. At this stage, the PD-10 column was equilibrated by running through approximately 25 ml Elution Buffer, followed by 2.5 ml of the supernatant of the chosen protein fraction that has just been centrifuged and by 3.5 ml Elution Buffer. These last 3.5 ml flow-through were collected, as they contained the protein. The Elution Buffer used was Binding Buffer

for half of the protein fraction and TBE 0.5 x for the other half of the fraction, as TBE was anticipated to make the protein more stable. The buffer-exchanged proteins were stored at 4 ºC overnight. Elution Buffer components are described in Table 2.5.5-1.

Table 2.5.5-1: Preparation of the Elution Buffers used for the PD-10 column.
Both Binding Buffer and TBE were dissolved in deionised H_2O, stirred at room temperature for 30 minutes and filter sterilised. These buffers were stored at room temperature for several months.

[Stock]	Chemicals used	Amount	Final conc (1 x)
Binding Buffer (1 x)	HEPES, Free acid (Melford), pH 7.9	0.30 g	2.5 mM
	NaCl (Fisher Scientific)	0.15 g	5 mM
	$MgCl_2$ (Fisher Scientific)	0.025 g	0.25 mM
[Stock]	**Chemicals used**	**Amount**	**Final conc (0.5 x)**
TBE (10 x)	UltraPure™ Tris (Invitrogen™)	54.5 g	45 mM
	Boric acid (Fisher Scientific)	27 g	45 mM
	EDTA (Fisher Chemical)	3.72 g	1 mM

2.5.6 Quantification with Bradford Assay and storage of proteins

The concentration of the purified and buffer-exchanged proteins was determined using a Quick Start™ Bradford Protein Assay (BIO RAD). This assay consisted of mixing 1 ml Quick Start ™ Bradford Dye Reagent, 1 x (BIO RAD), once warmed at room temperature, with 20 µl of the buffer-exchanged protein in disposable 1.5 ml

cuvettes (Kartell Labware). In order to mix thoroughly the two reagents, the cuvette was vortexed and then incubated at room temperature for about 5 to 10 minutes. The OD at 595 nm was measured with a Jenway 6305 Spectrophotometer (Jenway) against a blank, where the protein was replaced by deionised water.

The protein concentration was extrapolated from a standard curve of known concentration of Bovine Gamma Globulin, which had previously been plotted by replacing the 20 µl protein with several amounts of known Bovine Gamma Globulin 2 mg / ml (BIO RAD). Proteins were then stored as 500 µl aliquots at - 80 ºC.

2.5.7 Electrophoretic Mobility Shift Assay (EMSA) with DNA 130-mers

In order to determine if the protein under study interacts with specific sites in the DNA of *N. meningitidis*, an Electrophoretic Mobility Shift Assay (EMSA) was carried out using a native gel.

Primers for the promoter regions of the three genes under investigation were designed by Amie Williamson (James Moir's Lab), and are shown in Table 2.3.1-1 as NMB0430prot, NMB1048prot NMB1049prot. These primers were used for amplifying a region of 130 bp in length. PCR reactions and the program used were described in Section 2.3.1, but the extension time was decreased to 30 seconds and the final extension to 5 minutes. Agarose gels were prepared and run as described in Section 2.3.7 for 60 minutes, but a lower voltage of 80 V was used to get a sharper band separation. Band sizes were checked by applying 5 µl PCR products onto the gel and, if the size was correct, the PCR products were purified using the QIAquick PCR Purification Kit (QIAGEN) with a Sigma 1-13 microcentrifuge (Sigma). If multiple bands were seen, the entire PCR sample was loaded onto the gel and the

expected band was excised from the gel and DNA was purified. Concentrations of the purified promoter fragments were measured with a NanoDrop® ND-1000 Spectrophotometer (Thermo Scientific) and diluted to a concentration of 45 ng / µl with nuclease-free water (QIAGEN). The samples were then stored at -20 ºC.

Just before preparation of the protein samples to be loaded onto the native gels, a Bradford protein assay was carried out on the buffer-exchanged proteins stored into 0.5 x TBE buffer. Reactions were then prepared by mixing 5 picomoles of DNA to either a two-fold (10 picomoles) or a five-fold (25 picomoles) molar excess of the protein under study, to ensure that the protein was in excess and would saturate the promoter fragments. The DNA stock was diluted to a concentration of 45 ng / µl, and 10 µl were then used per reaction. This amount corresponded to 450 ng, which was converted to picomoles with the Life Science Calculator for DNA (http://calculators.mybiomath.com/nucleic_acid_calculators/convert-double-strand-dna-from-micrograms-to-picomoles/), where the parameters added were 130 bp as length of DNA and 0.45 µg as amount DNA. This resulted in approximately 5 picomoles of DNA added per reaction. The amount of the 6x His-tagged NMV_1164 protein to add was either 10 or 25 picomoles, and was calculated with the Life Science Calculator for Proteins (http://calculators.mybiomath.com/category/protein_calculators/). Parameters added to the calculator were 34.2 kDa protein size, and 10 or 25 picomoles protein amount, which resulted in 0.34 and 0.86 µg respectively. 100 µl of the protein were approximately diluted from 330 µg / ml to 100 µg / ml in 0.5 x TBE buffer. From the freshly made 100 µg / ml stock, 0.34 and 0.86 µg were needed, and these corresponded to 3.4 and 8.6 µl. To make up a reaction volume of 50 µl, with either 1 : 2 or 1 : 5 DNA to protein molar ratio, 10 µl of 45 ng / µl DNA were mixed with either 3.4 or 8.6 µl of the 100 µg / ml protein, 5.2

or 0 µl 0.5 x TBE buffer. 2 x Gel Shift Reaction buffer was mixed with an equal amount of DNA-protein solution, to obtain a final 1 x buffer concentration. 500 µl of 2 x Gel Shift Reaction buffer was prepared fresh by mixing 12 µl 1 M HEPES, 4 µl 1 M Tris, 2 µl 0.5 mM EDTA pH8, 5 µl 100 mM DTT, 60 µl 50 % (w / v) glycerol and 417 µl deionised H_2O, giving a 1 x final buffer concentration of approximately 24mM HEPES, 8 mM Tris, 2 µM EDTA pH8, 1 mM DTT, 6 % (w / v) glycerol. At this stage, 4 x Native PAGE Loading buffer was added to the reactions to a final 1 x concentration, and samples were incubated for 20 minutes at room temperature. 4 x Native PAGE Loading buffer was prepared with 100 ml 100 % (w / v) glycerol, 6.25 ml 1M Tris-HCl pH6.8, 0.375 ml 1% Bromophenol Blue dissolved in 100% Ethanol and 8.38 ml dH_2O. 30 µl of each reaction was loaded onto the EMSA gel. All the chemicals used in this section were provided by Fisher Scientific / Fisher Chemical and by Sigma-Aldrich®.

In order to resolve differences in mobility that might be caused by retardation of the 130-mers DNA due to DNA-protein interactions, a 12.5 % polyacrylamide gel was prepared instead of an agarose gel. The native gel was prepared with 0.5 ml filtered 50 % (w / v) glycerol (Fisher Chemical), 2 ml filtered 10 x TBE, 4.4 ml filtered deionised H_2O, 3.2 ml Acrylamide / Bis-acrylamide 40 % solution (19 : 1) (Sigma-Aldrich®), 150 µl 10 % (w / v) APS (Sigma) and 10 µl TEMED (Fluka). Solutions were filtered using a 0.45 µm filter (Millipore). The gel size was 6 cm long from the bottom of the wells, 8 cm wide and 1.0 mm thick, and was cast between two Mini-Protean® System Glass Plates (BIO RAD). Once set, the gel was pre-run for 30 minutes at 200 V in 0.5 x TBE running buffer and, after the 20 minutes incubation, 30 µl samples were loaded onto the gel, which was run for further 4 hours at 200 V

using a Power PAC 300 (BIO RAD). The gel was run at 4 ºC in order to prevent heating effects from disrupting the stability of the protein : DNA complex.

2.5.8 Sybr® Safe and Silver Staining of EMSA gels

The native gel was stained in 50 ml 0.5 x TBE with 5 µl SYBR® Safe DNA gel stain 10,000 x concentrate (Invitrogen™), giving the SYBR® Safe DNA gel stain 1 x solution a final concentration of 1 mg / L, which corresponds to 50 µg. The gel was subjected to gentle rocking at 15 rpm using a Gyro-Rocker® STR 9 (BIBBY Stuart) for about 30 minutes, and then rinsed with water. The DNA was visualised using the GeneGenius Bio Imaging System apparatus (Syngene) and the GeneSnap software, and a digital picture was saved as a JPEG file.

For an increased detection of the protein bands, a Silver Staining of the native gel was performed after SYBR® Safe DNA gel staining. The gel was rinsed with water and then immersed in fixing solution, which was composed of 50 % Ethanol (Fisher Scientific) and 10 % Glacial Acetic acid (Fisher Scientific) overnight at room temperature, whilst rocking at 15 rpm. The gel was subsequently stained with the ProteoSilver™ Silver Stain Kit (Sigma) by following the Technical Bulletin for PROT-SIL1 included within the kit. At the end, the gel was developed for about 4 to 5 minutes until the protein bands were clearly visible, before adding the ProteoSilver Stop Solution (Sigma). All these washes were performed whilst the gel was gently rocking. A picture of the gel was then taken with the GeneGenius Bio Imaging System apparatus (Syngene) and the GeneSnap software, and a digital picture was saved as a JPEG file.

2.5.9 Fluorescence Anisotropy

Fluorescence anisotropy was used to study the interactions between the protein NMV_1164 from *Neisseria meningitidis* strain 8013 and its potential binding sites within the promoter regions for *NMB0430*, *NMB1048* and / or *NMB1049*. Three potential binding sites for *NMB1048* were also checked for preferential binding of the protein. A negative control lacking a binding site for the protein, which was used for separate studies within the group, was designed by James Edwards (James Moir's Lab) and was tested for comparison.

Four complementary sets of primers for the promoter regions of all three genes were designed by Amie Williamson (James Moir's Lab), and are shown in Table 2.5.9-1. One oligonucleotide within each set contained a 5' hexachlorofluorescein (HEX^{TM}) label. Each 100 μM stock of complementary oligonucleotides, was mixed in an equimolar ratio and heated for 5 minutes to 95 ºC to denature secondary structures within the single stranded oligonucleotides, then cooled for 10 minutes to room temperature to allow the complementary strands to anneal. The resulting double stranded oligonucleotides, of 50 μM each, were further diluted to 0.5 μM with deionised filtered water.

Table 2.5.9-1: Primers designed for fluorescence anisotropy.

Nucleotide position refers to the primer's position relative to the starting codon of genes *NMB0430* and *NMB1048* in *N. meningitidis* MC58. NMB1048a-c refers to the intergenic regions between *NMB1048* and *NMB1049*. *NarP* was used as negative control. Underlined red letters correspond to mismatches. Yellow highlights indicate potential binding consensus. Abbreviations used: for: forward; rev: reverse. HEX: hexachlorofluorescein.

Primer	Primer Sequence (5' → 3')	Nucleotide position
HEX_NMB0430_ for	ATATCAATAAGATAATTTTCC	-135 / -115
NMB0430_ rev	GGAAAATTATCTTATTGATAT	-115 / -135
HEX_NMB1048a_for	CCAATCTTTTTTTTTGATAAC	113 / 133
NMB1048a_ rev	GTTATCAAAAAAAAAGATTGG	133 / 113
HEX_NMB1048b_for	ATCATCCGGAAAACTGATACA	135 / 155
NMB1048b_ rev	TGTATCAGTTTTCCGGATGAT	155 / 135
HEX_NMB1048c_ for	ACAATCCACCTAAAAGATTTC	194 / 214
NMB1048c_ rev	GAAATCTTTTAGGTGGATTGA	214 / 194
HEX_NarP_for (control)	ATTTATTGTAATTTTATTGCTGTC ATATTCATTAGAAGTATCATTTTA AGTTC	-
NarP_rev (control)	GAACTTAAAATGATACTTCTAAT GAATATGACAGCAATAAAATTAC AATAAAT	-

A fluorescence cuvette (Precision cells of Quartz Suprasil®, Hellma®) was prepared by mixing 976.4 µl 1 x binding buffer prepared in the previous sections (2.5 mM

HEPES Free acid pH 7.9, 5 mM NaCl, 0.25 mM $MgCl_2$) with 5 µl 1 M DTT, 6 µl 60 mg / ml acetylated BSA, 2.6 µl of 1 µg / ml DiDC (polydeoxyinosinic-deoxycytidylic acid) and 10 µl of 0.5 µM double stranded oligonucleotides, giving a final concentration of 0.98 x binding buffer (2.45 mM HEPES Free acid pH 7.9, 4.9 mM NaCl, 0.245 mM $MgCl_2$), 5 mM DTT, 360 µg / ml acetylated BSA and 0.0026 µg / ml DiDC and 5 nM each of the double stranded oligonucleotides. The method followed was adapted from James Edwards' protocol (Edwards *et al.*, 2012).

Fluorescence anisotropy measurements were carried out at 20 ºC using a FluoroMax-3 spectrofluorometer fitted with autopolarisers (Horiba Jobin Yvon). The excitation wavelength was set to 535 nm and the emission wavelength was set to 556 nm, with entrance and exit slits of 5 nm for both excitation and emission. The integration time was set to 0.1 seconds. The protein previously buffer-exchanged in 1 x Binding buffer (Section 2.5.5) was used, and anisotropy for 10 readings for each titration point was measured using the FluorEssence version: 3.0.0.19 software and Origin Version: 8.0951 (Horiba Jobin Yvon). Every time an aliquot of protein was added, the solution was mixed and left to equilibrate for 2 minutes before starting the new readings.

Chapter 3 - Defence against propionic acid toxicity in *Neisseria meningitidis*

3.1 Introduction

There are 9 conserved genetic islands which are found in all *Neisseria meningitidis* strains, but are absent from its closely related commensal *Neisseria lactamica*, as previously described in Section 1.7.2. One of these islands is involved in the putative metabolic 2-methylcitrate synthase pathway. This pathway is composed of several adjacent genes that are often referred to as the *prp* gene cluster (Horswill *et al.*, 2001). In *N. meningitidis* these genes still have putative functions, but these have been extrapolated by similarities with the gene sequences of other bacteria. The 2-methylcitrate cycle is used by several bacteria to oxidise a short chain fatty acid, propionic acid, to propionyl-CoA and to the pathway's end-products pyruvate and succinate (Garvey *et al.*, 2007).

In this chapter, several genes that are associated with the 2-methylcitrate synthase pathway will be investigated.

3.2 The *prp* operon

The 2-methylcitrate cycle is used by several bacteria to catabolise propionic acid, a short chain fatty acid, to the end-products of this pathway, which are pyruvate and succinate (Garvey *et al.*, 2007, Grimek & Escalante-Semerena, 2004) as shown in Figure 3.2-1. This pathway is needed to support bacterial growth in the presence of propionic acid or to limit toxicity of this compound to the cell, and is catabolised by

several enzymes clustered together, the *prp* gene cluster (Brämer & Steinbüchel, 2001), which form an operon (Upton & McKinney, 2007). These enzymes, however, may vary structurally between the different microorganisms, and their different organisations are shown in Figure 3.2-2. In *N. meningitidis* these enzymes still have a putative function.

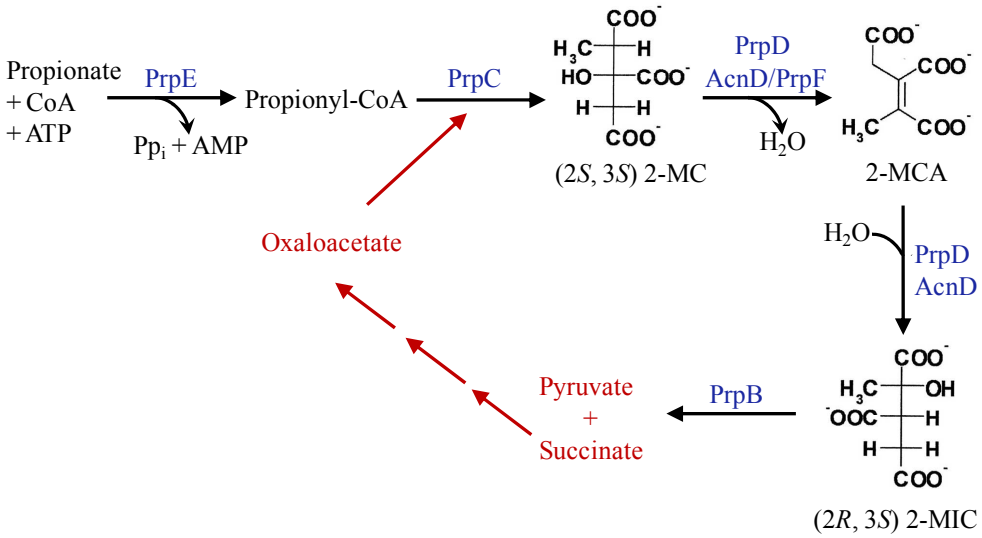

Figure 3.2-1: The 2-methylcitrate pathway with its intermediates.

The 2-methylcitrate pathway (black) is shown with its substrate, propionic acid. Propionic acid is oxidised to the end-products succinate and pyruvate with the help of pathway-specific enzymes (blue), and these products are both needed in the tricarboxylic acid cycle (TCA cycle) (red). Oxaloacetate, derived from the TCA cycle, enters the 2-methylcitrate cycle and is needed to break down propionyl-CoA into the pathway-specific compound 2-methylcitrate. The gene encoding PrpE is not present in all bacteria. Some bacteria possess the gene encoding PrpD, whereas in others *prpD* is replaced by *AcnD* and *prpF*. Abbreviations used: 2-MC: 2-methylcitrate. 2-MCA: 2-methyl-*cis*-aconitate. 2-MIC: 2-methylisocitrate (Figure adapted from Garvey *et al.*, 2007 and Grimek & Escalante-Semerena, 2004).

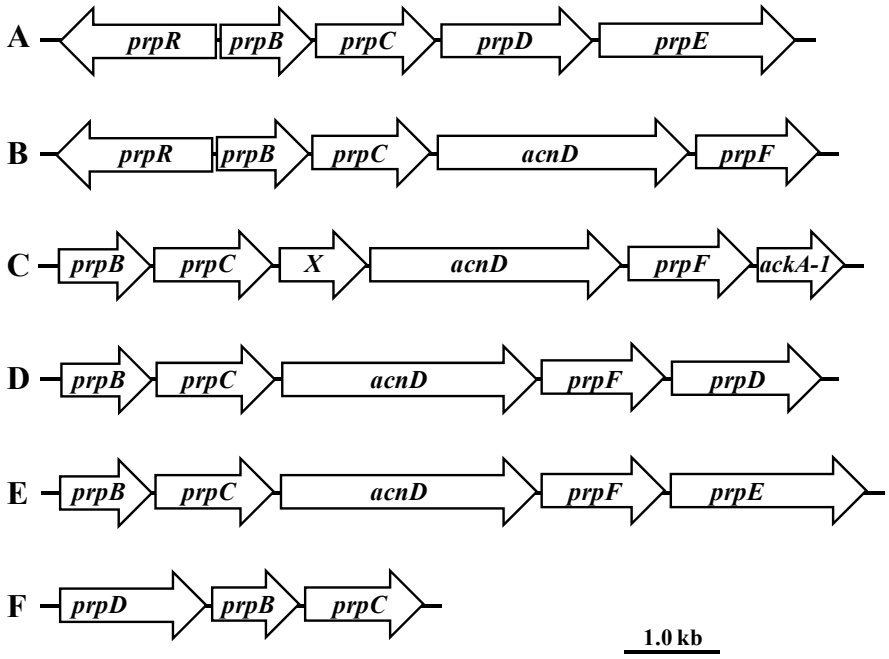

Figure 3.2-2: Comparison of the structural variations of the *prp* operon in several bacteria.

A: *Salmonella enterica* serovar Typhimurium, *Escherichia coli*. **B:** *Ralstonia eutropha* CH34, *Shewanella oneidensis*. **C:** *Neisseria meningitidis* and *Neisseria gonorrhoeae*. "*X*": gene encoding a putative hypothetical protein. **D:** *Ralstonia eutropha* HF39, *Bordetella pertussis*, *Pseudomonas aeruginosa*, *Pseudomonas putida* KT2440. **E:** *Vibrio cholerae*. **F:** *Corynebacterium glutamicum* (Figure adapted from Grimek & Escalante-Semerena, 2004).

Several studies have been carried out in order to verify the function of the genes belonging to the *prp* gene cluster in several organisms, but this has not yet been followed up with *N. meningitidis*. The *prpB* and *prpC* genes have been found to encode for enzymes that are specific to the 2-methylcitrate pathway, and are therefore always found adjacent to each other in all bacteria that have this pathway. *prpB* encodes the 2-methylisocitrate lyase (PrpB) (Grimek *et al.*, 2003) and *prpC* encodes the 2-methylcitrate synthase (PrpC) (Horswill & Escalante-Semerena,

1999b). The *prpD* gene encodes for the Fe/S-independent 2-methylcitrate dehydratase (PrpD) (Horswill & Escalante-Semerena, 2001), but it is not always present in the *prp* gene cluster, as it is often replaced by two less specific enzymes that have overlapping activities. These two enzymes are encoded by the genes *acnD* (translating into aconitate hydratase) and *prpF* (translating into aconitate hydratase – accessory protein, PrpF) (Garvey *et al.*, 2007, Grimek & Escalante-Semerena, 2004). When non ortholog addition or replacement of *prpD* with *acnD* and *prpF* was investigated, the 2-methylcitrate cycle was confirmed to be still functional, showing that both enzymes were active, and were needed together, in order to replace the function of PrpD (Grimek & Escalante-Semerena, 2004). The first step in the 2-methylcitrate cycle, which consists in the conversion of propionate to propionyl-CoA, is achieved by the *prpE* gene (encoding propionyl-CoA synthetase, PrpE) (Horswill & Escalante-Semerena, 1999a). This gene is only found in a few bacteria containing the 2-methylcitrate pathway and, when present, is always found as the most downstream gene of the *prp* operon.

Several studies published, which included mutants for inactivation of specific genes belonging to the 2-methylcitrate pathway, confirmed the involvement of each gene to this pathway, as the knockouts resulted in a slow down or eventual arrest of bacterial growth when propionic acid was supplemented in the growth medium: the knockouts, in fact, generated accumulation of toxic metabolites within the cell, such as propionyl-CoA or 2-methylcitrate (Plassmeier *et al.*, 2007, Brock & Buckel, 2004); *prpE* deficient mutants, however, were able to carry on growing, even though to a lesser extent, as propionyl-CoA could be formed by an acetyl-CoA synthetase ortholog (Palacios *et al.*, 2003). No homologues of PrpE are present in *N. meningitidis*: the presence of the *ackA-1* gene (*NMB0435*) (encoding a

propionate/acetate kinase) within the *prp* gene cluster suggests that it could replace *prpE* but with a lower affinity, as AckA-1 transforms propionate to propionyl phosphate. Propionyl phosphate is subsequently metabolised into propionyl-CoA with the help of the *pta* gene (*NMB0631*) (encoding a phosphotransacetylase; Pta). The supposition that AckA-1 has a lower affinity to propionate compared to PrpE is based on the evidence from studies from Starai using acetate kinase versus acetyl-CoA synthetase, rather than propionate kinase versus propionyl-CoA synthetase (Starai & Escalante-Semerena, 2004). Therefore, an analogous relationship in propionate activation was inferred here. Two possible pathways showing affinity of an AckA / Pta reaction compared to the acetyl-CoA synthetase are shown in Figure 3.2-3.

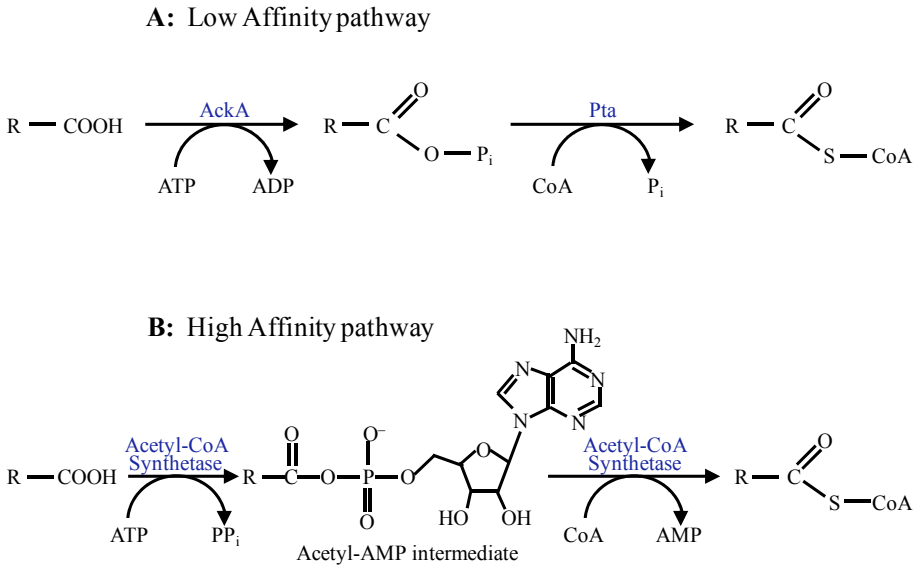

Figure 3.2-3: Pathway for the conversion of acetate to acetyl-CoA.
Affinity is defined by the concentration of acetate in the medium that is optimally used by each pathway. **A:** The low affinity pathway (AckA / Pta) is used when acetate concentrations are high ($\geq$ 30 mM). **B:** The high affinity pathway (acetyl-CoA synthetase) is used when acetate concentrations are < 10 mM (Figure adapted from Starai & Escalante-Semerena, 2004).

3.3 Characterisation of *prpC* and the *prp* operon in *N. meningitidis*

A *prpC* gene was identified in *N. meningitidis* strain MC58 following a BLAST search (NCBI) and was annotated in the genome sequence as a methylcitrate synthase (*NMB0431*) (Tettelin *et al.*, 2000). The *prpC* gene of *N. meningitidis* strain MC58 is 1155 bp long and is predicted to encode a protein of 384 amino acids with a theoretical molecular weight of 42.819 kDa. The putative PrpC protein from *N. meningitidis* revealed between 75 and 78 % similarity to the amino acid sequence of the PrpC proteins of several other β-proteobacteria, such as *Ralstonia* spp. and *Burkholderia* spp.

prpC is always found in bacteria that possess the 2-methylcitrate pathway. It is found within a cluster of a variable number of genes, and is defined as belonging to the *prp* operon. Table 3.3-1 shows all the genes that belong to the putative *prp* gene cluster in *N. meningitidis* MC58, and their annotated names. To test if the *prp* gene cluster is functional and forms an operon in *N. meningitidis* MC58, several genes belonging to this pathway were disrupted with an antibiotic resistance cassette, and the different mutants were investigated and described later on in this chapter.

Table 3.3-1: Genes involved in the 2-methylcitrate cycle in *Neisseria meningitidis* MC58.

All these genes have still a putative function.

Locus	Gene abbreviation	Protein common name
NMB0430	*prpB*	2-methylisocitrate lyase (carboxyphosphoenolpyruvate phosphomutase)
NMB0431	*prpC*	2-methylcitrate synthase
NMB0432	-	No putative function predicted
NMB0433	*acnD*	Aconitate hydratase
NMB0434	*prpF*	AcnD - accessory protein PrpF
NMB0435	*ackA-1*	Propionate kinase (acetate kinase)
NMB0631	*pta*	Phosphotransacetylase (Pta)

3.4 Distribution of the *prpC* gene in *Neisseria*

The *prpC* gene is found in most, but not all, *Neisseria* spp. that have been sequenced so far (*N. elongata, N. flavescens, N. gonorrhoeae, N. meningitidis, N. mucosa, N. sicca, N. subflava, N. wadsworthii and N. weaveri*), even though the genome sequence of the majority of these strains is not fully available yet. Isolates from several of these human-specific bacteria, such as *N. flavescens, N. sicca* and *N. subflava*, were occasionally found in immunocompromised patients and eventually lead to endocarditis, meningitis or septicaemia (Heiddal *et al.*, 1993, Sinave & Ratzan, 1987, Pollack *et al.*, 1984).

The *prpC* gene is not found in the most closely related commensal *Neisseria*, such as *N. lactamica*. This gene is also absent from the other close commensal *N. cinerea* and *N. polysaccharea*. *prpC* and the gene cluster to which it belongs are probably an adaptation that might have occurred to help *N. meningitidis* survive in human adults which, unlike human infants, are rich in anaerobic bacteria producing propionic acid. Alternatively, *N. lactamica* may have gone through selective gene loss, as the *prp* gene cluster may be less important in this species. Infants, in fact, are the optimal environment for *N. lactamica*'s growth, and the nasopharynx of human infants contains fewer anaerobic bacteria that synthesise propionic acid. Investigations for understanding if the gene was needed in pathogenicity or survival will be discussed in Chapter 6. The relationship between the 10 of the most common *Neisseria* species is shown in Figure 3.4-1, where phylogeny was based on 636 completely conserved core neisserial genes (Marri *et al.*, 2010).

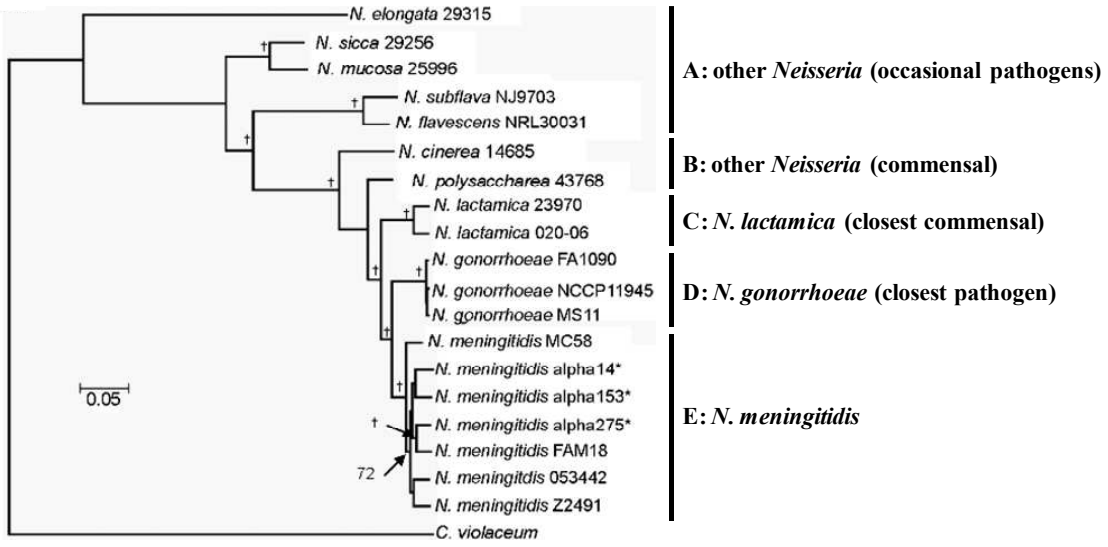

Figure 3.4-1: Phylogenetic relationship between *Neisseria* spp.
Phylogeny was based on 636 core genes from *Neisseria* spp. and the outgroup *Chromobacterium violaceum* (Figure adapted from Marri *et al.*, 2010).

3.5 Construction of knockout mutants of the *prpC*, *NMB0432* and *ackA-1* genes of *N. meningitidis*

In order to investigate the role played by PrpC, by the conserved hypothetical protein NMB0432, and by the putative propionate / acetate kinase NMB0435, all three belonging to the *prp* cluster, knockouts of *prpC*, *NMB0432* and *ackA-1* genes from *N. meningitidis* strain MC58 were constructed in this study. Construction of each single mutant knockout was achieved by inserting a spectinomycin or tetracycline resistance cassette within each gene of interest (Figure 3.5-1).

To generate the knockouts, the three genes with their flanking regions were amplified using the primers described in Table 2.3.1-1. The *prpC* gene (*NMB0431*) was amplified using primers NMB0431-for and NMB0431-rev (Figure 3.5-2). The conserved hypothetical gene adjacent to the *prpC* gene (*NMB0432*) was amplified with primers NMB0432-for and NMB0432-rev (Figure 3.5-3). The third gene, the *ackA-1* gene (*NMB0435*) was amplified with NMB0435-for and NMB0435-rev. *ackA-1* was the only gene that was flanked by the *N. meningitidis* DNA uptake sequence, GCCGTCTGAA (Figure 3.5-4). The relevant restriction sites where the spectinomycin or tetracycline cassette was inserted are also shown in these figures.

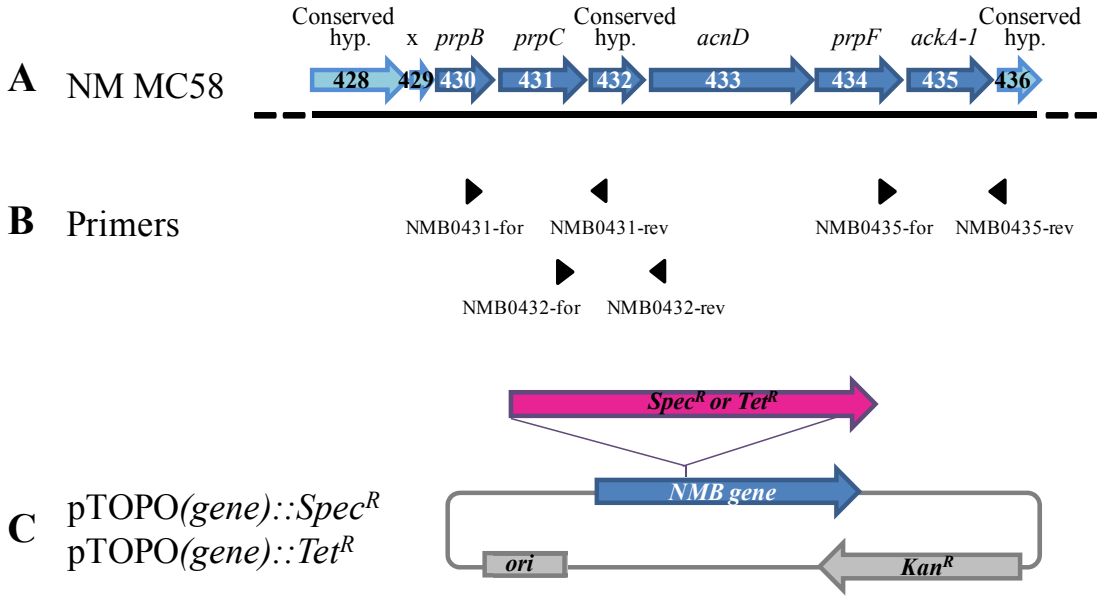

Figure 3.5-1: The ORF map of the *prp* gene cluster of *N. meningitidis* MC58, with primers and plasmid used for the construction of knockouts.

A: The relevant region of *N. meningitidis* MC58 genome representing the genes belonging to the *prp* gene cluster (dark blue arrows) and its flanking genes (light blue arrows) is shown with the orientation of each gene. Gene numbers correspond to the numbering given in the MC58 complete genome, where the number within each arrow is preceded by "NMB0" (NCBI GenBank accession number AE002098.2). **B:** The position of the three sets of primers used for constructing the knockouts is shown with black arrows. **C:** The pCR®-Blunt II-TOPO® vector (gray) is shown with its relevant features (gray box and gray arrow) and with the place of insertion of the mutant gene (blue arrow). The spectinomycin and tetracycline resistance cassettes and their place of insertion are also shown in the diagram (pink arrow). NM MC58: *N. meningitidis* strain MC58. Conserved hyp.: gene coding for a conserved hypothetical protein. 429, which corresponds to *NMB0429*, encodes a very short hypothetical protein.

GAACTTCGTGATTATGGCGCGTACCGATGCGCTGGCGGTAGAAGGTTTGGATGCCGCTATCGAACGCG
CCCAAGCTTGTGTCGAAGCCGGTGCGGACATGATTTTCCCTGAAGCCATGACCGATTTGAACATGTAC
CGCCAATTTGCAGATGCGGTGAAAGTGCCCGTGTTGGCGAACATTACCGAGTTTGGTTCCACTCCGCT
TTATACCCAAAGCGAGCTGGCTGAAAACGGCGTGTCGCTGGTGCTGTATCCGCTGTCATCGTTCCGTG
CAGCAAGCAAAGCCGCTCTGAATGTTTACGAAGCGATTATGCGCGATGGCACTCAGGCGGCGGTGGTG
GACAGTATGCAAACCCGTGCCGAGCTGTACGAGCATCTGAACTATCATGCCTTCGAGCAAAAACTGGA
TAAATTGTTTCAAAAATGATTTACCGCTTTCAGACTGCCTTTCAACAAATCCGCATCGGTCGTCTGAA
AACCCGAAACCCATAAAAACACAAAGGAGAAATACCATGACTGAAACTACTCAAACCCCGACCCTCAA
ACCTAAAAAATCCGTTGCGCTTTCTGGCGTTGCGGCCGGTAATACCGCTTTGTGTACCGTTGGCCGTA
CCGGCAACGATTTGAGCTATCGCGGTTACGACATTCTGGATTTGGCACAAAAATGCGAGTTTGAAGAA
GTCGCCCACCTGCTGATTCACGGCCATCTGCCCAACAAATTCGAGCTGGCCGCTTATAAAACCAAGCT
CAAATCCATGCGCGGCCTGCCTATCCGTGTGATTAAAGTTTTGGAAAGCCTGCCTGCACATACCCATC
CGATGGACGTAATGCGTACCGGCGTATCCATGCTGGGCTGCGTTCATCCTGAACGTGAAAGCCATCCG
GAAAGTGAAGCGCGCGACATCGCCGACAAACTGATCGCCAGCCTCGGCAGCATCCTCTTGTACTGGTA
TCAATATTCGCACAACGGCAAACGCATTGAGGTTGAAAGCGACGAAGAGACCATCGGCGGTCATTTCC
TGCAACTGTTGCACGGCAAACGCCCAAGCGAATCACACATCAAAGCCATGCACGTTTCACTGATTCTG
TATGCCGAACACGAGTTCAACGCTTCTACCTTTACCGCCCGCGTGATCGCCGGTACAGGCTCTGATAT
GTACTCCAGCATTACCGGAGCAATCGGCGCGTTGAAAGGTCCGAAACACGGCGGCGCGAACGAAGTGG
CTTACGATATTCAAAAACGCTACCGCAATGCCGACGAAGCTGAAGCCGACATCCGCGAACGCATCGGC
CGCAAAGAAATCGTGATCGGTTTCGGTCATCCGGTGTACACCATTTCCGACCCTCGCAACGTTGTCAT
TAAAGAAGTGGCACGCGGTTTGAGCAAAGAAACCGGCGATATGCGCCTCTTTGACATTGCCGAACGTT
TGGAAAGCGTGATGTGGGAAGAGAAAAAAATGTTCCCGAATCTGGACTGGTTCTCTGCCGTTTCCTAC
CAAAAATTGGGCGTACCGACCGCTATGTTCACACCGCTGTTCGTAATTTCCCGTACAACCGGTTGGAG
CGCACACGTTCTTGAGCAACGCAAAGACGGCAAAATCATCCGTCCGAGCGCAAACTACACAGGCCCTG
AAGATTTGGCGTTTGTGGAGATTGAAGAACGATAATTGAAGAATGCAATAGCAGTTTGTTCTTTAATT
TCGGTATGCAAAGCTAAGGATTTCAGACGACCTTGCCTTATTGGAAAGGTTGTCTGAAATAAGTTTAA
TCTAATAGGAGAAGATAATCCTGTATTGGCGCAAGTAACAGGATAAGAAACATGGAAGATTTATATAT

Figure 3.5-2: The *prpC* sequence with its flanking regions used for constructing the mutant.

The *prpC* gene (blue) with the ATG start codon (green) and the TAA stop codon (red) and its flanking regions (black) give a product 1690 bp long. Primers NMB0431-for and NMB0431-rev were used (highlighted in yellow). The reverse primer's mismatches are also shown (red), where "TT" in the sequence was considered "CC" in the primer. The PsiI site (TTATAA) is also shown (highlighted in blue) with the two bases within which the restriction enzyme cuts (brown). Primers NMB0431bis-for and NMB0431bis-rev were used for colony pick PCR screening in *N. meningitidis* (underlined in blue).

TGCGCCTCTTTGACATTGCCGAACGTTTGGAAAGCGTGATGTGGGAAGAGAAAAAAATGTTCCCGAAT
CTGGACTGGTTCTCTGCCGTTTCCTACCAAAAATTGGGCGTACCGACCGCTATGTTCACACCGCTGTT
CGTAATTTCCCGTACAACCGGTTGGAGCGCACACGTTCTTGAGCAACGCAAAGACGGCAAAATCATCC
GTCCGAGCGCAAACTACACAGGCCCTGAAGATTTGGCGTTTGTGGAGATTGAAGAACGATAATTGAAG
AATGCAATAGCAGTTTGTTCTTTAATTTCGGTATGCAAAGCTAAGGATTTCAGACGACCTTGCCTTAT
TGGAAAGGTTGTCTGAAATAAGTTTAATCTAATAGGAGAAGATAATCCTGTATTGGCGCAAGTAACAG
GATAAGAAACATGGAAGATTTATATATAATACTCGCTTTGGGTTTGGTTGCGATGATTGCCGGATTTA
TCGATGCGATTGCGGGCGGGGGTGGTTTGATTACGCTGCCCGCACTCTTGTTGGCAGGTATTCCTCCC
GTGTCGGCAATTGCCACCAACAAGCTGCAAGCAGCCGCTGCTACGTTTTCAGCTACGGTTTCTTTTGC
ACGCAAAGGTTTGATTGATTGGAAGAAAGGTCTCCCGATTGCCGCAGCATCGTTTGTAGGCGGCGTGG
CCGGTGCATTATCGGTCAGCTTGGTTTCCAAAGATATTCTGCTGGCGGTCGTGCCGGTTTTGTTGATA
TTTGTCGCACTGTATTTTGTGTTTTCGCCCAAGCTCGACGGCAGTAAGGAAGGCAAAGCCAGAATGTC
TTTTTTTCTGTTCGGGCTGACGGTCGCACCGCTTTTGGGTTTTTACGACGGTGTGTTCGGACCGGGTG
TCGGCTCGTTTTTTCTGATTGCCTTTATTGTTTTGCTCGGCTGCAAGCTGTTGAACGCGATGTCTTAC
ACCAAATTGGCGAACGTTGCCTGCAATCTTGGTTCGCTATCGGTATTCCTGCTGCACGGTTCGATTAT
TTTCCCGATTGCGGCAACGATGGCGGTCGGTGCGTTTGTCGGTGCGAATTTAGGTGCGAGATTTGCCG
TCCGCTTCGGTTCGAAGCTGATTAAGCCGCTGCTGATTGTCATCAGCATTTCGATGGCTGTGAAATTG
TTGATAGACGAGAGAAATCCGCTGTATCAGATGATTGTTTCGATGTTTTAAACCCTTTCAGACGACCC
CTTCAAAACGTCGGCTGAAACCTCAAACCACAAGAAAAACAGATCCACAGGAGAACCGACAGGCTGCC
AACCAACGTTACCGCAAACCGCTGCCCGGTACGGATTTGGAATACTACGACGCGCGTGCGGCGTGTGA

Figure 3.5-3: The *NMB0432* gene with its flanking regions used for constructing the mutant.

The *NMB0432* gene (blue) with the ATG start codon (green) and the TAA stop codon (red) and its flanking regions (black) give a product 1208 bp long. Primers NMB0432-for and NMB0432-rev were used (highlighted in yellow). The ClaI site (ATCGAT) and AclI site (AACGTT) are also shown (highlighted in blue) with the site where the restriction enzymes cut (brown).

CGGACAATGGACGGCCACCAAAGCGGTCATGAGCCGTAGCGCACGCGTGATGATGGAAGGTTGGGTCA
GGGTGCCTGAGGATTGTTTTTAAATTGACGTAGCATGGGTTTGCCCGCGAGCCATAAAAAGGTCGTCT
GAAAAACAAGTAAACATCAAATCACTGACCATTCCTTTCCCTTGCCCTGTGGCGGAAGGCGGCAAATC
ACAAGGAAGAACACGGAAACCCCGATAAAAGACAGCTTCCCGTATTACCGTCATTCCCGCGCAGGCGG
GAATCCAGACCTGTCAATATGGAGGATTGGCAGGGGAAAACAGGTTTCGTGAGTTCTACATTCTGGAT
TCCCGCCACAGCCTGTCCTCGCGTAGGCGGGGACGGAATAACGATAGAAAATGCGGCATACGCTTTGC
CCAAAGAGGCCGTCTGAAACACCTTGCGCCTGATGTCTGCCTTTTTCAGACGACCCCACACCAAAAAA
ACAACCACAAACTACAAGGAGAAACATCATGTCCGACCAACTCATCCTCGTTCTGAACTGCGGCAGTT
CATCGCTCAAAGGCGCCGTTATCGACCGAAAAAGCGGCAGCGTCGTCCTAAGCTGCCTCGGCGAACGC
CTGACCACGCCCGAAGCCGTCATTACGTTCAACAAAGACGGCAACAAACGCCAAGTTCCCCTGAGCGG
CCGAAATTGCCACGCCGGCGCGGTGGGTATGCTTTTGAACGAACTGGAAAAACACGGTCTGCACGACC
GCATCAAAGCCATCGGCCACCGCATCGCCCACGGCGGCGAAAAATACAGCGAGTCTGTTTTGATCGAC
CAGGCCGTAATGGACGAACTCAATGCCTGCATTCCGCTTGCGCCGCTGCACAACCCCGCCAACATCAG
CGGCATCCTTGCCGCACAGGAACATTTCCCCGGTCTGCCCAATGTCGGCGTGATGGATACTTCGTTCC
ACCAAACCATGCCGGAGCGTGCCTACACTTATGCCGTGCCGCGCGAGTTGCGTAAAAAATACGCTTTC
CGCCGCTACGGTTTCCACGGCACCAGTATGCGTTACGTTGCCCCTGAAGCCGCACGCATCTTGGGCAA
ACCTCTGGAAGACATCCGCATGATTATTGCCCACTTAGGCAACGGCGCATCCATTACCGCCATCAAAA
ACGGCAAATCCGTCGATACCAGTATGGGTTTCACGCCGATCGAAGGTTTGGTAATGGGTACACGTTGC
GGCGACATCGATCCGGGCGTATACAGCTATCTGACTTCCCACGCCGGGATGGATGTTGCCCAAGTGGA
TGAAATGCTGAACAAAAAATCAGGTTTGCTCGGTATTTCCGAACTTTCCAACGACTGCCGCACCCTCG
AAATCGCCGCCGACGAAGGCCACGAAGGCGCGCGCCTCGCCCTCGAAGTCATGACCTACCGCCTCGCC
AAATACATCGCTTCGATGGCTGTGGGCTGCGGCGGCGTTGACGCACTCGTGTTCACCGGCGGTATCGG
CGAAAACTCGCGTAATATCCGTGCCAAAACCGTTTCCTATCTTGATTTCTTGGGTCTGCACATCGACA
CCAAAGCCAATATGGAAAAACGCTACGGCAATTCGGGCATTATCAGCCCGACCGATTCTTCTCCGGCT
GTTTTGGTTGTCCCGACCAATGAAGAACTGATGATTGCCTGCGACACTGCCGAACTTGCCGGCATCTT
GTAGCCAAAAAAGGGACGAGTCCGCAAAAATGCCGTCTGAAACCCCAAACGCCCGATTAGGCTGATGA
GGATTTTAGACGGCATTGTTCATTTTTTTGTTATCTTGCATTTTTGTGCGGACGGTGGAATTTCATCC
TGTAAACATAAATATTTGTCGGAAAACAGAAACCCTCCGCCGCCATTTCTACGAAAGCAGGAAACCAG
CAACGCAAAGCGACAGGGATTTGTTGGAAATGACCGAAACCGAACGAACCGGATTCCCGCCTGCGCGG
GAATGACGGGATTTTCTGTTTTTGTGGAAATGACGGGATTTTGAATTTCGGGCGTACAATACGGAAAA
CATGACGATAAGGAAACAAACCATGGCACAGTTTTTCGCTATTCATCCCGACAATCCCCAAGAACGCC

Figure 3.5-4: The *ackA-1* gene with its flanking regions used for constructing the mutant.

The *ackA-1* gene (blue) with the ATG start codon (green) and the TAG stop codon (red) and its flanking regions (black) give a product 1935 bp long. Primers NMB0435-for and NMB0435-rev were used (highlighted in yellow). Just outside the gene of interest there are two *N. meningitidis* DNA uptake sequences (orange). The BsmI site (TGCATTC) and ClaI site (ATCGAT) are also shown (highlighted in blue) with the site where the restriction enzymes cut (brown).

After amplification of each gene of interest using neisserial genomic DNA from strain MC58 and GoTaq® DNA polymerase as described in Section 2.3.1, the PCR products obtained corresponded to the expected fragment sizes of 1690 bp for the *prpC* gene, 1208 bp for the *NMB0432* gene, and 1935 bp for the *ackA-1* gene. Correct amplification of the three genes was confirmed by the agarose gels (Figure 3.5-5). The resulting blunt-ended PCR products were subsequently purified and cloned into the 3519 bp pCR®-Blunt II-TOPO® vector (Invitrogen™), which contained a kanamycin resistance cassette (Kan^R). The vector was transformed into *Escherichia coli* DH5α by heat shock, and *E. coli* was then grown at 37 ºC on selective LB agar plates. Only bacteria with successfully transformed plasmids were able to grow in the presence of kanamycin.

Mini-preparations of two colonies per transformed *E. coli* plate were grown in liquid LB medium with kanamycin overnight; bacteria were then harvested and plasmid DNA was purified as described in Section 2.3.4. Positive insertion of the genes of interest in the new plasmid was investigated at this stage by EcoRI restriction digest. The pCR®-Blunt II-TOPO® vector, in fact, has two distinct recognition sites for EcoRI, and these sites are located just a few bases before and after the inserted genes under study, whilst the three genes did not contain any EcoRI restriction site. After restriction digest, two fragments were generated, one of which was the original 3.5 kb TOPO vector and the other corresponded to the inserted PCR product, which was less than 2 kb in size for all the three genes under study (Figure 3.5-6). Sequencing results confirmed that the *prpC*, the *NMB0432* and the *ackA-1* regions were amplified correctly and without introducing any error.

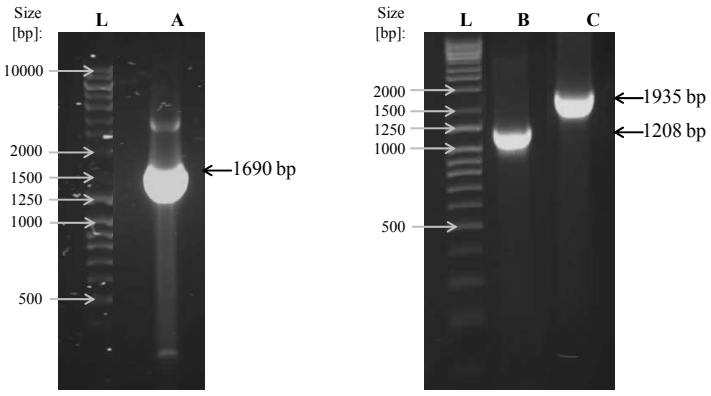

Figure 3.5-5: PCR products of the *prpC*, *NMB0432* and *ackA-1* genes with their relative flanking regions from *N. meningitidis* MC58.

The correct PCR products, fragments expected to be 1690 bp long for *prpC* (Lane A), 1208 bp for *NMB0432* (Lane B) and 1935 bp for *ackA-1* (Lane C), were successfully amplified. The Q-Step 4 Quantitative DNA ladder (YORBIO) (Lane L) was loaded on both gels to confirm the size of each DNA band.

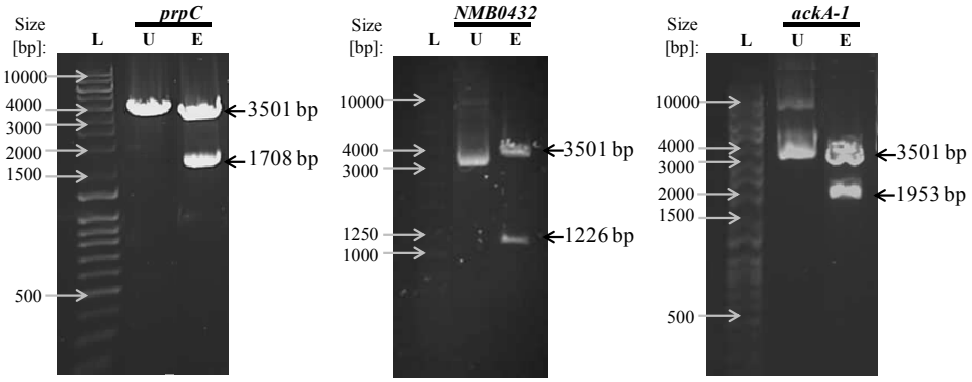

Figure 3.5-6: EcoRI screening for insertion of the genes *prpC*, *NMB0432* and *ackA-1* in the pCR®-Blunt II-TOPO® vector.

pCR®-Blunt II-TOPO® plasmids containing the genes under study, undigested and digested with EcoRI, were loaded on the gels. In the digested lanes (Lanes E) the top band corresponded to the 3.5 kb TOPO vector and the lower band corresponded to each gene of interest. The Q-Step 4 Quantitative DNA ladder (YORBIO) (Lane L) was loaded on all gels to confirm the size of the DNA bands. U: undigested plasmid. E: plasmid digested with EcoRI.

Once confirmed that the pCR®-Blunt II-TOPO® vectors were containing the genes under study, these were digested with different restriction enzymes that would cut only within each gene. The *prpC* gene was digested with PsiI, which cuts only once within the gene, and this was confirmed by sequencing (Figure 3.5-7A). The *NMB0432* gene was digested with ClaI and AclI, which would each cut just once within the gene, and the resulting fragment of 489 bp in length was eliminated, as shown in the gel and then confirmed by sequencing (Figure 3.5-7B). The *ackA-1* gene was digested with BsmI and ClaI, which would each cut only once within the gene, but only the BsmI enzyme worked, as confirmed by sequencing and by the missing small 389 bp fragment in the gel (Figure 3.5-7C). The three restriction enzymes AclI, BsmI and ClaI were creating sticky ended DNA, and therefore digests containing those enzymes were incubated with DNA Polymerase I (Klenow) and dNTPs during the last 30 minutes of the restriction digest incubation, in order to create blunt ended DNA needed for ligation with an antibiotic resistance cassette. The 5209 bp, 4238 bp and 5454 bp fragments were then purified from the gel for ligation with the spectinomycin resistance gene cassette ($Spec^R$) or the tetracycline resistance cassette (Tet^R).

The spectinomycin resistance gene cassette ($Spec^R$), also referred to as *Ω* cassette, is 1980 bp in size, and in this work it was generated from the digestion of the pHP45*Ω* plasmid, about 4.3 kb in size, with the SmaI restriction enzyme. This digest also created a second fragment, the pHP45 plasmid, which was 2320 bp long (Figure 3.5-8A). The tetracycline resistance gene cassette is 2.5 kb in size, and it was generated from the digestion of the pCMT18 plasmid with the EcoRV restriction enzyme (Figure 3.5-8B). Both cassettes were purified from the gel for ligation with the genes under investigation.

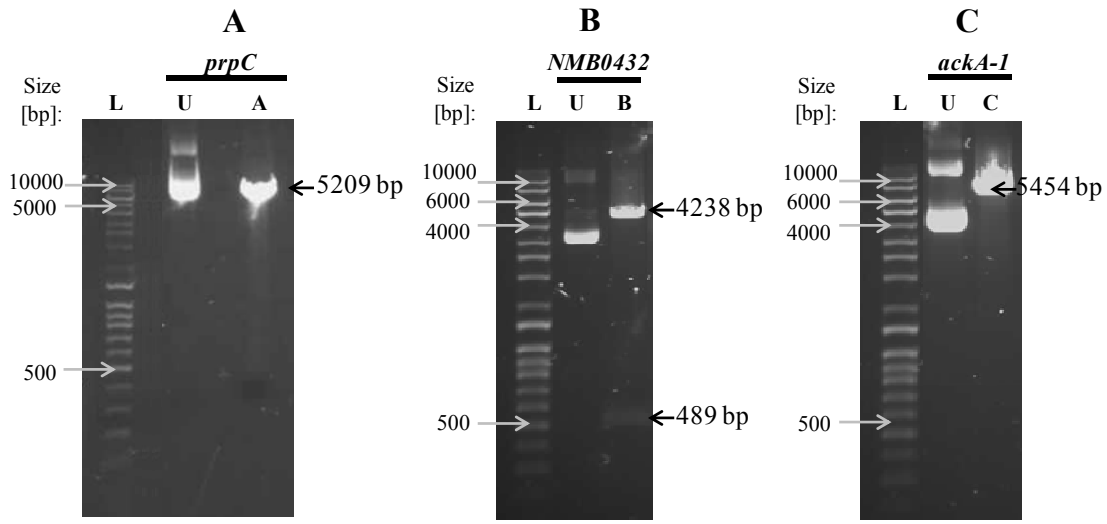

Figure 3.5-7: Restriction digests for the pCR®-Blunt II-TOPO® vector and its inserts, genes *prpC*, *NMB0432* and *ackA-1* for generating the knockouts.

pCR®-Blunt II-TOPO® plasmids containing the genes under study, undigested and digested with different restriction enzymes, were loaded on the gels. In the digested lanes (Lanes A-C) the top band corresponded to the 3.5 kb TOPO vector with most / all of the insert and the lower band present in Lane B, corresponded to part of the *NMB0432* gene. Lane A: plasmid digested with PsiI. Lane B: plasmid digested with ClaI and AclI (both sites in the *NMB0432* sequence were cut, thus the presence of the 489 bp fragment). Lane C: plasmid digested with BsmI and ClaI (only the BsmI site in the *ackA-1* sequence was cut). The Q-Step 4 Quantitative DNA ladder (YORBIO) (Lane L) was loaded on all gels to confirm the size of the DNA bands. U: undigested plasmid. A-C: plasmid digested with restriction enzymes.

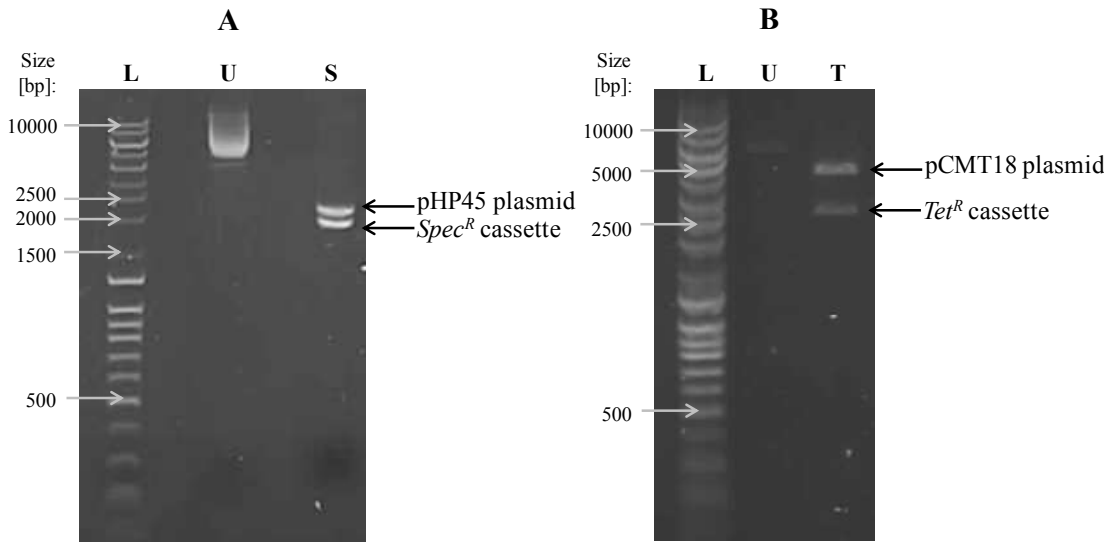

Figure 3.5-8: Spectinomycin and tetracycline resistance cassettes.

A: Lane U represents the undigested 4.3 kb pHP45*Ω* plasmid containing the spectinomycin resistance cassette (*Spec*^{R}). Lane S comprises the 1980 bp *Spec*^{R} cassette derived from the pHP45*Ω* plasmid after SmaI digest (lower band), and the 2320 bp pHP45 plasmid (upper band). **B:** Lane U represents the undigested pCMT18 plasmid containing the tetracycline resistance cassette (*Tet*^{R}). Lane S comprises the 2.5 kb *Tet*^{R} cassette derived from the pCMT18 plasmid after EcoRV digest (lower band), and the actual plasmid (upper band). The Q-Step 4 Quantitative DNA ladder (YORBIO) (Lane L) was loaded to confirm the size of the DNA bands.

At this stage, the spectinomycin resistance cassette was ligated to each of the three digested genes within the pCR®-Blunt II-TOPO® plasmids overnight at room temperature, and ligations were then transformed into *E. coli* DH5α with the heat shock procedure. The same procedure was also carried out with tetracycline resistance cassette and the *NMB0432* gene. The mutants were selected by plating each transformation onto selective LB agar plates containing 50 µg / ml of kanamycin and either 50 µg / ml spectinomycin or 20 µg / ml tetracycline. Mini-preparations of two colonies per transformation were grown in liquid LB medium

with both antibiotics overnight, and plasmid DNA was then extracted and purified as described in Section 2.3.4. An agarose gel was run after restriction digest with BamHI, in order to check for successful ligations with the *Spec*^{R} cassette. The pCR®-Blunt II-TOPO® vector, in fact, has one recognition site for BamHI just before the location of insertion of the genes under study, and the spectinomycin resistance cassette has two recognition sites at either ends of the cassette, whilst the three genes did not contain any BamHI restriction site. Positive ligation, therefore, resulted in the three fragments shown in Figure 3.5-9. A gel for the ligation of the *NMB0432* gene with the tetracycline cassette was not carried out; the colonies containing *Tet*^{R}, however, were verified by sequencing.

Sequencing results of the four new transformants confirmed that the three genes were disrupted with the spectinomycin resistance cassette, and that the *NMB0432* gene was disrupted with the tetracycline resistance cassette. Moreover, the *NMB0432* gene was inserted in the correct direction (plus / plus strand), but the *prpC* gene and the *ackA-1* gene were both inserted in the 5' to 3' direction (plus / minus strand) compared to the database sequence (NCBI GenBank accession number AE002098.2). A map of the pCR®-Blunt II-TOPO® plasmid showing the direction of insertion of each gene under study which was knocked out following ligation to the *Spec*^{R} or *Tet*^{R} cassette is shown in Figure 3.5-10. Direction was confirmed by both sequencing data and fragment sizes derived from BamHI digest.

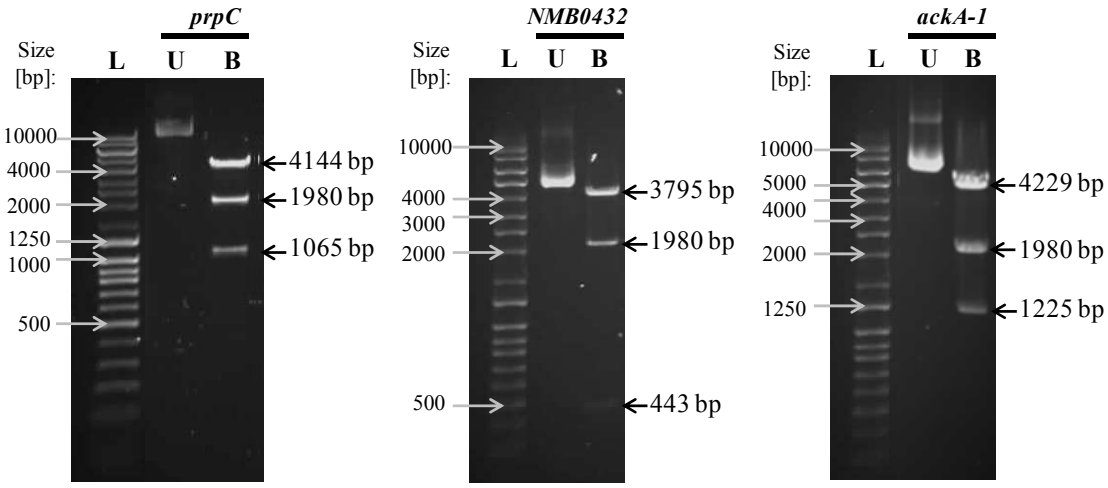

Figure 3.5-9: BamHI screening for insertion of the spectinomycin resistance cassette in the constructed plasmid containing *prpC*, *NMB0432* and *ackA-1* genes.

pCR®-Blunt II-TOPO® plasmids containing the genes under study disrupted with the spectinomycin cassette are shown both undigested and digested with BamHI. In the digested lanes (Lanes B) the top band corresponded to the 3.5 kb TOPO vector plus part of each gene under study, the middle band corresponded to the spectinomycin cassette and the lower band corresponded to the other part of each gene of interest. The Q-Step 4 Quantitative DNA ladder (YORBIO) (Lane L) was loaded on all gels to confirm the size of the DNA bands. U: undigested plasmid. B: plasmid digested with BamHI.

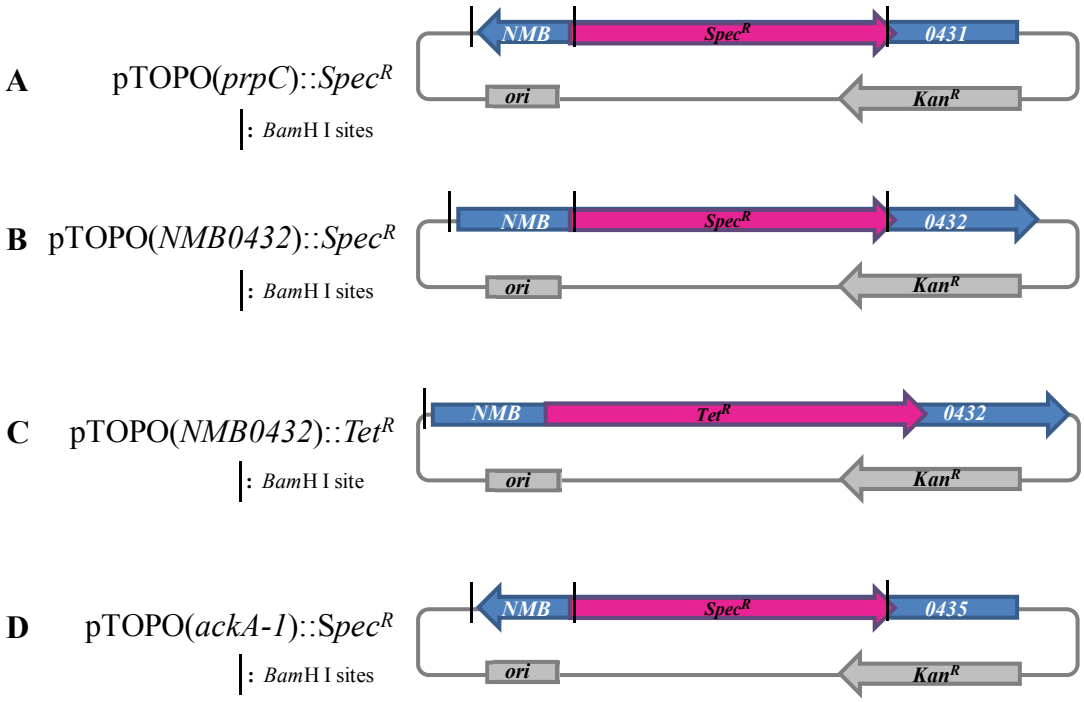

Figure 3.5-10: Plasmid maps of the pCR®-Blunt II-TOPO® vector containing the *prpC*, *NMB0432* and *ackA-1* gene, which were knocked out by the insertion of an antibiotic resistance cassette.

Two BamHI sites are found in both sides of the 2 kb spectinomycin resistance cassette, but none is found within the tetracycline resistance cassette. Another site is found just outside the location of insertion of the genes under study. **A-D:** direction of insertion of each gene under investigation from *N. meningitidis* MC58 (blue arrow) within the pCR®-Blunt II-TOPO® vector (gray). Spectinomycin or tetracycline resistance cassettes (pink arrows) disrupting the genes under study and the kanamycin resistance cassette (gray arrow) are also shown. Black vertical lines: BamHI cutting sites.

All three successful gene knockouts were transformed into wild-type *N. meningitidis* strain MC58 following the TSB method, as described in Section 2.3.9. The mutant strains were selected on CBA plates containing 5 % horse blood and either 50 µg / ml spectinomycin or 2.5 µg / ml tetracycline after overnight incubation at 37 ºC in a

5 % CO_2 atmosphere. Several colonies grown on each plate were screened by colony pick PCR for disruption of the genes by insertion of the 2 kb spectinomycin resistance cassette (Figure 3.5-11) and the 2.5 kb tetracycline resistance cassette (Figure 3.5-12). The original primers used for generating the knockouts were used for colony pick PCR for *NMB0432* and *ackA-1* disrupted genes. The *prpC* disrupted gene, however, failed to amplify in *N. meningitidis* and for this reason a new set of primers, primer NMB0431bis-for and primer NMB0431bis-rev (described in Table 2.3.1-1) was used to amplify the *prpC::Spec*^{R} gene from colony pick. Amplifying a smaller region, as the annealing site for both forward and reverse primers was located within the actual *prpC* gene, gave the expected results.

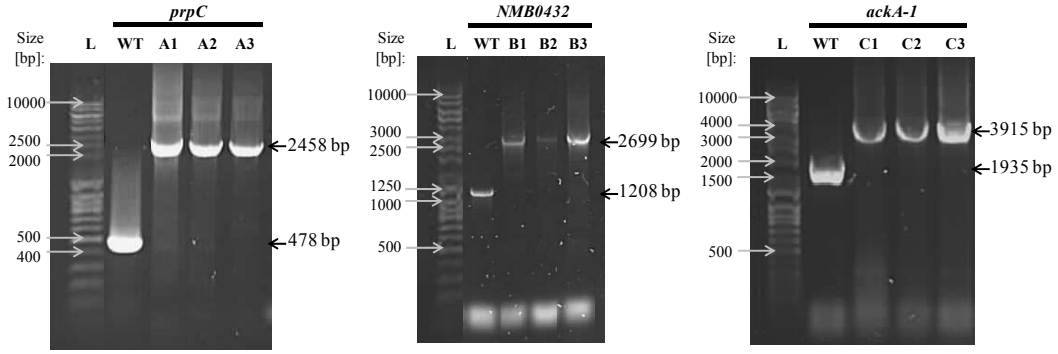

Figure 3.5-11: Colony pick PCR screening for *prpC*, *NMB0432* and *ackA-1* genes disrupted with spectinomycin cassette in *N. meningitidis* strain MC58.

Lanes A1-A3: *prpC* deficient mutants containing the 1980 bp spectinomycin resistance cassette. Lanes B1-B3: *NMB0432* deficient mutants (without the removed 489 bp fragment) containing the 1980 bp spectinomycin resistance cassette. Lanes C1-C3: *ackA-1* deficient mutants containing the 1980 bp spectinomycin resistance cassette. The Q-Step 4 Quantitative DNA ladder (YORBIO) (Lane L) was loaded on all gels to confirm the size of the DNA bands. WT: wild-type gene under study of *N. meningitidis* MC58.

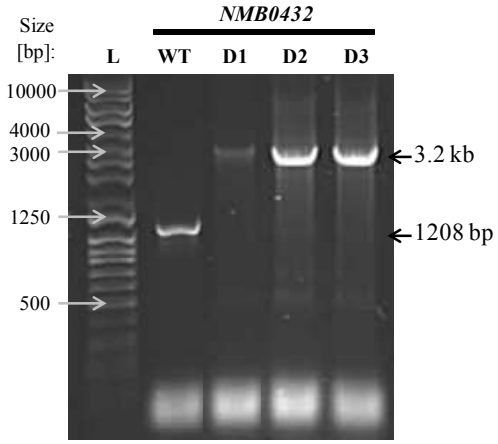

Figure 3.5-12: Colony pick PCR screening for the *NMB0432* gene disrupted with tetracycline cassette in *N. meningitidis* strain MC58.
WT: wild-type *NMB0432* gene of *N. meningitidis* MC58. Lanes D1-D3: *NMB0432* deficient mutants (with the removed 489 bp fragment) containing the 2.5 kb tetracycline resistance cassette. The Q-Step 4 Quantitative DNA ladder (YORBIO) (Lane L) was loaded on the gel to confirm the size of the DNA bands.

Picking from the actual transformation plates resulted in amplification of both *N. meningitidis* wild-type and mutant genes (example for the *ackA-1*::*Spec*^{R} mutant is shown in Figure 3.5-13). However, after re-plating the same colonies onto fresh plates and picking them again, the wild-type band disappeared and only the bands for the mutant strains were visible, confirming that the three genes were disrupted. The wild-type band seemed to have been caused by the background of the wild-type bacteria that did not transform and were plated following the transformation process.

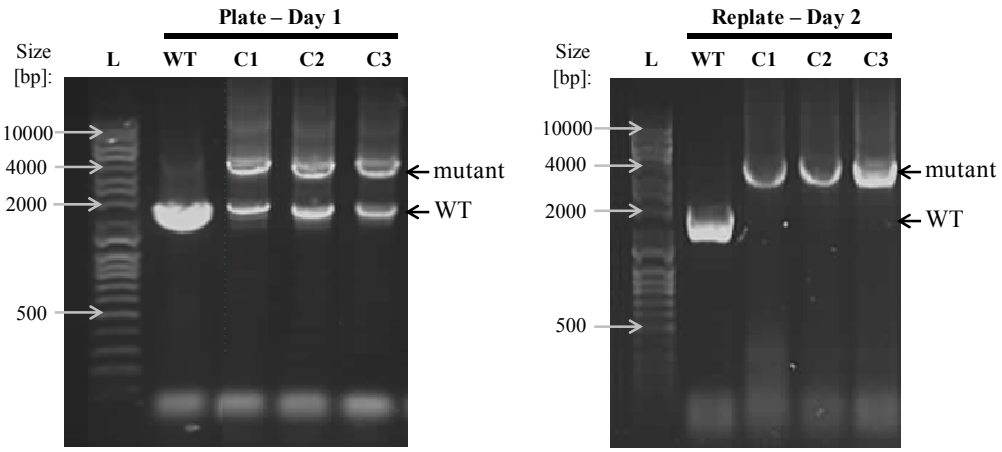

Figure 3.5-13: Comparison of the colony pick PCR screening from the first plate after transformation into *N. meningitidis* and after re-plating.

Three colonies were picked from the first plate after transformation for colony pick PCR (Plate – Day 1). The same colonies were re-plated and picked again the following day (Re-plate – Day 2). The wild-type background band has disappeared from the re-plated colonies. Lanes C1-C3: *ackA-1* deficient mutants containing the 1980 bp spectinomycin resistance cassette. The Q-Step 4 Quantitative DNA ladder (YORBIO) (Lane L) was loaded on all gels to confirm the size of the DNA bands. WT: wild-type gene under study of *N. meningitidis* MC58.

3.6 Effects of propionic acid on growth of *N. meningitidis*

To test the effects of propionic acid on toxicity or increased sensitivity in *N. meningitidis*, both wild-type and *prpC::Spec*^{R} strains were grown in rich medium supplemented with varying concentrations of propionic acid.

Bacteria were incubated in Mueller Hinton Broth (MHB) medium with 10 mM $NaHCO_3$ at 37 °C with shaking at 200 rpm for 24 hours. Growth was monitored by taking optical density measurements for triplicate cultures at 600 nm every 60 minutes. The results showed that 10 mM propionic acid were harmful and strongly

inhibited bacterial growth in both strains. However, no significant differences were noticed in growth rate when lower concentrations of propionic acid were added to the medium, as both strains were able to grow, and grew steadily, in a similar growth pattern (Figure 3.6-1). This indicated that *prpC* was not contributing to an increased resistance to the toxic effects of propionic acid. Inactivation of the *prpC* gene was therefore not fatal and did not increase sensitivity to propionic acid in the *prpC::Spec*^{R} strain.

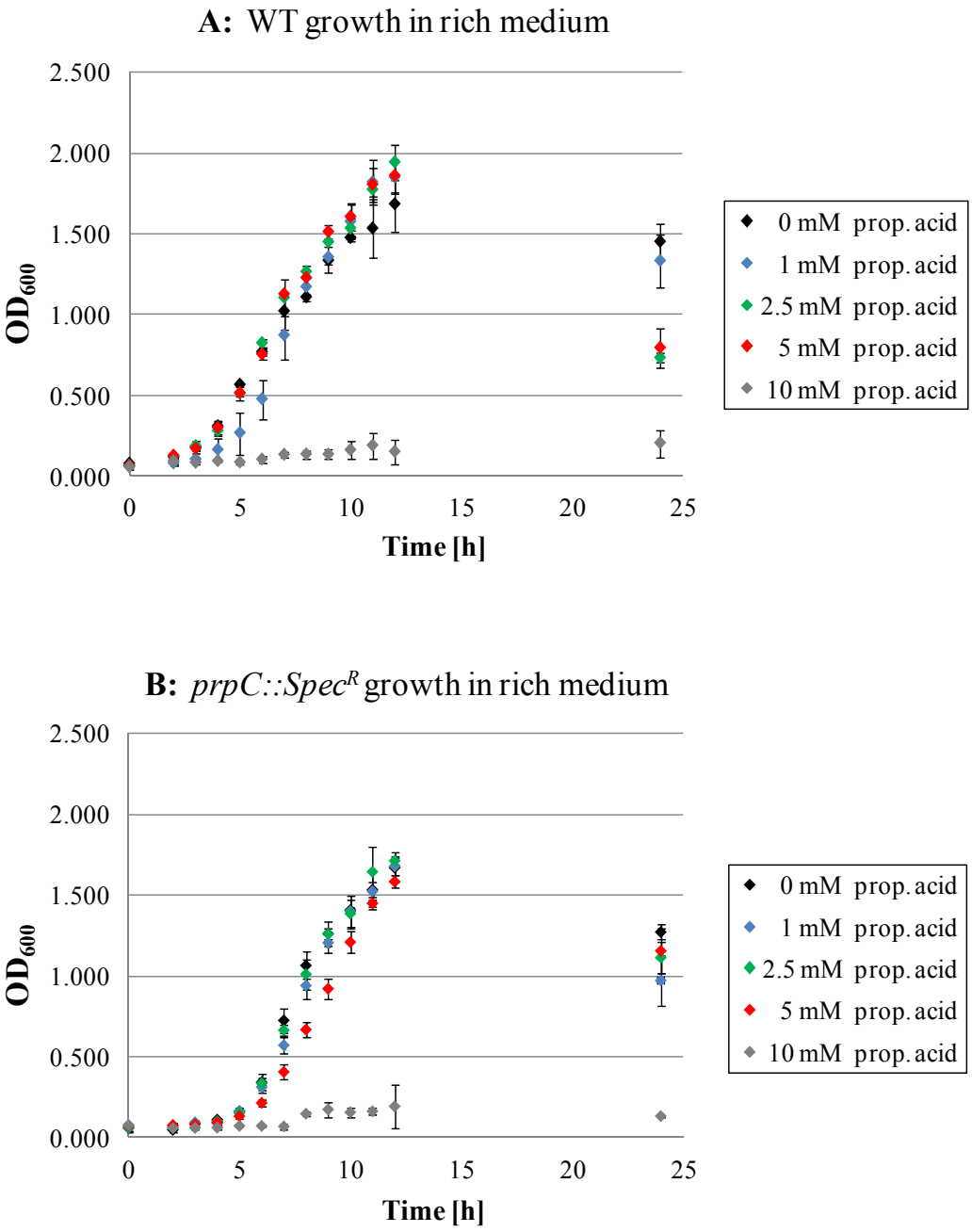

Figure 3.6-1: Growth curve for wild-type and *prpC::Spec*^{R} strains of *N. meningitidis* MC58 in rich medium with increasing concentrations of propionic acid.

A: Growth curve for wild-type bacteria. **B:** Growth curve for the *prpC* mutant strain. Bacteria were grown in Mueller Hinton Broth medium supplemented with varying concentrations of propionic acid. In both cases bacteria showed strong inhibition in growth when in the presence of high concentrations of propionic acid. When none or lower concentrations of propionic acid were used, both strains were able to grow.

As no significant differences were noticed between the two strains when grown in rich medium, further studies were carried out in Chemically Defined Medium (CDM), which was prepared as described in Table 2.2.4-1. Where neither Solution 4a (glucose) nor Solution 4b (sodium pyruvate) were added to the CDM, no cell growth occurred, even when propionic acid was supplemented into the medium, confirming that propionic acid cannot be used as sole source of carbon (Figure 3.6-2).

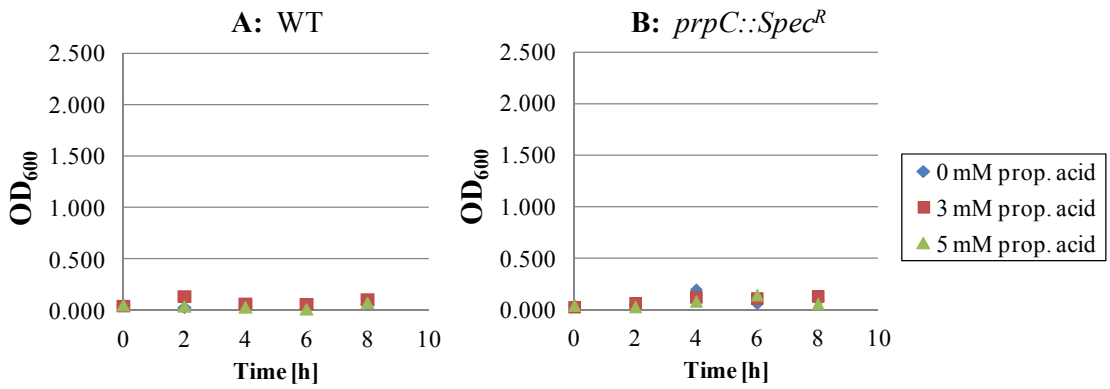

Figure 3.6-2: Growth curve for wild-type and *prpC::Spec*^{R} strains of *N. meningitidis* MC58 in minimal medium supplemented with only propionic acid. **A:** Growth curve for wild-type bacteria. **B:** Growth curve for the *prpC::Spec*^{R} mutant strain. Both strains are not able to grow on chemically defined medium supplemented with propionic acid, but lacking glucose and sodium pyruvate.

In CDM with 2.5 mM glucose wild-type and *prpC::Spec*^{R} bacteria grew similarly when no propionic acid was added, but showed a different phenotype when the medium was supplemented with propionic acid. Wild-type bacteria grown without

propionic acid reached the stationary phase after approximately 8 hours incubation and started to die afterwards, suggesting that carbon depletion was initiating at that point. Wild-type bacteria that were grown with the addition of 5 mM propionic acid, however, were able to continue their growth, instead of entering the stationary phase (Figure 3.6-3A). These results suggested that propionic acid could supplement growth in *N. meningitidis*.

The absence of *prpC* in the *prpC::Spec*^{R} strain did not bring about deleterious effects on the mutant's growth, as *prpC::Spec*^{R} in CDM with 2.5 mM glucose grew similarly to the wild-type when propionic acid was absent, reaching stationary phase after about 8 hours growth. When the mutants were grown in medium supplemented with 5 mM propionic acid, however, they had the same phenotype as when they were grown in medium with no propionic acid (Figure 3.6-3B). This behaviour indicated that the *prpC::Spec*^{R} mutant strain was unable to metabolise propionic acid, and also confirmed that the *prpC* gene is directly involved in propionic acid catabolism.

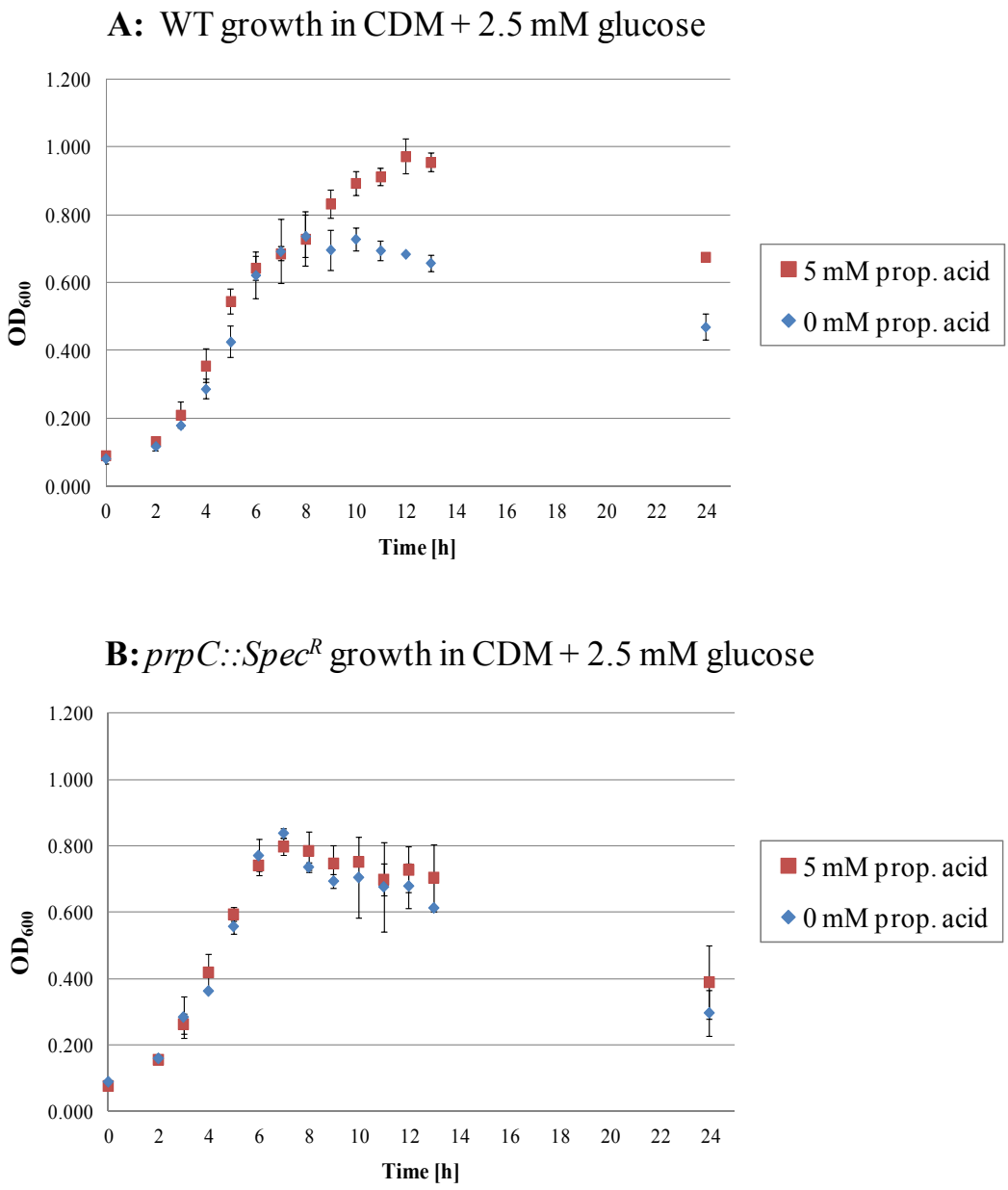

Figure 3.6-3: Growth curve of MC58 wild-type and *prpC::Spec*^{R} strains of *N. meningitidis* in CDM with 2.5 mM glucose and propionic acid.

A: Bacterial growth of wild-type *N. meningitidis*, with enhanced growth when in the presence of propionic acid. Instead of entering the stationary phase after 8 hours, wild-type bacteria used propionic acid for continued growth. **B:** Bacterial growth of *prpC::Spec*^{R} strain. Propionic acid did not have any influence in the mutant's growth, as the mutant was unable to utilise propionic acid due to the absence of the *prpC* gene.

Only the wild-type bacteria that were supplemented with 5 mM propionic acid started to break propionic acid down as an alternative source of carbon and were able to continue growth when bacteria under other conditions had already entered stationary or death phase. This was probably induced by the limiting glucose in the environment, which was used by all bacteria, and by the inability of the mutants to use propionic acid even when it was supplemented in the growth medium.

At this stage, new studies were carried out with CDM containing 5 mM sodium pyruvate. A double concentration of pyruvate (5 mM) was used compared to glucose (2.5 mM), in order to keep the number of carbon atoms added identical between the two minimal media. In this way, any divergence in phenotype between the two strains and the different media were easier to compare.

Bacteria grown in CDM supplemented with sodium pyruvate behaved similarly to bacteria grown in CDM with glucose: only wild-type bacteria were able to use propionic acid as an extra source of carbon to keep growing. Wild-type bacteria lacking propionic acid in their growth medium (Figure 3.6-4A) and *prpC::Spec*^{R} under all conditions (Figure 3.6-4B) started to die after approximately 6 hours incubation. The optical density of bacteria grown in CDM with sodium pyruvate was considerably lower compared to the one measured for CDM with glucose: bacteria incubated without propionic acid grew to an OD of 0.8 with glucose and only 0.4 with pyruvate. Therefore, sodium pyruvate was demonstrated not to be as good a substrate for *N. meningitidis* growth as glucose, and the effect of added propionic acid could be very clearly seen.

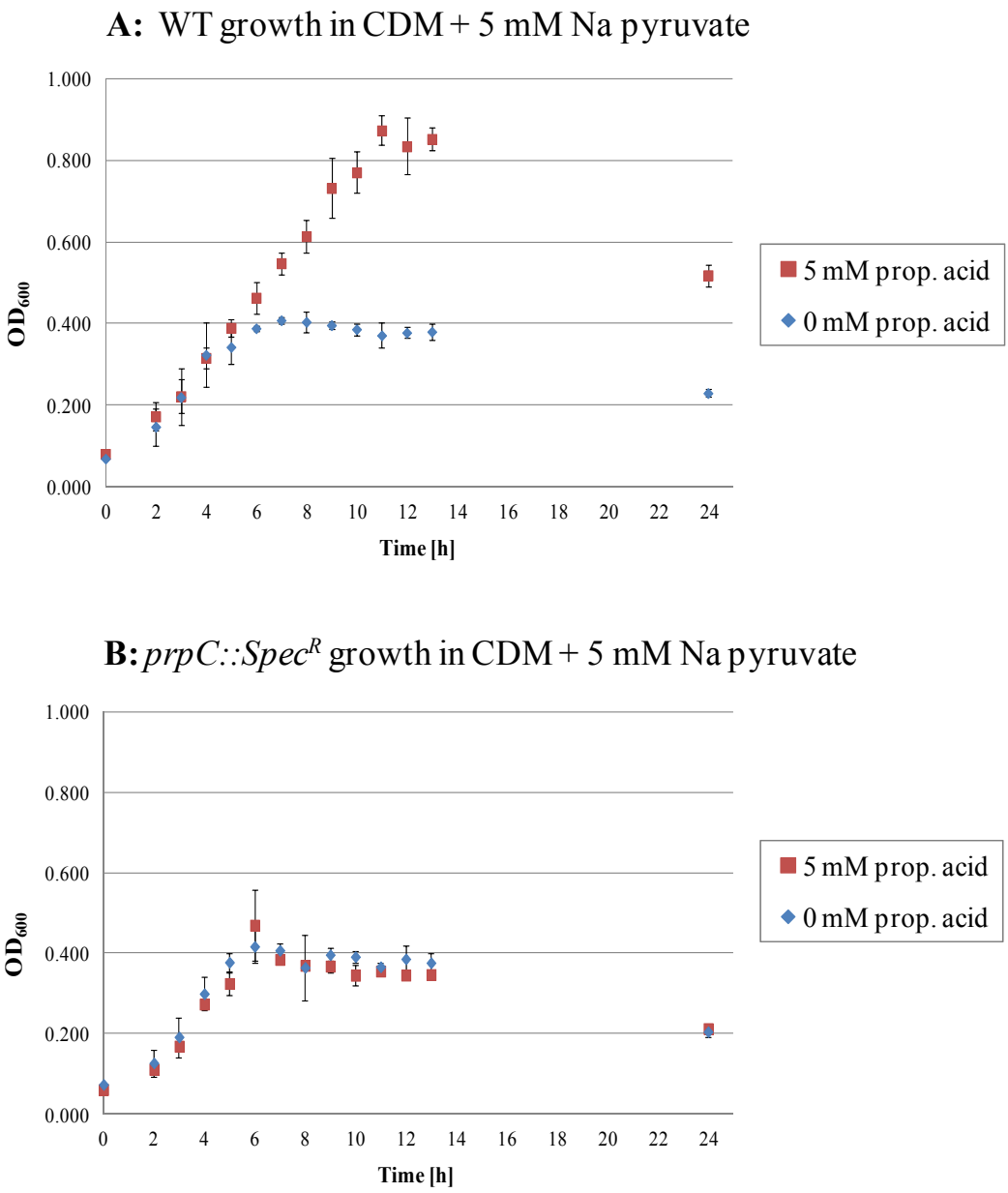

Figure 3.6-4: Growth curve of MC58 wild-type and *prpC::Spec*^{R} strains of *N. meningitidis* in CDM with 5 mM sodium pyruvate and propionic acid.

A: Bacterial growth of wild-type *N. meningitidis*, with enhanced growth when in the presence of propionic acid. Instead of entering the stationary phase, wild-type bacteria used propionic acid for continued growth. **B:** Bacterial growth of *prpC::Spec*^{R} strain. Propionic acid did not have any influence in the mutant's growth, as the mutant was unable to utilise propionic acid due to the absence of the *prpC* gene.

As mentioned above, MC58 wild-type and *prpC::Spec*^{R} mutant strains of *N. meningitidis* grew similarly when their growth in the same medium, supplemented with or lacking propionic acid, was compared, until the wild-type bacteria in minimal medium without propionic acid or the mutant strain under both growth conditions entered stationary phase. At this point, only wild-type bacteria started to utilise propionic acid. From the figures shown above, both strains seemed to have a similar doubling time when grown in the same medium with or without propionic acid during the exponential growth phase. The doubling times for each dataset were extrapolated from the linear equations that were derived from plots of $Log_{10}(OD_{600})$ against time. The gradient of the linear trendline during exponential growth phase was automatically calculated by excel and given within the equation, as shown in the example graph below (Figure 3.6-5). The doubling time was then calculated by dividing $\log_{10}$ (2) by each gradient. Results were then averaged with each corresponding datasets (Table 3.6-1 and Figure 3.6-6).

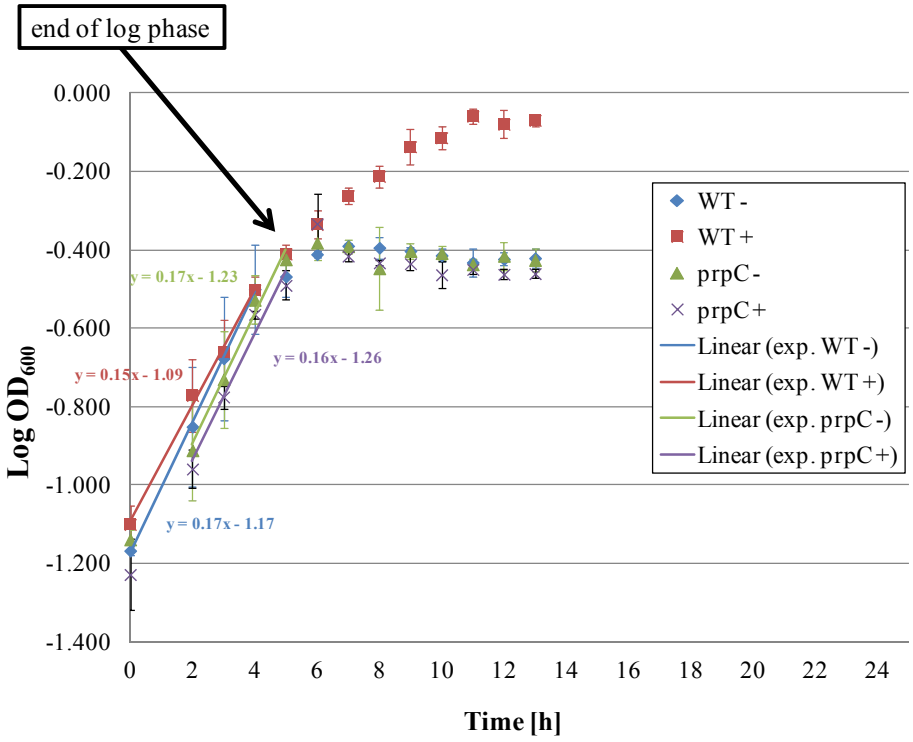

Figure 3.6-5: Log_{10} OD of MC58 wild-type and *prpC::Spec*^{R} strains of *N. meningitidis* in CDM supplemented with 5 mM sodium pyruvate and propionic acid.

A logarithmic graph was plotted for the OD values gathered during the growth curve. Trendlines for exponential growth phase were added to the graph, and the gradient was automatically calculated by excel. The doubling time of each strain under each condition was then extrapolated from the equations by dividing $\log_{10}$ (2) by their relative gradient. WT+: wild-type bacteria grown in CDM with pyruvate and 5 mM propionic acid. WT-: wild-type bacteria grown in CDM with pyruvate. *prpC*+: *prpC::Spec*^{R} mutants grown in CDM with pyruvate and 5 mM propionic acid. *prpC*-: *prpC::Spec*^{R} mutants grown in CDM with pyruvate.

Similarity in doubling time was confirmed and fell within the values from Table 3.6-1, where the actual doubling times calculated were extrapolated from at least 5 independent datasets. The same datasets were also plotted visually, where it was

easier to compare the doubling times for each growth medium. The doubling times were comparable within both strains for every growth medium: they were significantly shorter in rich MHB medium (approximately 80 minutes), but were similar within the two chemically defined media (100 and 110 minutes for CDM with glucose and pyruvate respectively) (Figure 3.6-6).

Table 3.6-1: Doubling time of MC58 wild-type and *prpC::Spec*^{R} mutant strains of *N. meningitidis* in the three different growth media with the addition of propionic acid, during exponential growth phase.

The summary of the doubling times was obtained from at least 5 independent sets of data for each strain. Both strains showed a shorter time of duplication when grown in rich medium compared to minimal medium. Doubling time of both strains grown in either minimal medium was not significantly different. -: growth medium not supplemented with propionic acid. +: growth medium supplemented with 5 mM propionic acid.

Doubling time [hours] / Strain	Average in MHB	Average in CDM+glucose	Average in CDM+pyruvate
MC58 WT -	1.27 ± 0.12	1.72 ± 0.19	1.76 ± 0.19
MC58 WT +	1.31 ± 0.06	1.59 ± 0.14	1.76 ± 0.17
prpC::Spec^R -	1.21 ± 0.10	1.70 ± 0.08	1.78 ± 0.22
prpC::Spec^R +	1.32 ± 0.12	1.65 ± 0.09	1.84 ± 0.24

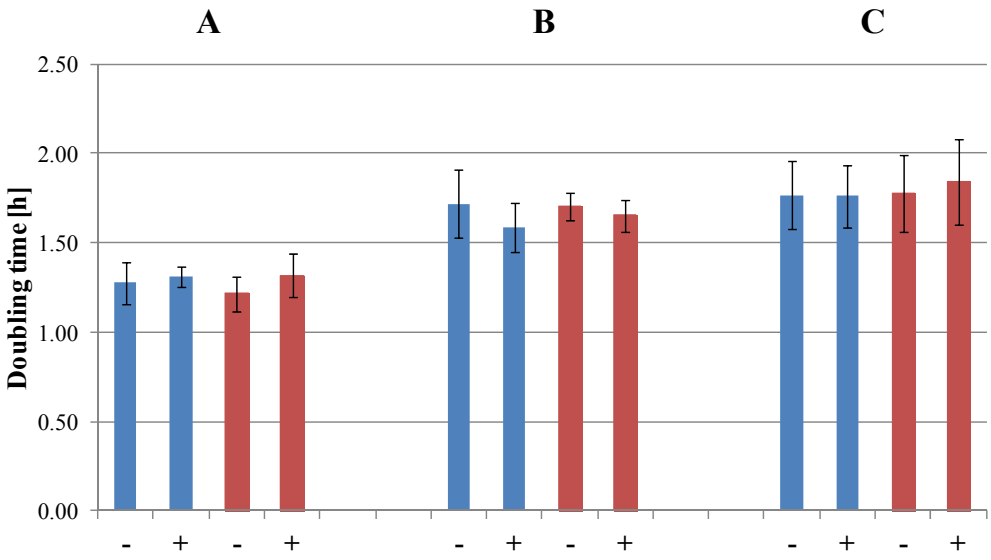

Figure 3.6-6: Doubling time of MC58 wild-type and *prpC::Spec*^{R} mutant strains of *N. meningitidis* in the three different growth media with the addition of propionic acid, during exponential growth phase.

A: Doubling time for growth in rich, MHB medium. **B:** Doubling time for growth in minimal medium, CDM with 2.5 mM glucose. **C:** Doubling time for growth in minimal medium, CDM with 5 mM sodium pyruvate. At least 5 independent sets of data were used for extrapolating the average doubling time of each strain. Doubling time was extrapolated from the exponential growth. Wild-type (blue columns) and *prpC::Spec*^{R} mutant (red columns) showed similar doubling times when the strains were compared within the same growth medium, independently of the presence or absence of propionic acid. -: growth medium not supplemented with propionic acid. +: growth medium supplemented with 5 mM propionic acid.

The delay in propionic acid utilisation in minimal media could be explained by the fact that wild-type bacteria needed several hours to be able to adapt to the new media containing propionic acid in order to activate the 2-methylcitrate pathway and, consequently, to be capable of starting to catabolise propionic acid. Another possible explanation for the delay in propionic acid utilisation could be due to the fact that the

prp gene cluster needs to be activated, possibly by the presence of the 2-methylcitrate compound within the cell (Palacios *et al.*, 2003). In order to build up an optimal concentration of 2-methylcitrate for activating this pathway, enough propionyl-CoA needed to be raised first, as this compound is the substrate of *prpC,* a crucial enzyme belonging to the pathway being investigated. The *prpC::Spec*^{R} mutant confirmed this result by being unable to metabolise propionic acid, a substrate needed in the metabolic pathway which was disrupted by the *prpC* gene knockout.

3.7 Utilisation of propionic acid in *N. meningitidis*

As shown in the previous section, propionic acid appears to be utilised as an extra source of carbon during late exponential phase in *N. meningitidis* MC58. To confirm these findings, samples for both strains and from all three growth media were collected at 60 minute intervals, and the content of propionic acid was measured by gas chromatography (GC). Chromatograms were automatically plotted and the area for propionic acid was extrapolated. A representative chromatogram is shown in Figure 3.7-1, where samples for bacteria grown in CDM with 2.5 mM glucose and none or 5 mM propionic acid were collected at the start of the growth curve.

Initially, propionic acid controls containing varying amounts of propionic acid were measured by gas chromatography, in order to check for differences in the readings which were caused by the different growth media compared with standard controls made with deionised water. Reproducibility of data, threshold levels for propionic acid detection and its volatility in the media over an extended period of time were checked. GC results for the controls were comparable independently of the growth

medium used. Moreover, the presence of propionic acid resulted in different peak sizes, depending on the amount of propionic acid that was added in solution. To check how volatile the short fatty acid was, controls were made with all three growth media, Mueller Hinton Broth, Chemically Defined medium with 2.5 mM glucose and Chemically Defined medium with 2.5 mM sodium pyruvate, supplemented with 5 mM propionic acid but which were not inoculated with bacteria, and were incubated in 30 ml polystyrene universal tubes (Sterilin®) at 37 ºC to replicate an extended growth culture over a three days period; GC readings taken twice per day, starting at time 0 when the incubation was just set up, showed that there was no significant loss in concentration of propionic acid. This control experiment confirmed that the decrease in concentration of propionic acid during bacterial incubation was due solely to its actual utilisation by the bacteria present in the medium, and not by its volatility.

Samples for both MC58 wild-type and *prpC::Spec*^{R} strains that were grown in media where propionic acid was not added were checked too. Gas chromatography results were always null, as no propionic acid was ever detected from cultures which were not supplied with propionic acid. When propionic acid was added into the media *prpC::Spec*^{R} mutant bacteria, as anticipated, were not able to use propionic acid under any growth condition. Wild-type bacteria, however, showed some differences.

When incubated in Mueller Hinton Broth medium, neither wild-type nor *prpC::Spec*^{R} bacteria used the propionic acid that was supplemented in the medium (Figure 3.7-2). Both strains entered quickly the exponential growth phase and did not need to utilise propionic acid for enhancing bacterial growth, as the medium was already rich in carbon. Major differences, however, were seen when bacteria were

grown in Chemically Defined Medium (CDM) with either 2.5 mM glucose or 5 mM sodium pyruvate supplemented with 5 mM propionic acid. MC58 wild-type bacteria started to use propionic acid after 5 to 6 hours incubation, independently of the CDM used (Figure 3.7-3). Growth curves from the previous section (Figure 3.6-3 and Figure 3.6-4) showed that wild-type bacteria supplemented with propionic acid followed enhanced growth, thus avoiding entering stationary phase, after approximately 7-8 hours in CDM with glucose, and already after 5-6 hours in CDM with pyruvate. This meant that propionic acid utilisation began in late exponential / stationary phase in CDM supplemented with glucose, and concomitant with entry into stationary phase in CDM supplemented with pyruvate.

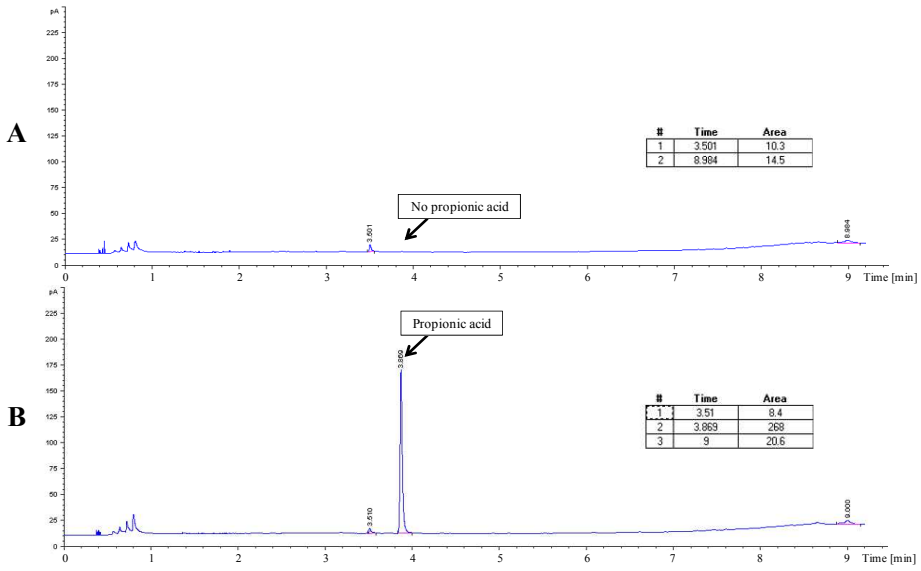

Figure 3.7-1: Representative GC chromatograms showing the absence / presence of propionic acid.

Bacteria were grown aerobically overnight at 37 ºC in media containing none or 5 mM propionic acid. Samples were collected every 60 minutes and GC chromatograms were checked for the area of propionic acid. No peak for propionic acid was detected in samples where this fatty acid was not added **(A)** and varying peak sizes were detected over time in the media where propionic acid was added and utilised **(B)**.

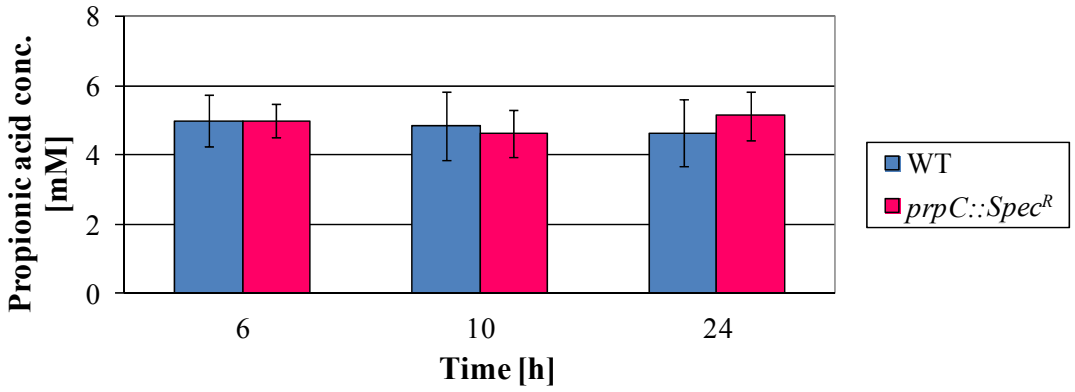

Figure 3.7-2: Propionic acid was not utilised in MHB medium.

Gas chromatography results for a few samples of MC58 wild-type and *prpC::Spec*^{R} showed that the amount of propionic acid in the rich medium remained constant throughout the 24 hours incubation period.

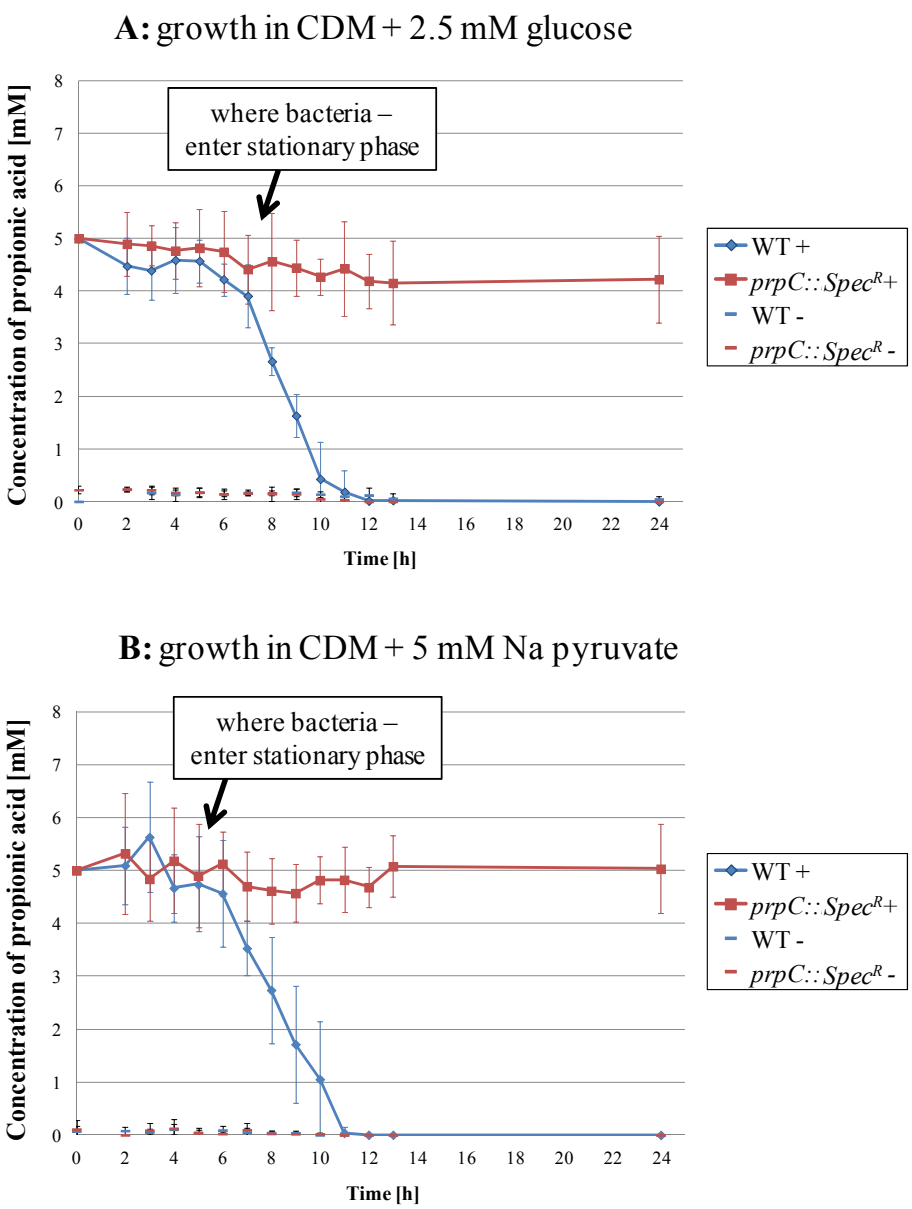

Figure 3.7-3: Propionic acid was utilised in minimal media.

Concentration of propionic acid versus time for bacteria grown in CDM media with 2.5 mM glucose (**A**) and 5 mM sodium pyruvate (**B**), with or without addition of 5 mM propionic acid. In both panels, gas chromatography results for MC58 wild-type and *prpC::Spec*^{R} *N. meningitidis* showed that propionic acid supplemented in both chemically defined media was utilised only by the wild-type strain, and was completely depleted after 24 hours growth. Controls where no propionic acid was added showed that propionic acid was not present throughout the growth curve for both bacteria. -: No propionic added to the medium. +: 5 mM propionic acid added at the start.

Samples from both MC58 wild-type and *prpC::Spec*^{R} bacteria that were grown where propionic acid was not added to the media were checked by gas chromatography and results, which showed that no propionic acid was detected throughout the whole growth curve, demonstrated that propionic acid is not synthesised under any experimental conditions that were investigated in this work. Moreover, *prpC::Spec*^{R} mutant bacteria were never able to utilise propionic acid, indicating that the 2-methylcitrate pathway is not functional on inactivation of the putative methylcitrate synthase *prpC* gene *NMB0431*. This result confirmed the involvement of the *prpC* gene in the pathway, and showed that the gene is indispensable for the pathway to be functional.

3.8 *prpC* gene expression in *N. meningitidis* in the presence of propionic acid

To check if the 2-methylcitrate pathway was activated during growth in media supplemented with propionic acid, and to check therefore if *prpC* gene expression increased in the same manner as propionic acid was being catabolised by the wild-type *N. meningitidis* MC58, as shown by gas chromatography, time course studies of the expression of the *prpC* gene were performed in all three media.

Wild-type bacteria were grown either in rich medium or in minimal medium, which was supplemented with none or 5 mM propionic acid, at 37 °C and shaking at 200 rpm over a period of 12 hours. An initial 1 ml aliquot was removed from each culture after 4 hours incubation, and every 2 hours following that, until the last 12 hours samples were collected. Each aliquot was spun down for 60 seconds at 12000 rpm with a Sigma 1-13 microcentrifuge (Sigma), and the pellets were immediately stored at - 80 ºC overnight, until RNA was extracted and reverse transcribed to cDNA for

Quantitative Real-Time PCR (RT-PCR) studies. All the procedures used in this step were described in Sections 2.3.12 – 2.3.14.

RT-PCR studies were carried out to check the expression level of the *prpC* gene in MC58 wild-type, and expression was then compared to the one from the *prpC::Spec*^{R} strain. The data obtained from each study was calibrated with the wild-type bacteria grown in MHB which was not supplemented with propionic acid. The data was also compared and normalised to the housekeeping *metK* gene (*NMB1799*), which encodes S-adenosylmethionine synthetase, so that discrepancies due to different amounts of starting total RNA extracted from each sample could be eliminated. The expression of the *gltA* gene (*NMB0954*), encoding the citrate synthase, was also checked as an extra control, and was then compared to the *prpC* gene. Data for the average fold change in expression of the triplicates that were set up in each 96-Well Optical Reaction Plate (Applied Biosystems) were plotted on a logarithmic scale in base 10.

Wild-type bacteria that were initially grown in Mueller Hinton Broth (MHB) medium with propionic acid showed a gradual increase in *prpC* expression, despite not using propionic acid for growth. Interestingly, also the culture that was grown without this fatty acid behaved similarly, and this could be explained by the expression of *prpC* not being induced directly by propionic acid. *gltA* levels did not vary much, but the increase in its expression coincided with increase in the *prpC* gene (Figure 3.8-1A).

Wild-type bacteria grown in minimal media had a higher expression of the gene earlier in the growth curve compared to those grown in rich medium. Bacteria

incubated in CDM with 2.5 mM glucose showed a similar pattern of *prpC* expression to the ones grown in MHB. Expression in this second case, however, started earlier, as after 8 hours growth its levels were significantly higher than in MHB. Expression level was also very pronounced, as 40-fold (without propionic acid) or 20-fold (when the medium was supplemented with propionic acid) increase in expression was seen (Figure 3.8-1B). A major increase in expression level happened between 6 hours and 8 hours growth, and this corresponded to the turning point seen at 8 hours, when wild-type bacteria had already started to utilise propionic acid for supporting growth instead of entering the stationary phase.

In CDM with 5 mM sodium pyruvate, *prpC* gene in wild-type bacteria was highly induced during the whole growth: a large amount of expression was already obvious when the first sample was collected after 4 hours incubation. Increase varied between 5 and 25-fold when compared to the calibrator (Figure 3.8-1C). The high levels of the gene expression under study that were recorded at all times might have been due to the fact that bacteria struggled to grow in pyruvate, and therefore they might have activated the 2-methylcitrate pathway sooner, in order to be able to catabolise propionic acid as an extra source of carbon. In fact, bacteria that were not supplied with propionic acid, when grown in this medium, started to die already after only 5 or 6 hours incubation.

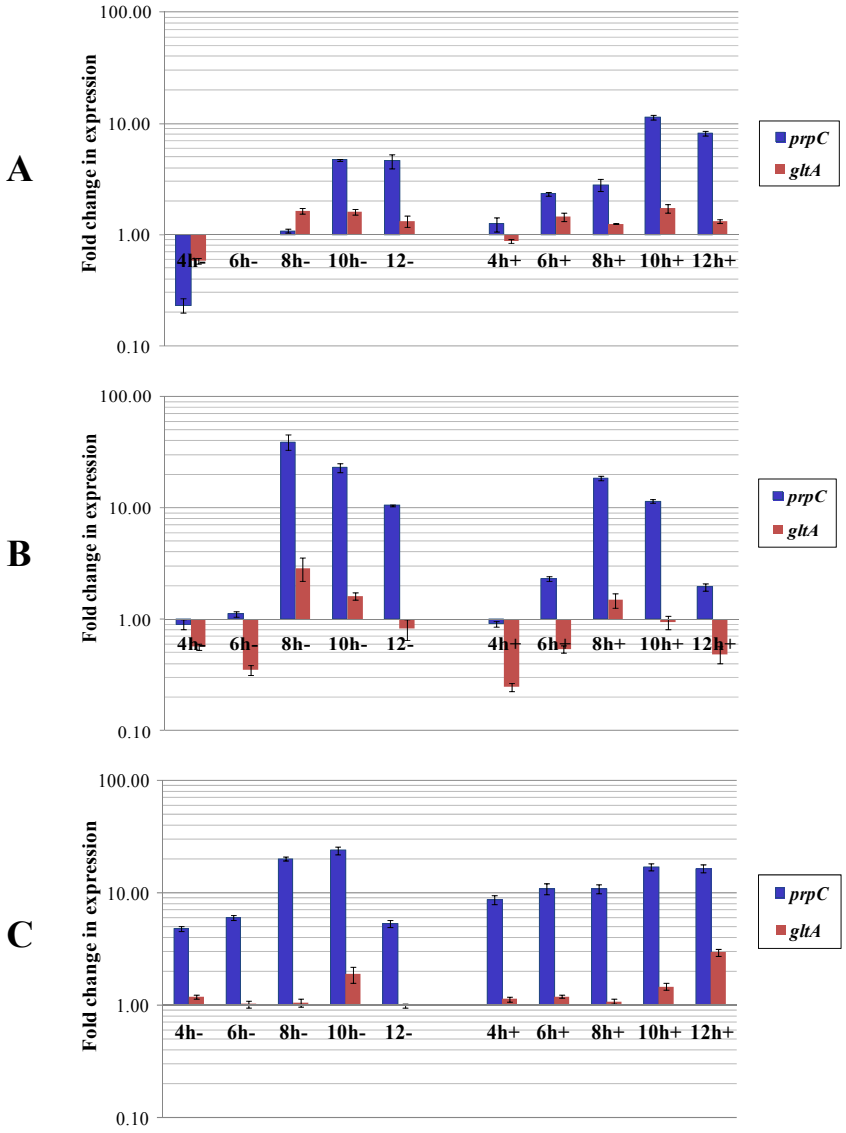

Figure 3.8-1: Average fold change of *prpC* and *gltA* gene expression in MC58 wild-type *N. meningitidis* in different growth media in a time course experiment. Relative expression of *prpC* was plotted for wild-type cultures grown in MHB (**A**) and in CDM with 2.5 mM glucose (**B**) or 5 mM sodium pyruvate (**C**) with 0 or 5 mM propionic acid. Data was normalised with *metK* and calibrated with the wild-type culture that was grown for 6 hours in MHB without propionic acid. Expression of *prpC* increased throughout the time course, and this was independent of the absence / presence of propionic acid. Expression level was higher in minimal medium; the gene was constantly expressed in CDM with pyruvate. Expression of *gltA* (encoding citrate synthase) did not vary much, and followed the pattern of *prpC* gene expression, but to a much lower extent. - / +: growth media with 0 / 5 mM propionic acid added at the start.

prpC gene expression was higher when nutrient availability was poor: the poorer the nutrient availability, the higher the *prpC* gene expression. In fact, when *N. meningitidis* was entering stationary phase or when the growth medium did not have a good carbon substrate, the gene was always highly expressed. Moreover, the *prpC* gene expression for the *prpC::Spec*^{R} mutant was always down-regulated, as expected, since the gene was knocked out.

3.9 Role of *NMB0432* and *ackA-1* in propionic acid utilisation

The genes *NMB0432*, encoding a conserved hypothetical protein, and *ackA-1* (*NMB0435*), encoding an acetate (or propionate) kinase, from *N. meningitidis* MC58 were knocked out with insertion of either a tetracycline resistance cassette (*NMB0432*) or a spectinomycin resistance cassette (*NMB0432* and *ackA-1*) within the genes being investigated, as described in Section 3.5.

Growth curves under the same conditions tested with the MC58 wild-type and the *prpC::Spec*^{R} strain from the previous sections were investigated, and the three new mutants, *NMB0432::Tet*^{R}, *NMB0432::Spec*^{R} and *ackA-1::Spec*^{R} showed the same phenotype as *prpC::Spec*^{R}. This meant that, when grown in rich medium, all strains grew similarly over the 13 hours incubation. In chemically defined medium with either 2.5 mM glucose or 5 mM sodium pyruvate, bacteria grew similarly and, in both cases, only wild-type bacteria supplemented with 5 mM propionic acid were able to grow further (Figure 3.9-1).

At this stage, propionic acid utilisation within CDM medium containing pyruvate was investigated with gas chromatography. As expected from the growth curve results and from the identical behaviour noticed with the *prpC::Spec*^{R} strain, the

three mutants were unable to catabolise propionic acid, and only the wild-type bacteria did (Figure 3.9-2).

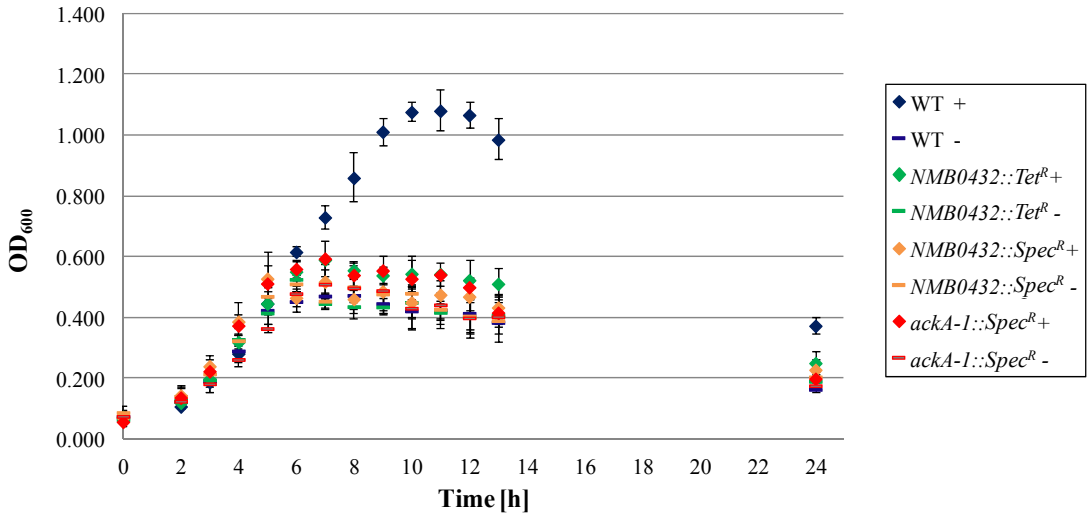

Figure 3.9-1: Growth curve of MC58 wild-type, *NMB0432::Spec^R/Tet^R* and *ackA-1::Spec^R* strains of *N. meningitidis* in CDM with 5 mM sodium pyruvate and propionic acid.

Propionic acid was necessary for continued growth of wild-type *N. meningitidis* in minimal medium. The three mutant strains that were grown either with or without supplementation of propionic acid, as well as the wild-type strain that was grown with no propionic acid, all entered stationary and death phase several hours earlier than wild-type bacteria supplemented with propionic acid. Strains tested here were *NMB0432::Tet^R* and *NMB0432::Spec^R*, where the *NMB0432* gene was knocked out either with tetracycline or with spectinomycin resistance cassette, and *ackA-1::Spec^R*, where the *ackA-1* gene (*NMB0435*) was knocked out with insertion of a spectinomycin resistance cassette. -: CDM medium with 5 mM sodium pyruvate and no supplementation of propionic acid. +: CDM medium with 5 mM sodium pyruvate and 5 mM propionic acid added at the start of the bacterial growth.

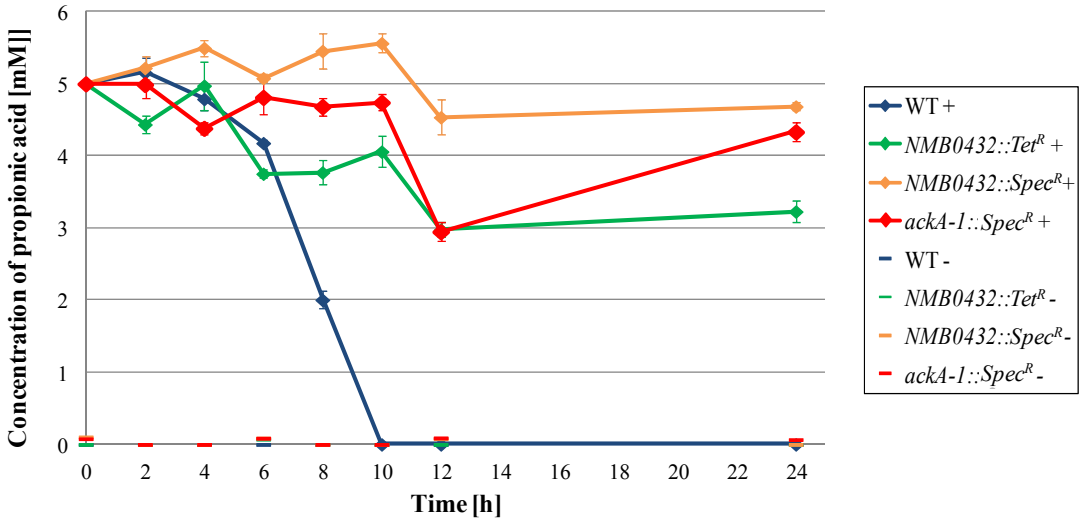

Figure 3.9-2: Propionic acid utilisation in MC58 wild-type, *NMB0432::Spec^R/Tet^R* and *ackA-1::Spec^R* strains of *N. meningitidis* in CDM with 5 mM sodium pyruvate and propionic acid.

Propionic acid was utilised only by the wild-type strain grown in 5 mM propionic acid. The three mutant strains were not able to use it. Strains tested here were MC58 wild-type, *NMB0432::Tet^R* and *NMB0432::Spec^R*, where the *NMB0432* gene was knocked out either with tetracycline or with spectinomycin resistance cassette, and *ackA-1::Spec^R*, where the *ackA-1* gene (*NMB0435*) was knocked out with insertion of a spectinomycin resistance cassette. -: CDM medium with 5 mM sodium pyruvate and no supplementation of propionic acid. +: CDM medium with 5 mM sodium pyruvate and 5 mM propionic acid added at the start of the bacterial growth.

The results illustrated in this section showed that both *NMB0432* and *ackA-1* genes were directly involved in the catabolism of propionic acid as, when they are disrupted, bacteria were not able to utilise the short fatty acid. Moreover, as they behaved in the exact same way as bacteria with the disrupted *prpC* gene, these genes appeared to belong to the 2-methylcitrate pathway. This was an interesting point as *NMB0432* has no predicted role associated with this pathway. In fact, this gene,

which contains a predicted permease domain, is absent from the *prp* operon in the other bacteria that possess the 2-methylcitrate pathway, with an exception of its closely related *Neisseria gonorrhoeae*. The *NMB0432* gene, therefore, might be a late addition to the *prp* gene cluster of *Neisseria* for helping them with propionic acid acquisition, due to the specific niche where these bacteria live. Likewise, the *ackA-1* gene is not found within the *prp* operon in any other bacteria, so it could be needed for adaptation in *Neisseria*.

3.10 The *prp* gene cluster is an operon

In order to check if the genes predicted to belong to the *prp* operon in *N. meningitidis* MC58 were actually organised in a fully functional operon, several mutants with disrupted genes from the *prp* gene cluster were tested.

From the previous sections within this chapter, I have demonstrated that the *prpC*, *NMB0432* and *ackA-1* (*NMB0435*) genes were all needed to catabolise propionic acid, which is the substrate for the 2-methylcitrate pathway, and this pathway is composed of genes belonging to the *prp* gene cluster. Because of being involved in the 2-methylcitrate pathway, these genes were checked for expression levels in Chemically Defined Medium containing 5 mM sodium pyruvate and 5 mM propionic acid. This medium was chosen because it was shown to be overexpressing the *prpC* gene more consistently than the other media, so that exact timing for expression levels was not so important (refer to Figure 3.8-1C). Total RNA was extracted from 1 ml of each culture grown for 6 hours, and cDNA was then reverse transcribed for expression studies. Mutants analysed were *prpC::Spec*^{R} (for gene *NMB0431*), *NMB0432::Spec*^{R} and *ackA-1::Spec*^{R} (for gene *NMB0435*), where the gene under

study was disrupted with a spectinomycin cassette. An extra mutant for the gene *NMB0432*, *NMB0432::Tet*^{R}, was created by disrupting this gene with a tetracycline cassette.

When grown in CDM with pyruvate for 6 hours, all strains except *prpC::Spec*^{R} did indeed confirm that the *prpC* gene was up-regulated compared to the calibrator control, the calibrator being wild-type bacteria grown for 6 hours in MHB without supplementation of propionic acid.

In wild-type bacteria, the three genes contiguous and downstream of the *prpC* gene were also similarly expressed to the *prpC* gene, independently of the presence or absence of propionic acid within the medium (Figure 3.10-1A). Expression data also confirmed that the *prpC* gene (*NMB0431*) in the *prpC::Spec*^{R} mutant was down-regulated, and the same was valid for the two following genes, *NMB0432* and *NMB0433*. Expression levels for the gene *NMB0434* was not checked for this strain (Figure 3.10-1B).

When both *NMB0432* mutant strains were analysed, the gene upstream of *NMB0432* was expressed similarly to the *prpC* gene (*NMB0431*) from the wild-type, as expected. The disrupted gene, however, behaved in two different ways: in the *NMB0432::Tet*^{R} strain the *NMB0432* gene and its downstream genes were still up-regulated, whereas in the *NMB0432::Spec*^{R} strain these genes, including *NMB0432*, were down-regulated (Figure 3.10-1C). This difference in behaviour was due to the fact that the tetracycline cassette has no transcriptional terminators, but the spectinomycin cassette possesses two of them, one at either end of the cassette (Prentki & Krisch, 1984).

ackA-1::Spec^R did not affect gene expression of the genes analysed and appeared to behave in the same way as wild-type bacteria. This was due to the fact that *ackA-1* (*NMB0435*) is the last gene within the *prp* gene cluster, and therefore this mutant did not have any effect in any of the genes upstream from it (Figure 3.10-1D).

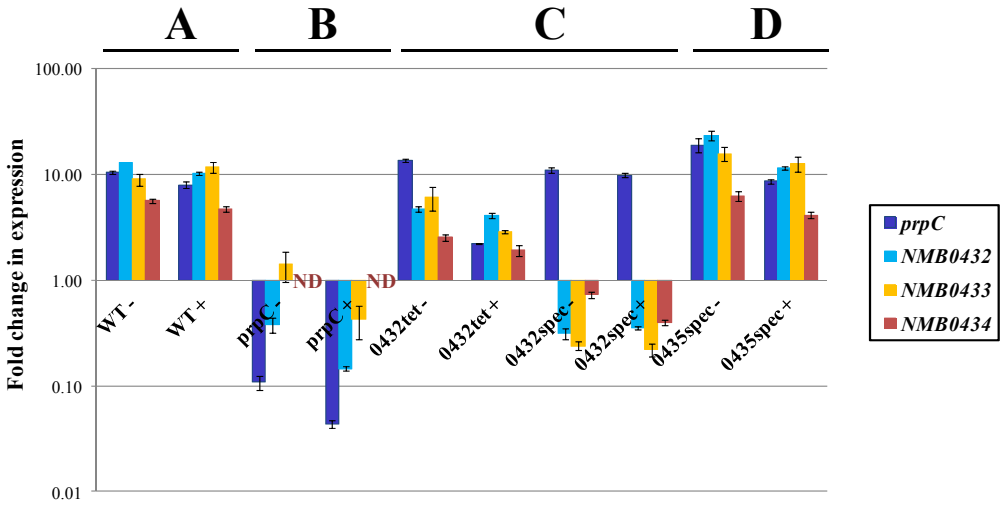

Figure 3.10-1: Average fold change in expression of several genes from the *prp* gene cluster in wild-type and mutant strains in *N. meningitidis* MC58.

Relative expression of the *prpC* gene (*NMB0431*) and the three downstream genes was plotted for wild-type cultures and for several single mutant strains with mutations in the genes from the *prp* gene cluster. All cultures were grown in CDM + 5 mM sodium pyruvate with or without supplementation of 5 mM propionic acid, and samples were collected after 6 hours growth. Data was normalised with *metK* and calibrated with the wild-type culture that was grown for 6 hours in MHB without addition of propionic acid. All downstream genes of each mutant in question were down-regulated, except for the *NMB0432::Tet*^{R} (tetracycline cassette, unlike the spectinomycin cassette, has no transcriptional terminators). -: medium with no supplementation of propionic acid. +: medium with 5 mM propionic acid. Bacterial strains used: MC58 wild-type and single mutant strains for *prpC* (disrupted with Spec), *NMB0432* (disrupted with Tet or Spec) and *NMB0435* (disrupted with Spec). *prpC*: encodes 2-methylcitrate synthase. *metK*: gene encoding S-adenosylmethionine synthetase. ND: no data collected for *NMB0434* in *prpC::Spec*^{R} mutant.

Gene expression showed that the adjacent genes studied here were linked together, as they were regulated in the same way and down-regulated by disruption with antibiotic resistance cassettes containing transcriptional terminators. However, in order to confirm once more if they were expressed as an operon, total RNA was extracted and cDNA generated prior to analysis by running a PCR to amplify all intergenic regions present in the operon. Only the intergenic regions between polycistronically expressed genes would be amplified and, therefore, seen when run on an agarose gel.

Total RNA from wild-type *N. meningitidis* MC58 grown in CDM with 5 mM sodium pyruvate and 5 mM propionic acid was extracted and purified. Purified total RNA was then reverse transcribed to cDNA using the SuperScript^{TM} II Reverse Transcriptase kit (Invitrogen^{TM}) as described in Section 2.3.13, and stored at -80 ºC to avoid degradation. The strain and the medium for growth were chosen because the genes in the *prp* gene cluster were up-regulated under those conditions. A PCR with reactions prepared as described in Section 2.3.1 and with primers from Table 2.3.14-1 was run with both purified total RNA and the corresponding cDNA, and a 0.8 % agarose gel was consequently run for 60 minutes (Figure 3.10-2). Bands were expected to be seen only from the cDNA samples, as the RNA would not be able to amplify unless contaminated with genomic DNA. Primers were chosen so that each pair would amplify the region located between each gene belonging to the *prp* gene cluster. The intergenic regions just before the start or just after the last gene of the *prp* cluster were amplified too, to verify that the two adjacent genes were not transcribed together as part of the same operon.

PCR reactions worked fine, as cDNA amplified correctly. The first and last lane of the cDNA samples did not show any band, and this was due to the fact that both regions were found outside the *prp* gene cluster. All other regions amplified correctly, despite one lane resulting in a smeared product. RNA should not have amplified at all, but products for two of the intergenic regions were present, even though in a much lower intensity compared to the same samples for cDNA. This meant that both samples were probably contaminated with genomic DNA, despite all RNA samples having been treated with the On-Column DNase Digestion (QIAGEN) during RNA purification (Figure 3.10-3). Nonetheless, the increase in band intensity in the cDNA lanes indicates that messenger RNA contained the intergenic region between each of the genes in the *prp* cluster. Moreover, despite the intergenic region between genes *NMB0433* and *NMB0434* failing to amplify, these two genes were confirmed to belong to the same *prp* gene cluster: in fact, they were up-regulated or down-regulated similarly in all *N. meningitidis* mutant strains tested, as previously shown in Figure 3.10-1.

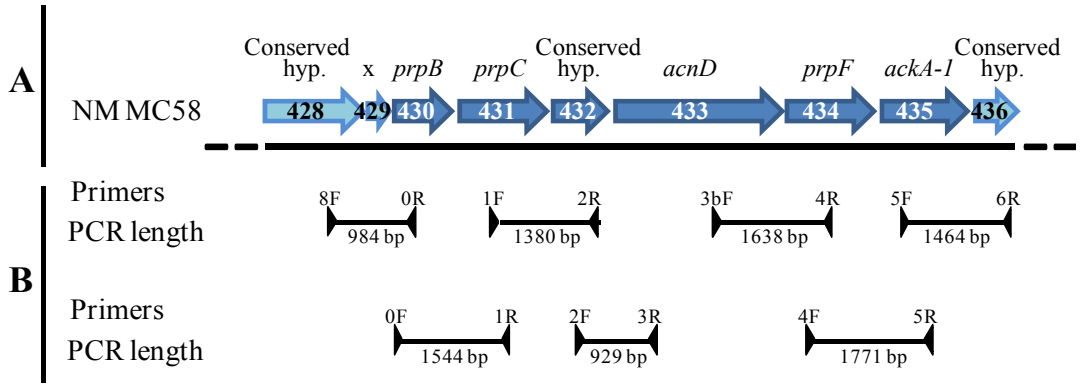

Figure 3.10-2: ORF map of the *prp* gene cluster of *N. meningitidis* MC58, with primers used to amplify the intergenic regions.

A: The relevant region of *N. meningitidis* MC58 genome representing the genes belonging to the *prp* gene cluster (dark blue arrows) and its flanking genes (light blue arrows) is shown with the orientation of each gene. Gene numbers correspond to the numbering given in the MC58 complete genome, where the number within each arrow is preceded by "NMB0" (NCBI GenBank accession number AE002098.2). **B:** The position of all sets of primers used to amplify the intergenic regions within and adjacent to the *prp* gene cluster (black arrows) and the products' relative length (black lines). NM MC58: *N. meningitidis* strain MC58 wild-type. Conserved hyp.: gene coding for a conserved hypothetical protein. 429, which corresponds to *NMB0429*, encodes a very short hypothetical protein. 8: *NMB0428*; 0: *NMB0430*; 1: *NMB0431*; 2: *NMB0432*; 3: *NMB0433*; 4: *NMB0434*; 5: *NMB0435*; 6: *NMB0436*. F: Forward primer. R: Reverse primer.

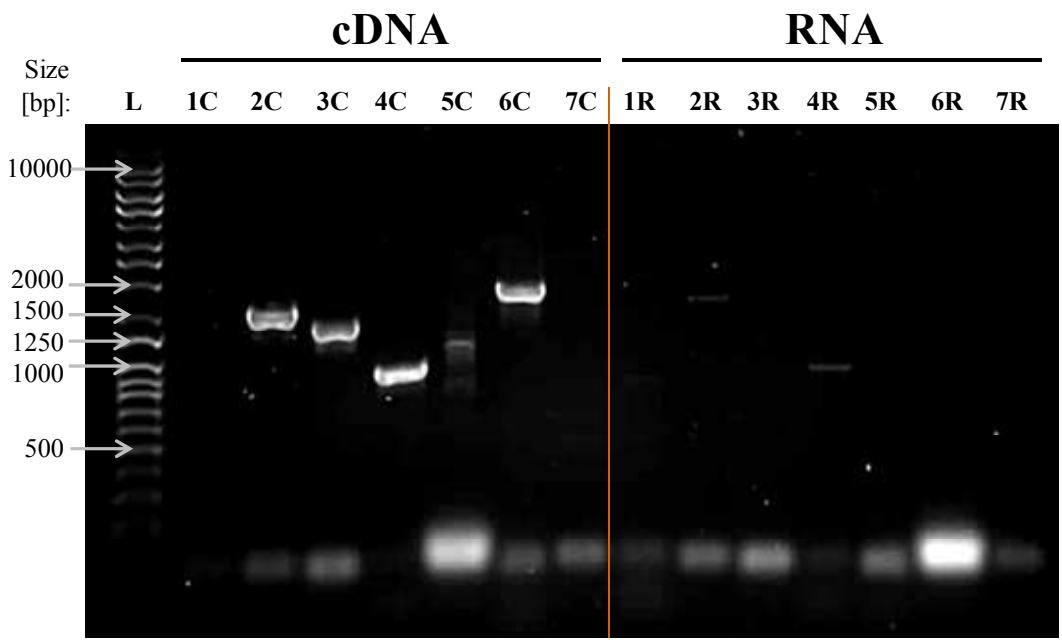

Figure 3.10-3: Amplification of cDNA versus RNA for the intergenic regions of the *prp* operon in wild-type *N. meningitidis* MC58.

Amplification of the intergenic regions of the *prp* operon was run using cDNA as template, and RNA as negative control. Wild-type bacteria grown in Chemically Defined Medium supplemented with 5 mM sodium pyruvate and 5 mM propionic acid were chosen because the genes are overexpressed under those conditions. In lanes 1C and 7C no bands were expected, as they corresponded to the intergenic regions just outside the *prp* gene cluster. Lane 5C failed to amplify the correct product and resulted in a smeared product, whereas lanes 2R and 4R showed little contamination in the samples. Intergenic regions between the genes analysed and their corresponding PCR fragment sizes for the cDNA are as follows: 1: *NMB0428-NMB0430*, no fragment expected (which would be 984 bp in length). 2: *NMB0430-NMB0431*, 1544 bp. 3: *NMB0431-NMB0432*, 1380 bp. 4: *NMB0432-NMB0433*, 929 bp. 5: *NMB0433-NMB0434*, 1638 bp. 6: *NMB0434-NMB0435*, 1771 bp. 7: *NMB0435-NMB0436*, no fragment expected (which would be 1464 bp). C: cDNA. R: RNA. The Q-Step 4 Quantitative DNA ladder (YORBIO) (Lane L) was loaded on the gel to confirm the size of the DNA bands seen.

3.11 *prpC* gene expression in enriched growth medium

prpC gene expression for bacteria that were grown in both rich and minimal medium after supplementation of several amino acids or Vitox was investigated. As already shown in Figure 3.8-1, expression of the *prpC* gene after 6 hours growth was lower in Mueller Hinton Broth (MHB) medium when compared to CDM containing 5 mM sodium pyruvate. This result indicated that *prpC* gene expression was greater when bacteria were grown in a poor medium. In order to try to understand what makes the expression in rich medium 6-fold lower, several amino acids and Vitox were added into both growth media, and their effect was checked.

Initially, *N. meningitidis* was grown for 6 hours with supplementation of different amino acids. Samples were collected, RNA extracted and reverse transcribed to cDNA as described in Sections 2.3.12 – 2.3.14. The data collected from the RT-PCR run were calibrated with the wild-type bacteria grown in MHB without propionic acid, and were normalised to the housekeeping *metK* gene (*NMB1799*). Wild-type bacteria that were grown in MHB medium supplemented with amino acids usually showed a decrease in *prpC* expression compared to the control, and this decrease depended on the various amino acids that were added in the medium, with L-cysteine hydrochloride having the most down-regulating effect (Figure 3.11-1A). Addition of amino acids into CDM with pyruvate, however, did not induce a significant change in *prpC* gene expression (Figure 3.11-1B). Even L-cysteine hydrochloride, in this case, did not alter the gene regulation.

At this stage Vitox, a commercially available culture medium supplement, was investigated instead. Vitox was supplemented at the manufacturer's recommended

concentration in all three growth media (MHB and CDM with either glucose or sodium pyruvate). As Vitox (Oxoid) contains essential growth factors, it was hypothesised that even growth in minimal medium should have a down-regulating effect over the *prpC* gene. *prpC* gene expression was down-regulated indeed (Figure 3.11-2A). Further investigations for underpinning which compound was more likely to be responsible for reducing expression were carried out. A laboratory-made Vitox was prepared fresh on the day, and all components that were present in the commercial Vitox were used at the same final concentration (Table 2.2.4-2). The samples of five independent growth curves were collected, and each time all Vitox components were made up fresh. *prpC* expression in CDM with 5 mM sodium pyruvate did not decrease, and was comparable to the expression of wild-type bacteria grown in minimal medium without Vitox (Figure 3.11-2B). Even when *N. meningitidis* was grown in minimal medium with only some of the reagents found in Vitox, expression did not change.

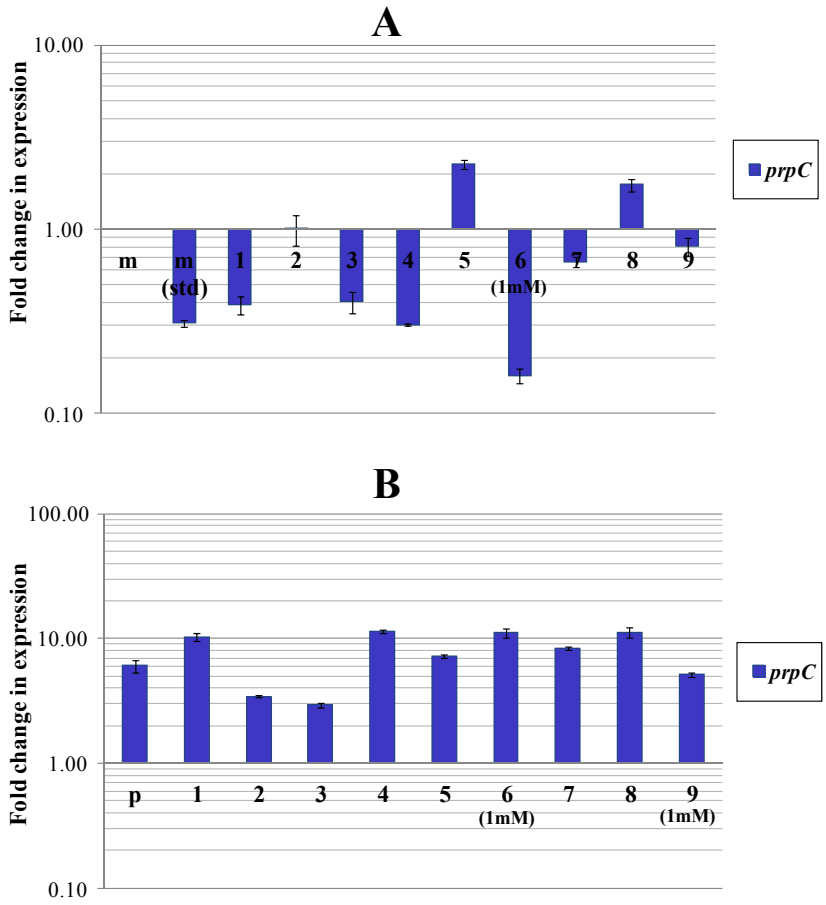

Figure 3.11-1: Average fold change of *prpC* gene expression in MC58 wild-type *N. meningitidis* in growth media enriched with amino acids.

Relative expression of *prpC* (encoding 2-methylcitrate synthase) was plotted for wild-type cultures grown in MHB **(A)** and in CDM with 5 mM sodium pyruvate **(B)** with supplementation of 5 mM amino acids (or 1 mM when specified). Data was normalised with *metK* (S-adenosylmethionine synthetase) and was calibrated with the wild-type culture that was grown for 6 hours in MHB without propionic acid. Expression level was higher in minimal medium: the gene was constantly expressed in CDM with pyruvate, but it was down-regulated in the presence of certain amino acids in MHB. Abbreviations used: m: MHB. p: CDM with 5 mM sodium pyruvate. std: amino acid solution always present in minimal media (see Table 2.2.4-1, Solution 3), but here also added to MHB. 1: L-alanine, L-isoleucine, L-leucine, L-methionine, L-valine. 2: L-phenylalanine, L-tryptophan. 3: L-aspartic acid, L-glutamic acid. 4: L-lysine, L-proline. 5: L-asparagine. 6: L-cysteine hydrochloride. 7: L-threonine. 8: L-histidine. 9: L-tyrosine.

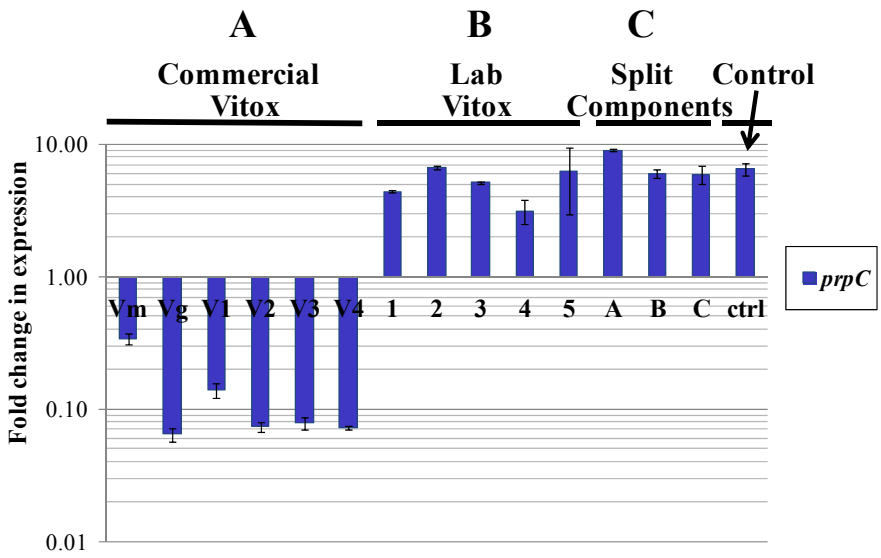

Figure 3.11-2: Average fold change of *prpC* gene expression in MC58 wild-type *N. meningitidis* in growth media enriched with Vitox.

Relative expression of *prpC* (2-methylcitrate synthase) was plotted for wild-type cultures grown in MHB (Vm), in CDM with glucose (Vg) and in CDM with sodium pyruvate (V1-V4, 4 independent repeats) enriched with commercial Vitox **(A)**; in CDM with sodium pyruvate and laboratory prepared Vitox (1-5, 5 independent repeats with freshly prepared Vitox each time) **(B)**; and in CDM with sodium pyruvate and some of the components present in Vitox **(C)**: adenine and guanine (in lane A), vitamin B_{12}, PABA, cocarboxylase, thiamine hydrochloride (in lane B) and thiamine hydrochloride alone (in lane C). *prpC* gene expression decreased when using commercial Vitox, but remained unchanged when laboratory Vitox and split components were used. The control (last lane) was wild-type bacteria grown in CDM with 5mM pyruvate. Data was normalised with *metK* (S-adenosylmethionine synthetase) and was calibrated with the wild-type culture that was grown for 6 hours in MHB without propionic acid.

Amino acids did not influence regulation in poor medium, but *prpC* gene expression was higher when nutrient availability was poor, and this was confirmed by a significant down-regulation of the *prpC* gene expression in all media containing

commercially available Vitox. Interestingly, though, expression was not affected when all components of Vitox were made up in the laboratory, despite having added them into the growth medium at the same concentration found in the commercial Vitox. To avoid chemicals becoming inactive or solutions decaying, all chemicals were ordered new for the purpose of this study and all components were prepared fresh on the day. Gene expression, however, did not decrease. Further investigations on the effects of Vitox are needed. The start point could be to test *prpC* gene expression in bacteria grown in CDM with a higher concentration of glucose, as commercial Vitox was dissolved in distilled water containing 0.55 M glucose, which was subsequently diluted into the growth medium to a final concentration of 11.10 mM glucose. Laboratory Vitox, instead, did not contain any glucose as chemicals were dissolved directly in deionised water.

3.12 Co-culture of *N. meningitidis* with *Veillonella*

In the previous sections it was shown that the *prp* gene cluster present in *N. meningitidis* MC58 was needed to catabolise propionic acid in minimal medium: in wild-type bacteria it supported growth whilst wild-type grown in an environment lacking this short fatty acid and all mutants grown with or without it reached stationary phase.

Veillonella spp. isolated from mouth washes by Dr. Stacey Fergusson (James Moir's lab), were used for co-culture growth with *N. meningitidis* wild-type and with the *prpC::Spec*^{R} mutant strain. Both bacteria were grown in Chemically Defined Medium with the addition of 5 mM sodium L-lactate instead of glucose or propionic acid, as *Veillonella* spp. needed lactate for growth (Rogosa, 1956) and *N.*

meningitidis could utilise lactate as an important energy source, especially during colonisation and growth in the nasopharyngeal tissue (Exley *et al.*, 2005).

Veillonella spp. metabolise lactate by breaking it down to propionate through fermentation, following the equation: 3 lactate → 2 propionate + 1 acetate + 1 CO_2 + 1 H_2O, thus supplying propionic acid into the minimal medium. Only wild-type *N. meningitidis* would be able to use it as a carbon source for growth and, for this reason, the hypothesis that was formulated stated that co-culture of both bacteria would show an enhanced growth in wild-type bacteria, but not in the *prpC::Spec*^{R} mutant strain.

Veillonella spp., which constitute an important part of the normal flora found in both intestine and nasopharynx of humans, are Gram-negative anaerobic cocci, whereas *N. meningitidis* are aerobic but facultative anaerobic bacteria. For this reason, initial studies involved growth of both bacteria microaerobically, where they were grown in 20 ml of medium and were shaken at 90 rpm at 37 ºC in a microbial C25KC incubator shaker (New Brunswick Scientific Ltd.) over a three-day period. All bacteria, however, struggled to grow. Further studies involved growth under the same conditions just described, but with shaking at 200 rpm instead of 90 rpm. In this instance, all bacteria except *Veillonella* that was grown on its own were able to proliferate. Co-culture of both bacteria resulted in an enhanced growth, detectable after already 6 hours incubation (Figure 3.12-1). From this preliminary experiment it was not possible to distinguish the role of each bacterium during growth, but a possible explanation would be that bacteria grown together were able to form a sort of symbiosis to help them proliferate. This symbiosis, however, did not depend on the propionate that could have been produced by *Veillonella*'s catabolism of lactate,

as both co-cultures, either containing MC58 wild-type or *prpC::Spec*^{R} mutant strain of *N. meningitidis*, grew similarly, without significant differences.

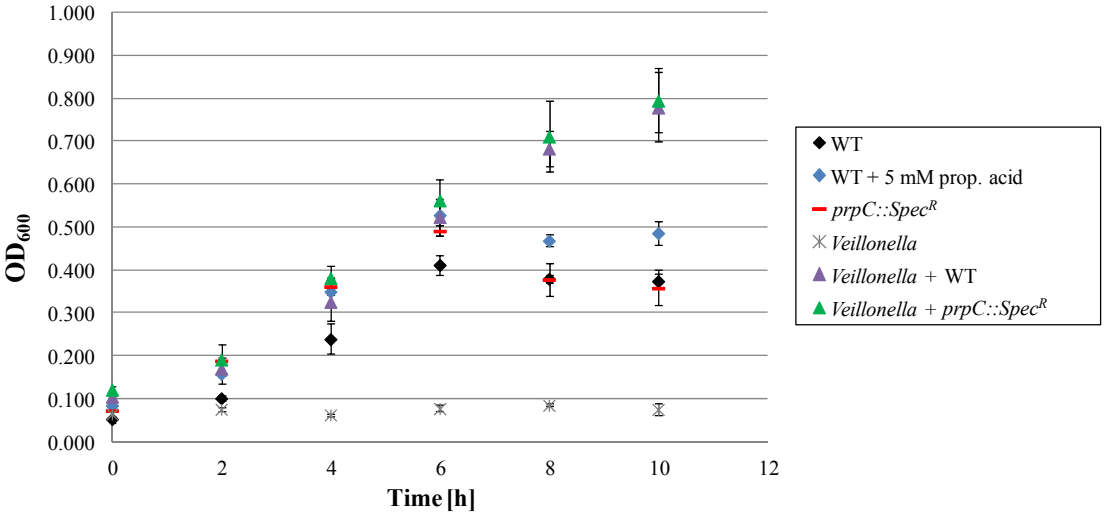

Figure 3.12-1: Growth curve of MC58 wild-type and *prpC::Spec*^{R} strains of *N. meningitidis*, and co-culture with *Veillonella* spp.

Co-culture of *Veillonella* and *Neisseria* resulted in a delay in entering stationary phase, even for the *prpC::Spec*^{R} strain, as continued growth was still seen after 10 hours incubation. Wild-type *N. meningitidis* did not seem to utilise propionic acid for enhanced growth, as they entered stationary phase after 6 hours, as all other *Neisseria*. Bacteria were grown in CDM supplemented with 5 mM sodium L-lactate and, when stated, with an additional 5 mM propionic acid. WT: wild-type *N. meningitidis* MC58. *prpC::Spec*^{R}: *N. meningitidis* MC58 with disrupted *prpC* gene (*NMB0431*).

Preliminary studies with co-cultures of *Veillonella* spp. and *N. meningitidis* showed that *N. meningitidis* was able to grow in an aerobic environment in minimal medium

with addition of 5 mM sodium L-lactate, and growth in this medium was similar to growth in CDM medium containing 5 mM sodium pyruvate.

Co-culture supported further growth compared to single strains, as the latter entered stationary phase sooner, and this was independent of supplementation of 5 mM propionic acid to the medium. However, at this stage, it was not possible to determine if the product contained both *Veillonella* spp. and *N. meningitidis*.

Bacterial growth curves showed that propionic acid was probably not used in minimal medium with lactate, as wild-type bacteria that were supplied with it entered stationary phase at the same time as the *prpC::Spec*^{R} mutant strain, and as co-culture of the mutant strain did not show a decreased growth.

Further investigations need to be carried out by repeating bacterial growth curves. Samples for the wild-type *N. meningitidis* MC58 grown in medium that was supplemented with propionic acid should be collected at different time points, and propionic acid content could be measured by gas chromatography to verify if wild-type *N. meningitidis* are indeed unable to use propionic acid when grown in the presence of lactate, or if the growth pattern is just an artefact due to lactate in the medium. Co-cultures could also be plated every few hours during the growth curve, and both bacteria could be counted from each plate, in order to verify if the growth seen is due to the presence of both bacteria.

3.13 Discussion

In this chapter the putative 2-methylcitrate pathway, needed for the catabolism of propionic acid, was investigated. In *N. meningitidis* strain MC58, a BLAST search

revealed that this pathway is composed of 6 genes, two of which are crucial to the pathway (*NMB0430* and *NMB0431*), as they are found in all bacteria that possess the 2-methylcitrate pathway (Suvorova *et al.*, 2012, Upton & McKinney, 2007, Brämer & Steinbüchel, 2001). These genes encode 2-methylisocitrate lyase and 2-methylcitrate synthase respectively. A knockout for *NMB0431* (*prpC::Spec*^{R} mutant) was created in this work, and it confirmed its involvement in this pathway, since in the absence of this gene bacteria were not able to use propionic acid under any condition tested.

Another two genes belonging to this pathway in *N. meningitidis* MC58 (*NMB0433* and *NMB0434*) replace the more specific *prpD* gene present in other bacteria, and are both needed for metabolising 2-methylcitrate to 2-methylisocitrate (Grimek & Escalante-Semerena, 2004, Horswill & Escalante-Semerena, 2001).

The following two genes, however, were found associated with the *prp* gene cluster only within *Neisseria* spp. The putative *NMB0432* gene, with no assigned function, was exclusively present in just three neisserial strains: *N. meningitidis*, *N. gonorrhoeae* and *N. flavescens*, even though the presence of the other genes encoding for enzymes belonging to the 2-methylcitrate pathway was confirmed in 10 different strains so far. The *ackA-1* gene (*NMB0435*), instead, was present in all 10 *Neisseria* spp. containing the *prp* gene cluster, and partly replaced the more specific *prpE* gene present in other bacteria, which encodes propionyl-CoA synthetase, an enzyme responsible for catabolising the first reaction amongst the pathway (Horswill & Escalante-Semerena, 1999a). As both genes were present only in three *Neisseria* species, knockouts of *NMB0432* (*NMB0432::Spec*^{R} and *NMB0432::Tet*^{R} mutant) and

NMB0435 (*NMB0435::Spec*^{R}) were investigated as part of this work to check if they were involved in the pathway indeed.

Growth curves for the wild-type and mutant strains showed that bacteria did not need propionic acid to grow in rich medium, but propionic acid was needed for optimal growth in minimal medium. Only the wild-type could achieve a more favourable growth, and this was confirmed with the mutants, which were not able to utilise propionic acid, showing that *NMB0431*, *NMB0432* and *NMB0435* were crucial for the 2-methylcitrate pathway. This hypothesis was further confirmed when samples from bacterial growth curves that were collected every hour were analysed by gas chromatography: propionic acid content measured from both chemically defined media studied revealed that only the wild-type strain was able to metabolise this short chain fatty acid, and this started to be utilised earlier when in the presence of a poorer carbon source, suggesting that expression of the genes belonging to the 2-methylcitrate pathway might be controlled by poor nutrient availability. These results were consequently confirmed with studies of the expression of *prpC* in wild-type bacteria, as expression was clearly higher in chemically defined media, especially when supplemented with sodium pyruvate, a poorer carbon source than glucose.

Gene expression studies for all mutants containing the spectinomycin cassette confirmed that the genes that were knocked out and their downstream genes were co-regulated, enhancing the hypothesis that these genes belong to an operon. The spectinomycin cassette, in fact, contained strong transcriptional terminators in each side (Prentki & Krisch, 1984). The mutant containing the tetracycline cassette, however, did not stop up-regulation of the genes downstream, as the cassette did not have transcriptional terminators (Heurlier *et al.*, 2008). Despite this, propionic acid

could not be utilised in *NMB0432::Tet*^{R} mutant, as confirmed by gas chromatography.

The hypothesis that all six genes were organised as an operon was further confirmed when amplification of the intergenic regions between the six genes from cDNA extracted from cultures grown under conditions that enhanced *prpC* expression, gave a clearly visible PCR product, whereas the intergenic region flanking both sides of the operon failed to amplify.

BLAST analysis using *NMB0432* as a query indicates that this gene is homologous to TauE, a family of integral membrane proteins that are involved in the transport of anions across the cytoplasmic membrane during the metabolism of taurine. TauE belongs to the *tauE* gene cluster, which appears to be fully absent from *N. meningitidis*. Other bacteria possess TsaS or CysZ, which are the most closely related proteins of known function, but still have low sequence identity with TauE. These proteins are involved in the uptake of sulphates or sulfonates. For this reason, it was hypothesised that proteins with similarities to TauE could be involved in the transport of anions across the membrane (Weinitschke *et al.*, 2007). This could suggest transport of propionic acid into the cell, and is in line with the inability of the mutants for this gene to utilise propionic acid, even when the gene was disrupted and did not block transcription of the downstream genes. Putative transmembrane helices for *NMB0432* were predicted using a transmembrane helices programme based on a hidden Markov model (TMHMM) (Appendix D). TMHMM output predicted 8 transmembrane helices for NMB0432 and that both N-terminal and C-terminal are located in the cytoplasm.

Since *Neisseria* lack *prpE*, and *ackA-1* translates into a propionate kinase and is responsible only for generating propionyl phosphate, a second enzyme, Pta, a phosphotransacetylase, has been related to the second part of the reaction, involving the production of propionyl-CoA. Thus these two enzymes are needed for replacing the full activity of prpF, even though with a lower affinity (Starai & Escalante-Semerena, 2004). In *Neisseria* Pta has similarity to the *NMB0631* gene, which is not specific to the 2-methylcitrate pathway. PrpE has a high affinity for propionate, and in *Salmonella enterica* its K_M corresponded to approximately 20 μM (Horswill & Escalante-Semerena, 2002), whereas acetate kinase from *Corynebacterium glutamicum* gave a much higher K_M of about 15 mM (Reinscheid *et al.*, 1999). These numbers showed that acetate kinase had a much lower affinity to propionate than PrpE. For this reason, an active transport of propionate towards the cytoplasm might be more important in *Neisseria* than in other bacteria.

Chapter 4 - Investigations of a pathogen-specific genetic island in *N. meningitidis*

4.1 Introduction

There are 9 conserved genetic islands which are found in all *Neisseria meningitidis* strains, but are absent from its closely related commensal *Neisseria lactamica*, as previously described in Section 1.7.2. One of these pathogenic islands is composed of two genes, *NMB1048* and *NMB1049* in *N. meningitidis* MC58. These two genes are divergently transcribed and still have putative functions. The product NMB1048 belongs to a family of bacterial proteins that are functionally uncharacterised and which are usually between 489 and 517 amino acids in length. NMB1048 corresponds to a protein that is 489 amino acids long and it has similarities to predicted membrane proteins and a family of putative transporters or permeases. The second gene, *NMB1049,* encodes a 304 amino acids uncharacterised LysR-Type transcriptional regulator.

Following a protein BLAST search (NCBI), these two genes appeared to also be present in four other *Neisseria* species: *N. gonorrhoeae*, *N. elongata*, *N. sicca* and *N. wadsworthii*, even though high identity (99 %) was seen only with *N. gonorrhoeae.* In fact, BLAST of the other three species resulted in poor identity (varying between 59 and 64 %). The pathogenic *N. gonorrhoeae* is often associated with gonorrhoea, whereas the other three bacteria were occasionally found in immunocompromised patients and eventually led to endocarditis, meningitis or septicaemia (Heiddal *et al.*, 1993, Wong & Janda, 1992).

As this genetic island is not present in the majority of commensal *Neisseria* spp. but only in the occasional pathogens, it could potentially serve as an adaptation that might have occurred to help *N. meningitidis* survive in human adults during infection. Investigations for understanding if this genetic island was needed in pathogenicity or survival into the human blood are later discussed in Chapter 6, where the *NMB1049* gene was further analysed.

In this chapter, the two genes (*NMB1048* and *NMB1049*) belonging to an uncharacterised pathogenic island from *Neisseria meningitidis* strain MC58 have been knocked out and their effects on growth and gene expression were compared to the wild-type bacteria.

4.2 Construction of knockout mutants for the putative *NMB1048* and *NMB1049* genes of *N. meningitidis*

In order to investigate the role played by NMB1048 and NMB1049, both belonging to a yet uncharacterised pathogenic island, knockouts of both genes from *N. meningitidis* strain MC58 were constructed in this study. Construction of each single mutant knockout was achieved by inserting a spectinomycin resistance cassette within each gene of interest (Figure 4.2-1).

In order to generate the knockouts, the two genes with their flanking regions were amplified using the primers described in Table 2.3.1-1. The sequence of the putative *NMB1048* gene, which encodes a hypothetical integral membrane protein, is shown in Figure 4.2-2. The sequence for the putative *NMB1049* gene, which encodes a hypothetical LysR-Type transcriptional regulator, is shown in Figure 4.2-3. Only *NMB1048* was flanked by the *N. meningitidis* DNA uptake sequence,

GCCGTCTGAA. The relevant restriction sites where the spectinomycin cassette was inserted are also shown in these figures.

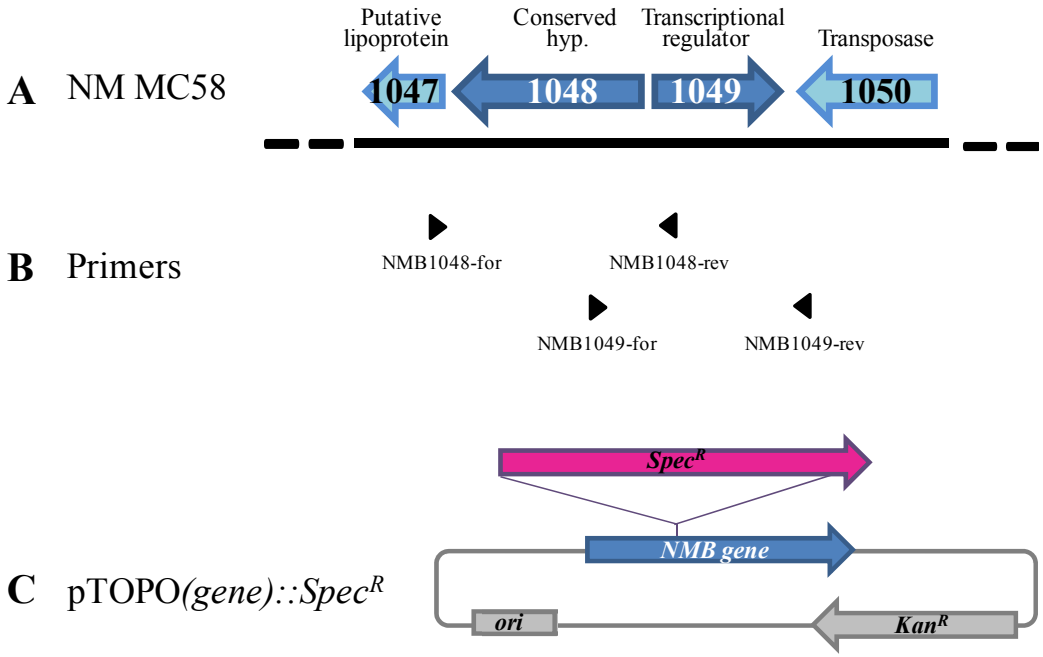

Figure 4.2-1: The ORF map of the uncharacterised pathogenic island of *N. meningitidis* MC58, with primers and plasmid used for the construction of knockouts.

A: The relevant region of *N. meningitidis* MC58 genome representing the genes belonging to the uncharacterised gene cluster (dark blue arrows) and its flanking genes (light blue arrows) is shown with the orientation of each gene. Gene numbers correspond to the numbering given in the MC58 complete genome, where the number within each arrow is preceded by "NMB" (NCBI GenBank accession number AE002098.2). **B:** The position of the two sets of primers used for constructing the knockouts is shown with black arrows. **C:** The pCR®-Blunt II-TOPO® vector (gray) is shown with its relevant features (gray box and gray arrow) and with the place of insertion of the mutant gene (blue arrow). The spectinomycin resistance cassette and its place of insertion are also shown in the diagram (pink arrow). NM MC58: *N. meningitidis* strain MC58. Conserved hyp.: gene coding for a conserved hypothetical protein.

TGCCGAATCGATGGGGTGGATAATGCCCAAACTGGTCTCTTCCGAATAATCGCCTGCCAGCGTTTTGG
CAAAATGCTCCAGCTTGTGTTTGTATTGCAGCAGGGATTCCGCTTCGGGCAACAGTATTTCGCCCGCC
CGCGTCAATACCATGCCTTTCCCCGTGCGCCTGAACAGCGGCGTGCCGACATATTCTTCAAGGGCTTT
AATTTGGGCAGAAACGGCAGGCTGGGAAAGGAAAAGTCGTTTGGCGGCTTGGGTAAGGTTGCCCTCGT
GCGCGACGGCGACAAATGATTTTAATTGTACGGCATCCATATATCCCTCCTTGTGCGGATGTTTTCTA
TATTTGTGCAATCGAAATCTTTTAGGTGGATTGTTGCTGAAAATTAACTTTTTAATCAAGTGGTTTGT
AAATTGTATCAGTTTTCCGGATGATGGTTATCAAAAAAAAAGATTGGTTTTATTGCCTGTTTGGGCTT
TAAATGGGGTTACGGCTTCCGAACGCAGCCCGTATCAAAAAGAAAAGTCATGCGCCCCTTTTACGAGG
CGCGATATATAAGGAGGAAGGTTATGGAAAAACATAATGGGACTTATCGGGATTTGCACCGTCCAGCT
TCGGAATTTGCGACGCGGGACGAATATTTGGAACATGAATTGCAGATTATGCAACCAAAACGCTGGCG
GCCCAACCTGCCCTTTCGCGATTACCGCTTCGAGTGGGAGGATTTGATTCCTGCGATGGCGGGAACGA
TTGGAAAAGTGGTGATGGTGGGGGCGGTGGCGGCGGCGTTTGCCGCACCTTTGGGGCTGCCTGACAGC
TTTGTACTGGAAAATGTGCGCTATGAGCTTTTAATCGCCGCCGCGTTTATCTTATTGGTATCGGGCTT
TTTTCTGCCCGGCGCCAACCTGCCCGGTACGCACGGGCCGCTGATTCCGATGATTCCCATCGTTGTGT
CGGCAGGCGGGCATCCTTTGGCGTTCGGCATTTCGATTGCGGTTTTAGGTCTGCTGATGGCTTTATTT
CGCGGCGGCAGTATTATGGCGAAGCTGACAAGCAACGGCGTATGCGGCGGATTATTACTCTATTTGGG
CTTTATCGGCACGACGGGGCAGGTAAAAAAATTGTTTTCGTGGGCAGGCGGTTTTAATATGCCCTACA
TCGCTTTTACCGTCATTATTGTAACGATTGTGATGTACGCTTTGTTGGAGCATTGGAAAAAACGCTGG
TTAGCCGTGCCTTTGGGATGCTTGATTGCCGGTGTGGTGGCATTTGCATTGGGTGCGCCGTTTGAGTT
TCACACCGCCCCCGGCCTGCCTCCAATGAGTCCTGCTTATTGGTGGGGTGAAAACAGCGGCTGGCATC
TGGGGTTGCCGACGGCAGAAAGTTTTTTGGTTGTCTTTCCATTTGCGGTATTGGCTGTTGCAATGTGG
TCGCCCGATTTTTTAGGACATCAAGTGTTCCAAAAAATCAGCTATCCGGAAAAAACCGATAAGGTATT
GATGAATATAGACGACACCATGACAAGTTGTTCTGTCCGTCAAGCAGTGGGTTCTATTTTAGGGGGTG
CAAATTTTACCTCTTCTTGGGGAACTTATATCGTACCGGCATCGATTGCCAAACGCCCCATTCCGGGC
GGTGCGGTTTTAACGGCGGTTTTATGTATTATCGCCGGGTTATGGGGCTATCCGATGGACTTGGCGAT
TTGGCAGCCGGTATTGAGCGTAGCCTTGGTCGTAGGCGTATACTTACCGCTTTTGGAAGCGGGCATGG
AAATGACGCGCAAAGGCAAAACCACCCAATCCGCCGCCATCGTGGTGTTCTCTTCCGCCTTGGTCAAT
CCGGTTTTCGGCTGGGCGTTGACGATGCTGTTGGATAATTTGGGCTTAATCGGCTGCAAAGAGCGCAG
TGCGCAATTAGGTTTCGCCGGACGCGTGTTGATACCCGCAGTAGGTTTCTTGATCTTGTGTGTGGCGA
TGGGTGCGGTCGGGATGCTGCCCGGTATCCCGCCGTTTTTGGAACACTTCAAATCTTTGGGCTAGGCT
GAAATCGGAAATGCCGTCTGAACCGCTTTCAGACGGCATTTTTGCAAACAGGCAAAATGACGGCGGCG
GGATTTTTTATTTTCCCGATTGAAGTATAATGTTGCCGGGCTTCAACCGGATATTCAAAACGGTTTGT
TCCAACACTCGGAACGGCGCATAAAACGCCGCCCTTCGCGTTATCCCGAACGGGGCGGCTAATCAGAT

Figure 4.2-2: Reverse complement of *NMB1048* gene with its flanking regions used for constructing the mutant.

The *NMB1048* gene (blue) with the ATG start codon (green) and the TAG stop codon (red) and its flanking regions (black) give a product 2081 bp long. Primers NMB1048-for and NMB1048-rev were used (highlighted in yellow) to generate the knockout. The same primers were used for colony pick PCR screening in *N. meningitidis*. One *N. meningitidis* DNA uptake sequence (orange) is found just outside the gene of interest. The ClaI site (ATCGAT) and SspI site (AATATT) are also shown (highlighted in blue) with the site where the restriction enzymes cut (brown).

GATAAAGCCCAAATAGAGTAATAATCCGCCGCATACGCCGTTGCTTGTCAGCTTCGCCATAATACTGC
CGCCGCGAAATAAAGCCATCAGCAGACCTAAAACCGCAATCGAAATGCCGAACGCCAAAGGATGCCCG
CCTGCCGACACAACGATGGGAATCATCGGAATCAGCGGCCCGTGCGTACCGGGCAGGTTGGCGCCGGG
CAGAAAAAAGCCCGATACCAATAAGATAAACGCGGCGGCGATTAAAAGCTCATAGCGCACATTTTCCA
GTACAAAGCTGTCAGGCAGCCCCAAAGGTGCGGCAAACGCCGCCGCCACCGCCCCCACCATCACCACT
TTTCCAATCGTTCCCGCCATCGCAGGAATCAAATCCTCCCACTCGAAGCGGTAATCGCGAAAGGGCAG
GTTGGGCCGCCAGCGTTTTGGTTGCATAATCTGCAATTCATGTTCCAAATATTCGTCCCGCGTCGCAA
ATTCCGAAGCTGGACGGTGCAAATCCCGATAAGTCCCATTATGTTTTTCCATAACCTTCCTCCTTATA
TATCGCGCCTCGTAAAAGGGGCGCATGACTTTTCTTTTTGATACGGGCTGCGTTCGGAAGCCGTAACC
CCATTTAAAGCCCAAACAGGCAATAAAACCAATCTTTTTTTTTGATAACCATCATCCGGAAAACTGAT
ACAATTTACAAACCACTTGATTAAAAAGTTAATTTTCAGCAACAATCCACCTAAAAGATTTCGATTGC
ACAAATATAGAAAACATCCGCACAAGGAGGGATATATGGATGCCGTACAATTAAAATCATTTGTCGCC
GTCGCGCACGAGGGCAACCTTACCCAAGCCGCCAAACGACTTTTCCTTTCCCAGCCTGCCGTTTCTGC
CCAAATTAAAGCCCTTGAAGAATATGTCGGCACGCCGCTGTTCAGGCGCACGGGGAAAGGCATGGTAT
TGACGCGGGCGGGCGAAATACTGTTGCCCGAAGCGGAATCCCTGCTGCAATACAAACACAAGCTGGAG
CATTTTGCCAAAACGCTGGCAGGCGATTATTCGGAAGAGACCAGTTTGGGCATTATCCACCCCATCGA
TTCGGCAAAACTCGTCGCGCTGACGGACAATATCGGTCAAACAGCCCCCAAAACGCGCCTGCACATCC
AATACGGAATGAGCGGCGAAATCCTCTCGCGCATCCAACACAAAACCCTGCACGGCGGCTTTATACTC
GGCAACGCCGCCCAACGCGGCATCCGCAGCGTATTCCTGCAAAACCTGACCTACGCGCTGATTTGCCC
GCAAAGCCAATATCCCCATCTGACCCGCTCCCTTCCGCAGAGCCTGCAAGAATGCGTATGGATAGAAA
TGTCGGGCGTGTCCGGAAGTAGGAAGCACCTGCACCAGTTTTGGCGCAGCAACCGGCTCTCACCCAAA
AAACAGATCTTGTGCGACTACCCCCAAACCATTATCGATTTGGTTGCAGGCGGTATAGGTGTGGCAAT
GGTGCCGGGAAACAAAGCCGAAGCGGCGGCAAAAGAAGGCGCGGGCGTGGCTATTATCGAATCGTGCC
GCCACAGTATGCCGCTCAATTTCATTTATGCGGAAGAATACGAGGATAATCCCCACGTCTCACTCCTG
CTCGAGTGCATTGAAAAAGTATGGGGAGTGCAGGCGGTGCAGCCGCCCGTTGTCTCGGACAACTGAAA
TAAATCCTGCTTTGCTGATTGTTTTAAAATAGAAATTTGAATTTTATCACGCTGAAAACACTGAAAAC
GCCATCCGCATTCTCTCAAATACGGCTTAAAATGCCCTTTGGAAATGCCGTTATAGTGGATTAACAAA
AATCAGGACAAGGCGACGAAGCCGCAGACAGTACAAATAGTACGGAACCGATTCACTTGGTGCTTCAG
CACCTTAGAGAATCGTTCTCTTTGAGCTAAGGCGAGGCAACGCCGTACTGGTTTTTGTTAATCCACTA
TAAACTGACGCAAATACCGTTTTGCACAATTCCAAAAGTTTTCAATTCCGTTAATGCGATTTTGCCGT
TTGGCGAAATGCGTACTGTTCCAGTCGTGGATTGAACCCCCACCCTGTATAGTTCTTTCGAAGCATTG
GGGTATTGTTTTTTCAAAGCATCTTGGATTCGGATTTCAAGTGCAACACTAGTGTATTAGTGGTTGGA
ACAGATTCAAGAATAAAACACTTGGCGTTTCGTAGCCAAGTGTTTTTCTTGGTCGGTGGTTCAACTCA

Figure 4.2-3: *NMB1049* gene with its flanking regions used for constructing the mutant.

The *NMB1049* gene (blue) with the ATG start codon (green) and the TGA stop codon (red) and its flanking regions (black) give a product 2043 bp long. Primers NMB1049-for and NMB1049-rev were used (highlighted in yellow) to generate the knockout. The same primers were used for colony pick PCR screening in *N. meningitidis*. The two BspEI sites are also shown (highlighted in blue) with the two bases within which the restriction enzyme cuts (brown).

Following amplification of both genes using neisserial genomic DNA from *N. meningitidis* strain MC58 and GoTaq® DNA polymerase as described in Section 2.3.1, the PCR products obtained corresponded to the expected fragment sizes of 2081 bp for the *NMB1048* gene and 2043 bp for the *NMB1049* gene. Correct amplification of the genes was confirmed by agarose gel (Figure 4.2-4). The resulting blunt-ended PCR products were subsequently purified and cloned into the 3519 bp pCR®-Blunt II-TOPO® vector (Invitrogen™), which contained a kanamycin resistance cassette (Kan^R). The vector was transformed into *Escherichia coli* DH5α by heat shock, and *E. coli* was then grown at 37 ºC on selective LB agar plates. Only bacteria with successfully transformed plasmids were able to grow in the presence of kanamycin.

Mini-preparations of two colonies per transformed plated *E. coli* were grown in liquid LB medium with kanamycin overnight; bacteria were then harvested and plasmid DNA was purified as described in Section 2.3.4. Positive insertion of the genes of interest in the new plasmid was investigated at this stage by EcoRI restriction digest, as the pCR®-Blunt II-TOPO® vector contains two restriction sites just a few bases before and after the inserted genes under study. After restriction digest, two fragments were generated, one of which was the original 3.5 kb TOPO vector and the other corresponded to the inserted PCR product, which was just over 2 kb in size for both genes under investigation (Figure 4.2-5). Sequencing results at this stage confirmed that both *NMB1048* and *NMB1049* genes have been inserted in the vector and that they were amplified correctly, without introducing any error.

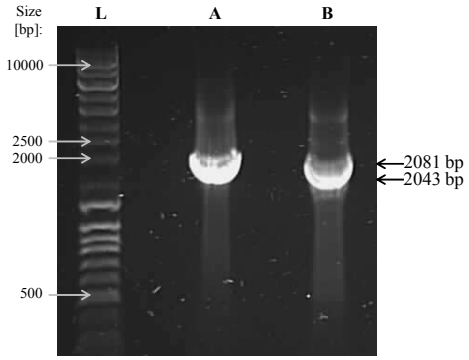

Figure 4.2-4: PCR products of the *NMB1048 and NMB1049* genes with their relative flanking regions from *N. meningitidis* MC58.

The correct PCR products, fragments expected to be 2081 bp long for *NMB1048* (Lane A) and 2043 bp for *NMB1049* (Lane B), were successfully amplified. The Q-Step 4 Quantitative DNA ladder (YORBIO) (Lane L) was loaded on both gels to confirm the size of each DNA band.

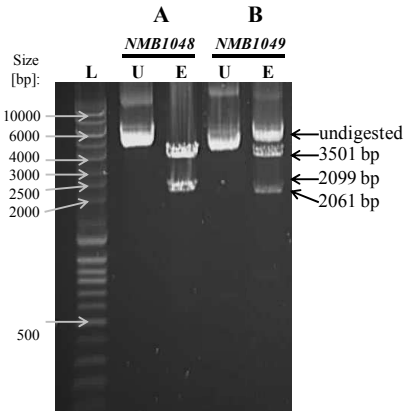

Figure 4.2-5: EcoRI screening for insertion of the genes *NMB1048* and *NMB1049* in the pCR®-Blunt II-TOPO® vector.

pCR®-Blunt II-TOPO® plasmids containing the genes under study, undigested and digested with EcoRI, were loaded on the gels. **A:** In the digested lane the top band corresponded to the 3.5 kb TOPO vector and the lower band corresponded to the *NMB1048* gene. **B:** Partial digestion in lane E, where the top band corresponded to the undigested plasmid, the middle band was the 3.5 kb TOPO vector and the lower band was the *NMB1049* gene. The Q-Step 4 Quantitative DNA ladder (YORBIO) (Lane L) was loaded on both gels to confirm the size of the DNA bands. U: undigested plasmid. E: plasmid digested with EcoRI.

Once confirmed that the pCR®-Blunt II-TOPO® vectors were containing the genes under study, these were digested with different restriction enzymes that would cut only within each gene. The *NMB1048* gene was digested with ClaI and SspI, which would each cut just once within the gene, and the resulting fragment of 971 bp in length was eliminated, as shown in the gel and then confirmed by sequencing (Figure 4.2-6A). The *NMB1049* gene was digested with BspEI, the recognition site of which was present in two different locations within the gene, and a fragment size of 705 bp in length was eliminated, as shown in the gel and then confirmed by sequencing (Figure 4.2-6B). Two restriction enzymes, ClaI and BspEI, were creating sticky ended DNA, and therefore digests containing those enzymes were incubated with DNA Polymerase I (Klenow) and dNTPs during the last 30 minutes of the restriction digest incubation, in order to create the blunt ended DNA needed for ligation with the antibiotic resistance cassette. Both 4629 bp and 4857 bp fragments were then purified from the gel for ligation with the spectinomycin resistance gene cassette (*Spec*^{R}).

The spectinomycin resistance gene cassette (*Spec*^{R}), also referred to as *Ω* cassette, was generated from the digestion of the pHP45*Ω* plasmid, about 4.3 kb in size, with the SmaI restriction enzyme. This digest created two fragments, the pHP45 plasmid which was 2320 bp long, and the spectinomycin resistance gene cassette which was 1980 bp in size, as shown previously in Figure 3.5-8A. The 1980 bp fragment was purified from the gel for ligation with *NMB1048* and *NMB1049* genes. Successful ligation of the antibiotic resistance to each gene was needed in order to disrupt the function of the genes.

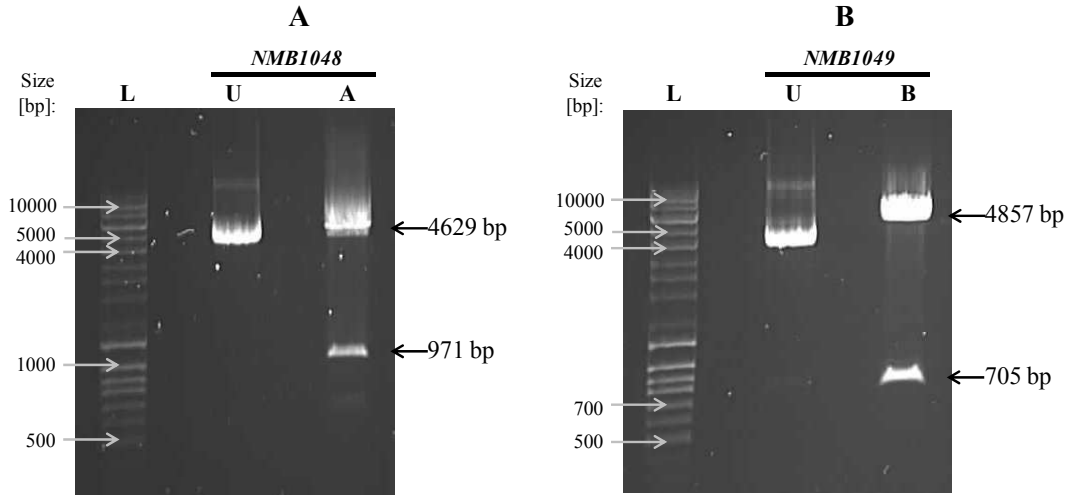

Figure 4.2-6: Restriction digests for the pCR®-Blunt II-TOPO® vector and its inserts, genes *NMB1048* and *NMB1049* for generating the knockouts.
pCR®-Blunt II-TOPO® plasmids containing the genes under study, undigested and digested with different restriction enzymes, were loaded on the gels. In the digested lanes (Lanes A and B) the top band corresponded to the 3.5 kb TOPO vector with part of the insert and the lower band corresponded to the deleted part of the gene under study. Lane A: plasmid digested with ClaI and SspI. Lane B: plasmid digested with BspEI, which cut twice within the gene. The Q-Step 4 Quantitative DNA ladder (YORBIO) (Lane L) was loaded on both gels to confirm the size of the DNA bands. U: undigested plasmid. A-B: plasmid digested with restriction enzymes.

At this stage, the spectinomycin resistance cassette was ligated to the digested genes within the pCR®-Blunt II-TOPO® plasmids at room temperature overnight, and ligations were then transformed into *E. coli* DH5α by heat shock, as explained in Section 2.3.3. The mutants were selected by plating each transformation onto selective LB agar plates containing 50 μg / ml kanamycin and 50 μg / ml

spectinomycin. Mini-preparations of two colonies per transformation were grown in liquid LB medium with both antibiotics overnight, and plasmid DNA was then extracted and purified as described in Section 2.3.4. An agarose gel was run after restriction digest with BamHI for the genes knocked out with the spectinomycin resistance cassette, in order to check for successful ligations. The pCR®-Blunt II-TOPO® vector has one recognition site for BamHI just before the location of insertion of the genes under study. The spectinomycin resistance cassette has two recognition sites for BamHI at either ends of the cassette. Positive ligation, therefore, resulted in three fragments, which corresponded to the 3.5 kb TOPO vector plus part of each gene investigated, the 2 kb spectinomycin resistance cassette, and a small fragment with the rest of the gene (Figure 4.2-7).

Sequencing results of the new transformants confirmed that each gene was disrupted with the spectinomycin resistance cassette. The *NMB1048* gene was inserted in the correct direction (plus / plus strand). The *NMB1049* gene, however, was inserted in the 5' to 3' direction (plus / minus strand) compared to the database sequence (GenBank AE002098). A map of the pCR®-Blunt II-TOPO®plasmid showing the direction of insertion of each gene under study which was knocked out following ligation to the spectinomycin cassette is shown in Figure 4.2-8. Direction was confirmed by both sequencing data and fragment sizes derived from BamHI digest.

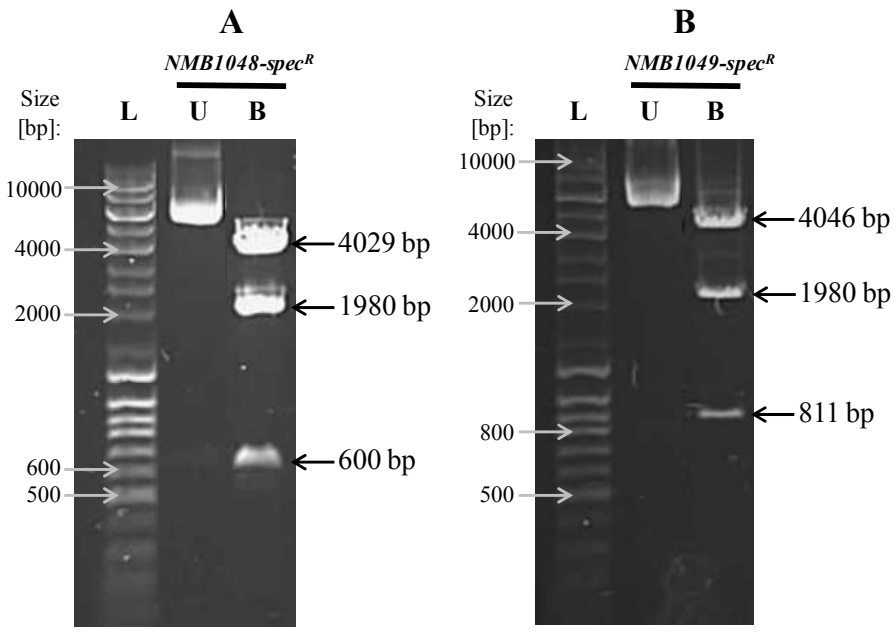

Figure 4.2-7: BamHI screening for insertion of the antibiotic resistance cassette in the constructed plasmids containing *NMB1048* and *NMB1049* genes.

Both gels show the pCR®-Blunt II-TOPO® plasmids containing the genes under study disrupted with the spectinomycin cassette. In the digested lanes (Lanes B) the top band corresponded to the 3.5 kb TOPO vector with part of each gene under study, the middle band corresponded to the spectinomycin cassette and the lower band corresponded to the other part of each gene of interest. The Q-Step 4 Quantitative DNA ladder (YORBIO) (Lane L) was loaded on all gels to confirm the size of the DNA bands. U: undigested plasmid. B: plasmid digested with BamHI.

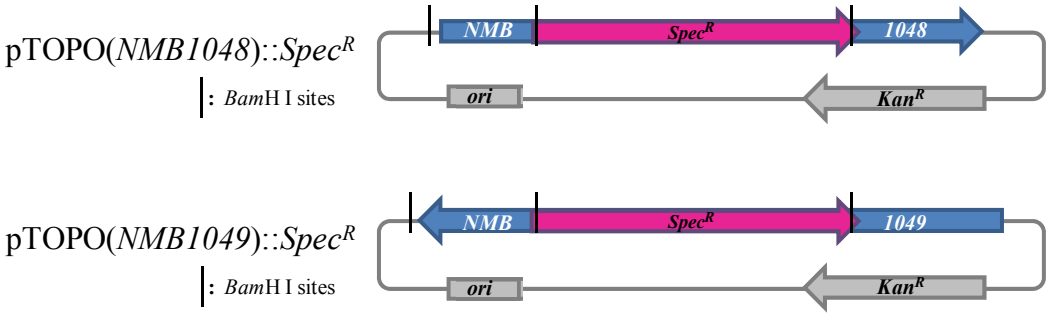

Figure 4.2-8: Plasmid maps of the pCR®-Blunt II-TOPO® vector containing the *NMB1048* and *NMB1049* genes knocked out by insertion of an antibiotic resistance cassette.

Two BamHI sites are found in both sides of the 2 kb spectinomycin resistance cassette, and the third site is found just outside the location of insertion of the genes under study. Gray: pCR®-Blunt II-TOPO® vector. Gray arrow: gene belonging to the vector that confers resistance to kanamycin. Blue arrow: *N meningitidis* MC58 gene under investigation, and its direction of insertion into the plasmid. Pink arrow: gene that confers resistance to spectinomycin. Black vertical lines: BamHI cutting sites.

Both successful gene knockouts were transformed into wild-type *N. meningitidis* strain MC58 following the TSB method, as described in Section 2.3.9. The mutant strains were selected on CBA plates containing 5 % horse blood and 50 µg / ml spectinomycin after overnight incubation at 37 ºC in a 5 % CO_2 atmosphere. Several colonies grown on each plate were screened by colony pick PCR for disruption of the genes by insertion of the 2 kb antibiotic Figure 4.2-9. The original primers used for generating the knockouts were used for colony pick PCR for both *NMB1048* and *NMB1049* disrupted genes.

Picking from the actual transformation plates resulted in amplification of both *N. meningitidis* wild-type and mutant genes (an example with the *NMB1049::Spec*^{R} mutant is shown in Figure 4.2-10). Mutants grew overnight and showed several colonies on the CBA plate already the following day, except for the *NMB1049::Spec*^{R} mutant which needed two days incubation before showing any colonies from the original transformation plate. After picking several colonies and re-plating them into fresh plates, however, the wild-type band disappeared and only the bands for the mutant strains were visible, confirming that the genes being investigated were disrupted. The background wild-type band seemed to have been caused by the wild-type bacteria that did not transform but that were plated during the transformation process.

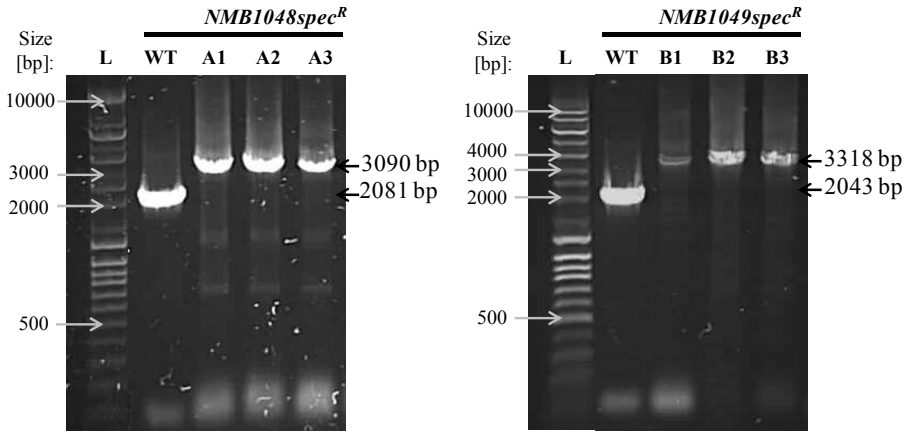

Figure 4.2-9: Colony pick PCR screening for *NMB1048* and *NMB1049* genes disrupted with spectinomycin resistance cassette in *N. meningitidis* strain MC58. Lanes A1-A3: *NMB1048::Spec*^{R} mutants containing the 1980 bp spectinomycin resistance cassette (with the removed 971 bp fragment). Lanes B1-B3: *NMB1049::Spec*^{R} mutants containing the 1980 bp spectinomycin resistance cassette (without the 705 bp fragment from the gene, which had been previously removed). The Q-Step 4 Quantitative DNA ladder (YORBIO) (Lane L) was loaded on all gels to confirm the size of the DNA bands. WT: wild-type gene of *N. meningitidis* MC58 under study.

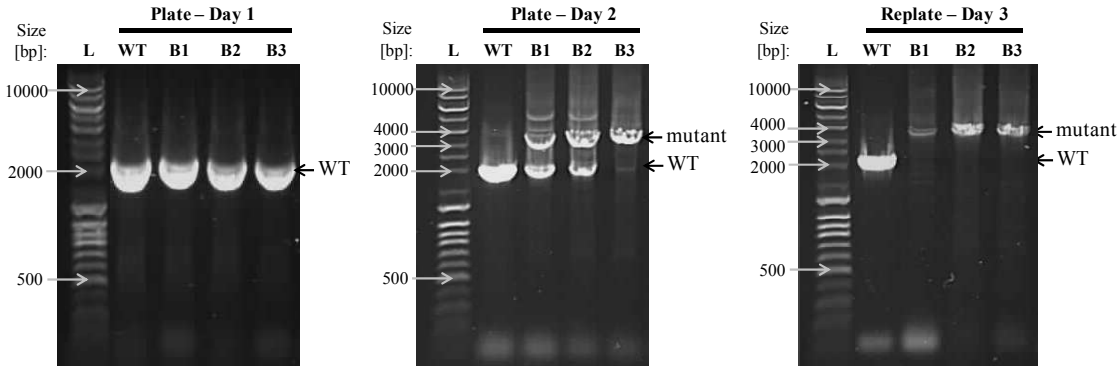

Figure 4.2-10: Comparison of the colony pick PCR screening from the first plate after transformation into *N. meningitidis* and after re-plating.

No colonies were visible in the first plate after transformation for colony pick PCR after overnight incubation, but three picks at random within the plate gave wild-type colonies (Plate – Day 1). After two days incubation, several colonies were grown, and three were picked (Plate – Day 2). The same three colonies were picked and re-plated again the following day (Re-plate – Day 3). The wild-type background band has disappeared from the re-plated colonies. Lanes B1-B3: *NMB1049::Spec*^{R} mutants containing the 1980 bp spectinomycin resistance cassette. The Q-Step 4 Quantitative DNA ladder (YORBIO) (Lane L) was loaded on all gels to confirm the size of the DNA bands. WT: wild-type gene under study of *N. meningitidis* MC58.

A knock-out of the *NMB1049* gene with the chloramphenicol resistance cassette was also created, as shown in Appendix C. Investigations of this mutant, however, still need to be carried out.

4.3 *prpC* and *NMB1048* gene expression in *N. meningitidis* MC58 under different growth conditions

In this chapter, studies were carried out to investigate if the NMB1049 protein was responsible for regulating the expression of the *prp* gene cluster and the *NMB1048*

gene. Several RT-PCRs were performed to check the expression levels of the *prpC* gene, which is crucial to the 2-methylcitrate pathway, and the *NMB1048* gene in MC58 wild-type, and expression was then compared to the one obtained from the *NMB1049::Spec*^{R} mutant strain. The data obtained from each study was calibrated with the wild-type bacteria grown for 6 hours in MHB which was not supplemented with propionic acid (control sample). The data was also compared and normalised to the housekeeping *metK* gene (*NMB1799*), which encodes S-adenosylmethionine synthetase, so that discrepancies due to different amounts of starting total RNA extracted from each sample could be eliminated. Data for the average fold change in expression of the triplicates that were set up in each 96-Well Optical Reaction Plate (Applied Biosystems) were plotted on a logarithmic scale in base 10.

Initial RT-PCR results seemed to show that the NMB1049 protein was both up-regulating the expression of *NMB1048* and down-regulating *prpC* (*NMB0431*) gene expression. A preliminary model was built following these outcomes, where it was hypothesised that NMB1049, a hypothetical LysR-Type protein, was responsible for regulating both the *prp* gene cluster (genes *NMB0430-NMB0435*) and the divergently transcribed *NMB1048* gene (Figure 4.3-1). The signal molecule was thought to involve C3 compounds, such as sodium pyruvate or propionic acid, as both genes under study were constantly highly expressed when wild-type bacteria were grown in the presence of sodium pyruvate or under propionic acid conditions.

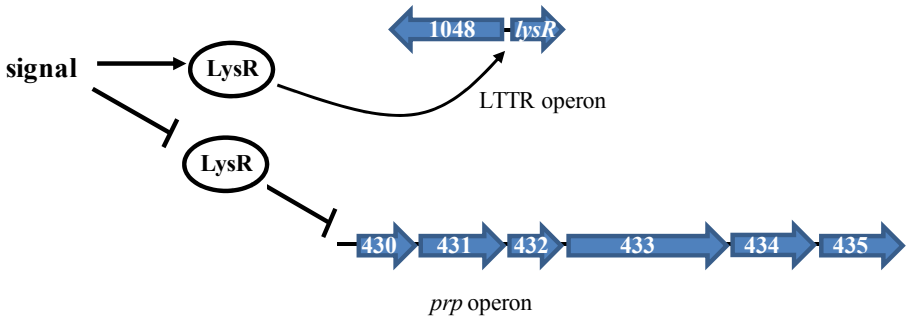

Figure 4.3-1: Hypothetical model for genes regulated by NMB1049.
Model showing that the LysR protein, encoded by *NMB1049,* might up-regulate transcription of *NMB1048* and down-regulate the expression of the *prp* operon when in the presence of a signal molecule. Gene numbers correspond to the numbering given in the MC58 complete genome, where the number within each arrow is preceded by "NMB" (NCBI GenBank accession number AE002098.2).

Further data collection and analysis, however, showed that there was a lot of variability in gene expression within the same bacterial strains, even when they were run under the same conditions, when samples were collected and RNA was extracted on different days. This variability between sample repeats could be due to some or all of the steps carried out starting from sample collection after 6 hours incubation during growth to the cDNA run on a different 96-Well Optical Reaction Plate (Applied Biosystems) on an ABI 7000 Sequence Detection System Analyser (Applied Biosystems). Analysis was done as a relative quantification and was directly compared to the data that had been collected previously, therefore both experimental and machine-specific variability were to be kept into account. As the steps just described introduced a lot of variability in gene expression within each strain and under the same conditions, data collected in this way could not be used to

support the model. A few examples of the gene expression variability just described are clearly shown in Figure 4.3-2. In this specific case wild-type bacteria were grown for 6 hours in MHB over four different days.

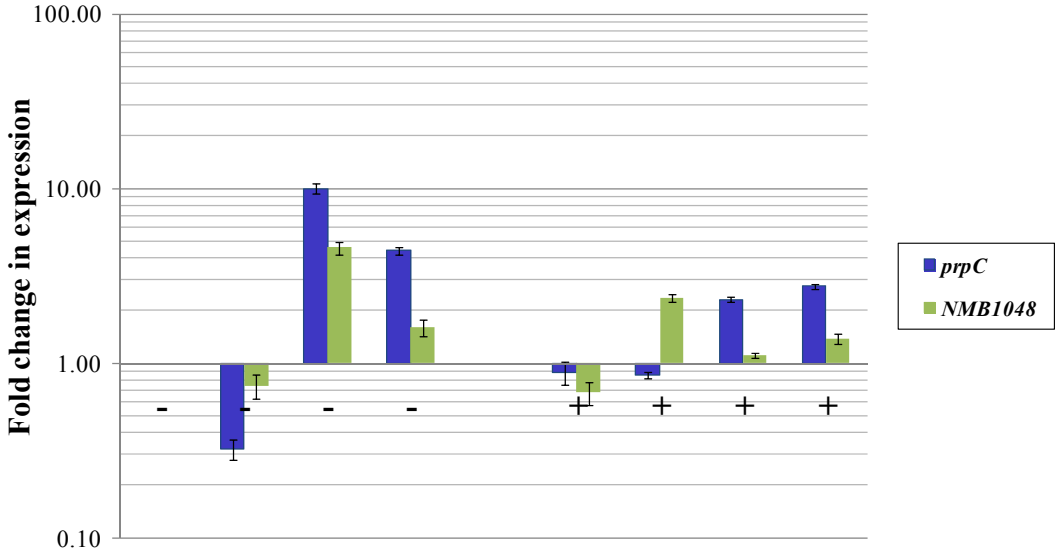

Figure 4.3-2: Variability of gene expression between independent repeats under the same conditions.

In this example, four independent repeats for wild-type bacteria grown in MHB medium were measured for gene expression after 6 hours incubation. Each sample was both collected and run in different days and showed a lot of variability. The data was normalised with *metK* gene (encoding S-adenosylmethionine synthetase). -: MHB medium not supplemented with propionic acid. +: MHB medium supplemented with 5 mM propionic acid.

In order to overcome all the variability seen in gene expression due to the samples being collected after 6 hours incubation from a number of independent growth curves, the data for each culture was now collected several times over a period of 12

hours. 1 ml aliquot was removed from each culture after 4 hours incubation, and every 2 hours following that, until the last 12 hours samples were collected. Total RNA was then extracted and an RT-PCR was run with the newly reverse transcribed cDNA, as described in Sections 2.3.12 – 2.3.14.

Wild-type bacteria that were initially grown in Mueller Hinton Broth (MHB) medium with propionic acid showed a gradual increase in both *prpC* and *NMB1048* gene expression, despite not using propionic acid for growth. Interestingly, the culture that was grown without this fatty acid also behaved similarly. The gradual increase seen with the *NMB1048* expression, however, was more pronounced as it reached over 20-fold up-regulation. The *NMB1049::Spec*^{R} mutant strain showed similar gene expression for *prpC*. However, expression of *NMB1048* was induced to a much lower extent in the *NMB1049* deficient mutant (Figure 4.3-3A).

Wild-type bacteria grown in minimal media had a higher expression of the *NMB1048* gene earlier in the growth curve compared to the rich medium. Bacteria incubated in CDM with 2.5 mM glucose showed a similar pattern of *prpC* expression to the ones grown in MHB. Expression in this second case, however, started earlier, as after 8 hours growth its levels were significantly higher than in MHB. Expression level was also very pronounced, as a 40-fold (without propionic acid) or a 20-fold (when the medium was supplemented with propionic acid) increase in expression was seen. *NMB1048* gene expression, instead, was high throughout the whole growth curve, and reached a 65-fold (without propionic acid) or a 30-fold (with propionic acid) increase. In this case, *prpC* expression in the *NMB1049::Spec*^{R} mutant strain was comparable to the one for the wild-type bacteria, whereas *NMB1048* expression was considerably lower in all the time points measured (Figure 4.3-3B). A major increase

in expression level, particularly with the *prpC* gene, happened between 6 hours and 8 hours growth, and this corresponded to the turning point seen at 8 hours, when wild-type bacteria had already started to utilise propionic acid for supporting growth instead of entering the stationary phase.

In CDM with 5 mM sodium pyruvate, both *prpC* and *NMB1048* genes in wild-type bacteria were highly induced during the whole growth: a large amount of expression of both genes was already obvious when the first sample was collected after 4 hours incubation. *prpC* expression varied between 5 and 25-fold, whereas NMB1048 expression was usually higher and varied between 6 and 75-fold (except for one data point) when compared to the calibrator. Once more, the expression of the *prpC* gene in the *NMB1049::Spec*^{R} mutant strain was comparable to the one for the wild-type bacteria, whereas *NMB1048* expression was considerably lower in all the time points measured (Figure 4.3-3C). The high levels of gene expression seen at all times for both genes in wild-type bacteria might be explained by the fact that bacteria find pyruvate to be a poor carbon substrate for growth, and therefore started to catabolise propionic acid sooner, as an extra source of carbon. In fact, bacteria that were not supplied with propionic acid, when grown in this medium, started to die already after only 5 or 6 hours incubation. Alternatively, the constantly high expression level of the *prpC* gene throughout the period of growth in pyruvate can explain the early utilisation of propionic acid in these cultures, compared to cultures grown in CDM with glucose or in MHB, where expression was lower.

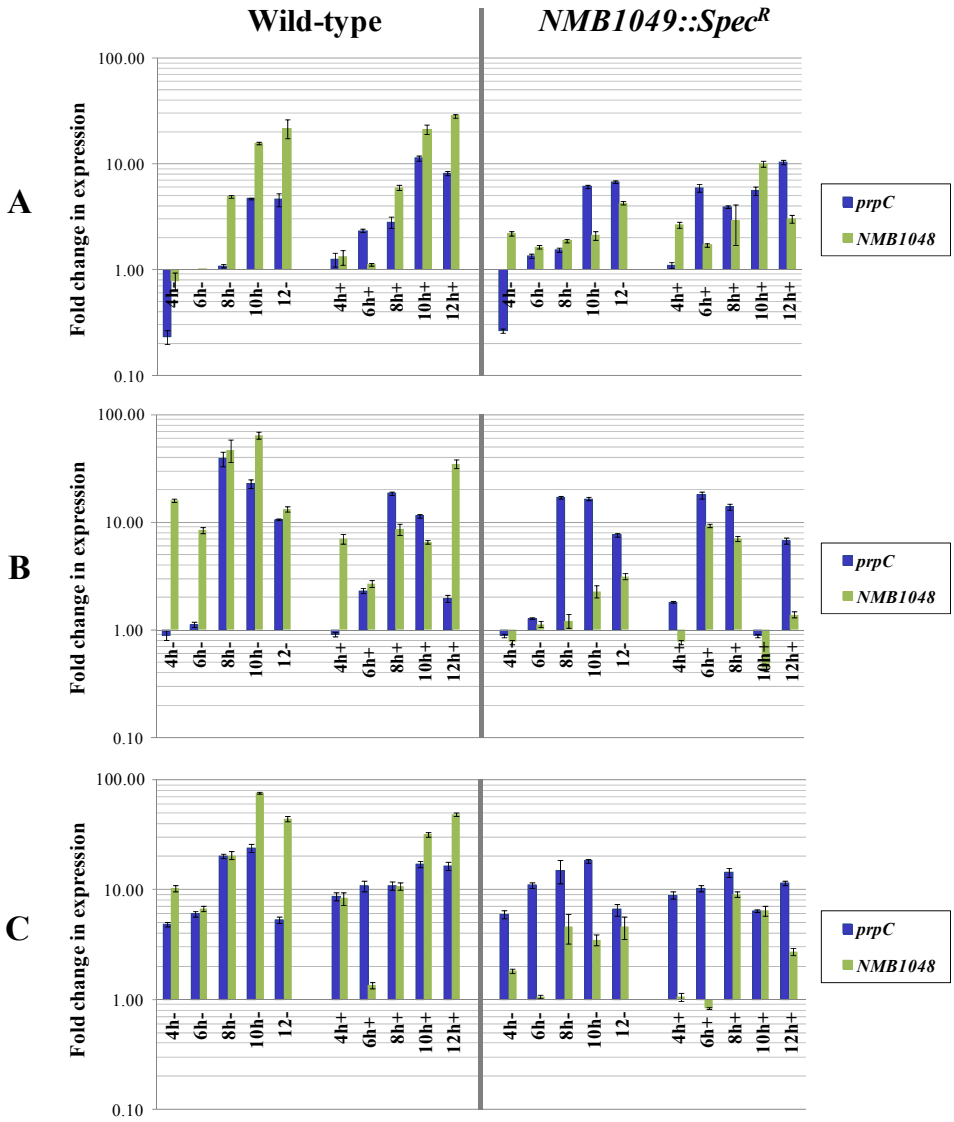

Figure 4.3-3: Average fold change of *prpC* and *NMB1048* gene expression in *N. meningitidis* MC58 wild-type and *NMB1049::Spec*^{R} mutant strain.

Relative expression of *prpC* (2-methylcitrate synthase) and *NMB1048* was plotted for wild-type cultures grown in MHB (**A**) and in CDM with 2.5 mM glucose (**B**) or 5 mM sodium pyruvate (**C**) with 0 or 5 mM propionic acid. Data was normalised with *metK* (S-adenosylmethionine synthetase) and was calibrated with the wild-type culture that was grown for 6 hours in MHB without propionic acid. Expression of *prpC* and *NMB1048* increased throughout the time course, and this was independent on the absence / presence of propionic acid. *prpC* expression level was similar in wild-type and *NMB1049::Spec*^{R} mutant. *NMB1048* expression level was considerably lower in the *NMB1049::Spec*^{R} mutant. - / +: growth media with 0 / 5 mM propionic acid added at the start.

Both *prpC* and *NMB1048* gene expressions were higher when nutrient availability was poor. In fact, when *N. meningitidis* was entering stationary phase or when the growth medium did not have a good carbon substrate, these genes were always highly expressed. As a consequence, it could be deduced that *prpC* and *NMB1048* were co-regulated, but also that *prpC* was not regulated by NMB1049, as there was no change in *prpC* expression between the wild-type and the *NMB1049::Spec*^{R} mutant. A new model was therefore built following these results, where NMB1049, a hypothetical LysR-Type protein, was only found responsible for regulating the divergently transcribed *NMB1048* gene (Figure 4.3-4). The idea that the signal molecule, which was thought to involve C3 compounds such as sodium pyruvate or propionic acid in preliminary studies, could involve propionic acid was now discarded, as the *NMB1048* gene under investigation did not have any significant changes in expression due to the presence or absence of this short fatty acid.

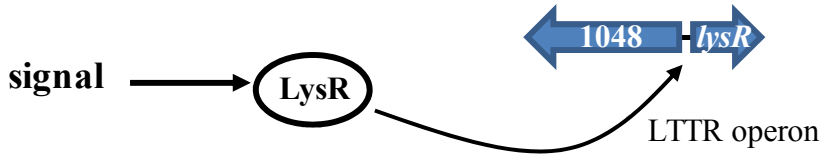

Figure 4.3-4: Actual model for genes regulated by NMB1049.
LysR protein, encoded by *NMB1049,* up-regulates transcription of *NMB1048* when in the presence of a signal molecule. 1048 corresponds to *NMB1048,* whose nomenclature was given in the MC58 complete genome (NCBI GenBank accession number AE002098.2).

Preliminary results showed that NMB1049 was likely to be a repressor of the *prp* operon, as in the *NMB1049::Spec*^{R} mutant strain expression of *prpC* was higher than in wild-type bacteria. This hypothesis, however, was studied further because of the high variability between experiments, and was soon discarded when gene expression was measured as a time course. Time course gene expression, in fact, showed that *prpC* was always similarly expressed in both bacterial strains under investigation.

The uncharacterised pathogenic island under study is composed of genes *NMB1048* and *NMB1049*. NMB1049 has similarity to a LysR-Type transcriptional regulator (LTTR), as it contains the two functional domains typical of LTTR proteins, the N-terminal Helix-Turn-Helix domain and the C-terminal substrate-binding domain. LTTRs typically regulate genes that are adjacent and transcribed divergently in the genome. *NMB1048* is adjacent and divergently transcribed to *NMB1049*. Moreover, *NMB1048* gene expression has been shown to be more up-regulated in the wild-type strain, as the mutant strain deficient in *NMB1049* did not have such high expression. For this reason, it can be hypothesised that NMB1049 is an activator of *NMB1048*.

This 2-genes pathogenic island could be facilitating transport into the bacterial cell of the C3 compound sodium pyruvate. NMB1048, in fact, has similarity to an uncharacterised putative transmembrane protein. When wild-type *N. meningitidis* bacteria were grown in minimal medium and especially when in the presence of sodium pyruvate, there was a constant up-regulation of the expression of *NMB1048*, whereas in the *NMB1049::Spec*^{R} mutant the expression of *NMB1048* was induced to a much lower extent.

4.4 Effects of the different media on growth of *N. meningitidis*

To test if NMB1048 can be a sodium pyruvate transporter and to confirm the results shown in the previous section, which were suggesting that the *prp* operon was still fully functional and that propionic acid did not have any effects on this uncharacterised pathogenic island composed of genes *NMB1048* and *NMB1049* as the *NMB1049::Spec*^{R} mutant did not have any effect on the expression of *prpC*, *N. meningitidis* MC58 wild-type, *NMB1048::Spec*^{R} and *NMB1049::Spec*^{R} strains were grown in all media with or without propionic acid.

Bacteria were incubated in Mueller Hinton Broth (MHB) medium with 10 mM $NaHCO_3$ at 37 °C with shaking at 200 rpm for 24 hours. Growth was monitored by taking optical density measurements for triplicate cultures at 600 nm every 60 minutes. The results showed that all three strains were able to grow, and grew steadily, independently on the addition of propionic acid into the culture (Figure 4.4-1). Inactivation of *NMB1048 or NMB1049* genes was therefore not fatal and did not increase sensitivity to 5 mM propionic acid in the mutant strains, as shown in the previous chapter.

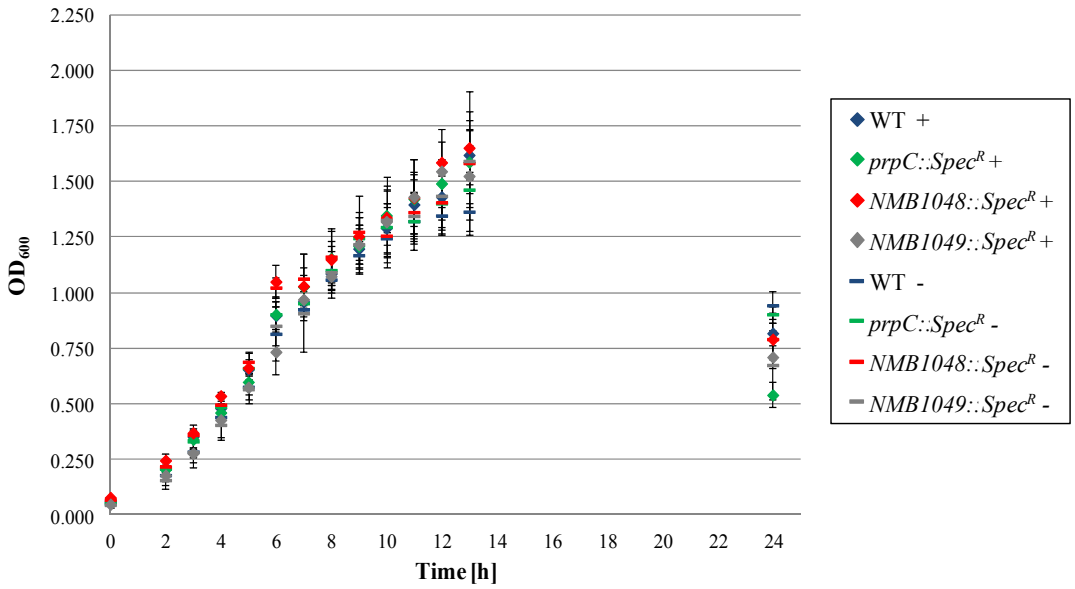

Figure 4.4-1: Growth curve for wild-type, *prpC*, *NMB1048* and *NMB1049* mutant strains of *N. meningitidis* MC58 in rich medium with propionic acid.
All strains of bacteria grown in Mueller Hinton Broth medium supplemented with none or 5 mM propionic acid grew steadily.

As no significant differences were noticed between wild-type and the mutant strains when grown in rich medium, further studies were carried out in Chemically Defined Medium (CDM), which was prepared as described in Table 2.2.4-1. In CDM with 2.5 mM glucose wild-type, *NMB1048::Spec*^{R} and *NMB1049::Spec*^{R} bacteria grew similarly when no propionic acid was added: all strains reached stationary phase after approximately 8 hours incubation and started to die afterwards, suggesting that carbon depletion was initiating at that point. Bacteria that were grown with the addition of 5 mM propionic acid, however, were able to continue their growth and did not enter stationary phase, except for the *prpC::Spec*^{R} mutant (Figure 4.4-2A). These results suggested that propionic acid could supplement growth in *N. meningitidis* and, despite inactivation of genes *NMB1048* and *NMB1049*, propionic

acid was still utilised. This behaviour confirmed that both genes belonging to the uncharacterised island under investigation were not directly involved in propionic acid catabolism. At this stage, new studies were carried out with CDM containing 5 mM sodium pyruvate. Compared to glucose, a double concentration of pyruvate was used in order to keep the number of carbon atoms added identical between the two minimal media. In this way, any divergence in phenotype between the two strains and the different media was easier to compare.

When grown in CDM supplemented with 5 mM sodium pyruvate and 5 mM propionic acid all bacteria grew continually for a period of over 10 hours, except for the *prpC::Spec*^{R} mutant strain which started to die after approximately 6 hours incubation, and this growth was comparable to when bacteria were grown in minimal medium with glucose and propionic acid. In the absence of propionic acid, all strains started to die after approximately 6 hours incubation, like the *prpC::Spec*^{R} mutant that was unable to use propionic acid as an extra carbon source (Figure 4.4-2B). The optical density of bacteria grown in CDM with sodium pyruvate was considerably lower compared to the one measured for CDM with glucose: bacteria incubated without propionic acid grew to an OD of 0.8 - 1 with glucose and only 0.4 with pyruvate. Therefore, sodium pyruvate was demonstrated to be not as good a substrate for *N. meningitidis* growth as glucose, and the effect of added propionic acid could be very clearly seen. Sodium pyruvate appeared to be utilised at the same rate in wild-type and the mutant strains, as growth and doubling time was comparable. This suggested that *NMB1048::Spec*^{R} and *NMB1049::Spec*^{R} mutant strains were probably not directly involved in the transport of sodium pyruvate.

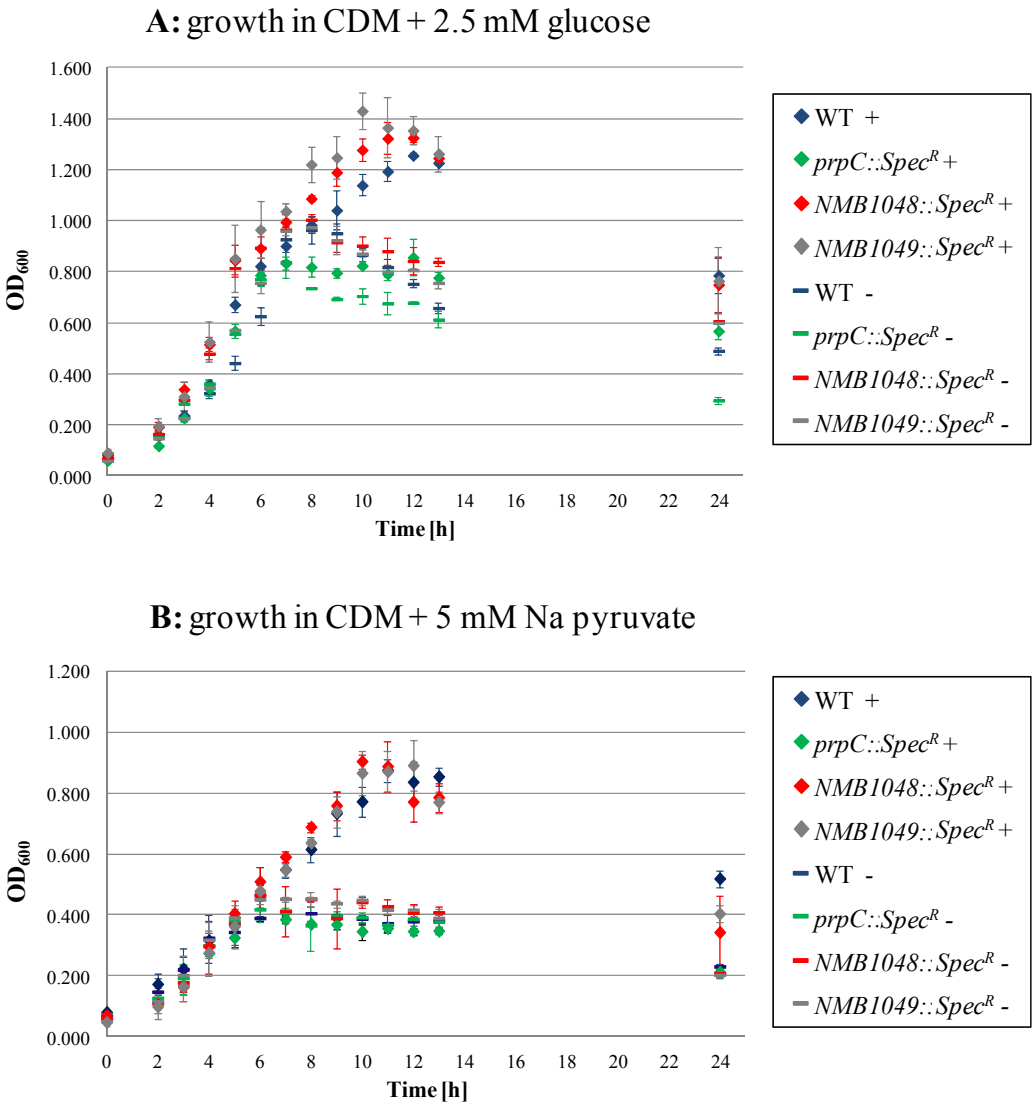

Figure 4.4-2: Growth curves for wild-type, *prpC*, *NMB1048* and *NMB1049* mutant strains of *N. meningitidis* MC58 in CDM media with propionic acid.
All bacterial strains grown in both minimal media used propionic acid as an extra carbon source for continued growth, with the exception of the *prpC::Spec*^{R} mutant strain.

Both *NMB1048::Spec*^{R} and *NMB1049::Spec*^{R} mutants grew in a similar way as the wild-type MC58 strain in all media and under all conditions investigated. Moreover, from the figures shown above, all strains showed a similar doubling time when their

growth was compared to the same medium with or without propionic acid during the exponential growth phase. Similarity in doubling time was confirmed and fell within the values from Table 4.4-1, where the actual doubling times calculated were extrapolated from at least 4 independent datasets. The same datasets were also plotted visually, where it was easier to compare the doubling times for each growth medium. Doubling times were significantly shorter in rich MHB medium (approximately 80 minutes), but were similar within the two chemically defined media (approximately 100 minutes) (Figure 4.4-3). The doubling time for each dataset was extrapolated in the same way as described in Figure 3.6-5.

Table 4.4-1: Doubling time of MC58 wild-type, *NMB1048::Spec^R* and *NMB1049::Spec^R* mutant strains of *N. meningitidis* in the three different growth media with the addition of propionic acid, during exponential growth phase.

The summary of the doubling times was obtained from at least 4 independent sets of data for each strain. All strains showed a shorter time of duplication when grown in rich medium compared to minimal medium. Doubling time of all strains grown in either minimal medium was not significantly different. -: growth medium not supplemented with propionic acid. +: growth medium supplemented with 5 mM propionic acid.

Doubling time / Strain [hours]	Average in MHB	Average in CDM+glucose	Average in CDM+pyruvate
MC58 WT -	1.27 ± 0.12	1.72 ± 0.19	1.76 ± 0.19
MC58 WT +	1.31 ± 0.06	1.59 ± 0.14	1.76 ± 0.17
NMB1048::Spec^R -	1.30 ± 0.09	1.56 ± 0.25	1.70 ± 0.07
NMB1048::Spec^R +	1.21 ± 0.15	1.62 ± 0.19	1.76 ± 0.15
NMB1049::Spec^R -	1.24 ± 0.13	1.66 ± 0.13	1.56 ± 0.13
NMB1049::Spec^R +	1.17 ± 0.14	1.50 ± 0.11	1.57 ± 0.20

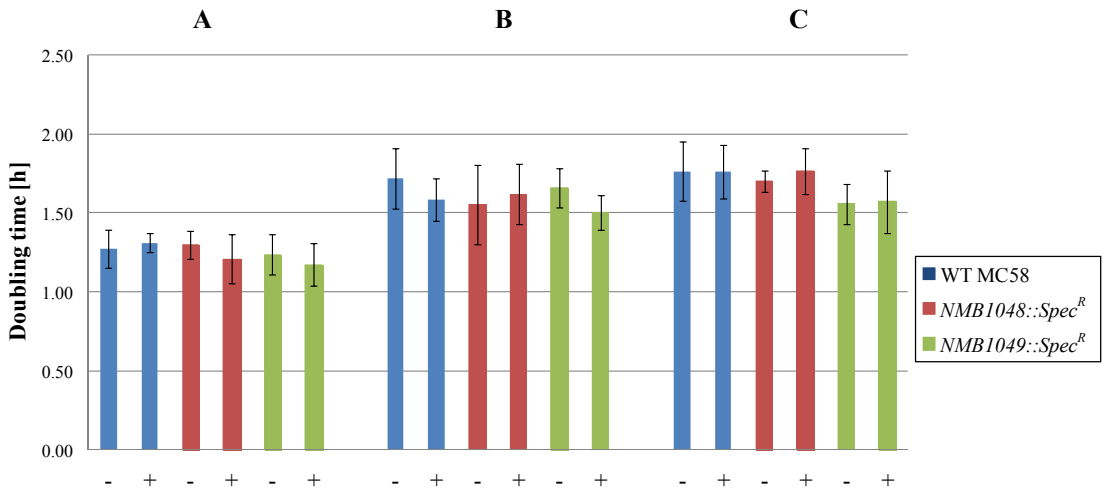

Figure 4.4-3: Doubling time of MC58 wild-type, *NMB1048::Spec*^{R} and *NMB1049::Spec*^{R} mutant strains of *N. meningitidis* in the three different growth media.

A: Doubling time for growth in rich medium (MHB). **B:** Doubling time for growth in minimal medium, CDM with 2.5 mM glucose. **C:** Doubling time for growth in minimal medium, CDM with 5 mM sodium pyruvate. A minimum of 4 independent sets of data were used for extrapolating the average doubling time of each strain. Doubling time was extrapolated from the exponential growth. All three strains showed similar doubling times when the strains were compared within the same growth medium, independently of the presence or absence of propionic acid. -: growth medium not supplemented with propionic acid. +: growth medium supplemented with 5 mM propionic acid.

No significant differences were noticed in growth or doubling time when the wild-type and both *NMB1048::Spec*^{R} and *NMB1049::Spec*^{R} mutants were compared within the same medium. Therefore, despite inactivation of either of the genes, sodium pyruvate seemed to be still used at a similar rate. The absence of the putative transporter NMB1048 did not appear to have any negative influence on sodium pyruvate uptake. Moreover, as both mutant strains behaved similarly to the wild-type

bacteria, the hypothesis that propionic acid could still be used by the mutants was still valid.

4.5 Effects of propionic acid on *NMB1048*

As shown in the previous section, propionic acid does not have any direct effects on the uncharacterised pathogenic island composed of genes *NMB1048* and *NMB1049,* and appears to be utilised as an extra source of carbon during late exponential phase in *N. meningitidis* MC58 wild-type, *NMB1048::Spec*^{R} and *NMB1049::Spec*^{R} mutants when bacteria were grown in minimal medium. To confirm these findings, samples from all growth media were collected every 60 minutes, and the content of propionic acid was measured by gas chromatography (GC).

When incubated in Mueller Hinton Broth medium, neither wild-type bacteria nor *prpC::Spec*^{R}, *NMB1048::Spec*^{R} nor *NMB1049::Spec*^{R} mutant strains used the propionic acid that was supplemented in the medium (Figure 4.5-1). All strains entered quickly the exponential growth phase and did not need to utilise propionic acid for enhancing bacterial growth, as the medium was already rich in carbon. Major differences, however, were seen when bacteria were grown in Chemically Defined Medium (CDM) with either 2.5 mM glucose or 5 mM sodium pyruvate supplemented with 5 mM propionic acid. MC58 wild-type bacteria started to use propionic acid after 5 to 6 hours incubation, independently of the CDM used (Figure 4.5-2). Growth curves from the previous section (Figure 4.4-2) showed that wild-type bacteria supplemented with propionic acid followed enhanced growth, thus avoiding entering stationary phase, after approximately 7-8 hours in CDM with glucose, and already after 5-6 hours in CDM with pyruvate. This meant that

propionic acid utilisation began in late exponential / stationary phase in CDM supplemented with glucose, and concomitant with entry into stationary phase in CDM supplemented with pyruvate.

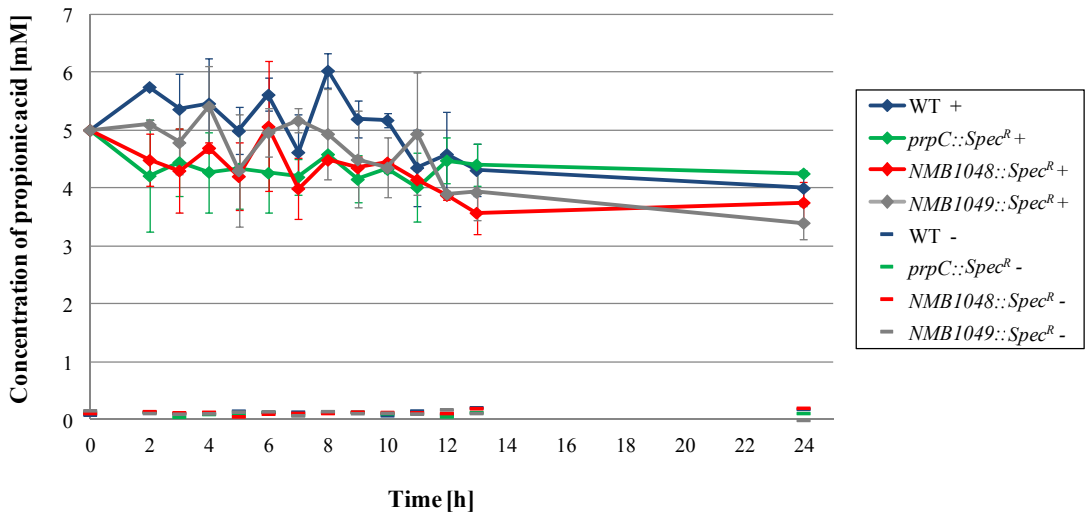

Figure 4.5-1: Propionic acid was not utilised in rich medium.

Gas chromatography results for *N. meningitidis* MC58 wild-type and all mutant strains tested showed that the amount of propionic acid in MHB medium remained constant throughout the 24 hours incubation period.

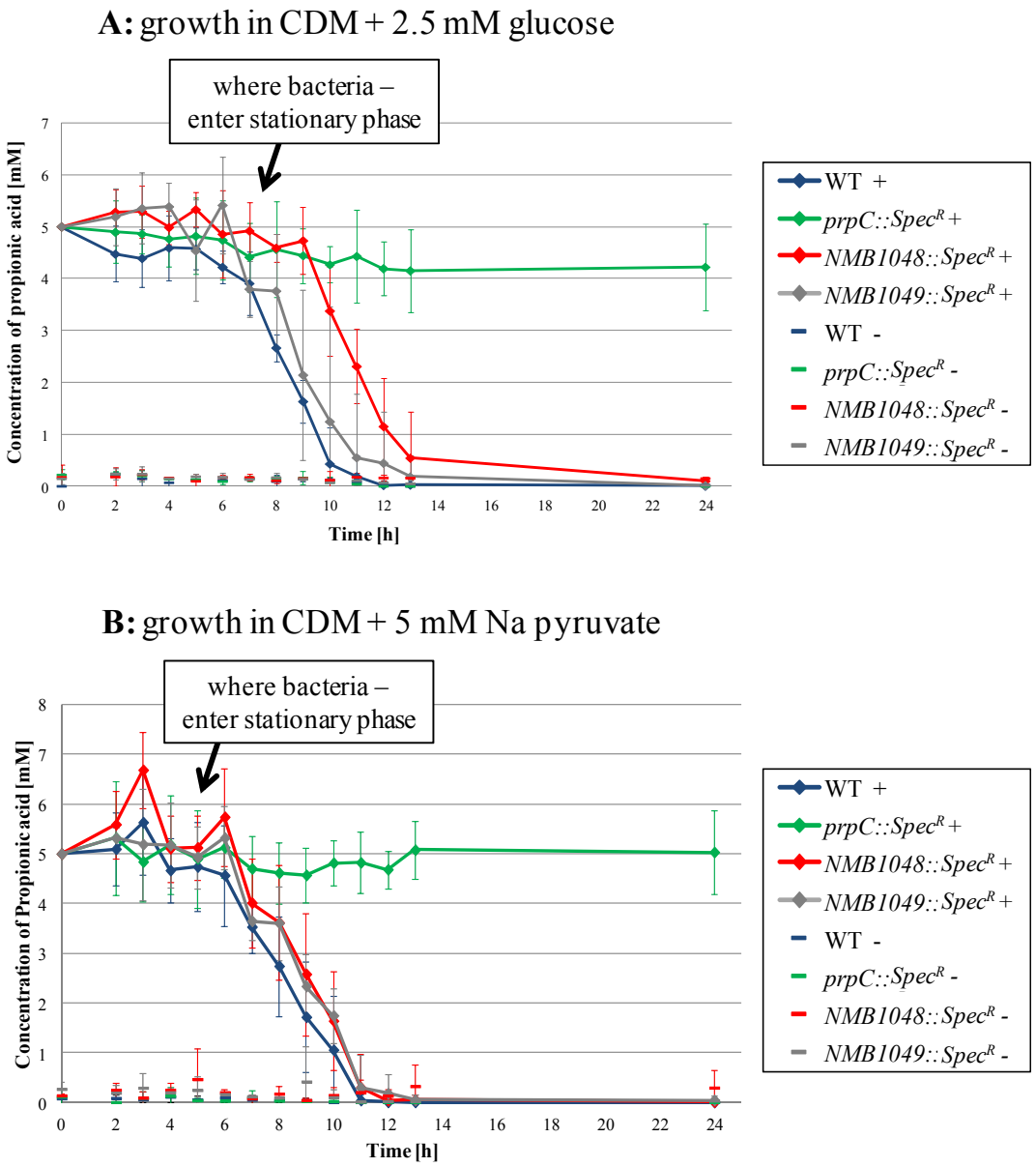

Figure 4.5-2: Propionic acid was utilised in minimal media.

Concentration of propionic acid versus time for bacteria grown in CDM media with 2.5 mM glucose (**A)** and 5 mM sodium pyruvate **(B)**, with or without addition of 5 mM propionic acid. In both panels, gas chromatography results showed that propionic acid supplemented in both chemically defined media was utilised by all strains tested, with the exception of the *prpC::Spec*^{R} mutant, and was completely depleted after 24 hours growth. Controls where no propionic acid was added showed that propionic acid was not present throughout the growth curve for any bacteria. -: No propionic added to the medium. +: 5 mM propionic acid added at the start.

Samples taken from all strains tested in the absence of propionic acid showed that no propionic acid was detected throughout the whole growth curve, demonstrating that propionic acid is not synthesised under any experimental conditions that were investigated in this work. When 5 mM propionic acid was added into either minimal media, there was no significant difference in propionic acid utilisation between wild-type and both *NMB1048::Spec*^{R} and *NMB1049::Spec*^{R} mutant bacteria, suggesting that the absence of this uncharacterised pathogenic island did not have any direct negative influence on the functioning of the 2-methylcitrate pathway.

4.6 Studies of the *N. meningitidis* double mutant for genes *NMB0432* and *NMB1048*

NMB1049, which encodes a putative LTTR protein, has been shown in this chapter to be involved in the regulation of the *NMB1048* gene. *NMB1048*, which encodes a putative transmembrane protein, has been speculated here to be involved in the transport of sodium pyruvate, as gene expression showed that this gene was highly expressed in wild-type but not in the *NMB1049::Spec*^{R} mutant strain when grown in minimal medium supplemented with sodium pyruvate. Despite inactivation of *NMB1048* or *NMB1049*, however, sodium pyruvate appeared to be still used at a similar rate. This meant that the absence of the putative transporter NMB1048 did not appear to have any negative influence on sodium pyruvate uptake.

One possible explanation on why the absence of *NMB1048* did not seem to have any effect in the transport of sodium pyruvate could be due to this putative transporter being redundant and replaced by another transporter. The uncharacterised *NMB0432* gene belonging to the *prp* gene operon, which is a putative transporter and has been demonstrated to be directly involved in the 2-methylcitrate pathway and to be crucial

for propionic acid metabolism in Chapter 3, could be a C3 compound transporter for propionic acid and sodium pyruvate. Therefore, a strain containing disrupted copies of both *NMB0432* and *NMB1048* genes might grow poorly on sodium pyruvate.

To understand if *NMB0432* and *NMB1048* genes were involved in sodium pyruvate transport, a double mutant for both genes was created. The double mutant was constructed as described in Section 2.3.9. During the TSB transformation, however, wild-type bacteria were replaced with the *NMB1048::Spec*^{R} mutant strain, which was spread on CBA plates containing 5 % Defibrinated Horse Blood (TCS biosciences) and 50 μg / ml spectinomycin. The gene to be inserted into this strain was the *NMB0432* that was previously disrupted with tetracycline (described in Section 3.5). The new transformants were spread onto CBA plates containing also 2.5 μg / ml tetracycline. Double mutants were screened by PCR, where several colonies grown on the plate were picked twice, once for checking that the gene *NMB1048* was actually disrupted with spectinomycin, and once for verifying positive insertion of the *NMB0432* gene containing the tetracycline resistance cassette. New stocks for this *NMB0432::Tet*^{R}*-NMB1048::Spec*^{R} double mutant strain were stored at - 80 ºC.

Growth curves under the same conditions tested with the *N. meningitidis* MC58 wild-type and the mutant strains for *NMB0432* and *NMB1048* were investigated, and in rich medium the new double mutant grew similarly to all the bacteria tested over the 13 hours incubation period, showing that absence of the two genes at the same time was not fatal. When grown in chemically defined medium with 5 mM of both sodium pyruvate and propionic acid, the double mutant strain showed the same phenotype as the *NMB0432::Tet*^{R} mutant, and this meant that it was not able to catabolise propionic acid. Moreover, the double mutant grew at the same rate as wild-type

bacteria in the absence of propionic acid, therefore sodium pyruvate was probably entering the cell and being used normally (Figure 4.6-1).

At this stage, propionic acid utilisation within the CDM medium containing pyruvate was investigated with gas chromatography. As expected from the growth curve results and from the identical behaviour noticed with the *NMB0432::Tet*^{R} strain, the double mutant was not able to catabolise propionic acid, unlike the wild-type and the *NMB1048::Spec*^{R} mutant bacteria (Figure 4.6-2).

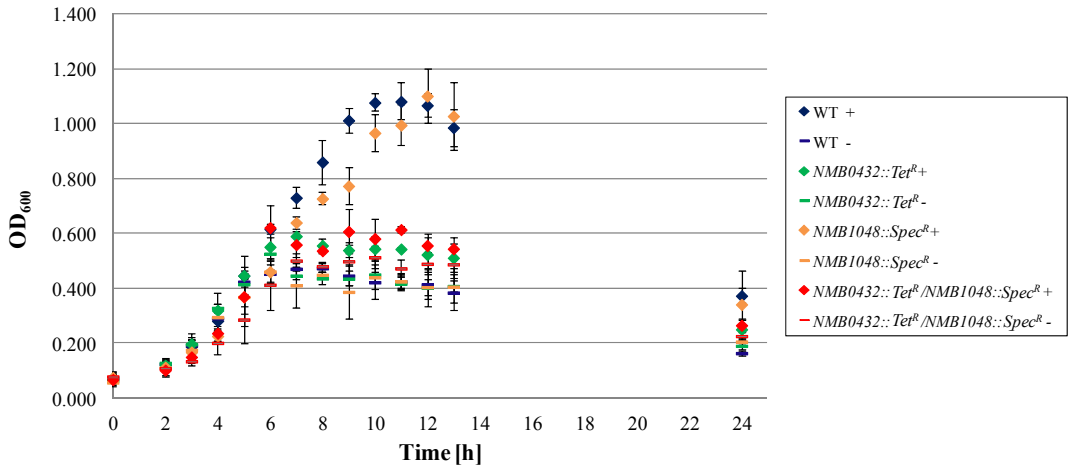

Figure 4.6-1: Growth curve of MC58 *N. meningitidis* wild-type, *NMB0432::Tet*^{R} and *NMB01048::Spec*^{R} compared to the double mutant.

Propionic acid was necessary for continued growth of wild-type *N. meningitidis* and *NMB01048::Spec*^{R} in minimal medium. The other two mutant strains that were grown either with or without supplementation of propionic acid, as well as the wild-type and mutant for *NMB1048* that were grown with no propionic acid, all entered stationary and death phase several hours earlier. The double mutant had the same phenotype as the single mutants for *NMB0432*. -: CDM medium with 5 mM sodium pyruvate and no supplementation of propionic acid. +: CDM medium with 5 mM sodium pyruvate and 5 mM propionic acid added at the start of the bacterial growth.

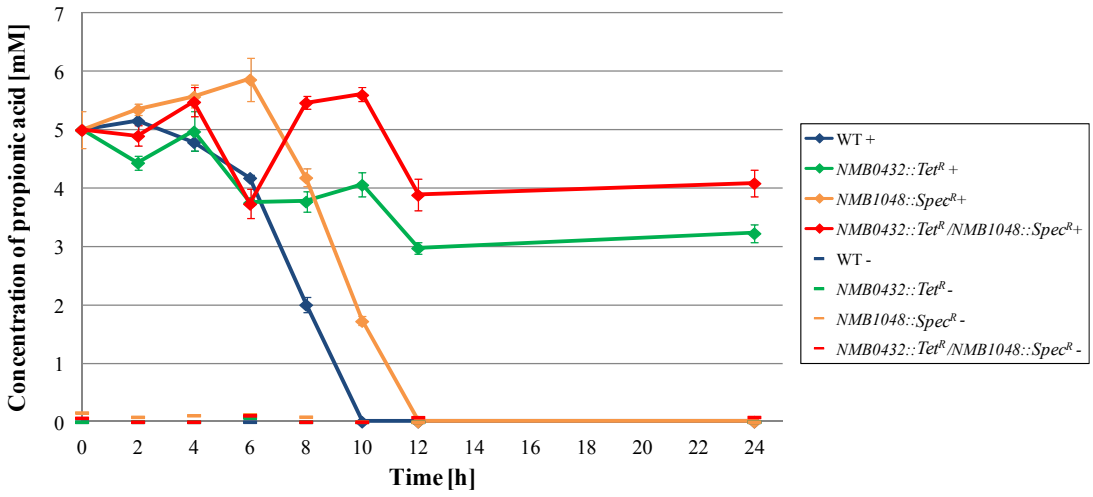

Figure 4.6-2: Propionic acid utilisation in MC58 *N. meningitidis* wild-type, *NMB0432::Tet*^{R} and *NMB01048::Spec*^{R} compared to the double mutant.
Propionic acid was utilised only by the wild-type and *NMB01048::Spec*^{R} strain grown in 5 mM propionic acid. The double mutant strain, like the *NMB0432::Tet*^{R} strain, was not able to catabolise it. -: CDM medium with 5 mM sodium pyruvate and no supplementation of propionic acid. +: CDM medium with 5 mM sodium pyruvate and 5 mM propionic acid added at the start of the bacterial growth.

The results illustrated in this section showed that the knock-out of both *NMB0432* and *NMB1048* genes simultaneously gave the double mutant strain the same phenotype seen with the single mutant for the *NMB0432* gene. Neither of them was able to utilise propionic acid. Moreover, the absence of both genes did not decrease or slow down bacterial growth in minimal medium with sodium pyruvate. Following these outcomes, the double mutant's expression of the genes belonging to the *prp* gene operon was expected to be similar to the expression for the *NMB0432::Tet*^{R} mutant. Difference in gene expression between these two strains, however, showed that the genes tested were less up-regulated in the double mutant. The

NMB0432::Tet^{R} mutant, instead, had all genes downstream of *NMB0432* only slightly down-regulated, as the tetracycline resistance cassette does not contain transcriptional terminators (Heurlier *et al.*, 2008). Further investigations need to be carried out, as this was based on samples taken on one single occasion and run in triplicates (Figure 4.6-3).

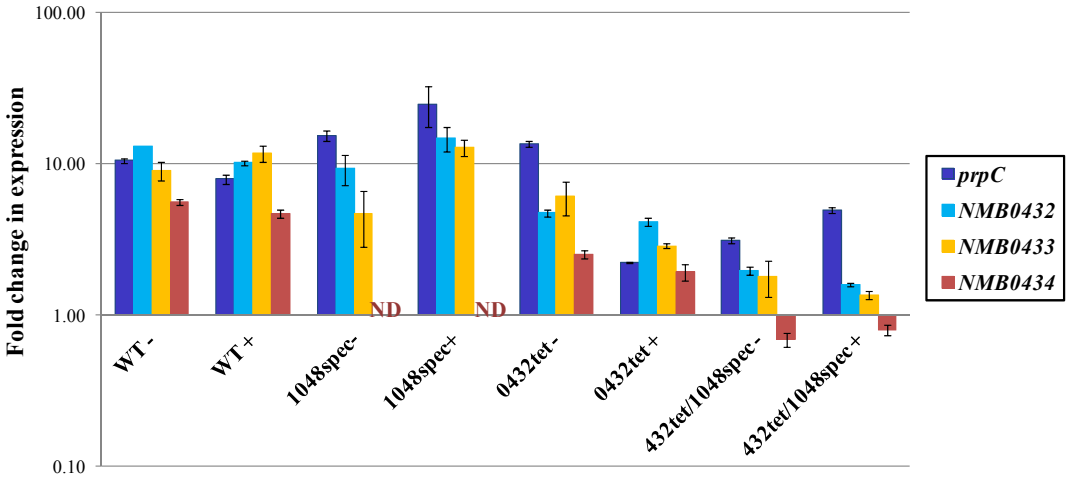

Figure 4.6-3: Average fold change in expression of several genes from the *prp* gene cluster in wild-type and mutant strains in *N. meningitidis* MC58.

All cultures were grown in Chemically Defined Medium with 5 mM sodium pyruvate with (+) or without (-) supplementation of 5 mM propionic acid, and samples were collected after 6 hours growth. Data was normalised with the *metK* gene and was calibrated with the wild-type culture that was grown for 6 hours in MHB without addition of propionic acid. Level of expression of each gene depended on the strain tested. The double mutant shows a net decrease of gene expression, and this includes the *prpC* (*NMB0431*) gene. ND: no data collected for *NMB0434* in *NMB1048::Spec*^{R} mutant.

Down-regulation of expression of the genes tested (*NMB0431-NMB0434*) belonging to the *prp* operon in the *NMB0432::Tet*^{R}*-NMB01048::Spec*^{R} double mutant compared to the wild-type and single mutants could be suggesting that the putative *NMB0432* and *NMB1048* transporters can compensate for each other's absence regarding the expression of the *prpC* gene. Why exactly this happens, however, is still unclear, as it has been shown not to depend on sodium pyruvate.

4.7 *prpC* and *NMB1048* gene expression in enriched growth medium

prpC and *NMB1048* gene expression for wild-type bacteria that were grown in both rich and minimal medium after supplementation of Vitox was investigated. *N. meningitidis* was grown for 6 hours and samples were collected, RNA extracted and reverse transcribed to cDNA as described in Sections 2.3.12 – 2.3.14. Vitox (Oxoid) is a commercially available culture medium supplement and was added at the manufacturer's recommended concentration in all three growth media (MHB and CDM with either glucose or sodium pyruvate). Laboratory Vitox was prepared by adding each component to the same final concentration as the commercial Vitox. The concentration of each component is described in Table 2.2.4-2. The data collected from the RT-PCR run were calibrated with the wild-type bacteria grown in MHB without propionic acid, and were normalised to the housekeeping *metK* gene (*NMB1799*).

As already shown in Figure 4.3-3, expression of both genes after 6 hours growth was considerably lower in Mueller Hinton Broth (MHB) medium when compared to CDM containing 5 mM sodium pyruvate. This result indicated that expression of *prpC* and *NMB1048* genes was greater when bacteria were grown in a poor medium.

When commercial Vitox (Oxoid) was added to the media under investigation, expression of both genes was down-regulated even further, as Vitox contains essential growth factors. However, when laboratory Vitox or the split components, which are composed of only a few chemicals present in the Vitox, were tested, both genes were up-regulated as much as when wild-type bacteria were grown in minimal medium with sodium pyruvate. Laboratory-made Vitox appeared not to have any effect on bacterial growth (Figure 4.7-1).

The same phenotype for *prpC* gene expression was seen in both wild-type and *NMB01049::Spec*^{R} mutant. The second gene under study, which is *NMB1048,* was down-regulated in the mutant when compared to the wild-type under the same conditions. In the mutant strain, however, a modest up-regulation was seen in minimal medium when grown in the presence of either the commercial or the laboratory-made Vitox. *NMB1048* expression in the mutant was similar to the one seen in rich medium with or without addition of Vitox (Figure 4.7-1B).

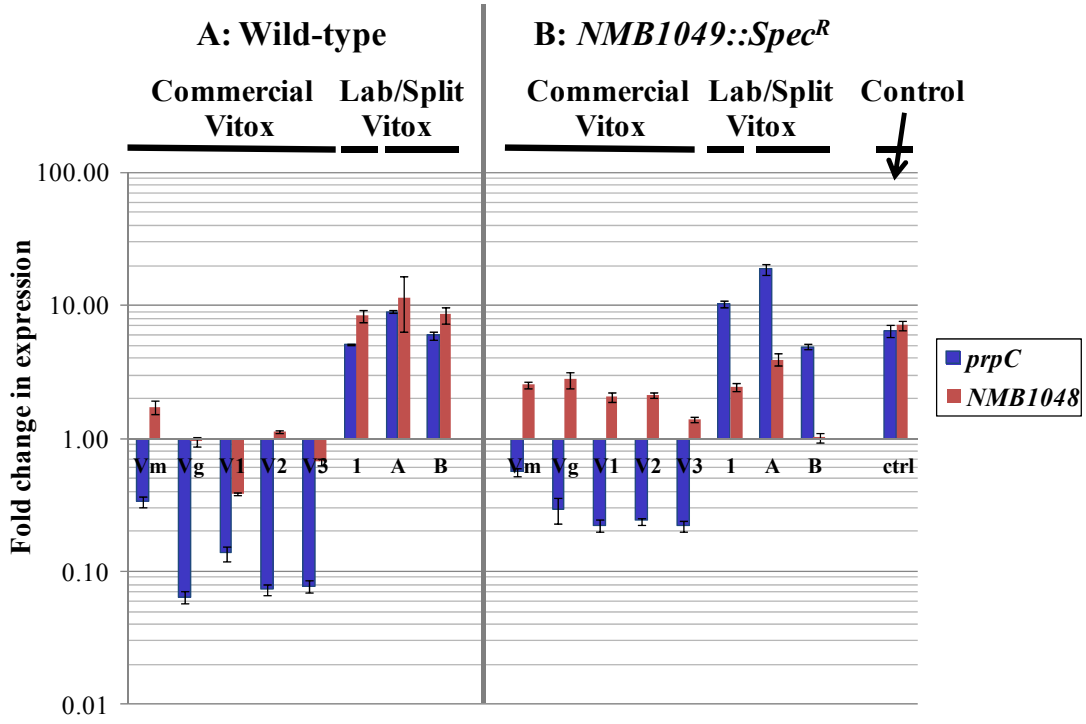

Figure 4.7-1: Average fold change of *prpC* and *NMB1048* gene expression in growth media enriched with Vitox.

Relative expression of *prpC* (2-methylcitrate synthase) and the putative *NMB1048* was plotted for wild-type and *NMB01049::Spec*^{R} mutant cultures grown in MHB (Vm), in CDM with glucose (Vg) and in CDM with sodium pyruvate (V1-V3, 3 independent repeats) enriched with commercial Vitox; in CDM with sodium pyruvate and laboratory prepared Vitox (1) with freshly prepared components each time; and in CDM with sodium pyruvate and some of the components present in Vitox: adenine and guanine (in lane A) and vitamin B_{12}, PABA, cocarboxylase, thiamine hydrochloride (in lane B). *prpC* gene expression was always down-regulated when using commercial Vitox, but remained unchanged when laboratory Vitox and split components were used. *NMB1048* gene expression was down-regulated with commercial Vitox in wild-type bacteria but increased about two-fold compared to the calibrator in the *NMB01049::Spec*^{R} mutant. The control (last lane) was wild-type bacteria grown in CDM with 5mM pyruvate. Data was normalised with *metK* (S-adenosylmethionine synthetase) and was calibrated with the wild-type culture that was grown for 6 hours in MHB without propionic acid.

prpC and *NMB1048* gene expression were higher when nutrient availability was poor, and this was confirmed in wild-type bacteria by a significant down-regulation of both genes in all media containing commercially available Vitox. Interestingly, though, expression was not affected when all components of Vitox were made up in the laboratory, despite having added them into the growth medium at the same concentration found in the commercial Vitox.

4.8 Discussion

In this chapter the uncharacterised pathogenic island from *N. meningitidis* strain MC58, composed of the *NMB1048* and *NMB1049* genes, was investigated. A BLAST search revealed that this pathway is rare in other *Neisseria* spp. but is always present in *N. meningitidis* strains.

NMB1048 encodes a protein that has similarity to the DUF3360, a family of uncharacterised proteins which are probably transporters. Putative transmembrane helices for *NMB1048* were predicted using a transmembrane helices programme based on a hidden Markov model (TMHMM) (Appendix E). TMHMM outputs predicted 11 transmembrane helices and suggested that the N-terminal is located outside and the C-terminal is located in the cytoplasm. *NMB1049* encodes a putative LysR-Type transcriptional regulator. LTTRs are known to up-regulate their adjacent gene, which is divergently transcribed within the genome. In this case the divergently transcribed gene from *NMB1049* is *NMB1048*.

Knockouts for *NMB1048* (*NMB1048::Spec*^{R}) and *NMB1049* (*NMB1049::Spec*^{R}) were created in this work, and they both showed the same phenotype as the wild-type bacteria under any conditions tested. Growth curves and gas chromatography

analysis confirmed that the mutants did not need propionic acid to grow in rich medium, but they were able to use propionic acid for optimal growth in minimal medium.

As already mentioned in Chapter 3, expression of the genes belonging to the 2-methylcitrate pathway might be controlled by poor nutrient availability, as propionic acid started to be utilised earlier when in the presence of a poor carbon source. This hypothesis was further confirmed in this chapter, as *prpC* gene expression was constantly high in minimal medium. *NMB1048* gene expression led to similar results in the wild-type strain, as the gene was highly up-regulated in a similar manner as *prpC*. In the *NMB1049::Spec*^{R} mutant strain, *prpC* showed to have the same regulation as in wild-type bacteria, but expression of *NMB1048* was consistently lower than in the wild-type bacteria. These results indicated that the putative LTTR encoded by *NMB1049* is responsible for regulating expression of *NMB1048* but not *prpC*.

prpC and therefore *NMB0432*, as the latter gene always has similar expression as *prpC*, and *NMB1048* were always highly up-regulated in minimal medium, especially when the medium was supplemented with sodium pyruvate. Both *NMB0432* and *NMB1048* encode for proteins that have putative functions, and could be transporters. As they were regulated similarly, a double mutant was created (*NMB0432::Tet*^{R}*-NMB1048::Spec*^{R} mutant). *NMB1048*, encoding a putative transmembrane protein, was thought to be replaced, at least partially, by another gene, *NMB0432*. This second gene, *NMB0432*, has been confirmed to be fundamental for propionic acid metabolism in Chapter 3 and it encodes a protein that has similarities to putative transporters. The *NMB0432* gene, containing a predicted

permease domain, might be a late addition to the *prp* gene cluster of *Neisseria* for helping these bacteria acquiring propionic acid, due to the specific niche where these bacteria live. However, as these genes were highly expressed in minimal media, especially in the presence of sodium pyruvate, and because they both have similarities to transporters, it was hypothesised in this work that they could both be involved and have overlapping functions in the transport of the C3 compound sodium pyruvate. Growth curves showed that absence of both genes simultaneously was not lethal. Gas chromatography revealed that propionic acid was not utilised, as it was already seen with the *NMB0432::Tet*^{R} strain.

prpC gene expression was constantly highly regulated after 6 hours incubation in minimal medium with sodium pyruvate, independently of the supplementation of propionic acid in the medium, in all strains tested with the exception of the double mutant. In this strain, all downstream genes from, and including the *prpC* gene (*NMB0431-NMB0434*), were shown to be down-regulated. The strain deficient in *NMB1048*, instead, had all genes up-regulated like the wild-type bacteria and the strain deficient in *NMB0432* had the genes downstream of the *prpC* (*NMB0431*) only slightly down-regulated, as the tetracycline cassette has no transcriptional terminators (Heurlier *et al.*, 2008). Despite not being regulated by NMB1049, both *prpC* and *NMB1048* appeared to be co-regulated. Low expression of both genes in the double mutant could indicate that *NMB0432* and *NMB1048* are possibly compensating for each other, as expression of either of the two genes in the *NMB0432::Tet*^{R} and *NMB1048::Spec*^{R} mutants is high and similar to the wild-type bacteria.

A possibility as to why both *prpC* and *NMB1048* genes are highly up-regulated in the wild-type strain in minimal medium could be explained by a fairly recent study, where it was discovered that *NMB0573* is responsible for up-regulating both *prpC* and *NMB1048* (Ren *et al.*, 2007). *NMB0573* encodes the Lrp protein (leucine-responsive regulatory protein), which is a global regulator that consists of an adaptive response to nutrient poor conditions. The expression of *NMB1048*, therefore, is activated by both NMB1049, as shown in this work, and Lrp. Whilst the regulation of *NMB1048* and *prpC* is similar in response to growth conditions, co-regulation of both genes could also be explained by Lrp.

Chapter 5 - Investigations of a pathogen-specific regulator in *N. meningitidis*

5.1 Introduction

There are 9 conserved genetic islands which are found in all *Neisseria meningitidis'* strains, but are absent from its closely related commensal *Neisseria lactamica*. One amongst these islands is composed of two genes (*NMB1048* and *NMB1049* in *N. meningitidis* MC58) that are divergently transcribed. This island has been previously described in Section 1.7.2 and in Chapter 4.

When subjected to BLAST, NMB1048 was shown to belong to a family of bacterial proteins that are functionally uncharacterised. The sequence of NMB1049, however, resulted in specific hits for two conserved domains that are always present in LysR-Type transcriptional regulators: the Helix-Turn-Helix (HTH) domain and the LysR-Type transcriptional regulator (LTTR) substrate-binding domain (Figure 5.1-1). The HTH domain recognises and binds to the DNA that is regulated by this protein, whereas the LTTR substrate-binding domain is responsible for the different regulation of the gene to which it has bound, thanks to a co-factor binding motif (Schell, 1993). The LTTR protein can usually have a dual activity, meaning that it can both up-regulate a certain gene or cluster of genes and down-regulate a different gene or operon. This family of proteins usually activates the expression of the adjacent and divergently transcribed gene or of genes found elsewhere within the genome, whilst repressing its own expression due to negative auto-regulation (Figure 5.1-2) (Pérez-Rueda & Collado-Vides, 2001).

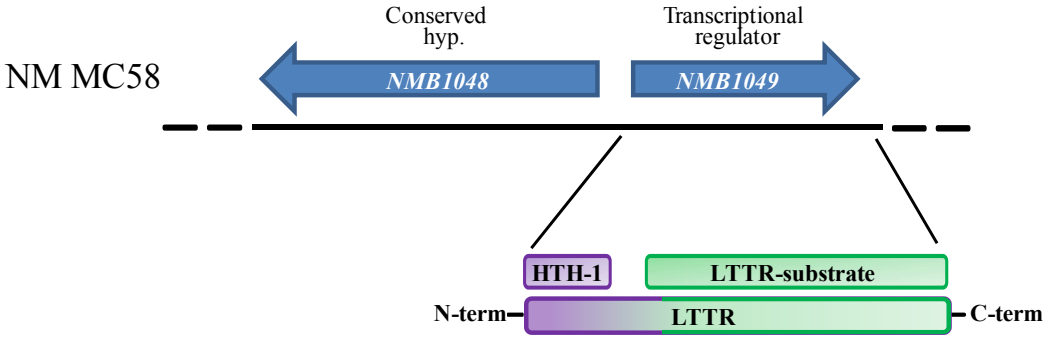

Figure 5.1-1: LysR-Type conserved domains in NMB1049.

The relevant region of *N. meningitidis* MC58 genome representing the genes belonging to the *NMB1048-NMB1049* pathogenic gene cluster (dark blue arrows) is shown with the orientation of both genes. Conserved domains in NMB1049 have similarities to a LysR-Type Transcriptional regulator (LTTR) protein and comprise a Helix-Turn-Helix (HTH) domain at the N-Terminus and a LTTR substrate-binding domain at the C-Terminus. Gene numbers correspond to the numbering given in the MC58 complete genome (NCBI GenBank accession number AE002098.2). Conserved hyp.: gene coding for a conserved hypothetical protein.

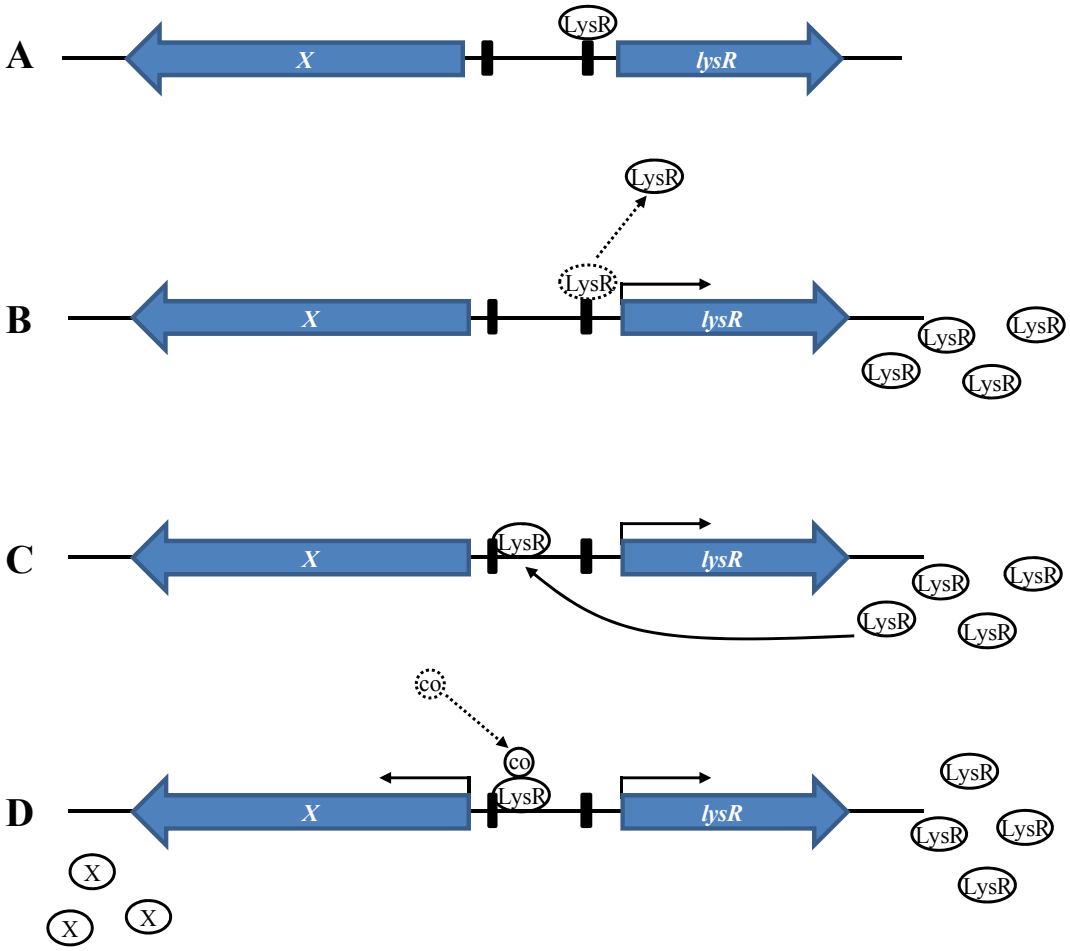

Figure 5.1-2: Classical model for LTTR-dependent transcriptional regulation. **A:** The LysR protein binds to its own promoter and represses its gene regulation. **B:** Once the LysR protein dissociates from its promoter, the *lysR* gene starts being transcribed. **C:** Abundance of LysR protein is more likely to bind upstream of the promoter region of the divergently transcribed target gene. **D:** When the co-inducer is present and interacts with LysR, transcription of the target gene is activated (Figure adapted from Maddocks & Oyston, 2008).

LTTR proteins are folded in a similar manner and are, therefore, thought to be originating from a common ancestor (Pérez-Rueda & Collado-Vides, 2001, Henikoff *et al.*, 1988). The highest similarity amongst LTTRs is given by the amino acid

sequence forming the Helix-Turn-Helix domain, which consists of 66 N-terminal residues. Amongst these residues, amino acids 23 to 42 have sequence identity of at least 40 % between all LTTR proteins with the HTH binding motif (Schell, 1993).

LysR-Type transcriptional regulators are the most abundant types of transcriptional regulators and are composed of between 276 and 324 amino acids. They have a regulatory function over genes with different disparate functional roles, such as genes implicated in metabolic processes, virulence, quorum sensing, oxidative stress response, attachment and secretion, etc. (Maddocks & Oyston, 2008). In *N. meningitidis* strain MC58, for instance, three LTTRs are found following protein BLAST search, and these are OxyR (NMB0173), which is responsible for activating genes for the defence against oxidative stress; CrgA (NMB1856), which is needed for down-regulating genes involved in pili and capsule formation upon contact with the host's epithelial cells in order to enhance adhesion; and MetR (NMB2055), which regulates the expression of methionine biosynthetic genes (Sainsbury *et al.*, 2012, Ieva *et al.*, 2008, Deghmane *et al.*, 2002). OxyR and MetR are found in all *Neisseria* spp. sequenced so far, whereas CrgA is present only in the three closely related *N. meningitidis*, *N. gonorrhoeae* and *N. lactamica*. The putative NMB1049 protein, which is 305 amino acids in length, has similarities to the type 2 periplasmic binding protein which is usually coupled to transporters or chemotaxis receptors, but no actual genes have been identified to be regulated by NMB1049 to date.

In this study, the protein NMV_1164 from *Neisseria meningitidis* serogroup C strain 8013 has been overexpressed and purified for its characterisation. NMV_1164 is a 33.4 kDa protein which, in this work, contains 6x His-tag residues. This protein has 100 % identity with NMB1049 from *Neisseria meningitidis* serogroup B strain

MC58 and, for this reason, NMV_1164 has been chosen for studying the protein's possible interactions with *NMB0430*, *NMB1048* and *NMB1049*. Preliminary studies from chapter 4 hypothesised that this gene encoding a LTTR was responsible for regulating both the *prp* gene cluster (genes *NMB0430-NMB0435*) and the divergently transcribed *NMB1048* gene (Figure 5.1-3). For this reason, this hypothesis was further studied in this chapter by investigating the interactions between the NMV_1164 (NMB1049) protein and the intergenic regions of DNA where possible promoter regions for LTTR were found. The choice for promoter regions will be investigated in Sections 5.5 and 5.6.

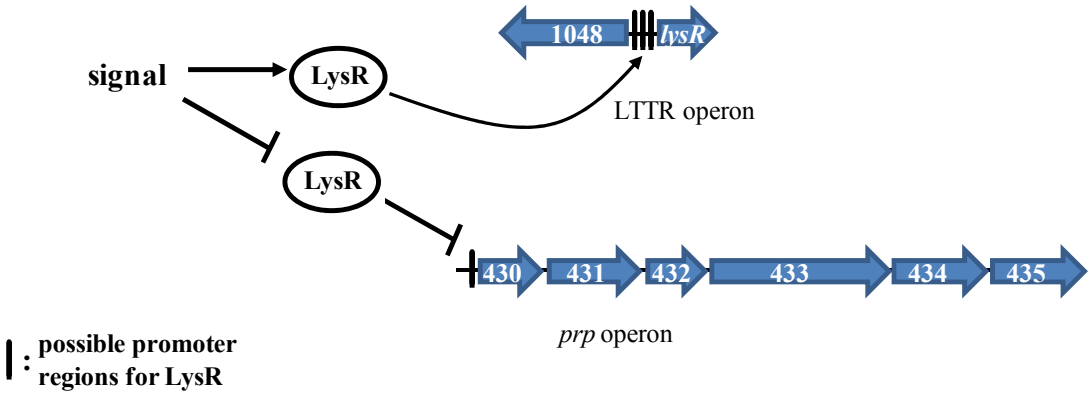

Figure 5.1-3: Hypothetical model for genes regulated by NMB1049.
LysR protein encoded by *NMB1049* might regulate transcription of *NMB1048* and the *prp* operon when in the presence of a signal molecule. Three possible promoter regions were found in the intergenic region between *NMB1048* and *NMB1049*, and one promoter region was found upstream of the *prp* operon. Gene numbers correspond to the numbering given in the MC58 complete genome, where the number within each arrow is preceded by "NMB" (NCBI GenBank accession number AE002098.2).

5.2 Transformation of *NMV_1164*

The *NMV_1164* gene cloned into pET28b (+) vector was kindly donated by Dr Vladimir Pelicic, Imperial College London, and was transformed into *E. coli* BL21 (DE3) following the standard heat-shock procedure. Positive insertion was confirmed by sequencing, where primers T7 term (TATGCTAGTTATTGCTCAGCGGT) and T7 (TAATACGACTCACTATAGGG) from the Technology Facility (University of York) were used. Sequencing results gave 100 % identity with the original sequence for that specific gene and, therefore, also for *NMB1049*.

5.3 Expression and purification of NMV_1164

NMV_1164 transformed into *E. coli* BL21 (DE3) was successfully overexpressed in auto-induction medium, following the protocol from Section 2.2.3. All the following steps and reagents' preparation used for extracting and purifying the protein were carried out as described in Section 2.5. Purification was performed on an ÄKTAprime plus apparatus (Amersham Biosciences) and the flow-through was monitored by absorbance at 280 nm with the Primeview 5.0 Software. After initial equilibration of the 1 ml HisTrap^{TM} column (GE Healthcare) with HEPES Buffer A (HBA) binding buffer (with an imidazole concentration of 15 mM), the soluble fraction protein suspension was flowed through the column. Non-specific proteins were not retained by the column, thus giving high absorbance readings at 280 nm. After running the protein suspension, the HisTrap^{TM} column was equilibrated with binding buffer again, and the column was then washed with an increasing gradient of HEPES Buffer B (HBB) elution buffer (with an imidazole concentration of 1 M). The rising concentration of imidazole, which reached 1 M value after 40 ml of initial addition of the elution buffer B, allowed the His-tagged protein of interest to depart

from the column. Several 5 ml fractions were collected during the elution step. Fractions 4 and 5 appeared to be containing the most NMV_1164 protein, as the absorbance peak reached its summit at that moment (Figure 5.3-1). At that point only about 40 % of HBB elution buffer, and therefore 60 % HBA binding buffer, had passed through the column, suggesting that about 400 mM imidazole were required for the protein to unbind from the column. Fractions 4 and 5 were further analysed by SDS-PAGE and Coomassie Brilliant Blue Staining (Figure 5.3-2).The NMV_1164 protein was successfully purified, as the fraction collected showed a clear band corresponding to approximately 35 kDa. The expected 6x His-tagged protein of interest is, in fact, 34.2 kDa in size. All the fractions containing the protein of interest, however, also showed the presence of a second, weaker band, above the expected band. This extra band seemed to be just below 70 kDa in size, which could probably correspond to NMV_1164 protein dimers. Fractions 4 and 5, which showed the most intense protein band, also appeared to contain a third and much fainter band at approximately 100 kDa. This extra band could have been caused by the correct protein aggregating and forming protein trimers or other higher order oligomers.

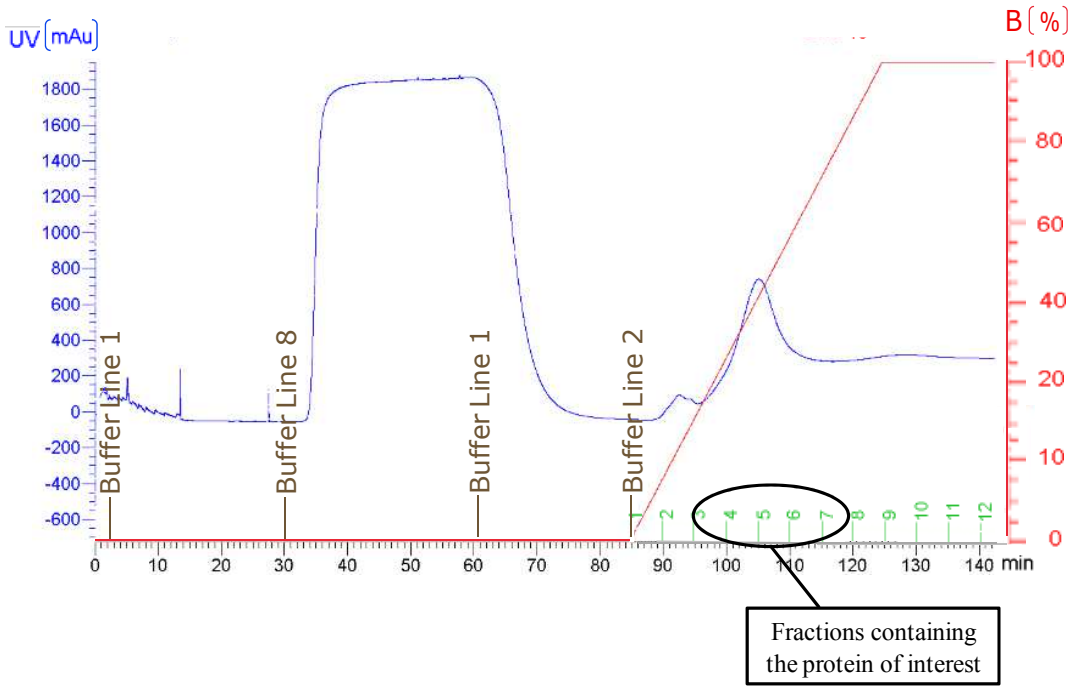

Figure 5.3-1: Purified NMV_1164 protein in fractions 4 and 5.

Absorbance measurements at 280 nm (blue line) and amount of HEPES Buffer B elution buffer added during elution (red line) are shown for the protein being purified. The sharp peak and its matching elution fractions (black circle) show that fractions 4 and 5 contain most of the protein when approximately 40 % of the HEPES Buffer B is running through. "Buffer Line #" (brown) indicate which buffer is running through the column. Buffer Line 1: HEPES Buffer A binding buffer. Buffer Line 8: Soluble fraction protein. Buffer Line 2: HEPES Buffer B elution buffer added with an increasing concentration and HEPES Buffer A binding buffer added with a decreasing concentration. Green numbers at the bottom right: elution tubes collected. B [%]: percentage of HEPES Buffer B used, where 0 equals to 15 mM imidazole (from HEPES Buffer A) and 100 % equals to 1 M imidazole (from HEPES Buffer B).

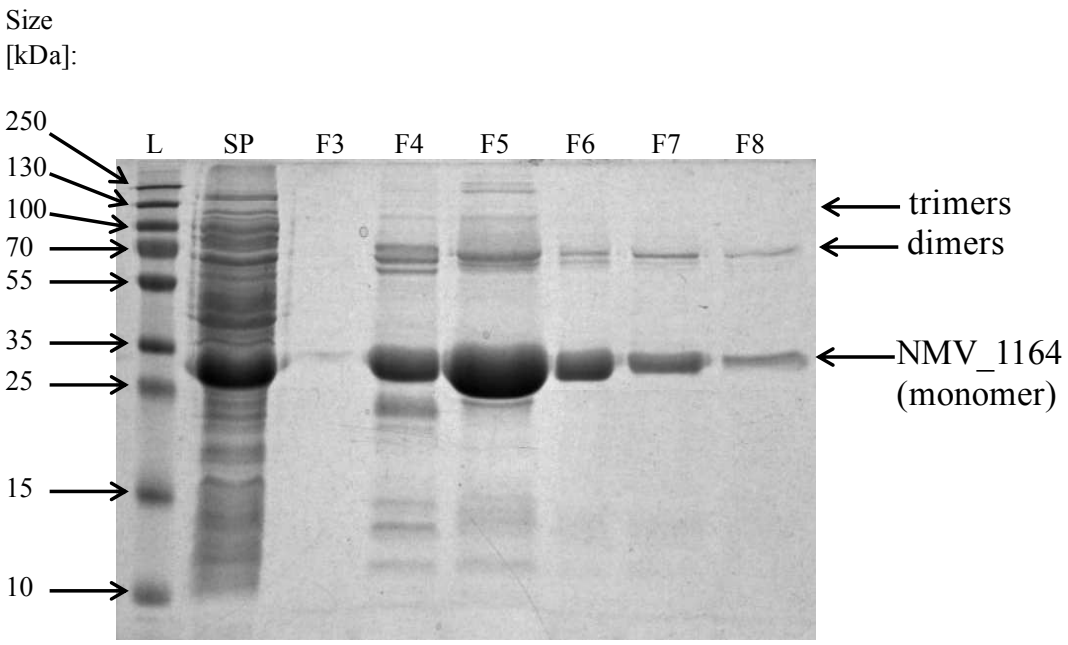

Figure 5.3-2: Purified protein fractions.

Purification of the protein of interest showed that the expected band of 34.2 kDa was present, and that protein fractions 4 and 5 contained most of the protein. L: PageRuler^{TM} Plus Prestained Protein Ladder (Thermo Scientific). SP: Soluble fraction protein suspension. F#: fractions collected during the protein purification step, corresponding to the fractions collected in Figure 5.3-1.

The bands present in the SDS-PAGE gel clearly showed that the correct protein was collected, but they also suggested that protein oligomers, especially dimers, were present despite having used SDS load Buffer containing 5 mM β-mercaptoethanol. Polymers could have formed due to the presence of five cysteine residues in the amino acid sequence of the NMV_1164 protein. These cysteine residues could have covalently bonded to each other to form disulphide bonds, linking more than one protein together.

5.4 Buffer-exchange and quantification of NMV_1164

The fractions shown to contain a high concentration of NMV_1164 protein were cloudy, and this meant that the protein was unstable and already started to precipitate. Cloudy fractions were centrifuged upon collection in order to get rid of the precipitated proteins and were then buffer-exchanged into 1 x Binding Buffer or 0.5 x TBE (both solutions were prepared as described in Table 2.5.5-1 with a PD-10 Desalting Column (GE Healthcare) to prevent any further loss of the protein. At this stage the protein was quantified with a Quick Start™ Bradford Protein Assay (BIO RAD). The assay was carried out by measuring the OD at 595 nm, and the value obtained was then added to an equation derived from a standard curve which was previously plotted by diluting a Bovine Gamma-Globulin Standard of known concentration, as described in the manufacturer's protocol (Figure 5.4-1). The OD value obtained was applied to the graph's equation as y value, and the concentration x was consequently extrapolated by re-arranging the equation as follows: protein concentration [µg / ml] = ($OD_{595\ nm}$ – 0.0137) / 0.0005 (Table 5.4-1, column 3). Protein concentration in µM was then derived from the following formula: Molar concentration [mol / L] = concentration [g / L] / protein molar mass [Da], where the 6x His-tagged protein molar mass is 34235 Da (Table 5.4-1, column 4).

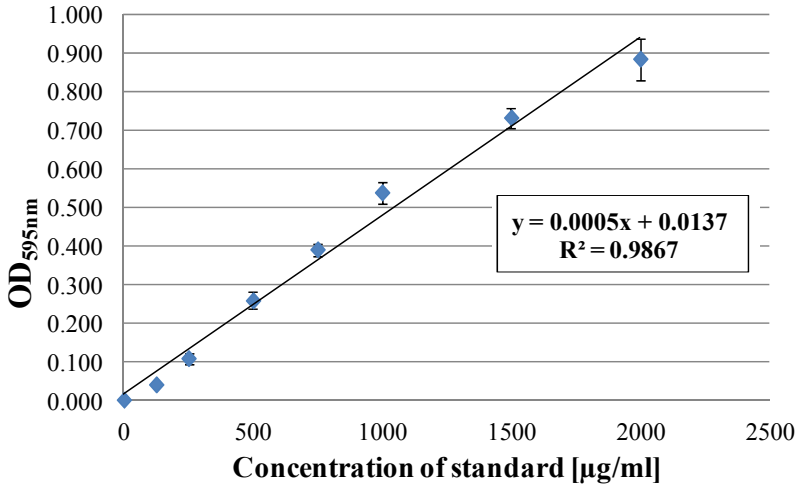

Figure 5.4-1: Standard curve for Bradford Protein Assay.

Concentration of standard measured using Bradford Protein Assay and Bovine Gamma-Globulin Standard. An equation was automatically created for the best line of fit of the linear trendline.

Table 5.4-1: Protein concentration from the Bradford Protein Assay.

OD values were measured at 595 nm in triplicates. BB: 1 x Binding Buffer (2.5 mM HEPES Free acid, pH 7.9, 5 mM NaCl and 0.25 mM $MgCl_2$). TBE: 0.5 x TBE (45 mM UltraPure™ Tris, 45 mM Boric acid and 1 mM EDTA).

Protein fraction	OD_{595nm}	[Protein] (µg / ml)	[Protein] (µM)
Fraction 4 in BB	0.165 ± 0.01	302.60 ± 28.84	8.84 ± 0.84
Fraction 5 in BB	0.238 ± 0.01	448.60 ± 16.37	13.10 ± 0.48
Fraction 6 in BB	0.154 ± 0.01	279.93 ± 18.90	8.18 ± 0.55
Fraction 7 in BB	0.033 ± 0.01	37.93 ± 15.01	1.11 ± 0.44
Fraction 4 in TBE	0. 179 ± 0.01	329.93 ± 26.63	9.64 ± 0.78
Fraction 5 in TBE	0. 250 ± 0.01	473.27 ± 23.01	13.82 ± 0.67
Fraction 6 in TBE	0.141 ± 0.01	254.60 ± 29.05	7.44 ± 0.85
Fraction 7 in TBE	0.052 ± 0.02	76.60 ± 30.20	2.24 ± 0.88

5.5 Electrophoretic Mobility Shift Assay (EMSA) with DNA 130-mers

Preliminary results suggested that protein NMB1049 might be binding to the promoter regions of genes *NMB0430*, *NMB1048* and / or *NMB1049*. In order to verify if this was the case, an Electrophoretic Mobility Shift Assay (EMSA) was carried out by using the homologous NMV_1164 protein, and checking its possible interactions with the promoter regions of all three genes belonging to *Neisseria meningitidis* MC58. *NMV_1164* from *Neisseria meningitidis* strain 8013, as previously stated, has 100 % identity with *NMB1049* from *Neisseria meningitidis* MC58.

Promoter regions for studying the interactions between the DNA (possible LTTR boxes) and the protein of interest (LysR-Type transcriptional regulator) were chosen because they were next to or contained the following interrupted palindromic sequence: ATC–N_9–GAT. This sequence and the most generally accepted T–N_{11}–A, in fact, are conserved amongst LysR-Type transcriptional regulators and are known as the LTTR box, to which the LysR-Type transcriptional regulators bind (Maddocks & Oyston, 2008). The intergenic region preceding the *prp* operon contains just one palindromic sequence which is very similar, and within acceptance, to the expected one (ATC–N_5–GAT) (Figure 5.5-1A). The intergenic region between the two divergently transcribed genes *NMB1048* and *NMB1049*, instead, contains three perfectly matching palindromic sequences (Figure 5.5-1B). Primers used to amplify the intergenic regions containing the LTTR boxes are described in Table 2.3.1-1 and were designed by Amie Williamson (Moir's lab). The presence of three LTTR boxes near to each other could suggest that either the protein NMB1049 (and therefore

NMV_1164) has a higher affinity for one of these sequences or the protein binds to the intergenic region between *NMB1048* and *NMB1049* in the form of a homodimer or homotrimer. LTTR proteins are known to sometimes aggregate in multimers when in the presence of the correct co-inducer (Maddocks & Oyston, 2008).

A

ATGAAACCAATTCAGATGTTTTCCCCTTTTCTGAATAATCCCCTTGTTTTCTTCTTGTCTGCGGTTTT
GCCGCATAATTCCGAACGGTCTGCTGTTTTTCTTTGATTCGTTTTAAATATCAATAAGATAATTTTTC
CCATATATTTTTAATGATTGGATTGGGATGCCCGACGCGTCGGATGGCTGTGTTTTGCCGTCCGAATG
TGATGGAAGCCTGTCCATACTGAAAAAAAGTCTATAAAGGAGAAATATGATGAGTCAACACTCTGCCG
GAGCACGTTTCCGCCAAGCCGTGAAAGAATCGAATCCGCTTGCCGTCGCCGGTTGCGTCAATGCTTAT

B

CGCCAGCGTTTTGGTTGCATAATCTGCAATTCATGTTCCAAATATTCGTCCCGCGTCGCAAATTCCGA
AGCTGGACGGTGCAAATCCCGATAAGTCCCATTATGTTTTTCCATAACCTTCCTCCTTATATATCGCG
CCTCGTAAAAGGGGCGCATGACTTTTCTTTTTGATACGGGCTGCGTTCGGAAGCCGTAACCCCATTTA
AAGCCCAAACAGGCAATAAAACCAATCTTTTTTTTTGATAACCATCATCCGGAAAACTGATACAATTT
ACAAACCACTTGATTAAAAAGTTAATTTTCAGCAACAATCCACCTAAAAGATTTCGATTGCACAAATA
TAGAAAACATCCGCACAAGGAGGGATATATGGATGCCGTACAATTAAAATCATTTGTCGCCGTCGCGC
ACGAGGGCAACCTTACCCAAGCCGCCAAACGACTTTTCCTTTCCCAGCCTGCCGTTTCTGCCCAAATT

Figure 5.5-1: Intergenic regions containing possible LTTR boxes.

A: The intergenic region (black) between genes *NMB0429* and *NMB0430* (blue) is shown with the ATG starting codons for both genes (green) and the TGA stop codon for *NMB0429* (red). Primers NMB0430prot-for and NMB0430prot-rev (highlighted in yellow) were used to amplify the DNA region containing the possible LTTR box (orange). **B:** The intergenic region (black) between the divergent genes *NMB1048* and *NMB1049* (blue) is shown with both genes' starting codons (green). Primers NMB1048prot-for (1st yellow highlight) and NMB1048prot-rev (2nd yellow highlight) and primers NMB1049prot-for (2nd yellow highlight) and NMB1049prot-rev (3rd yellow highlight) were used to amplify the DNA region next to or containing the three possible LTTR boxes (orange).

Potential promoter regions for *NMB0430*, *NMB1048* and *NMB1049* of *Neisseria meningitidis* MC58 containing possible LTTR boxes were successfully amplified by PCR. The 130 bp bands were clearly visible from the 0.8 % agarose gel (Figure 5.5-2) and therefore samples were subjected to PCR purification (QIAGEN). One of the products, however, showed an extra band at about 600 bp and, for this reason, the full PCR product was run on a gel and the expected 130 bp band was excised and gel extracted (QIAGEN). Concentrations of the purified promoter fragments were measured with a NanoDrop® ND-1000 Spectrophotometer (Thermo Scientific) and diluted to a final concentration of 45 ng / µl with nuclease-free water (QIAGEN). The DNA was then stored at -20 ºC until ready to be used.

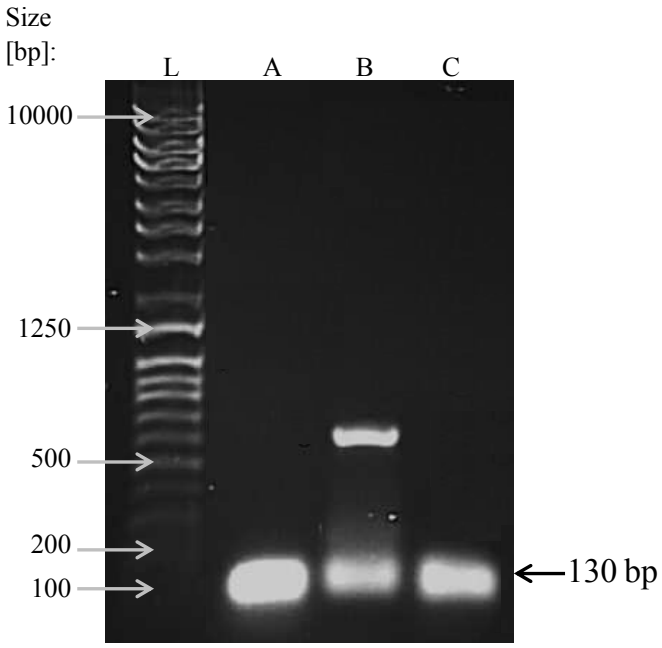

Figure 5.5-2: Potential promoter regions for use with EMSA.
The expected fragment size of all three products was 130. A: promoter region for *NMB0430*. B: promoter region for *NMB1048*. C: promoter region for *NMB1049*. L: Q-Step 4 Quantitative DNA ladder (YORBIO).

The three promoter regions just purified and fraction 5 of the protein of interest that was buffer-exchanged in 0.5 x TBE buffer in Section 5.4 were mixed together in a DNA to protein molar ratio of 1 : 2 and 1 : 5. The binding reactions were established by using 450 ng of DNA (which corresponded to 10 µl of the 45 ng / µl DNA stocks, giving 5 picomoles DNA per reaction) and a two-molar or 5-molar excess of 6x His-tagged NMV_1164 protein (resulting in 10 or 25 picomoles protein per reaction).

To make up a reaction volume of 50 µl with either 1 : 2 or 1 : 5 DNA to protein molar ratio, 10 µl DNA (45 ng / µl stock) were mixed with either 3.4 or 8.6 µl protein (100 µg / ml stock) and the volume was adjusted to 18.6 µl with 0.5 x TBE buffer. At this point, 18.6 µl 2 x Gel Shift Reaction buffer and 12.8 µl 4 x Native PAGE loading buffer were added to each reaction, as described in Section 2.5.7. Each reaction was incubated at room temperature for 20 minutes prior to being loaded onto the native gel that had been pre-run at 200 V in 0.5 x TBE running buffer. The gel was then run for four further hours and stained in 1 x SYBR® Safe DNA gel stain 10,000 x concentrate (Invitrogen™) for 30 minutes. The DNA was then visualised by UV illumination (Figure 5.5-3). The lane where only the protein was added did not show any band, as expected. All the other lanes, however, showed only one band of DNA, suggesting that no protein-DNA complex has been formed. To further investigate this result, and to check that the protein was present in the gel and not trapped in the well, a Silver Staining of the same EMSA gel was carried out and the protein-DNA interaction was checked (Figure 5.5-4). This result confirmed that there were no protein-DNA interactions and that the protein was running through the gel, as all the lanes that were loaded with it showed a smear, whereas the lanes containing only the DNA did not show any smear.

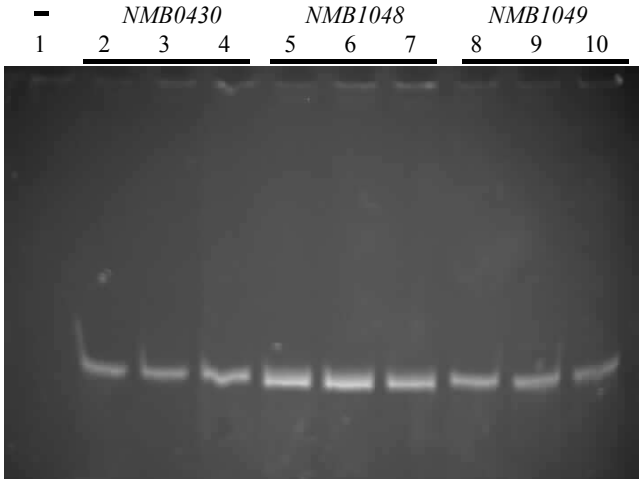

Figure 5.5-3: EMSA results after SYBR® Safe staining.

The 130-mer promoter regions of *NMB0430*, *NMB1048* and *NMB1049* with or without the 6x His-tagged NMV_1164 protein show no differences in running distance through the gel. 1: Protein only. 2: *NMB0430*. 3: *NMB0430*+prot (1:2). 4: *NMB0430*+prot (1:5). 5: *NMB1048*. 6: *NMB1048*+prot (1:2). 7: *NMB1048*+prot (1:5). 8: *NMB1049*. 9: *NMB1049*+prot (1:2). 10: *NMB1049*+prot (1:5).

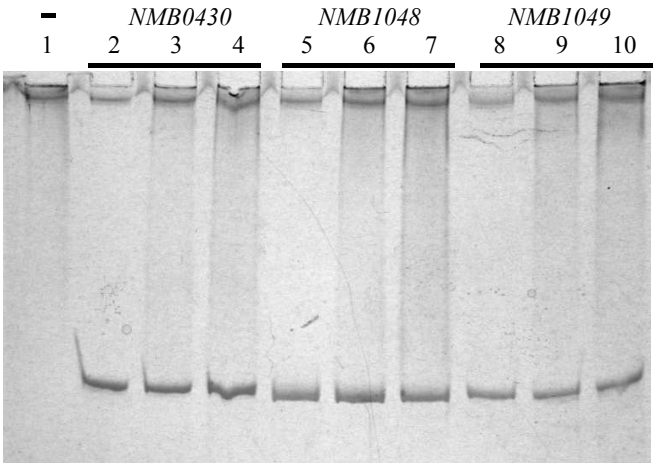

Figure 5.5-4: EMSA results after Silver Staining.

The 130-mer promoter regions of *NMB0430*, *NMB1048* and *NMB1049* with or without the 6x His-tagged NMV_1164 protein show smears in the lanes where the protein is present. 1: Protein only. 2: *NMB0430*. 3: *NMB0430*+prot (1:2). 4: *NMB0430*+prot (1:5). 5: *NMB1048*. 6: *NMB1048*+prot (1:2). 7: *NMB1048*+prot (1:5). 8: *NMB1049*. 9: *NMB1049*+prot (1:2). 10: *NMB1049*+prot (1:5).

All the protein lanes showed smears, thus suggesting that the conditions for running the EMSA gel were not ideal despite the sharp bands obtained with the DNA. The final salt concentration in each EMSA reaction might have still been too high, or the protein was not stable enough and was already starting to dissociate inside the well or whilst running within the gel. Moreover, only a small percentage of the protein could still be functionally active, or the protein might even be requiring some unknown co-factors before being able to bind to DNA.

5.6 Fluorescence anisotropy

Fluorescence anisotropy was used to quantitatively analyse the strength of the interactions in solution between the purified protein fraction 5, containing the 6x His-tagged NMV_1164 protein that was buffer-exchanged in Binding buffer in Section 5.4, and the fluorescently tagged DNA containing the sequence for the protein's potential binding site.

Fluorescence anisotropy allows measurements of the rate of tumbling in solution, where the small molecules rotate very rapidly and the emitted light is depolarised. This means that when the DNA marked with a fluorophore is not bound to the protein, the DNA will rotate fast and the fluorescence anisotropy ratio, which is the ratio between polarised and depolarised light emitted, results in a low value. When the DNA marked with a fluorophore binds to the protein, however, the newly formed complex will move slower due to the higher molecular weight, and therefore the fluorescence anisotropy value increases. Fluorescence anisotropy should give a better idea of the interactions occurring between the protein and the DNA, as the possible artefacts due to the gel when running an EMSA gel are eliminated.

Potential sequences of DNA where the protein could bind were found once within the promoter region of *NMB0430* and three times between the promoter regions of the two divergently transcribed *NMB1048* and *NMB1049* genes, as already explained in the previous section, and corresponded to the palindromic sequences that formed the potential LTTR boxes (Figure 5.6-1). The primers used are described in Table 2.5.9-1 and were designed by Amie Williamson (Moir's lab). The DNA thought to be binding to the protein under study and a control DNA that was completely unrelated to it were labelled at the 5' end with a hexachlorofluorescein (HEX™).

A

ATGAAACCAATTCAGATGTTTTCCCCTTTTCTGAATAATCCCCTTGTTTTCTTCTTGTCTGCGGTTTT
GCCGCATAATTCCGAACGGTCTGCTGTTTTTCTTTGATTCGTTTTAAATATCAATAAGATAATTTTTC
CCATATATTTTTAATGATTGGATTGGGATGCCCGACGCGTCGGATGGCTGTGTTTTGCCGTCCGAATG
TGATGGAAGCCTGTCCATACTGAAAAAAAGTCTATAAAGGAGAAATATGATGAGTCAACACTCTGCCG
GAGCACGTTTCCGCCAAGCCGTGAAAGAATCGAATCCGCTTGCCGTCGCCGGTTGCGTCAATGCTTAT

B

CGCCAGCGTTTTGGTTGCATAATCTGCAATTCATGTTCCAAATATTCGTCCCGCGTCGCAAATTCCGA
AGCTGGACGGTGCAAATCCCGATAAGTCCCATTATGTTTTTCCATAACCTTCCTCCTTATATATCGCG
CCTCGTAAAAGGGGCGCATGACTTTTCTTTTTGATACGGGCTGCGTTCGGAAGCCGTAACCCCATTTA
AAGCCCAAACAGGCAATAAAACCAATCTTTTTTTTTGATAACCATCATCCGGAAAACTGATACAATTT
ACAAACCACTTGATTAAAAAGTTAATTTTCAGCAACAATCCACCTAAAAGATTTCGATTGCACAAATA
TAGAAAACATCCGCACAAGGAGGGATATATGGATGCCGTACAATTAAAATCATTTGTCGCCGTCGCGC
ACGAGGGCAACCTTACCCAAGCCGCCAAACGACTTTTCCTTTCCCAGCCTGCCGTTTCTGCCCAAATT

Figure 5.6-1: Primers were designed to include possible LTTR boxes.

A: The intergenic region (black) between genes *NMB0429* and *NMB0430* (blue) is shown with the ATG starting codons for both genes (green) and the TGA stop codon for *NMB0429* (red). Primers HEX_NMB0430_ for and NMB0430_ rev (highlighted in yellow) corresponded to the double stranded DNA region containing the possible LTTR box (orange). The mismatch of both primers is shown (highlighted in red), where "T" in the sequence was considered as "C". **B:** The intergenic region (black) between the divergent genes *NMB1048* and *NMB1049* (blue) is shown with both genes' starting codons (green). The three sets of primers HEX_NMB1048_for and NMB1048_ rev (distinguished as a, b and c) corresponded to the double stranded DNA regions containing one possible LTTR box each pair (orange).

Anisotropy readings were taken using a fixed amount of double stranded 21-mer DNA (5 nM) and varying concentrations of the protein under study, which was continuously added into the same cuvette after intervals of every 10 readings. Anisotropy readings for DNA only were also taken, where the varying amounts of proteins added were replaced by varying amounts of 1 x Binding Buffer (2.5 mM HEPES Free acid, pH 7.9, 5 mM NaCl and 0.25 mM $MgCl_2$), the buffer in which the protein was stored. A graph for visualising the binding affinity of the NMV_1164 protein to the various DNA sequences was then drawn using SigmaPlot, where the actual values plotted were obtained by subtracting the values from the background given by the DNA only to the values obtained for each sample containing both DNA and protein (Figure 5.6-2).

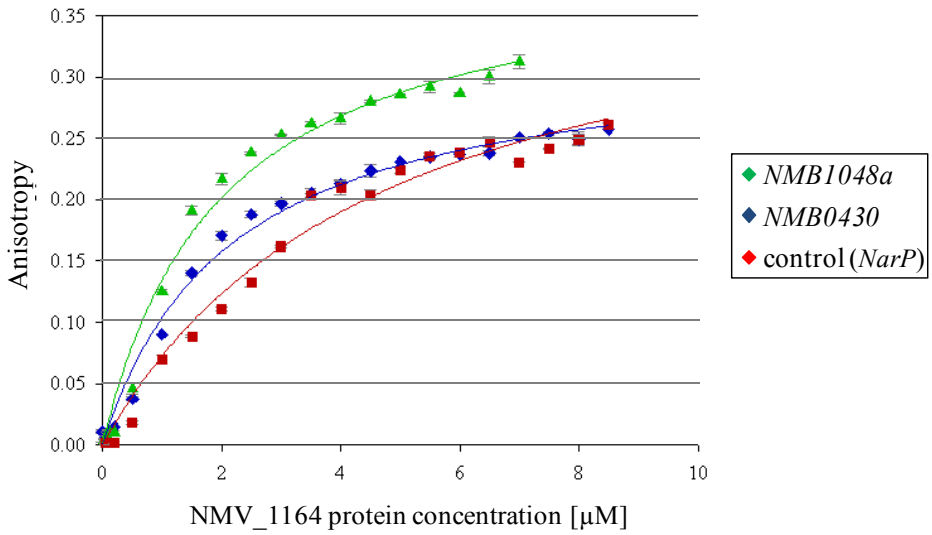

Figure 5.6-2: Binding affinity for the NMV_1164 protein with its potential LTTR boxes.

Average anisotropy for 10 repeats was plotted against the concentration of NMV_1164 in the presence of 5 nM DNA 21-mer duplex. The highest anisotropy values were seen when the protein was added to the *NMB1048a* binding site. A control DNA lacking the binding site for the protein under study was also tested, and its anisotropy values were similar to the ones seen for the *NMB0430* LTTR box.

Fluorescence anisotropy appeared to have partially worked, as there was an increase in its value with all double stranded DNA tested, and the binding curve showed that saturation was almost achieved when over 5 μM protein was added. Anisotropy increase, however, was also evident with the control DNA. Control DNA was predicted to give a steady flat line with no anisotropy variation, as the protein should not have interacted with DNA at all. The binding curve for NMV_1164 with the *NMB1048a* DNA showed that the curve approached saturation at a lower concentration of protein and this suggested that, despite the non-optimal conditions, the protein was likely to be interacting with the DNA indeed. The equilibrium dissociation constant (k_d) for each interaction was automatically calculated by SigmaPlot, and corresponded to the following values: k_d (NMB1048a): 1.98 μM; k_d (NMB0430): 2.14 μM; k_d (control): 4.70 μM. This low value of over 4 μM confirmed that interactions between NMV_1164 and the control DNA were very weak. When anisotropy was tested with DNA only, which meant that the solution was composed of either *NMB0430* or *NMB1048a* and that the protein was replaced with 1 x Binding Buffer, all readings showed no change in anisotropy, as expected (results not shown).

The weak affinity suggested that there were more factors which were influencing fluorescence anisotropy that needed to be taken into consideration, other than the expected specific interactions of the protein with its potential binding sites. In fact, despite having been added in excess, not all the NMV_1164 protein might have remained active after purification, thus impeding full saturation of DNA, or only a weak binding was occurring and therefore more protein was required for achieving full saturation. The apparent low affinity could also be due to the protein requiring multiple sets of the inverted repeats, and therefore binding to DNA as a trimer.

5.7 Conclusions on the expression and characterisation of NMV_1164

The 6x His-tagged NMV_1164 protein from *Neisseria meningitidis* serogroup C strain 8013 has been successfully purified, but was unstable *in vitro* and started forming aggregates soon after purification, making it difficult to work with. After centrifugation to eliminate the precipitated proteins, however, the concentration of the protein under investigation was still high enough. A stock solution of 100 μg / ml was made in 0.5 x TBE, allowing the protein to be easily added to the 450 ng DNA in a two-fold or five-fold molar excess. The protein in excess would allow for maximum interactions and binding of the protein-DNA complex. When diluted in 0.5 x TBE the protein showed an increased stability compared to when it was diluted in 1 x Binding Buffer, the reason being that TBE contained a low salt concentration and a slightly basic pH, conditions that improve nucleic acids handling and electrophoretic techniques.

This protein is found as a probable homodimer or homotrimer when run in a SDS-PAGE gel, despite the use of a reducing agent (5 mM β-mercaptoethanol). This does not necessarily mean that the protein exists in bacteria as a homooligomer, but that this could be the case. In fact, when subjected to BLAST, this protein had high identities with the LysR-Type transcriptional regulators, and the ones that have been characterised so far typically consist of several identical sub-units, most likely to be tetramers or dimers, as these would increase the affinity and specificity of the protein to its DNA binding site compared to their monomeric form (Knapp & Hu, 2010, Klemm *et al.*, 1998). When the purified NMV_1164 protein is heated to 95 ºC, however, it denatures and unfolds, possibly leading to an exposed hydrophobic core

that could interact with the hydrophobic core of another NMV_1164 protein, and so on, thus forming the homodimer or homotrimer seen in the gel. In order to avoid this oligomerisation, samples could also be tested and run after incubation at room temperature, and compared to the heated ones. The intergenic region between *NMB1048* and *NMB1049* contains 3 matching LTTR boxes (ATC–N_9–GAT), which could explain why the protein might be able to form dimers or trimers.

Further investigations to test the interactions between the protein under study and the DNA need to be carried out, starting with changing the conditions under which the protein is run in the EMSA gel. Salt concentrations in the protein stock or in the Gel Shift Reaction buffer can be lowered in order to increase electrostatic stabilisation. A higher amount of glycerol or other stabilising agents could be added during gel preparation, and a decrease in the time from when the samples are added in the well before entering the gel could all help in reducing possible protein aggregation or dissociation and smearing (Vagenende *et al.*, 2009, Hellman & Fried, 2007).

During fluorescent anisotropy the protein did not show a fully saturated binding curve and even the negative control behaved in a similar way, suggesting that changes in anisotropy were not due to protein-DNA interactions solely but also to interactions within the cuvette. Fluorescence anisotropy values are dependent on several factors, and not only on the binding of the protein to the DNA. The factors that could make a difference in the readings, in fact, are non-specific bindings forming the protein-DNA complex, shape, size and motion, and even protein aggregates. An increased amount of BSA could also be added to the cuvette in order to decrease non-specific binding. The difference in size was only due to the double stranded DNA used, which was a 21-mer for both *NMB0430* and *NMB1048* binding

sites, and a 53-mer for the control. This size difference could lead to a decrease in the movement of the control DNA even when not bound to the protein, thus increasing anisotropy values. A more appropriate control could be given by testing an unrelated DNA containing a HEX fluorophore that is 21 base pairs long. Alternatively, a longer experimental DNA of approximately 53 base pairs could be tested too. The fluorophore chosen, or its location within the DNA, could also have affected the affinity with the protein, and therefore a different position or fluorophore selection might lead to a positive assay.

From this work it cannot be clearly determined if the NMV_1164 protein regulates the expression of *NMB0430*, *NMB1048* or *NMB1049* by binding to their promoter regions. However, following fluorescence anisotropy a lower k_d was obtained when the protein was added in solution with one of the LTTR boxes for the *NMB1048* gene (*NMB1048a*). The other two LTTR boxes found between *NMB1048* and *NMB1049* (which are referred to as *NMB1048b* and *NMB1048c* in this work) still need to be tested, and they might reveal that a stronger interaction could be formed between either of these sites and the protein, thus saturating the DNA more readily and decreasing the k_d value even further, allowing the protein-DNA interactions to reach the plateau sooner.

More studies could also be performed regarding the motion of protein and DNA. By adding more protein, viscosity might also increase, as more Binding buffer is added together with the protein into the cuvette. Further investigations could be performed by changing some components in which the protein in stored (Moerke, 2009, Kuimova *et al.*, 2008). Alternatively, the protein could be concentrated using centrifugation devices following the ÄKTAPrime Plus purification. Finally, changes

in anisotropy could be due to aggregation of the protein in solution, which was not visible by eye as the concentration of the protein added into the cuvette was relatively low (8.5 μM maximum value). Precipitation of the protein, in fact, was very obvious straight after purification, when the protein was at its highest concentration.

To try to improve the protein solubility, NMV_1164 could be cloned into a vector that contains a soluble tag, such as maltose-binding protein (MBP) or glutathione *S*-transferase (GST) (Lichty *et al.*, 2005). One point to take into consideration, however, is that the protein might start to aggregate once the tag is cleaved off.

Once the protein is more stable, other biophysical experiments such as native mass spectrometry (NMS) or analytical ultracentrifugation (AUC) could be used to obtain information about the NMV_1164 protein and to investigate the ability of the protein to form homooligomers in solution, as there are three LTTR boxes present in the intergenic region between genes *NMB1048* and *NMB1049* (Heck, 2008, Lebowitz *et al.*, 2002).

Chapter 6 - Role of propionic acid metabolism in colonisation and disease models

6.1 Introduction

The 2-methylcitrate pathway is present in a few opportunistic pathogens, including *Neisseria meningitidis*, and is involved in the catabolism of propionic acid. To study the correlation of this pathway from *Neisseria meningitidis* with carriage or infection in the population, saliva and blood samples from several healthy individuals were investigated.

In this work, just over 300 saliva samples have been analysed for propionic acid content by gas chromatography and then compared to *Neisseria meningitidis* carriage using the Mann-Whitney U Test. It is known that carriage of *N. meningitidis* is present in 10 to 35 % of the population at any time (Caugant. *et al.*, 2007), but its correlation with the amount of propionic acid has never been investigated. A number of studies, however, have been performed to check short-chain fatty acid concentrations in dental plaque formation and accumulation, resulting in propionic acid ranges varying between 0.8 mM in mildly affected and 9.5 mM in severely affected individuals (Niederman *et al.*, 1997). Plaque formation studies, however, did not look into carriage of *N. meningitidis* during periodontal diseases, as this bacterium is not related to plaque. A hypothesis for this work stated that there was a statistical difference in the amount of propionic acid present in the saliva of carriers and non-carriers, and was then tested.

Despite colonising asymptomatically the nasopharynx of humans, *Neisseria meningitidis* can occasionally enter the bloodstream, thus becoming pathogenic. During infection, bacteria change their natural environment, and must therefore adapt to the new and more limiting environment of the host. Many studies of the infection have been performed by inoculating the bacteria in mice and rats (Yi *et al.*, 2003, Sun *et al.*, 2000). Results obtained from animal models, however, would probably not be as accurate in mimicking what happens in the bacteria's natural environment, as *Neisseria meningitidis* is an exclusively human pathogen. Improvements in mice models, though, are achieved through generating transgenic mice with human versions of CD46, for example, or by xenotransplanting human dermal microvessels (Melican *et al.*, 2013, Johansson *et al.*, 2003). Studies performed in human whole blood, on the other hand, would be more precise for checking the overall transcriptional changes of *N. meningitidis* during bacteraemia (Hedman *et al.*, 2012, Echenique-Rivera *et al.*, 2011). When studying human whole blood, however, a choice of the right anti-coagulant was needed, as it was important to take into consideration the effects caused by its addition to the blood so that it would not interfere with the serogroup under study (Ison *et al.*, 1995).

As an important part of this work, it was necessary to study the 2-methylcitrate pathway involvement in survival or virulence of the pathogen in human blood, as this pathway is only present in pathogenic *Neisseria.* Moreover, another gene belonging to a different pathogenic island, the *NMB1049* encoding a Lys-R Type transcriptional regulator, was also taken into consideration. Human whole blood from seven healthy individuals was infected *ex vivo* with wild-type, *prpC::Spec*^{R} and *NMB1049::Spec*^{R} mutant strains and a time-course growth of bacteria was monitored by counting colony forming units.

6.2 Collection and handling of human saliva

Saliva samples were collected by Professor Robert Read's group at the University of Sheffield as part of a trial investigation of meningococcal carriage. Healthy individuals were screened for any *Neisseria* species present in their oropharynx and Dr. Alice Deasy, University of Sheffield, gave access to the data where the various students were tested for *N. meningitidis* colonisation. Of the 302 student's saliva tested, 235 tested negative, whereas 67 tested positive to *Neisseria meningitidis*.

6.3 Correlation between propionic acid and *N. meningitidis* carriage

Propionic acid present in all saliva samples collected from both carriers and non-carriers for *Neisseria meningitidis* was measured by the 6890 N Network GC system gas chromatograph (Agilent Technologies) and compared to a standard curve. Control samples for plotting the standard curve were prepared by mixing a known amount of propionic acid to deionised water, and were acidified with 132 mM potassium phosphate (pH 3) prior to injection into the chromatograph. The y = 39.002x equation was extrapolated from the graph, and the concentration of propionic acid was calculated as follows: propionic acid [mM] = (area of propionic acid) / (39.002) (Figure 6.3-1).

The concentration of propionic acid present in the saliva of carriers and non-carriers for *N. meningitidis* was then used to visually check the distribution of the two datasets, and statistical tests were then performed to find a correlation between the amount of propionic acid and the presence of the bacterium.

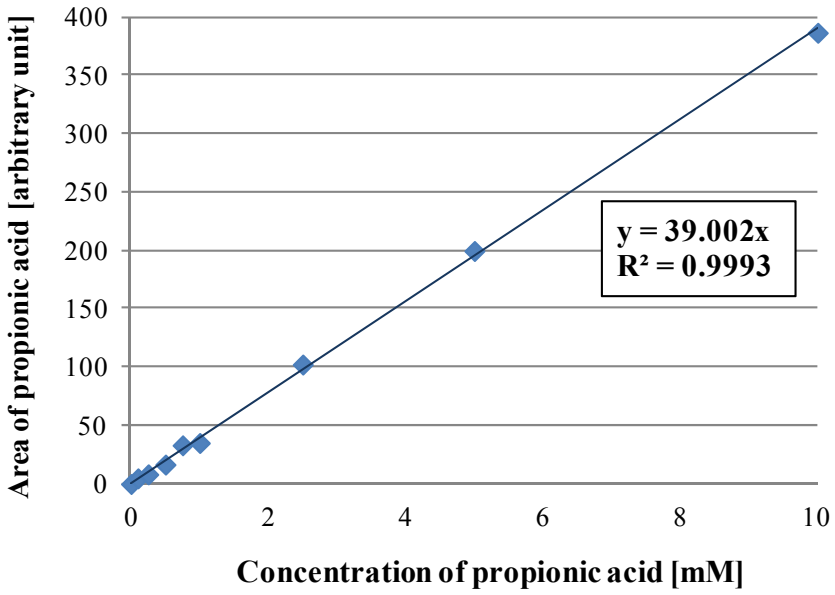

Figure 6.3-1: Standard curve showing the areas of propionic acid and their relative concentration.

The area of propionic acid was automatically measured by gas chromatography and plotted versus the concentration of propionic acid added in each control sample. Control samples were made up of deionised water and a known amount of propionic acid. R^2 is a measure of the goodness of fit for the given set of data. R^2 here is near to its maximum value of 1, implying that the regression line fits the data nicely and that the resulting equation is accurate.

Frequency distribution for the two datasets was plotted in a histogram by organising the values into bins of 0.1 mM intervals (Figure 6.3-2). Neither of the two datasets looked normally distributed, but this result could have just been an artefact of the choice of bins. Data distribution was therefore double checked and the same results were confirmed by the SPSS Statistics software, version 19 (IBM), which automatically generated a Q-Q (quantile – quantile) plot for each dataset (Figure

6.3-3). The SPSS program calculated the expected theoretical value for each data point based on the distribution of the whole dataset. Q-Q plots visually showed that both datasets deviated from the straight line when compared to their theoretical values, and these plots also showed bias to the right. This meant that the data were not following normal distribution. This method was more reliable than the histograms as the results did not depend on bin choices.

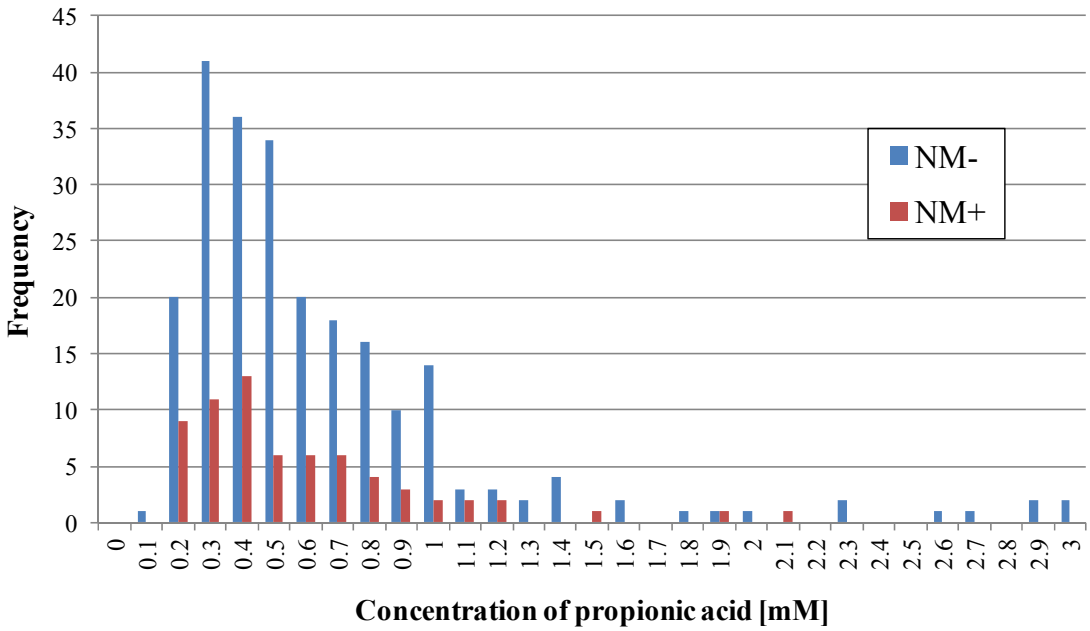

Figure 6.3-2: Frequency distribution for carriers and non-carriers of *Neisseria meningitidis*.

Both datasets are not normally distributed and have a strong tail on the right. NM-: non-carriers of *Neisseria meningitidis*. NM+: *Neisseria meningitidis* carriers.

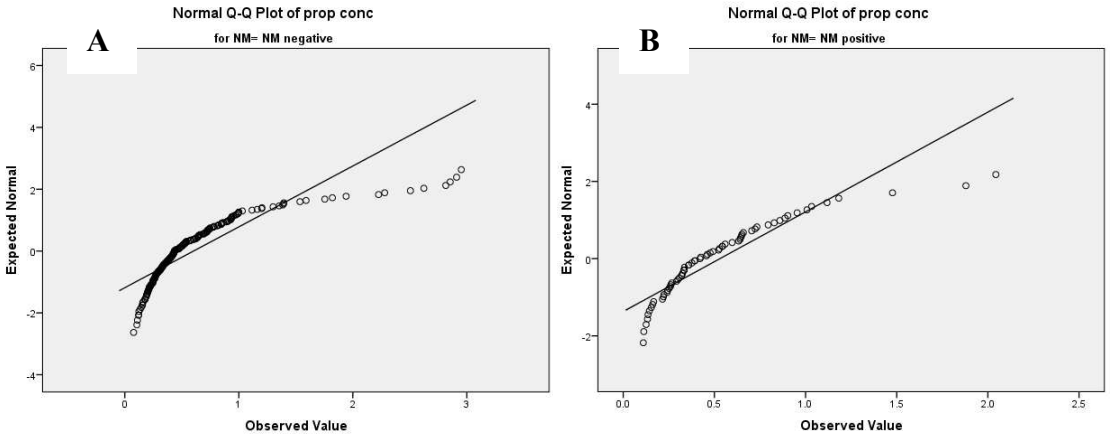

Figure 6.3-3: Quantile – Quantile Plots for probability distributions.
A: data distribution for non-carriers of *Neisseria meningitidis*. **B:** data distribution for *Neisseria meningitidis* carriers. The straight line corresponds to the y = x equation. Both datasets were not normally distributed as they deviated from the straight line and showed a strong tail at the right.

The SPSS Software also performed two non-parametric statistical tests, the Kolmogorov-Smirnov and Shapiro-Wilk normality tests in order to confirm the results previously obtained with the histogram and Q-Q plots. The null hypothesis corresponded to both datasets being normally distributed for the significance level of 0.05. As these tests gave a significance p-value of 0 for non-carriers of *Neisseria meningitidis* and between 0 and 0.003 for *Neisseria meningitidis* carriers, the null hypothesis was rejected, meaning that the data were not normally distributed. For the data to be normally distributed, in fact, the p-value should have been greater than 0.05 (Table 6.3-1).

Table 6.3-1: Normality tests for the carriers and non-carriers datasets.
Kolmogorov-Smirnov and Shapiro-Wilk tests showed that neither of the two datasets was normally distributed as the p-values were smaller than significance level chosen of 0.05 and therefore the null hypothesis of the datasets to be normally distributed was rejected. NM negative: non-carriers of *Neisseria meningitidis*. NM positive: *Neisseria meningitidis* carriers.

Tests of Normality

		Kolmogorov-Smirnov[a]			Shapiro-Wilk		
	NM isolated	Statistic	df	Sig.	Statistic	df	Sig.
prop conc	NM negative	.174	235	.000	.725	235	.000
	NM positive	.139	67	.003	.832	67	.000

a. Lilliefors Significance Correction

Differences between carriers and non-carriers of *Neisseria meningitidis* were graphically drawn in excel with a box-and-whisker plot. This type of visualisation did not depend on the statistical distribution of the two datasets and was, therefore, a non-parametric way of showing neatly the key values for both datasets (Figure 6.3-4). The medians corresponded to 0.44 for non-carriers and 0.42 for carriers of the bacterium. As they both fell within the interquartile range of the other plot and their value was so close to each other, no significant difference was seen between them.

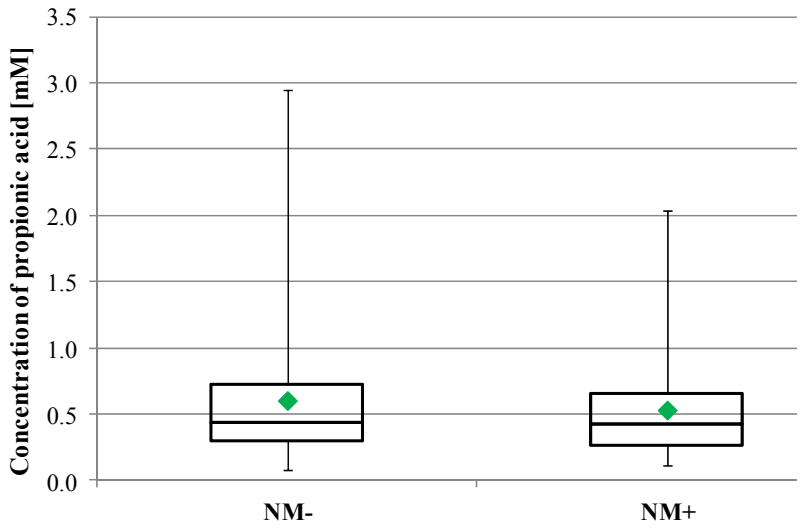

	NM-	NM+
MIN	0.08	0.11
Q1	0.29	0.26
Median	0.44	0.42
Q3	0.72	0.66
MAX	2.95	2.04
Mean	0.60	0.53

Figure 6.3-4: Frequency distribution of the concentration of propionic acid for carriers and non-carriers of *Neisseria meningitidis*.

This box plot summarises the five key numbers and the mean for the two datasets. Lower bar is the minimum and top bar is the maximum observed concentration of propionic acid, bottom of box is first quartile, middle bar is median value, top of box is third quartile. In green: the mean for each group. The key numbers were also summarised in the table. NM-: non-carriers of *Neisseria meningitidis*. NM+: *Neisseria meningitidis* carriers.

The two datasets were then checked with the SPSS Software for statistical differences using the Mann-Whitney U test, as the data was non-parametric and could be ranked. The null hypothesis stated that there was no difference between the two groups and a significance level of 0.05 was set. For a p-value smaller than 0.05 the null hypothesis was set to be rejected, whereas for a p-value greater than 0.05 the null hypothesis was set to be accepted. In this study, the test gave a p-value of 0.180 for the Mann-Whitney one-tailed U test, thus accepting the null hypothesis that there was no significant difference between carriers and non-carriers in respect to the propionic acid amount present in the saliva (Table 6.3-2). In order to be able to use

this test, however, both independent samples needed to be checked for distribution. For the test to be valid, in fact, the samples are required to have similar distribution. A one-way ANOVA test was performed for this reason, as it is considered a robust test against the normality assumption. For significance level of 0.05, the assumption made was that a p-value greater than 0.05 would imply that the two datasets were not statistically different. The SPSS Software computed a p-value of 0.5 so the data were confirmed not to be statistically different and, consequently, had similar distribution (Table 6.3-3).

Table 6.3-2: Rejected statistical difference for propionic acid for both carriers and non-carriers datasets.

Mann-Whitney one-tailed U test showing that the datasets failed to reach statistical significance (highlighted in red) as the p-value was greater than the chosen 0.05 significance level, the null hypothesis for which there was no difference between the two groups, was accepted. NM negative: non-carriers of *Neisseria meningitidis*. NM positive: *Neisseria meningitidis* carriers. Grouping variable: carriage or non-carriage of *Neisseria meningitidis.*

Mann-Whitney Test

Ranks

	NM isolated	N	Mean Rank	Sum of Ranks
prop conc	NM negative	235	153.96	36180.50
	NM positive	67	142.87	9572.50
	Total	302		

Test Statistics[a]

	prop conc
Mann-Whitney U	7294.500
Wilcoxon W	9572.500
Z	-.917
Asymp. Sig. (2-tailed)	.359
Asymp. Sig. (1-tailed)	.180

a. Grouping Variable: NM isolated

Table 6.3-3: Similar distribution between carriers and non-carriers datasets. Similar distribution for the two groups was confirmed by the one-way ANOVA test. Significance level of 0.05 was chosen with the assumption that for p-value greater than 0.05 both datasets has similar distribution.

Oneway

ANOVA

abs_deviation

	Sum of Squares	df	Mean Square	F	Sig.
Between Groups	865.921	1	865.921	.456	.500
Within Groups	570255.976	300	1900.853		
Total	571121.896	301			

6.4 Growth of *N. meningitidis* in human whole blood

In order to mimic the *in vivo* disease as closely as possible, bacteria were grown *in vitro* in Mueller Hinton Broth, a rich growth medium, supplemented with 10 mM $NaHCO_3$ until they reached a concentration of approximately 10^8 bacteria; this corresponded to bacteria which had entered early exponential phase. Following a first dilution in fresh MHB to a magnitude of 10^6 cells, bacteria were mixed to 100 % human whole blood to a concentration of 50000 CFU / ml (for blood from donors 1-4) or to 100000 CFU / ml (for blood from donors 5-7) and were grown at 37 ºC for two hours. Survival rate in the blood was investigated by counting the colony forming units (CFU) for each strain every 30 minutes over a 120 minutes incubation period. At time 0, the 20 µl inoculum spread onto each plate was expected to grow 1000 or 2000 CFU respectively.

6.5 Survival rate in human blood

Blood from the seven individuals was subdivided into two distinct groups following the results seen when counting the number of colonies grown in the plates: the first group was composed of bactericidal blood and the second was non-bactericidal. The records for both groups, with bactericidal blood belonging to four individuals and non-bactericidal blood belonging to three individuals, were averaged in order to obtain the two single datasets for each time point.

For the bactericidal blood group, the number of bacteria consistently dropped 15 / 20 - fold within the first 30 minutes following inoculation, and bacteria were not able to replicate over the full length of the experiment anymore, suggesting that blood was indeed involved in the killing of bacteria. After the two hours incubation, less than 10 % of all bacteria survived (Figure 6.5-1A). For the non-bactericidal blood group, however, bacteria tripled in number within the first 30 minutes and kept increasing, even though in a slower rate, until the end (Figure 6.5-1B). In both groups, bacterial counts for the *prpC::Spec*^{R} and *NMB1049::Spec*^{R} mutants showed no significant difference compared to the MC58 wild-type strain. This was indicating that both genes were not essential for survival and growth of *Neisseria meningitidis* in whole human blood.

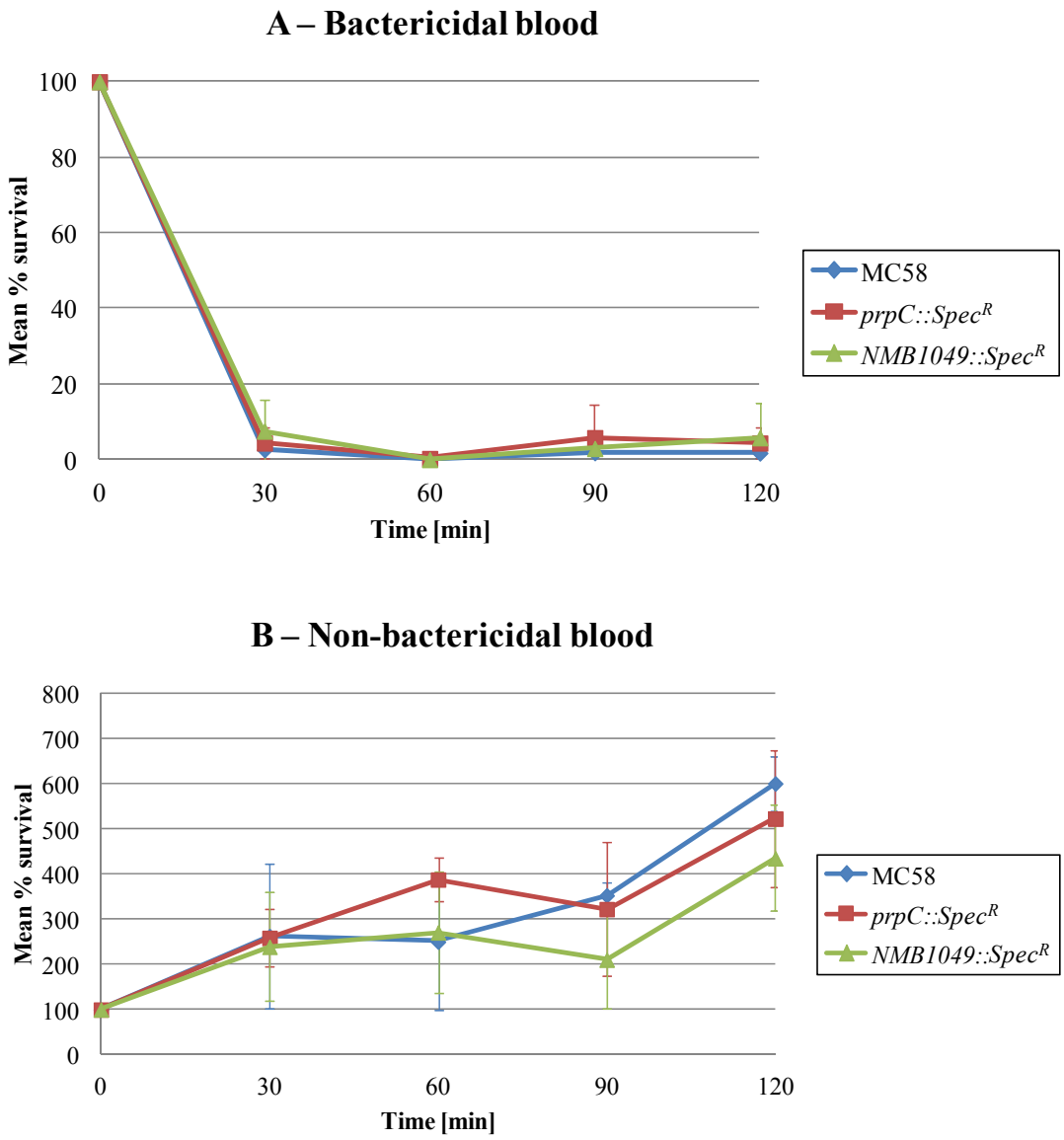

Figure 6.5-1: Mean survival of MC58 wild-type, *prpC* and *NMB1049* mutant strains in human whole blood expressed as percent of initial inoculum.

A: Blood from donors 1, 2, 3 and 7 showed bactericidal activity. **B:** Blood from donors 4, 5 and 6 showed that bacteria were not sensitive to blood and were capable of replicating.

The big overlapping error bars present in the mean percentage survival graph for the non-bactericidal blood were due to differences in the starting bacterial inoculum size

added into the three whole bloods. Bacterial viable count for two bloods with starting inoculum size of 100000 CFU / ml resulted in similar growth, whereas viable count for the smaller 50000 CFU / ml starting inoculum size, other than colony count throughout the experiment, resulted in less pronounced growth in the first hour (Figure 6.5-2). Lower starting material within the blood could have accounted for the different rate of neisserial growth. Wild-type and *NMB1049::Spec*^{R} strains showed a plateau between 30 minutes and 1 hour growth, indicating that these bacteria were under stress and were probably switching expression of some of the genes during that lapse of time, whereas the *prpC* mutant strain was behaving differently.

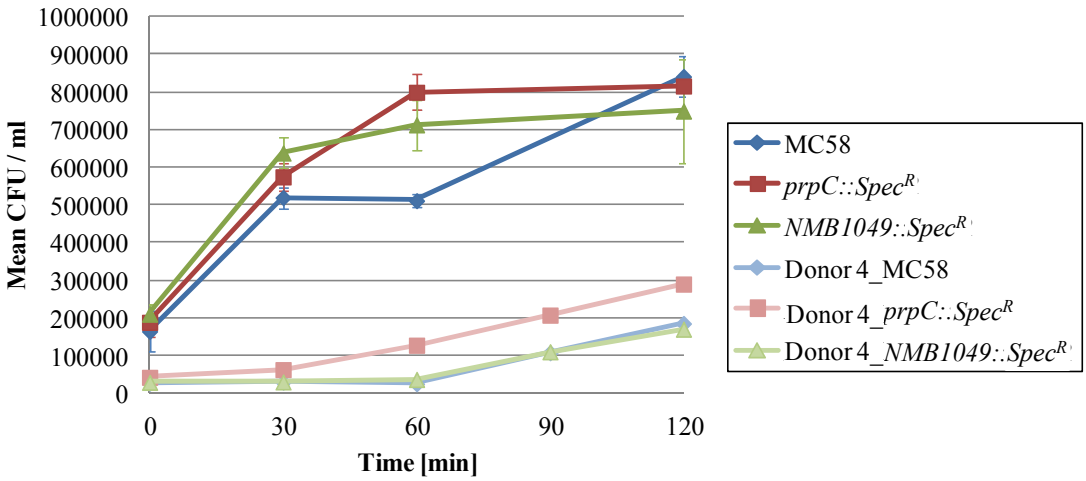

Figure 6.5-2: Growth of *Neisseria meningitidis* in non-bactericidal human whole blood.

Growth of meningococci in donors 5 and 6 was shown as a mean value for each strain, as the numbers of colonies grown in the plates over time were comparable. Bacterial growth for donor 4 (shown at the lower end of the graph as pale lines) was shown separately, as the starting inoculum size was half in respect to the inoculum size for the other two donors, and this discrepancy in starting material could account for the different rate of overall neisserial growth.

6.6 Discussion

Working with saliva and blood from real donors has revealed to be a harder task than expected, as the samples were not taken from a closed and controlled environment. Results obtained could therefore depend on many external but also individual-specific factors.

In regards to the saliva samples, the data for both carriers and non-carriers of *Neisseria meningitidis* were statistically not different from each other, and therefore propionic acid was not altered on meningococcal carriage. There were several possible reasons that could explain this lack of difference, such as the large rate of variation within the population, the time of the day when the saliva samples were collected, the type of diet of each individual, and specific bacterial colonisation in the nasopharyngeal region. More samples, especially for carriers of *Neisseria meningitidis,* could be collected and included in the statistical tests, to check whether higher sample sizes would give significant statistical difference amongst the two larger datasets.

The initial hypothesis made in this chapter was that a higher amount of propionic acid was expected in individuals that were colonised by *Neisseria meningitidis*. This carboxylic acid, in fact, is a substrate needed for the 2-methylcitrate metabolic pathway and can be utilised as an alternative substrate for growth (as explained in more details in Section 1.7.2 and Section 3.2. Likewise, an alternative hypothesis could speculate the fact that bacteria present in the carriers would be able to use propionic acid, thus leading to a lower concentration of this acid. The median for

both groups, however, was almost identical, as it had a value of 0.44 mM for non-carriers and 0.42 mM for carriers.

Despite the little difference for the median, the data showed positive bias, implying that there were several individuals whose saliva contained concentrations of propionic acid that were higher than normal, and these higher values were present in a larger number in non-carriers of *Neisseria meningitidis*. The saliva samples of 13 non-carriers contained over 1.5 mM propionic acid, versus two samples only for the carriers. This difference in the number of individuals could, however, be an artefact due to the size of the datasets, as individuals that were not colonised by the bacteria were over three times more abundant as compared to carriers (which corresponded to 235 versus 67 individuals).

A few saliva samples for the non-carriers, but none for carriers of *N. meningitidis*, contained a high concentration of at least 2.5 mM propionic acid. As mentioned above, this difference could be explained by chance, such as the varied food intake of the individuals, but it could also be explained by a higher presence of bacteria that produce propionic acid, such as Propionibacteria. The absence of *Neisseria meningitidis* carriage in these individuals would also imply that propionic acid cannot be utilised, as the 2-methylcitrate pathway is not present in non-carriers, this giving higher readings in the gas chromatograph.

Bacteria present in the saliva samples could be checked by pyrosequencing, where their diversity could be tested with 16S ribosomal RNA primers and all the data analysed (Yang *et al.*, 2011, Li *et al.*, 2010). A preliminary PCR was already run as described in Section 1.3.1 to check whether enough DNA could be gathered from the

saliva samples that were used above and which were stored at - 80 ºC. Several samples were chosen from both carriers and non-carriers of *Neisseria meningitidis,* and they had also been selected to include the full range of propionic acid: a few samples of each group containing very low, medium and maximum concentrations of propionic acid were chosen. Saliva samples were centrifuged for one minute with a Sigma 1-13 microcentrifuge (Sigma) to gather the particulates at the bottom of the tube, and 0.5 µl were mixed with 20 µl EB buffer (QIAGEN). Saliva samples at this stage were ready for use with PCR amplification and were stored at - 80 ºC. The universal primers U8F (5'-AGAGTTTGATYMTGGCTCAG-3') and U785R (5'-GGACTACCVGGGTATCTAAKCC-3') were used to amplify 16S bacterial rRNA, and the PCR amplified enough bacterial DNA from all saliva selected samples (Figure 6.6-1). One clear band was visible for each sample, and seemed to correspond to the expected 777 bp fragment. Pyrosequencing results of these samples might elucidate why the concentration of propionic acid was not statistically different between the two groups and could also help in finding a clear correlation between carriage of Propionibacteria and *Neisseria*, and the amount of propionic acid found in the saliva.

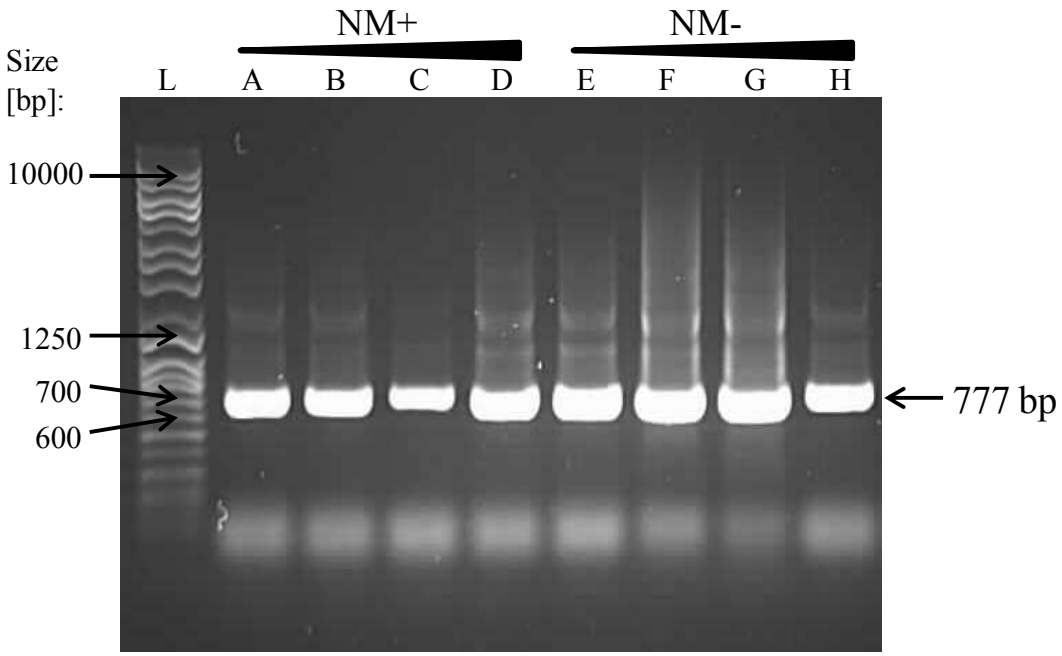

Figure 6.6-1: Amplification of 16S bacterial rRNA from human saliva samples. The expected 777 bp fragment was amplified and confirmed that enough bacterial RNA was present in all saliva samples for future pyrosequencing studies. **L:** Q-Step 4 Quantitative DNA ladder (YORBIO). Increasing amounts of propionic acid were present from left to right for both groups. **A-D:** *Neisseria meningitidis* carriers with 0.11 - 0.83 - 0.95 - 2.04 mM propionic acid. **E-H:** non-carriers for *Neisseria meningitidis* with 0.08 - 0.97 - 1.39 - 2.95 mM propionic acid.

Wild-type, *prpC::Spec*^{R} and *NMB1049::Spec*^{R} strains tested in blood in this chapter showed a significant sensitivity to being killed by about 60 % of the human whole blood from the donors tested. This result was very high when compared to the very little likelihood of the bacteria to cause septicaemia *in vivo*, but could be explained by the fact that a fairly high amount of bacteria was inoculated directly into the blood, most likely mimicking the incidence of disease once *N. meningitidis* has

already reached the blood, as in the reality only a small incidence of bacteria would enter the blood vessels *in vivo*.

As many as 10^9 *Neisseria meningitidis* bacteria can be present in 1 ml of blood from patients with fulminant disease. In studies *ex vivo* it was also shown that the number of bacteria inoculated into the blood had a direct effect on the blood's own bacterial killing effects. When bacteria were mixed with bactericidal blood at a starting concentration of 10^7 CFU / ml, they started to die straight away. When the starting concentration was increased to 10^9 CFU / ml, they went through a 45 minutes lag phase, before increasing in growth number (Hedman *et al.*, 2012). In my work I used a starting inoculum size of $0.5\text{-}1*10^5$ CFU / ml, which was well below the 10^9 CFU / ml loss of sensitivity to bactericidal blood tested. This meant that the bactericidal and non-bactericidal bloods seen here could be considered as such, and they would probably not behave differently if they were found in a similar situation in vivo.

Despite having been collected from seven healthy adult volunteers, the blood showed two radically different results in *Neisseria meningitidis* phenotype, independently of each strain tested. This difference in bacterial killing activity could be explained by some complement deficiencies or to other factors specific to the non-bactericidal blood donors. It is known that there are individuals that are more susceptible to septicaemia and meningitis, such as people with immunodeficiency problems. These people are an optimal target, as they have complement deficiencies or lack circulating antibodies that protect them against the meningococci (Skattum *et al.*, 2011, Tedesco, 2008).

Chapter 7 - General conclusions and future directions

Nine genomic islands of two or more genes have been identified in *Neisseria meningitidis*. As these islands are always absent from the closely related commensal *N. lactamica*, they can also be referred to as pathogenic islands. Their role in pathogenicity has been investigated for two islands in this work.

The role in pathogenesis for genomic island 4, composed of six genes (*NMB0430-NMB0435*), and genomic island 8, composed of two genes (*NMB1048-NMB1049*), has been clarified by growing *N. meningitidis* in human whole blood, thereby mimicking the conditions of infection. The results showed that both islands are not involved in pathogenicity per se, as knockouts for crucial genes within these pathways did not decrease blood bactericidal activity compared to the wild-type strain.

Genes belonging to the genomic island 4 encode proteins with still unknown functions or proteins with putative functions, which were extrapolated by BLAST search for similarity with genes present in other bacteria. In this work it has been shown for the first time that *N. meningitidis* can catabolise propionic acid as an extra carbon source, and that this is achieved through the six genes *NMB0430 – NMB0435* belonging to the 2-methylcitrate pathway (Figure 7-1). Knockouts of several genes amongst this pathway, in fact, led to the inability of the bacteria to use the short chain fatty acid. The results of this study indicate that the methylcitrate pathway plays an important role when *N. meningitidis* is grown in poor media, as it helps

bacteria to grow more. This pathway could give the meningococcus a survival advantage in the adult nasopharynx, which is rich in anaerobic bacteria producing propionic acid, or might be especially useful *in vivo* once it enters the blood vessels, as *N. meningitidis* will need to adapt quickly to the new challenging environment. Blood, in fact, contains fewer free nutrients, and propionic acid is amongst these. Propionic acid present in the blood derives from either food intake, as it is used as a common preservative, or from digestion of odd chain fatty acids and some amino acids. Moreover, propionic acid is produced by bacteria present in periodontal pockets. The main source of this short chain fatty acid, however, comes from bacteria present in the normal flora of the gut, where they produce it as metabolic end-product. Therefore, concentrations in the gut are always as high as 17.5 – 25 mM (Sellin, 1999). Propionic acid can then readily enter the blood by crossing the blood-gut barrier or the epithelial cells in the upper digestive tract, and is found in the blood in ranges varying between 3 – 5 mM (Wolever *et al.*, 1997). In a recent study, gene expression of the *prp* operon in *N. meningitidis* MC58 wild-type grown in human blood was shown to be up-regulated (Echenique-Rivera *et al.*, 2011). This meant that, when bacteria were grown in blood, they behaved similarly to when they were grown in poor medium, as documented in my results.

NMB0432, encoding a putative transporter, has been demonstrated in this work to be crucial in the 2-methylcitrate pathway. Propionic acid cannot be utilised by the mutant strain, even when this gene is disrupted by an antibiotic cassette lacking transcriptional terminators. This means that *NMB0432* is potentially involved in the transport of the fatty acid into the cell. For this reason, it would be interesting to study the protein structure and see whether propionic acid can actually physically bind and be transported into the cell.

ackA-1 (*NMB0435*) encodes a propionate kinase and, as with *NMB0432*, it has been demonstrated here to be necessary for propionate metabolism. From the database (NCBI GenBank accession number AE002098.2) it appears, however, that *N. meningitidis MC58* contains two putative acetate kinases: *ackA-1* (*NMB0435*) and *ackA-2* (*NMB1518*). In this work, *ackA-1* was hypothesised to be a propionate kinase, as it is found as an integral part of the *prp* operon in all *N. meningitidis* strains. For this reason, *ackA-2* is thought to be coding for a real acetate kinase. Studies designed to confirm this suggestion could be carried out by overexpressing both AckA-1 and AckA-2 in *E. coli* strain BL21 (DE3). A kinase assay could then be used to determine the activity of both proteins with propionic acid and acetic acid. Some work in this area has already begun in James Moir's laboratory, where Iain Wallace has measured affinity to acetate but none to propionate for the AckA-2 protein. This is in line with the results regarding the mutant for the *ackA-1* gene, where the 2-methylcitrate pathway was not functioning, and also confirms that *ackA-2* is an acetate kinase. AckA-1, on the other hand, has been found to have affinity with both propionate and acetate substrates.

As the K_M of the propionate kinase in *N. meningitidis* strain MC58 has been measured to be 20 mM for propionate, and the concentration of propionate found in the natural habitat of these bacteria is considerably lower, active transport of this fatty acid into the cell may be required, and is probably achieved through NMB0432. This could also explain why other microorganisms that utilise the 2-methylcitrate synthase pathway and that contain a gene encoding propionyl-CoA synthetase (PrpE) do not need to encode a protein for an active transport for propionate. PrpE, in fact, has a much higher affinity to propionate, as it has a K_M value of about 20 μM (Horswill & Escalante-Semerena, 2002).

Genes belonging to the genomic island 8 (*NMB1048* and *NMB1049*) encode two proteins with unknown functions. NMB1049 contains domains similar to the LysR-Type transcriptional regulators and has been shown in this work for the first time to be directly involved in the regulation of *NMB1048* (Figure 7-1). Moreover, the NMB1049 protein was successfully overexpressed as part of this research, but its binding to *NMB1048* was unsuccessful, probably due to inactivation of the protein. A development of the method of purification should therefore be carried out in order to keep the protein in its native functional state. The protein could therefore be cloned into a vector that contains a soluble tag such as glutathione *S*-transferase or maltose-binding protein (Lichty *et al.*, 2005).

Additional studies of the nine genomic islands will give more insights into the pathogenicity or survival capabilities of *N. meningitidis* and this could be very important, as it could help in the development of vaccines, especially those needed for the bacteria belonging to the serogroup B. These genomic islands are absent from *N. lactamica*, and therefore the design of new vaccines targeting the products of these genes would be advantageous, as they would not interfere with the colonisation of *N. lactamica*. *N. lactamica*, in fact, has already been proved to be important in stopping colonisation of *N. meningitidis* (Evans *et al.*, 2011).

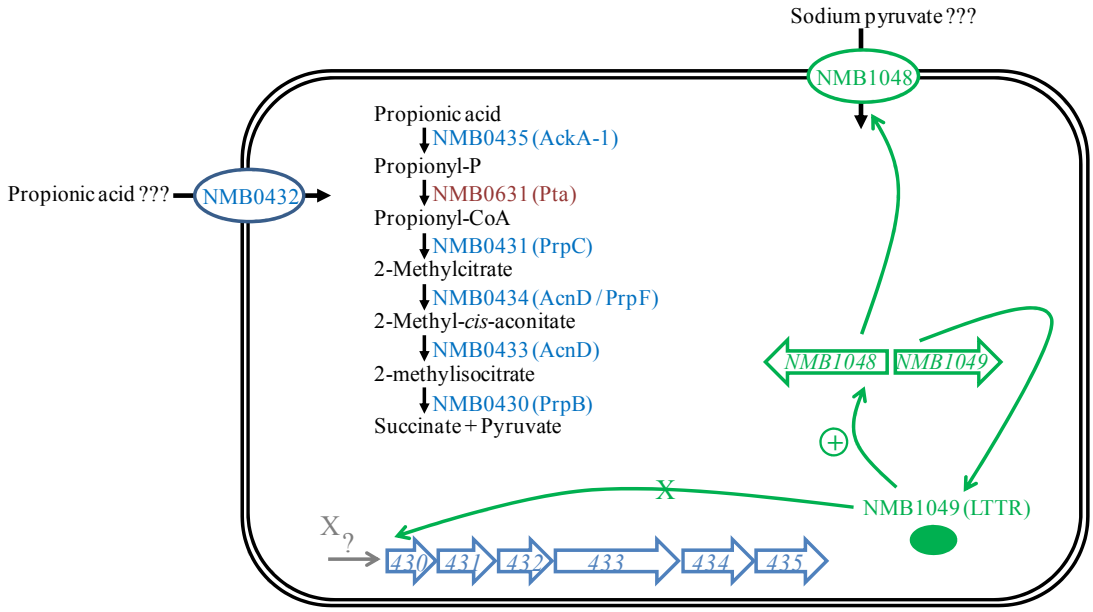

Figure 7-1: *Neisseria meningitidis* MC58 metabolism in regards to pathogenic islands 4 and 8.

The *prp* gene cluster (pathogenic island 4) is organised in an operon and the six genes it encodes (in blue) are all involved in the catabolism of propionic acid. NMB0432 is involved in the 2-methylcitrate pathway and is homologous to TauE, a family of integral membrane proteins. Pathogenic island 8 (in green) comprises two hypothetical genes, one of which encodes an LTTR protein. The LTTR protein activates the expression of the 2nd gene, *NMB1048*, which has still no function assigned to, but which belongs to the family of uncharacterised proteins DUF3360. The LTTR does not have any influence on the expression of the *prp* operon. Both pathogenic islands are regulated sharply by nutrient deprivation, which may be a prevalent problem for *N. meningitidis* in vivo. Gene numbers (*430-435* in blue) correspond to the numbering given in the MC58 complete genome, where the number is preceded by "*NMB0*". X (gray): unknown activator protein that binds to the *prp* operon promoter.

Another way forward to eradicating *N. meningitidis*, and therefore to eliminate the chances of infection and death caused by this bacterium, could involve analysing the

oral microbiome of infants, children and older people, and comparing it to the microbiome of young adults, as this is the age range most prone to infection caused by *N. meningitidis*. Several studies have already been carried out in separate laboratories, where bacterial swabs were taken with different techniques and at different locations within the mouth. These showed that children contained mostly aerobic bacteria (Bogaert *et al.*, 2011) and older people colonised an increasing number of anaerobic bacteria (Segata *et al.*, 2012). More accurate studies could therefore involve swabs taken from the same place within the mouth or throat and could be analysed by pyrosequencing. The data obtained in this way would then lead to more comparable results, which could contribute to the effective inoculation of beneficial bacteria that would stop *N. meningitidis* colonisation.

Appendices

Appendix - A

Construction of the *NMB0240::Spec*^{R} mutant of *N. meningitidis* MC58

The putative pathogenic island composed of genes *NMB0239* and *NMB0240* is thought to be involved in polyamine biosynthesis (Figure A-1). The first gene of this pathway, *NMB0240*, encodes spermidine synthase and has been successfully knocked-out with a spectinomycin resistance cassette, which was inserted after restriction digest with SspI (Figure A-2).

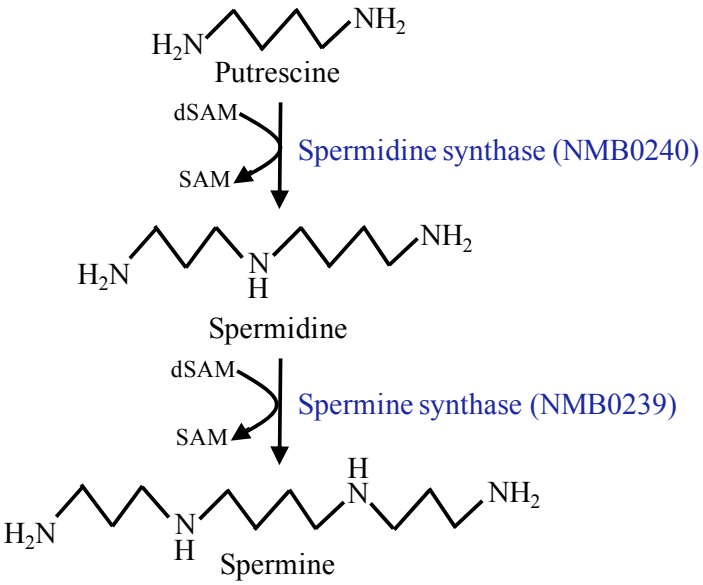

Figure A-1: The spermine synthase pathway with its intermediates.
Both *NMB0239* and *NMB0240* genes are specific to this pathway. Abbreviations used: dSAM: decarboxylated S-adenosylmethionine. SAM: S-adenosylmethionine (Figure adapted from Wimalasekera *et al.*, 2011).

CCTTATATTTTTTCAACACTTTGGGTGCGGCACTCGGATCGCTTGCCGCCGCCGAATTTTTCTACGTC
TTTTTTACCCTCTCCCAAACCATTGCGCTGACAGCCTGCTTTAACCTTCTGATTGCTGCTTCAGTATG
GCTGCGTTACAGAAAGGATGGATATAGTGAACACTAAACCGAATACTAGTTTGATTTATATGCTTTCT
TTCCTTAGCGGCTTATTGAGCTTGGGTATAGAAGTCTTGTGGGTGAGGATGTTTTCGTTCGCAGCACA
GTCCGTGCCTCAGGCATTTTCATTTACCCTTGCCTGTTTTCTGACCGGTATCGCCGTCGGCGCGTATT
TTGGCAAACGGATTTGCCGCAGCCGCTTTGTTGATATTCCCTTTATCGGGCAGTGCTTCTTGTGGGCG
GGTATTGCCGACTTTTTGATTTTGGGTGCTGCGTGGTTGTTGACGGGTTTTTCCGGCTTCGTCCACCA
CGCCGGTATCTTCATTACCCTGTCTGCCGTCGTCAGAGGGTTGATTTTCCCGCTCGTACACCATGTGG
GTACGGATGGCAACAAATCCGGACGACAGGTTTCCAATGTTTATTTCGCCAACGTTGCCGGCAGTGCA
TTGGGTCCGGTCCTTATCGGCTTTGTGATACTTGATTTCTTGTCCACCCAACAGATTTACCTGCTCAT
CTGTTTGATTTCTGCTGCTGTCCCTTTGTTTTGTACACTGTTCCAAAAAAGTCTCCGACTGAATGCAG
TGTCGGTAGCAGTTTCCCTAATGTTCGGCATCCTCATGTTCCTACTGCCGGATTCTGTCTTTCAAAATT
ATTGCTGACCGTCCGGATAGGCTGATTGAAAACAAACACGGCATTGTTGCGGTTTACCATAGAGATGG
TGATAAGGTTGTTTATGGGGCGAATGTATACGACGGCGCATACAATACCGATGTATTCAATAGTGTCA
ACGGCATCGAACGTGCCTATCTGCTACCCTCCCTGAAGTCTGGCATACGCCGCATTTTCGTCGTTGGA
CTGAGTACAGGTTCGTGGGCGCGCGTCTTGTCTGCCATTCCGGAAATGCAGTCGATGATCGTTGCGGA
AATCAATCCGGCATACCGTAGCCTTATCGCGGACGAGCCGCAAATCGCCCCGCTTTTGCAGGACAAAC
GTGTTGAAATTGTATTGGATGACGGTAGGAAATGGCTGCGTCGCCATCCTGATGAAAAATTCGACCTG
ATTTTGATGAATACGACTTGGTACTGGCGTGCCTATTCCACCAACCTGTTGAGTGCGGAATTTTTAAA
ACAGGTGCAAAGCCACCTTACCCCGGATGGTATTGTAATGTTTAATACCACGCACAGCCCGCATGCTT
TTGCTACCGCCGTACACAGTATTCCCTATGCATACCGCTATGGGCATATGGTAGTCGGCTCGGCAACC
CCGGTAGTTTTCCCTAATAAAGAACTGCTCAAGCAACGTCTCTCCCGGTTGATTTGGCCGGAAAGCGG
CAGGCACGTATTTGACAGCAGCACCGTGGATGCTGCAGCACAAAAGGTTGTCTCTCGTATGCTGATTC
AGATGACGGAACCTTCGGCTGGGGCGGAAGTTATTACCGACGATAATATGATTGTAGAATACAAATAC
GGCAGAGGGATTTAACCGTCTTAAAGGGTTTCAGGCAACGCAGGTTTTAGGTAACGTCCTGCTAGTTC
AAAAAAACCGCATCACAGCAGTCGGGACAAAATGGTTTAAACATTTTGTCCCGAATTCTTATTCCTAT
ATATAGTGGATTAACAAAAATCAGGACAAGGCGACGAAGCCGCAGACAGTACAAATAGTACGGAACCG

Figure A-2: The *NMB0240* sequence with its flanking regions used for constructing the mutant.

The *NMB0240* gene (blue) with the ATG start codon and the TAA stop codon (both in green) and its flanking regions (black) give a product 1516 bp long. Primers NMB0240-for and NMB0240-rev were used (highlighted in yellow) to generate the knockout. The reverse primer's mismatches are also shown (highlighted in red), where "A" and "T" in the sequence were both considered as "G" during the primer's design. The SspI site is also shown (highlighted in blue) with the two bases within which the restriction enzyme cuts (brown). Primers NMB0240bis-for and NMB0240bis-rev were used for colony pick PCR screening in *N. meningitidis* (underlined in blue).

Appendix - B

Construction of the *NMB0468::Spec*^{R} mutant of *N. meningitidis* MC58

The putative pathogenic island composed of genes *NMB0468* and *NMB0469* is thought to be involved in polyamine biosynthesis (Figure B-1). The first gene of this pathway, *NMB0468*, encodes arginine decarboxylase and has been successfully knocked-out with a spectinomycin resistance cassette, which was inserted after restriction digest with AclI (Figure B-2). Sequencing results of the new transformant confirmed that the gene was disrupted with the spectinomycin resistance cassette. From sequencing it cannot be determined if the restriction enzyme cut all three sites or just once, however, the spectinomycin cassette has been partially sequenced starting from the 3rd AclI site.

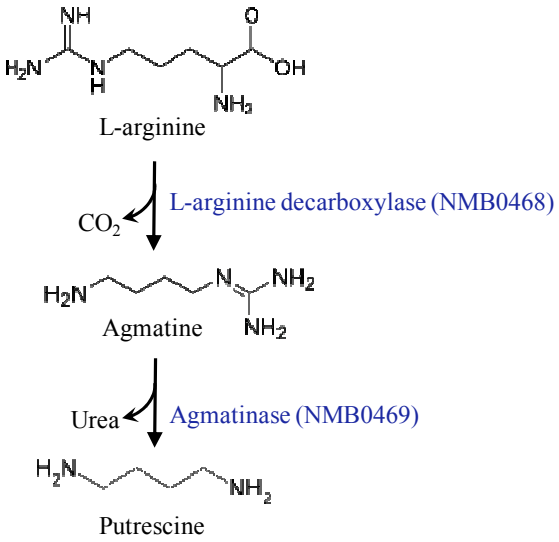

Figure B-1: The putrescine synthesis pathway.
Both *NMB0468* and *NMB0469* genes are specific to this pathway (Figure adapted from Stalon & Mercenier, 1984).

ATCGCTGACTCCTTTGATGGAAAGATGAACCAAAATGCCGTCTGAAGCGTTCAGACGGCATTTTGCCT
GTTCCTCATCAGGTATGAGGCAGGCTTTTCTTATTAAAAAAATGACATTTCACGCTGATTTGTTATAA
TCATTGCTTTTCAACACGACAGACGGAGCAGGTTTATTATGCCTATCCTTACCATCCGTGAAGTGTGC
AACATTAATCATTGGGGCATAGGTTATTATGATGTTGACGATTCCGGCGAAATCATCGTCCGCCCCAA
TCCCTCGCAACACAATCAAACTGTTTCACTGCAAAAACTGACTGAAGCCGTGCAACAAAAACATCAGG
CGCGCCTGCCTGTTTTGTTTTGTTTTCCGCAAATCCTCGAACACCGCCTCCGCGACATTAACCGCGCC
TTTCAGACGGCACGGGAAGAGTGCGGCTATAAGGGCGGTTATTGTTTGGTTTACCCTATCAAGGTCAA
CCAACACCGCCGCGTCATCGAATCGCTTATGTCAAGCGGACAACCGCATGGTTTGGAAGCTGGTTCTA
AAGCCGAACTGATGGCGGTTTTGGCACACGCCGGCAACCGGCAAACATTAATCGTCTGCAACGGCTAT
AAAGACCGTGAATATATCCGTTTCGCCTTGATGGGCGAAAAACTGGGGCATCAGGTTTATTTGGTGAT
TGAGAAGCTGTCCGAAATACAAATGGTATTGGAAGAGGCGGAAAAACTCGGCATCAAGCCCCGTTTGG
GTGTGCGCGCCAGACTGGCTTCCCAAGGTTCGGGAAAATGGCAGTCTTCGGGTGGGGAAAAATCAAAA
TTCGGCTTGTCGGCTTCCCAAGTTTTGCAACTGGTCGATATTTTGAAACAAAAAAACAGGCTGGATTG
CCTGCAGCTTTTGCATTTCCATTTGGGCTCGCAGCTTGGGAACATCCGTGATGTTGCCACAGGTGTAC
ACGAATCGGCTCGGTTTTATGTTGAGTTGCACAAACTGGGGGTAAATATCCGCTGTTTTGATGTAGGC
GGCGGGCTTGGCGTGGATTACGAAGGAAACCGCACACAATCGGATTGTTCCGTTAATTACAGCCTCAA
CGAATATGCCGCCACAGTCGTATGGGGCATCAGTCAGGCTTGTCTCGAACACGGGCTGCCGCATCCGA
CAATCATCACCGAGAGCGGGCGCGGCATTACCGCACATCACGCCGTTTTGGTTGCTAATGTTATAGGC
GTTGAACGTTACAAACCGCGCCGGCTGGATGCGCCATCGCCCGAAGCACCGCGTGTGTTGCACAGTAT
GTGGGAAACTTGGACGGATATTTCCGCCTCGCGGGAAAAACGTTCCTTACGCAGCTGGATACACGAAG
GGCAGTTTGATCTTGCTGATGTGCATAATCAGTATAATGTCGGGCTGTTGAGTTTGGCGCAACGTGCG
TGGGCGGAGCAACTGTATTTAAATATCTGTCATGAAGTCGGCGAATTGTTTAATGAAAAACACCGGTC
TCACCGAACCATTATTGACGAATTGCAAGAACGTTTTGCCGATAAGCTGTATGTCAATTTCTCACTCT
TCCAATCTTTGCCCGATGCTTGGGGCATAGATCAACTTTTCCCTGTTTGTCCCATTACCGGTTTGAAT
GAACCGATTGCGCGCCGCGCCGTGTTGTTGGACATTACCTGCGATTCAGACGGTACGATTGACCACTA
CATCGACGGAGACGGCATCGCCGGTACGATGCCTATGCCTGATTATCCCGAAGAAGAGCCGCCGCTTT
TAGGCTTTTTTATGGTGGGAGCATATCAGGAAATACTCGGCAATATGCACAATCTTTTCGGCGACACT
GCCACTGCCGATGTTGTTGTAGGGGAAGACGGACAATTTACCGTCATCGATTACGATGAAGGAAACAC
CGTTGCCGATATGCTCGAATACGTTTATCAAGATCCGAAAGAGCTGATGAAACGCTATCGCGAACAAA
TCGAACATTCAGACCTTCCTGCCTCGCAGGCTATGTCTTTCTTAAAAGAACTCGAAGCGGGGCTTAAT
GGTTATACCTATTTGGAAGACGAATAGACGCATCAAGGCATCGGATATGTCGTCTGAAGCCCGATTTT
CTTACTCAAACACCAATCATCACGACCGATTGAAACCAATTACAAGGAATCATTACGATGCAATACAG
CACACTGGCAGGACAAACCGACAACTCCCTCGTTTCCAATAATTTCGGGTTTTTGCGCCTGCCGCTTA

Figure B-2: The *NMB0468* sequence with its flanking regions used for constructing the mutant.

The *NMB0468* gene (blue) with the ATG start codon (green) and the TAG stop codon (red) and its flanking regions (black) give a product 1958 bp long. Primers NMB0468-for and NMB0468-rev were used (highlighted in yellow) to generate the knockout. The reverse primer's mismatch is also shown (highlighted in red), where "T" in the sequence was considered as "C" during the primer's design. The same primers were used for colony pick PCR screening in *N. meningitidis*. The three AclI sites are also shown (highlighted in blue) with the two bases within which the restriction enzyme cuts (brown).

Appendix - C

Construction of the *NMB1049::Chl*^{R} mutant of *N. meningitidis* MC58

The putative *NMB1049* gene that encodes a LysR-Type transcriptional regulator has been knocked-out with a spectinomycin resistance cassette, as described in Chapter 4. This gene, however, has also been successfully knocked-out with a chloramphenicol resistance cassette.

The chloramphenicol resistance gene cassette (*Chl*^{R}) was generated by PCR amplification of the pST2 plasmid with the primers Chloram-for (5'-AAGAATTGGAGCCAATCAATTC-3') and Chloram-rev (5'-TACACTAAATCAGTAAGTTGGC-3'). The resulting PCR fragment for chloramphenicol resistance gene was approximately 2 kb in size. This fragment was purified from the gel and subsequently used for ligation with *NMB1049*, in order to disrupt the function of the *NMB1049* gene.

The resistance cassette was inserted after restriction digest of *NMB1049* with BspEI (Figure C-1). Sequencing results showed that the 705 bp fragment was eliminated after digest with the restriction enzyme. Sequencing of the new transformant confirmed that the *NMB1049* gene was disrupted with the chloramphenicol resistance cassette.

GATAAAGCCCAAATAGAGTAATAATCCGCCGCATACGCCGTTGCTTGTCAGCTTCGCCATAATACTGC
CGCCGCGAAATAAAGCCATCAGCAGACCTAAAACCGCAATCGAAATGCCGAACGCCAAAGGATGCCCG
CCTGCCGACACAACGATGGGAATCATCGGAATCAGCGGCCCGTGCGTACCGGGCAGGTTGGCGCCGGG
CAGAAAAAAGCCCGATACCAATAAGATAAACGCGGCGGCGATTAAAAGCTCATAGCGCACATTTTCCA
GTACAAAGCTGTCAGGCAGCCCCAAAGGTGCGGCAAACGCCGCCGCCACCGCCCCCACCATCACCACT
TTTCCAATCGTTCCCGCCATCGCAGGAATCAAATCCTCCCACTCGAAGCGGTAATCGCGAAAGGGCAG
GTTGGGCCGCCAGCGTTTTGGTTGCATAATCTGCAATTCATGTTCCAAATATTCGTCCCGCGTCGCAA
ATTCCGAAGCTGGACGGTGCAAATCCCGATAAGTCCCATTATGTTTTTCCATAACCTTCCTCCTTATA
TATCGCGCCTCGTAAAAGGGGCGCATGACTTTTCTTTTTGATACGGGCTGCGTTCGGAAGCCGTAACC
CCATTTAAAGCCCAAACAGGCAATAAAACCAATCTTTTTTTTTGATAACCATCATCCGGAAAACTGAT
ACAATTTACAAACCACTTGATTAAAAAGTTAATTTTCAGCAACAATCCACCTAAAAGATTTCGATTGC
ACAAATATAGAAAACATCCGCACAAGGAGGGATATATGGATGCCGTACAATTAAAATCATTTGTCGCC
GTCGCGCACGAGGGCAACCTTACCCAAGCCGCCAAACGACTTTTCCTTTCCCAGCCTGCCGTTTCTGC
CCAAATTAAAGCCCTTGAAGAATATGTCGGCACGCCGCTGTTCAGGCGCACGGGGAAAGGCATGGTAT
TGACGCGGGCGGGCGAAATACTGTTGCCCGAAGCGGAATCCCTGCTGCAATACAAACACAAGCTGGAG
CATTTTGCCAAAACGCTGGCAGGCGATTATTCGGAAGAGACCAGTTTGGGCATTATCCACCCCATCGA
TTCGGCAAAACTCGTCGCGCTGACGGACAATATCGGTCAAACAGCCCCCAAAACGCGCCTGCACATCC
AATACGGAATGAGCGGCGAAATCCTCTCGCGCATCCAACACAAAACCCTGCACGGCGGCTTTATACTC
GGCAACGCCGCCCAACGCGGCATCCGCAGCGTATTCCTGCAAAACCTGACCTACGCGCTGATTTGCCC
GCAAAGCCAATATCCCCATCTGACCCGCTCCCTTCCGCAGAGCCTGCAAGAATGCGTATGGATAGAAA
TGTCGGGCGTGTCCGGAAGTAGGAAGCACCTGCACCAGTTTTGGCGCAGCAACCGGCTCTCACCCAAA
AAACAGATCTTGTGCGACTACCCCCAAACCATTATCGATTTGGTTGCAGGCGGTATAGGTGTGGCAAT
GGTGCCGGGAAACAAAGCCGAAGCGGCGGCAAAAGAAGGCGCGGGCGTGGCTATTATCGAATCGTGCC
GCCACAGTATGCCGCTCAATTTCATTTATGCGGAAGAATACGAGGATAATCCCCACGTCTCACTCCTG
CTCGAGTGCATTGAAAAAGTATGGGGAGTGCAGGCGGTGCAGCCGCCCGTTGTCTCGGACAACTGAAA
TAAATCCTGCTTTGCTGATTGTTTTAAAATAGAAATTTGAATTTTATCACGCTGAAAACACTGAAAAC
GCCATCCGCATTCTCTCAAATACGGCTTAAAATGCCCTTTGGAAATGCCGTTATAGTGGATTAACAAA
AATCAGGACAAGGCGACGAAGCCGCAGACAGTACAAATAGTACGGAACCGATTCACTTGGTGCTTCAG
CACCTTAGAGAATCGTTCTCTTTGAGCTAAGGCGAGGCAACGCCGTACTGGTTTTTGTTAATCCACTA
TAAACTGACGCAAATACCGTTTTGCACAATTCCAAAAGTTTTCAATTCCGTTAATGCGATTTTGCCGT
TTGGCGAAATGCGTACTGTTCCAGTCGTGGATTGAACCCCCACCCTGTATAGTTCTTTCGAAGCATTG
GGGTATTGTTTTTTCAAAGCATCTTGGATTCGGATTTCAAGTGCAACACTAGTGTATTAGTGGTTGGA
ACAGATTCAAGAATAAAACACTTGGCGTTTCGTAGCCAAGTGTTTTTCTTGGTCGGTGGTTCAACTCA

Figure C-1: The *NMB1049* sequence with its flanking regions used for constructing the mutant.

The *NMB1049* gene (blue) with the ATG start codon (green) and the TGA stop codon (red) and its flanking regions (black) give a product 2043 bp long. Primers NMB1049-for and NMB1049-rev were used (highlighted in yellow) to generate the knockout. The same primers were used for colony pick PCR screening in *N. meningitidis*. The two BspEI sites are also shown (highlighted in blue) with the two bases within which the restriction enzyme cuts (brown).

Appendix - D

TMHMM for the NMB0432 protein of *N. meningitidis* MC58

The putative NMB0432 protein containing 262 amino acids has similarities to TauE, a family of integral membrane proteins. A search with the TMHMM Server v. 2.0 for the NMB0432 protein sequence resulted in 8 transmembrane helices.

```
# WEBSEQUENCE Length: 262
# WEBSEQUENCE Number of predicted TMHs:  8
# WEBSEQUENCE Exp number of AAs in TMHs: 158.60079
# WEBSEQUENCE Exp number, first 60 AAs:  37.22885
# WEBSEQUENCE Total prob of N-in:        0.84138
# WEBSEQUENCE POSSIBLE N-term signal sequence
WEBSEQUENCE     TMHMM2.0        inside       1     4
WEBSEQUENCE     TMHMM2.0        TMhelix      5    24
WEBSEQUENCE     TMHMM2.0        outside     25    27
WEBSEQUENCE     TMHMM2.0        TMhelix     28    47
WEBSEQUENCE     TMHMM2.0        inside      48    74
WEBSEQUENCE     TMHMM2.0        TMhelix     75    97
WEBSEQUENCE     TMHMM2.0        outside     98   100
WEBSEQUENCE     TMHMM2.0        TMhelix    101   118
WEBSEQUENCE     TMHMM2.0        inside     119   129
WEBSEQUENCE     TMHMM2.0        TMhelix    130   147
WEBSEQUENCE     TMHMM2.0        outside    148   150
WEBSEQUENCE     TMHMM2.0        TMhelix    151   173
WEBSEQUENCE     TMHMM2.0        inside     174   192
WEBSEQUENCE     TMHMM2.0        TMhelix    193   215
WEBSEQUENCE     TMHMM2.0        outside    216   229
WEBSEQUENCE     TMHMM2.0        TMhelix    230   248
WEBSEQUENCE     TMHMM2.0        inside     249   262
```

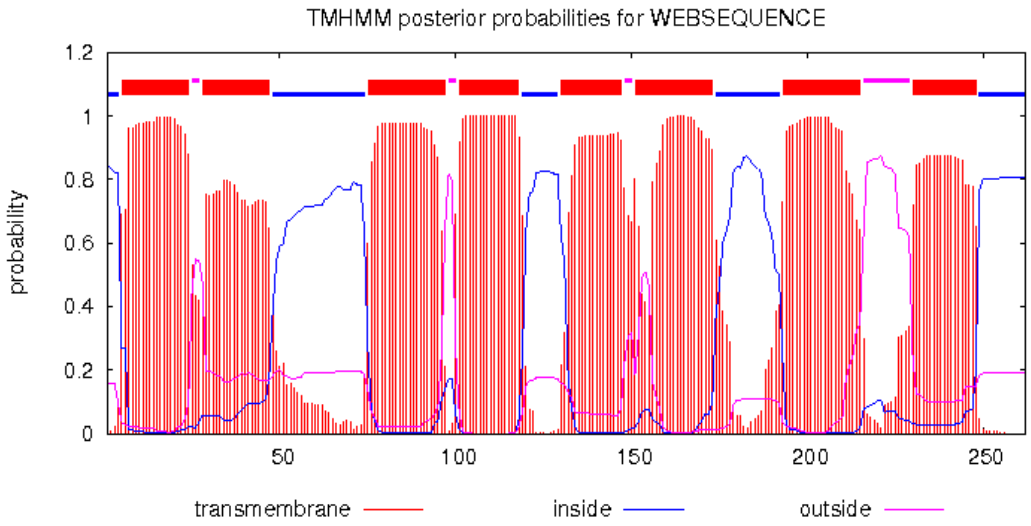

Figure D-1: TMHMM prediction for NMB0432.

The protein encoded by *NMB0432* contains 8 transmembrane helices.

Appendix - E

TMHMM for the NMB1048 protein of *N. meningitidis* MC58

The putative NMB1048 protein containing 489 amino acids belongs to the DUF3360, a family of proteins of unknown function. A search with the TMHMM Server v. 2.0 for the NMB1048 protein sequence resulted in 11 transmembrane helices.

```
# WEBSEQUENCE Length: 489
# WEBSEQUENCE Number of predicted TMHs:  11
# WEBSEQUENCE Exp number of AAs in TMHs: 242.56482
# WEBSEQUENCE Exp number, first 60 AAs:  2.74115
# WEBSEQUENCE Total prob of N-in:        0.06600
WEBSEQUENCE     TMHMM2.0        outside     1    63
WEBSEQUENCE     TMHMM2.0        TMhelix     64   86
WEBSEQUENCE     TMHMM2.0        inside      87   92
WEBSEQUENCE     TMHMM2.0        TMhelix     93   115
WEBSEQUENCE     TMHMM2.0        outside     116  124
WEBSEQUENCE     TMHMM2.0        TMhelix     125  147
WEBSEQUENCE     TMHMM2.0        inside      148  159
WEBSEQUENCE     TMHMM2.0        TMhelix     160  182
WEBSEQUENCE     TMHMM2.0        outside     183  191
WEBSEQUENCE     TMHMM2.0        TMhelix     192  212
WEBSEQUENCE     TMHMM2.0        inside      213  218
WEBSEQUENCE     TMHMM2.0        TMhelix     219  241
WEBSEQUENCE     TMHMM2.0        outside     242  264
WEBSEQUENCE     TMHMM2.0        TMhelix     265  287
WEBSEQUENCE     TMHMM2.0        inside      288  352
WEBSEQUENCE     TMHMM2.0        TMhelix     353  372
WEBSEQUENCE     TMHMM2.0        outside     373  376
WEBSEQUENCE     TMHMM2.0        TMhelix     377  399
WEBSEQUENCE     TMHMM2.0        inside      400  411
WEBSEQUENCE     TMHMM2.0        TMhelix     412  434
WEBSEQUENCE     TMHMM2.0        outside     435  455
WEBSEQUENCE     TMHMM2.0        TMhelix     456  478
WEBSEQUENCE     TMHMM2.0        inside      479  489
```

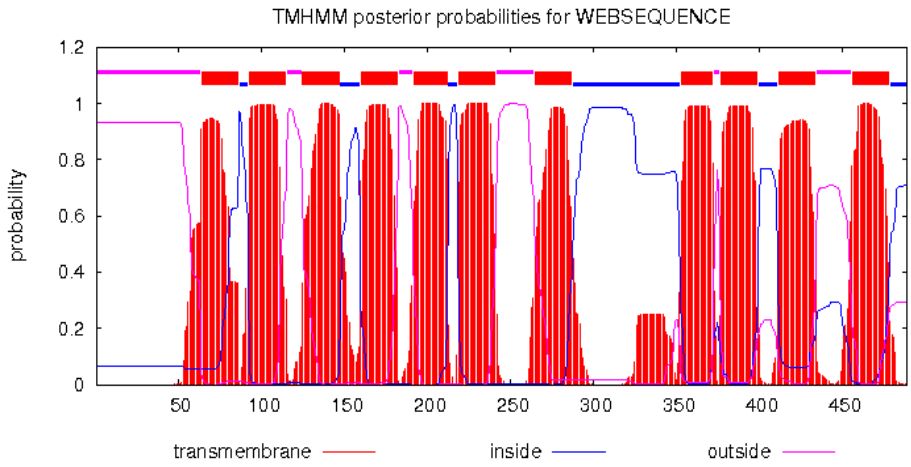

Figure E-1: TMHMM prediction for NMB1048.

The protein encoded by *NMB1048* contains 11 transmembrane helices.

References

Aas, J. A., Paster, B. J., Stokes, L. N., Olsen, I. and Dewhirst, F. E. (2005). Defining the normal bacterial flora of the oral cavity. *Journal of clinical microbiology,* 43(11): 5721-5732.

Alber, B. E. and Fuchs, G. (2002). Propionyl-coenzyme A synthase from Chloroflexus aurantiacus, a key enzyme of the 3-hydroxypropionate cycle for autotrophic CO2 fixation. *Journal of Biological Chemistry,* 277(14): 12137-12143.

Allison, K. and Clarridge, J. E. (2005). Long-term respiratory tract infection with canine-associated Pasteurella dagmatis and Neisseria canis in a patient with chronic bronchiectasis. *Journal of clinical microbiology,* 43(8): 4272-4274.

Amann, R. I., Ludwig, W. and Schleifer, K.-H. (1995). Phylogenetic identification and in situ detection of individual microbial cells without cultivation. *Microbiological reviews,* 59(1): 143-169.

Andersen, B., Steigerwalt, A., O'Connor, S., Hollis, D., Weyant, R., Weaver, R. and Brenner, D. (1993). Neisseria weaveri sp. nov., formerly CDC group M-5, a gram-negative bacterium associated with dog bite wounds. *Journal of clinical microbiology,* 31(9): 2456-2466.

Barrett, S., Schlater, L. K., Montali, R. J. and Sneath, P. (1994). A new species of Neisseria from iguanid lizards, Neisseria iguanae sp. nov. *Letters in applied microbiology,* 18(4): 200-202.

Bennett, J. S., Griffiths, D. T., McCarthy, N. D., Sleeman, K. L., Jolley, K. A., Crook, D. W. and Maiden, M. C. (2005). Genetic diversity and carriage dynamics of Neisseria lactamica in infants. *Infection and immunity,* 73(4): 2424-2432.

Bogaert, D., Keijser, B., Huse, S., Rossen, J., Veenhoven, R., van Gils, E., Bruin, J., Montijn, R., Bonten, M. and Sanders, E. (2011). Variability and diversity of nasopharyngeal microbiota in children: a metagenomic analysis. *PloS one,* 6(2): e17035.

Boisier, P., Nicolas, P., Djibo, S., Taha, M.-K., Jeanne, I., Maínassara, H. B., Tenebray, B., Kairo, K. K., Giorgini, D. and Chanteau, S. (2007). Meningococcal meningitis: unprecedented incidence of serogroup X—related cases in 2006 in Niger. *Clinical Infectious Diseases,* 44(5): 657-663.

Bojar, R. and Holland, K. (2004). Acne and Propionibacterium acnes. *Clinics in dermatology,* 22(5): 375-379.

Brämer, C. O. and Steinbüchel, A. (2001). The methylcitric acid pathway in Ralstonia eutropha: new genes identified involved in propionate metabolism. *Microbiology,* 147(8): 2203-2214.

Brandtzaeg, P. and van Deuren, M. (2012). Classification and pathogenesis of meningococcal infections. In: *Neisseria meningitidis*. Springer, pp. 21-35.

Branham, S. E. (1940). The meningococcus (Neisseria intracellularis). *Bacteriological reviews,* 4(2): 59-96.

Brock, M. and Buckel, W. (2004). On the mechanism of action of the antifungal agent propionate. *European Journal of Biochemistry,* 271(15): 3227-3241.

Brüggemann, H., Henne, A., Hoster, F., Liesegang, H., Wiezer, A., Strittmatter, A., Hujer, S., Dürre, P. and Gottschalk, G. (2004). The complete genome sequence of Propionibacterium acnes, a commensal of human skin. *Science,* 305(5684): 671-673.

Caesar, N., Myers, K. and Fan, X. (2013). Neisseria meningitidis Serotype B Vaccine Development. *Microbial pathogenesis*, 57: 33-40.

Catlin, B. W. and Schloer, G. M. (1962). A defined agar medium for genetic transformation of Neisseria meningitidis. *Journal of bacteriology,* 83(3): 470-474.

Caugant, D., Høiby, E., Rosenqvist, E., Frøholm, L. and Selander, R. (1992). Transmission of Neisseria meningitidis among asymptomatic military recruits and antibody analysis. *Epidemiology and infection,* 109(02): 241-253.

Caugant, D. A., Høiby, E., Magnus, P., Scheel, O., Hoel, T., Bjune, G., Wedege, E., Eng, J. and Frøholm, L. (1994). Asymptomatic carriage of Neisseria meningitidis in a randomly sampled population. *Journal of clinical microbiology,* 32(2): 323-330.

Caugant, D. A., Tzanakaki, G. and Kriz, P. (2007). Lessons from meningococcal carriage studies. *FEMS microbiology reviews,* 31(1): 52-63.

Chakravorty, S., Helb, D., Burday, M., Connell, N. and Alland, D. (2007). A detailed analysis of 16S ribosomal RNA gene segments for the diagnosis of pathogenic bacteria. *Journal of microbiological methods,* 69(2): 330-339.

Chippaux, J.-P. (2008). Control of meningococcal meningitis outbreaks in sub-Saharan Africa. *The Journal of Infection in Developing Countries,* 2(05): 335-345.

Claus, H., Maiden, M. C., Maag, R., Frosch, M. and Vogel, U. (2002). Many carried meningococci lack the genes required for capsule synthesis and transport. *Microbiology,* 148(6): 1813-1819.

Coureuil, M., Mikaty, G., Miller, F., Lécuyer, H., Bernard, C., Bourdoulous, S., Duménil, G., Mège, R.-M., Weksler, B. B. and Romero, I. A. (2009). Meningococcal type IV pili recruit the polarity complex to cross the brain endothelium. *Science,* 325(5936): 83-87.

D'amelio, R., Agostoni, A., Biselli, R., Brai, M., Caruso, G., Cicardi, M., Corvetta, A., Fontana, L., Misiano, G. and Perricone, R. (1992). Complement deficiency and antibody profile in survivors of meningococcal meningitis due to common serogroups in Italy. *Scandinavian journal of immunology,* 35(5): 589-595.

Davidsen, T. and Tønjum, T. (2006). Meningococcal genome dynamics. *Nature Reviews Microbiology,* 4(1): 11-22.

de Filippis, I. (2009). Quest for a broad-range vaccine against Neisseria meningitidis serogroup B: implications of genetic variations of the surface-exposed proteins. *Journal of medical microbiology,* 58(9): 1127-1132.

Deghmane, A. E., Giorgini, D., Larribe, M., Alonso, J. M. and Taha, M. K. (2002). Down ‐ regulation of pili and capsule of Neisseria meningitidis upon contact with epithelial cells is mediated by CrgA regulatory protein. *Molecular microbiology,* 43(6): 1555-1564.

Distler, W. and Kröncke, A. (1981). The lactate metabolism of the oral bacterium Veillonella from human saliva. *Archives of Oral Biology,* 26(8): 657-661.

Echenique-Rivera, H., Muzzi, A., Del Tordello, E., Seib, K. L., Francois, P., Rappuoli, R., Pizza, M. and Serruto, D. (2011). Transcriptome analysis of Neisseria meningitidis in human whole blood and mutagenesis studies identify virulence factors involved in blood survival. *PLoS pathogens,* 7(5): e1002027.

Edwards, J., Quinn, D., Rowbottom, K.-A., Whittingham, J. L., Thomson, M. J. and Moir, J. W. B. (2012). Neisseria meningitidis and Neisseria gonorrhoeae are differently adapted in the regulation of denitrification: single nucleotide polymorphisms that enable species-specific tuning of the aerobic-anaerobic switch. *Biochemical Journal,* 445(1): 69-79.

Ekins, A., Khan, A. G., Shouldice, S. R. and Schryvers, A. B. (2004). Lactoferrin receptors in gram-negative bacteria: insights into the iron acquisition process. *Biometals,* 17(3): 235-243.

European_Commission (2011). Regulations, Commission regulation (EU) No 1129/2011. *Official Journal of the European Union,* L 295.

Evans, C. M., Pratt, C. B., Matheson, M., Vaughan, T. E., Findlow, J., Borrow, R., Gorringe, A. R. and Read, R. C. (2011). Nasopharyngeal colonization by Neisseria lactamica and induction of protective immunity against Neisseria meningitidis. *Clinical Infectious Diseases,* 52(1): 70-77.

Exley, R. M., Goodwin, L., Mowe, E., Shaw, J., Smith, H., Read, R. C. and Tang, C. M. (2005). Neisseria meningitidis lactate permease is required for nasopharyngeal colonization. *Infection and immunity,* 73(9): 5762-5766.

Feil, E. J., Holmes, E. C., Bessen, D. E., Chan, M.-S., Day, N. P., Enright, M. C., Goldstein, R., Hood, D. W., Kalia, A. and Moore, C. E. (2001). Recombination within natural populations of pathogenic bacteria: short-term empirical estimates and long-term phylogenetic consequences. *Proceedings of the National Academy of Sciences,* 98(1): 182-187.

Garrity, G. M., Brenner, D., Krieg, N. and Staley, J. (2005). Class II. Betaproteobacteria class. nov. In: *Bergey's Manual® of Systematic Bacteriology*. 2nd ed. Springer, p. 777.

Garvey, G. S., Rocco, C. J., Escalante‐Semerena, J. C. and Rayment, I. (2007). The three‐dimensional crystal structure of the PrpF protein of Shewanella oneidensis complexed with trans‐aconitate: Insights into its biological function. *Protein science,* 16(7): 1274-1284.

Goldschneider, I., Gotschlich, E. C. and Artenstein, M. S. (1969). Human immunity to the meningococcus II. Development of natural immunity. *The Journal of experimental medicine,* 129(6): 1327-1348.

Granoff, D. M. (2010). Review of meningococcal group B vaccines. *Clinical Infectious Diseases,* 50(Supplement 2): S54-S65.

Grimek, T. L. and Escalante-Semerena, J. C. (2004). The acnD genes of Shewenella oneidensis and Vibrio cholerae encode a new Fe/S-dependent 2-methylcitrate dehydratase enzyme that requires prpF function in vivo. *Journal of bacteriology,* 186(2): 454-462.

Grimek, T. L., Holden, H., Rayment, I. and Escalante-Semerena, J. C. (2003). Residues C123 and D58 of the 2-methylisocitrate lyase (PrpB) enzyme of Salmonella enterica are essential for catalysis. *Journal of bacteriology,* 185(16): 4837-4843.

Hanahan, D. (1983). Studies on transformation of Escherichia coli with plasmids. *Journal of molecular biology,* 166(4): 557-580.

Hava, D. L. and Camilli, A. (2002). Large‐scale identification of serotype 4 Streptococcus pneumoniae virulence factors. *Molecular microbiology,* 45(5): 1389-1406.

Heck, A. J. (2008). Native mass spectrometry: a bridge between interactomics and structural biology. *Nature methods,* 5(11): 927-933.

Hedman, A. K., Li, M.-S., Langford, P. R. and Kroll, J. S. (2012). Transcriptional Profiling of Serogroup B Neisseria meningitidis Growing in Human Blood: An Approach to Vaccine Antigen Discovery. *PloS one,* 7(6): e39718.

Heiddal, S., Sverrisson, J. T., Yngvason, F. E., Cariglia, N. and Kristinsson, K. G. (1993). Native-valve endocarditis due to Neisseria sicca: case report and review. *Clinical Infectious Diseases,* 16(5): 667-670.

Hellman, L. M. and Fried, M. G. (2007). Electrophoretic mobility shift assay (EMSA) for detecting protein–nucleic acid interactions. *Nature protocols,* 2(8): 1849-1861.

Henikoff, S., Haughn, G. W., Calvo, J. M. and Wallace, J. C. (1988). A large family of bacterial activator proteins. *Proceedings of the National Academy of Sciences,* 85(18): 6602-6606.

Heurlier, K., Thomson, M. J., Aziz, N. and Moir, J. W. B. (2008). The nitric oxide (NO)-sensing repressor NsrR of Neisseria meningitidis has a compact regulon of genes involved in NO synthesis and detoxification. *Journal of bacteriology,* 190(7): 2488-2495.

Hill, D., Griffiths, N., Borodina, E. and Virji, M. (2010). Cellular and molecular biology of Neisseria meningitidis colonization and invasive disease. *Clinical Science,* 118: 547-564.

Holst, J. (2007). Strategies for development of universal vaccines against meningococcal serogroup B disease. *Human vaccines,* 3(6): 290-294.

Horstmann, R. D. (1992). Target recognition failure by the nonspecific defense system: surface constituents of pathogens interfere with the alternative pathway of complement activation. *Infection and immunity,* 60(3): 721-727.

Horswill, A. R., Dudding, A. R. and Escalante-Semerena, J. C. (2001). Studies of propionate toxicity in Salmonella enterica identify 2-methylcitrate as a potent inhibitor of cell growth. *Journal of Biological Chemistry,* 276(22): 19094-19101.

Horswill, A. R. and Escalante-Semerena, J. C. (1999a). The prpE gene of Salmonella typhimurium LT2 encodes propionyl-CoA synthetase. *Microbiology,* 145(6): 1381-1388.

Horswill, A. R. and Escalante-Semerena, J. C. (1999b). Salmonella typhimurium LT2 catabolizes propionate via the 2-methylcitric acid cycle. *Journal of bacteriology,* 181(18): 5615-5623.

Horswill, A. R. and Escalante-Semerena, J. C. (2001). In vitro conversion of propionate to pyruvate by Salmonella enterica enzymes: 2-methylcitrate dehydratase

(PrpD) and aconitase enzymes catalyze the conversion of 2-methylcitrate to 2-methylisocitrate. *Biochemistry,* 40(15): 4703-4713.

Horswill, A. R. and Escalante-Semerena, J. C. (2002). Characterization of the propionyl-CoA synthetase (PrpE) enzyme of Salmonella enterica: residue Lys592 is required for propionyl-AMP synthesis. *Biochemistry,* 41(7): 2379-2387.

Hugenholtz, P. and Pace, N. R. (1996). Identifying microbial diversity in the natural environment: a molecular phylogenetic approach. *Trends in biotechnology,* 14(6): 190-197.

Ieva, R., Roncarati, D., Metruccio, M. M. E., Seib, K. L., Scarlato, V. and Delany, I. (2008). OxyR tightly regulates catalase expression in Neisseria meningitidis through both repression and activation mechanisms. *Molecular microbiology,* 70(5): 1152-1165.

Imrey, P. B., Jackson, L. A., Ludwinski, P. H., England, A. r., Fella, G. A., Fox, B. C., Isdale, L. B., Reeves, M. W. and Wenger, J. D. (1995). Meningococcal carriage, alcohol consumption, and campus bar patronage in a serogroup C meningococcal disease outbreak. *Journal of clinical microbiology,* 33(12): 3133-3137.

Ison, C. A., Heyderman, R. S., Klein, N. J., Peakman, M. and Levin, M. (1995). Whole blood model of meningococcal bacteraemia—a method for exploring host-bacterial interactions. *Microbial pathogenesis,* 18(2): 97-107.

Jenkinson, H. F. and Lamont, R. J. (2005). Oral microbial communities in sickness and in health. *Trends in microbiology,* 13(12): 589-595.

Johansson, L., Rytkönen, A., Bergman, P., Albiger, B., Källström, H., Hökfelt, T., Agerberth, B., Cattaneo, R. and Jonsson, A.-B. (2003). CD46 in meningococcal disease. *Science,* 301(5631): 373-375.

Jolley, K. A., Appleby, L., Wright, J. C., Christodoulides, M. and Heckels, J. E. (2001). Immunization with recombinant Opc outer membrane protein from Neisseria meningitidis: influence of sequence variation and levels of expression on the bactericidal immune response against meningococci. *Infection and immunity,* 69(6): 3809-3816.

Khatami, A., Snape, M. D., Davis, E., Layton, H., John, T., Yu, L.-M., Dull, P. M., Gill, C. J., Odrjlin, T. and Dobson, S. (2012). Persistence of the immune response at 5 years of age following infant immunisation with investigational quadrivalent MenACWY conjugate vaccine formulations. *Vaccine,* 30(18): 2831-2838.

Klemm, J. D., Schreiber, S. L. and Crabtree, G. R. (1998). Dimerization as a regulatory mechanism in signal transduction. *Annual review of immunology,* 16(1): 569-592.

Knapp, G. S. and Hu, J. C. (2010). Specificity of the E. coli LysR-type transcriptional regulators. *PloS one,* 5(12): e15189.

Knapp, J. S. (1988). Historical perspectives and identification of Neisseria and related species. *Clinical microbiology reviews,* 1(4): 415-431.

Kuimova, M. K., Yahioglu, G., Levitt, J. A. and Suhling, K. (2008). Molecular rotor measures viscosity of live cells via fluorescence lifetime imaging. *Journal of the American Chemical Society,* 130(21): 6672-6673.

Lebowitz, J., Lewis, M. S. and Schuck, P. (2002). Modern analytical ultracentrifugation in protein science: a tutorial review. *Protein science,* 11(9): 2067-2079.

Lemon, K. P., Klepac-Ceraj, V., Schiffer, H. K., Brodie, E. L., Lynch, S. V. and Kolter, R. (2010). Comparative analyses of the bacterial microbiota of the human nostril and oropharynx. *MBio,* 1(3): e00129-10.

Lewis, V. P. and Yang, S.-T. (1992). Propionic acid fermentation by Propionibacterium acidipropionici: effect of growth substrate. *Applied microbiology and biotechnology,* 37(4): 437-442.

Li, L., Hsiao, W. W. L., Nandakumar, R., Barbuto, S. M., Mongodin, E. F., Paster, B. J., Fraser-Liggett, C. M. and Fouad, A. F. (2010). Analyzing endodontic infections by deep coverage pyrosequencing. *Journal of dental research,* 89(9): 980-984.

Lichty, J. J., Malecki, J. L., Agnew, H. D., Michelson-Horowitz, D. J. and Tan, S. (2005). Comparison of affinity tags for protein purification. *Protein expression and purification,* 41(1): 98-105.

Ligon, B. L. (2005). Albert Ludwig Sigesmund Neisser: discoverer of the cause of gonorrhea. *Seminars in Pediatric Infectious Diseases*, pp. 336-341. Elsevier.

Lindqvist, K. (1960). A Neisseria Species Associated with Infectious Keratoconjunctivitis of Sheep Neisseria Ovis Nov. Spec. *Journal of Infectious Diseases,* 106(2): 162-165.

Liu, Y., Zhang, Y.-G., Zhang, R.-B., Zhang, F. and Zhu, J. (2011). Glycerol/glucose co-fermentation: one more proficient process to produce propionic acid by Propionibacterium acidipropionici. *Current microbiology,* 62(1): 152-158.

MacLennan, J., Kafatos, G., Neal, K., Andrews, N., Cameron, J. C., Roberts, R., Evans, M. R., Cann, K., Baxter, D. N. and Maiden, M. C. J. (2006). Social behavior and meningococcal carriage in British teenagers. *Emerging infectious diseases,* 12(6): 950-957.

Maddocks, S. E. and Oyston, P. C. F. (2008). Structure and function of the LysR-type transcriptional regulator (LTTR) family proteins. *Microbiology,* 154(12): 3609-3623.

Maerker, C., Rohde, M., Brakhage, A. A. and Brock, M. (2005). Methylcitrate synthase from Aspergillus fumigatus. *FEBS Journal,* 272(14): 3615-3630.

Maiden, M. C. (2008). Population genomics: diversity and virulence in the Neisseria. *Current opinion in microbiology,* 11(5): 467-471.

Maniatis, T. (1989). *Molecular cloning: a laboratory manual/J. Sambrook, EF Fritsch, T. Maniatis*. New York: Cold Spring Harbor Laboratory Press.

Marri, P. R., Paniscus, M., Weyand, N. J., Rendón, M. A., Calton, C. M., Hernández, D. R., Higashi, D. L., Sodergren, E., Weinstock, G. M. and Rounsley, S. D. (2010). Genome sequencing reveals widespread virulence gene exchange among human Neisseria species. *PloS one,* 5(7): e11835.

Maruyama, K. and Kitamura, H. (1985). Mechanisms of growth inhibition by propionate and restoration of the growth by sodium bicarbonate or acetate in Rhodopseudomonas sphaeroides S. *The Journal of biochemistry,* 98(3): 819-824.

Masignani, V., Comanducci, M., Giuliani, M. M., Bambini, S., Adu-Bobie, J., Aricò, B., Brunelli, B., Pieri, A., Santini, L. and Savino, S. (2003). Vaccination against Neisseria meningitidis using three variants of the lipoprotein GNA1870. *The Journal of experimental medicine,* 197(6): 789-799.

Massari, P., Ram, S., Macleod, H. and Wetzler, L. M. (2003). The role of porins in neisserial pathogenesis and immunity. *Trends in microbiology,* 11(2): 87-93.

Matlho, G., Himathongkham, S., Riemann, H. and Kass, P. (1997). Destruction of Salmonella enteritidis in poultry feed by combination of heat and propionic acid. *Avian diseases*: 58-61.

McGuinness, B. T., Clarke, I. N., Lambden, P. R., Barlow, A. K., Heckels, J. E., Poolman, J. T. and Jones, D. M. (1991). Point mutation in meningococcal por A gene associated with increased endemic disease. *The Lancet,* 337(8740): 514-517.

McKee, A. S., McDermid, A. S., Ellwood, D. and Marsh, P. (1985). The establishment of reproducible, complex communities of oral bacteria in the chemostat using defined inocula. *Journal of Applied Microbiology,* 59(3): 263-275.

Melican, K., Veloso, P. M., Martin, T., Bruneval, P. and Duménil, G. (2013). Adhesion of Neisseria meningitidis to Dermal Vessels Leads to Local Vascular Damage and Purpura in a Humanized Mouse Model. *PLoS pathogens,* 9(1): e1003139.

Moerke, N. J. (2009). Fluorescence Polarization (FP) Assays for Monitoring Peptide - Protein or Nucleic Acid - Protein Binding. *Current protocols in chemical biology*, 1: 1-15.

Moore, P. S. (1992). Meningococcal meningitis in sub-Saharan Africa: a model for the epidemic process. *Clinical Infectious Diseases,* 14(2): 515-525.

Mourelatos, K., Eady, E. A., Cunliffe, W. J., Clark, S. M. and Cove, J. H. (2007). Temporal changes in sebum excretion and propionibacterial colonization in preadolescent children with and without acne. *British Journal of Dermatology,* 156(1): 22-31.

Mueller, J. E., Borrow, R. and Gessner, B. D. (2006). Meningococcal serogroup W135 in the African meningitis belt: epidemiology, immunity and vaccines. *Expert review of vaccines*, 5(3): 319-336.

Nassif, X., Lowy, J., Stenberg, P., O'Gaora, P., Ganji, A. and So, M. (1993). Antigenic variation of pilin regulates adhesion of Neisseria meningitidis to human epithelial cells. *Molecular microbiology,* 8(4): 719-725.

Ng, S. K. and Hamilton, I. R. (1971). Lactate metabolism by Veillonella parvula. *Journal of bacteriology,* 105(3): 999-1005.

Niederman, R., Buyle-Bodin, Y., Lu, B. Y., Robinson, P. and Naleway, C. (1997). Short-chain carboxylic acid concentration in human gingival crevicular fluid. *Journal of dental research,* 76(1): 575-579.

Olsen, S., Djurhuus, B., Rasmussen, K., Joensen, H., Larsen, S., Zoffman, H. and Lind, I. (1991). Pharyngeal carriage of Neisseria meningitidis and Neisseria lactamica in households with infants within areas with high and low incidences of meningococcal disease. *Epidemiology and infection,* 106(3): 445-457.

Pace, D., Pollard, A. J. and Messonier, N. E. (2009). Quadrivalent meningococcal conjugate vaccines. *Vaccine,* 27: B30-B41.

Palacios, S., Starai, V. J. and Escalante-Semerena, J. C. (2003). Propionyl coenzyme A is a common intermediate in the 1, 2-propanediol and propionate catabolic pathways needed for expression of the prpBCDE operon during growth of Salmonella enterica on 1, 2-propanediol. *Journal of bacteriology,* 185(9): 2802-2810.

Pérez-Rueda, E. and Collado-Vides, J. (2001). Common history at the origin of the position–function correlation in transcriptional regulators in archaea and bacteria. *Journal of molecular evolution,* 53(3): 172-179.

Perrin, A., Bonacorsi, S., Carbonnelle, E., Talibi, D., Dessen, P., Nassif, X. and Tinsley, C. (2002). Comparative genomics identifies the genetic islands that

distinguish Neisseria meningitidis, the agent of cerebrospinal meningitis, from other Neisseria species. *Infection and immunity,* 70(12): 7063-7072.

Piveteau, P. (1999). Metabolism of lactate and sugars by dairy propionibacteria: A review. *Le Lait,* 79(1): 23-41.

Plassmeier, J., Barsch, A., Persicke, M., Niehaus, K. and Kalinowski, J. (2007). Investigation of central carbon metabolism and the 2-methylcitrate cycle in< i> Corynebacterium glutamicum</i> by metabolic profiling using gas chromatography–mass spectrometry. *Journal of biotechnology,* 130(4): 354-363.

Plugge, C. M., van Leeuwen, J. M., Hummelen, T., Balk, M. and Stams, A. J. (2001). Elucidation of the pathways of catabolic glutamate conversion in three thermophilic anaerobic bacteria. *Archives of microbiology,* 176(1-2): 29-36.

Pollack, S., Mogtader, A. and Lange, M. (1984). Neisseria subflava endocarditis: case report and review of the literature. *The American journal of medicine,* 76(4): 752-758.

Prentki, P. and Krisch, H. M. (1984). In vitro insertional mutagenesis with a selectable DNA fragment. *Gene,* 29(3): 303-313.

Racloz, V. and Luiz, S. (2010). The elusive meningococcal meningitis serogroup: a systematic review of serogroup B epidemiology. *BMC infectious diseases,* 10(1): 175-183.

Racoosin, J. A., Whitney, C. G., Conover, C. S. and Diaz, P. S. (1998). Serogroup Y meningococcal disease in Chicago, 1991-1997. *JAMA: the journal of the American Medical Association,* 280(24): 2094-2098.

Rayner, C., Dewar, A., Moxon, E., Virji, M. and Wilson, R. (1995). The effect of variations in the expression of pili on the interaction of Neisseria meningitidis with human nasopharyngeal epithelium. *Journal of Infectious Diseases,* 171(1): 113-121.

Reinscheid, D. J., Schnicke, S., Rittmann, D., Zahnow, U., Sahm, H. and Eikmanns, B. J. (1999). Cloning, sequence analysis, expression and inactivation of the Corynebacterium glutamicum pta-ack operon encoding phosphotransacetylase and acetate kinase. *Microbiology,* 145(2): 503-513.

Ren, J., Sainsbury, S., Combs, S. E., Capper, R. G., Jordan, P. W., Berrow, N. S., Stammers, D. K., Saunders, N. J. and Owens, R. J. (2007). The structure and transcriptional analysis of a global regulator from Neisseria meningitidis. *Journal of Biological Chemistry,* 282(19): 14655-14664.

Riesbeck, K., Orvelid-Mölling, P., Fredlund, H. and Olcén, P. (2000). Long-term persistence of a discotheque-associated invasive Neisseria meningitidis group C

strain as proven by pulsed-field gel electrophoresis and porA gene sequencing. *Journal of clinical microbiology,* 38(4): 1638-1640.

Rogosa, M. (1956). A selective medium for the isolation and enumeration of the veillonella from the oral cavity. *Journal of bacteriology,* 72(4): 533-536.

Rogosa, M. (1964). The genus Veillonella I. General Cultural, Ecological, and Biochemical Considerations. *Journal of bacteriology,* 87(1): 162-170.

Rosenstein, N. E., Perkins, B. A., Stephens, D. S., Popovic, T. and Hughes, J. M. (2001). Meningococcal disease. *New England Journal of Medicine,* 344(18): 1378-1388.

Ryan, K. J., Ray, C. G., Nafees, A., Lawrence, D. W. and James, P. (2010). *Sherris medical microbiology*. 5th ed. McGraw Hill Medical, 542-549.

Sainsbury, S., Ren, J., Saunders, N. J., Stuart, D. I. and Owens, R. J. (2012). Structure of the regulatory domain of the LysR family regulator NMB2055 (MetR-like protein) from Neisseria meningitidis. *Acta Crystallographica Section F: Structural Biology and Crystallization Communications,* 68(7): 730-737.

Salmond, C. V., Kroll, R. G. and Booth, I. R. (1984). The effect of food preservatives on pH homeostasis in Escherichia coli. *Journal of general microbiology,* 130(11): 2845-2850.

Schell, M. A. (1993). Molecular biology of the LysR family of transcriptional regulators. *Annual Reviews in Microbiology,* 47(1): 597-626.

Schoen, C., Blom, J., Claus, H., Schramm-Glück, A., Brandt, P., Müller, T., Goesmann, A., Joseph, B., Konietzny, S. and Kurzai, O. (2008). Whole-genome comparison of disease and carriage strains provides insights into virulence evolution in Neisseria meningitidis. *Proceedings of the National Academy of Sciences,* 105(9): 3473-3478.

Seeliger, S., Janssen, P. H. and Schink, B. (2002). Energetics and kinetics of lactate fermentation to acetate and propionate via methylmalonyl‐CoA or acrylyl‐CoA. *FEMS microbiology letters,* 211(1): 65-70.

Segata, N., Haake, S. K., Mannon, P., Lemon, K. P., Waldron, L., Gevers, D., Huttenhower, C. and Izard, J. (2012). Composition of the adult digestive tract bacterial microbiome based on seven mouth surfaces, tonsils, throat and stool samples. *Genome Biol,* 13(6): R42.

Sellin, J. H. (1999). SCFAs: the enigma of weak electrolyte transport in the colon. *Physiology,* 14(2): 58-64.

Serruto, D., Bottomley, M. J., Ram, S., Giuliani, M. M. and Rappuoli, R. (2012). The new multicomponent vaccine against meningococcal serogroup B, 4CMenB: immunological, functional and structural characterization of the antigens. *Vaccine,* 30: B87-B97.

Sinave, C. P. and Ratzan, K. R. (1987). Infective endocarditis caused by Neisseria flavescens. *The American journal of medicine,* 82(1): 163-164.

Singh, N. and Victor, L. Y. (1992). Osteomyelitis due to Veillonella parvula: case report and review. *Clinical Infectious Diseases,* 14(1): 361-363.

Skattum, L., van Deuren, M., van der Poll, T. and Truedsson, L. (2011). Complement deficiency states and associated infections. *Molecular immunology,* 48(14): 1643-1655.

Snape, M. D. and Pollard, A. J. (2005). Meningococcal polysaccharide–protein conjugate vaccines. *The Lancet infectious diseases,* 5(1): 21-30.

Sneath, P. and Barrett, S. (1996). A new species of Neisseria from the dental plaque of the domestic cow, Neisseria dentiae sp. nov. *Letters in applied microbiology,* 23(5): 355-358.

Snyder, L. A. and Saunders, N. J. (2006). The majority of genes in the pathogenic Neisseria species are present in non-pathogenic Neisseria lactamica, including those designated as' virulence genes'. *BMC genomics,* 7(1): 128-138.

Stabler, R. A., Marsden, G. L., Witney, A. A., Li, Y., Bentley, S. D., Tang, C. M. and Hinds, J. (2005). Identification of pathogen-specific genes through microarray analysis of pathogenic and commensal Neisseria species. *Microbiology,* 151(9): 2907-2922.

Stalon, V. and Mercenier, A. (1984). L-arginine utilization by Pseudomonas species. *Journal of general microbiology,* 130(1): 69-76.

Starai, V. J. and Escalante-Semerena, J. C. (2004). Acetyl-coenzyme A synthetase (AMP forming). *Cellular and Molecular Life Sciences CMLS,* 61(16): 2020-2030.

Stephens, D. S. (2007). Conquering the meningococcus. *FEMS microbiology reviews,* 31(1): 3-14.

Studier, F. W. (2005). Protein production by auto-induction in high-density shaking cultures. *Protein expression and purification,* 41(1): 207-234.

Sun, Y.-H., Bakshi, S., Chalmers, R. and Tang, C. M. (2000). Functional genomics of Neisseria meningitidis pathogenesis. *Nature medicine,* 6(11): 1269-1273.

Suvorova, I. A., Ravcheev, D. A. and Gelfand, M. S. (2012). Regulation and Evolution of Malonate and Propionate Catabolism in Proteobacteria. *Journal of bacteriology,* 194(12): 3234-3240.

Swick, R. W. and Wood, H. G. (1960). The role of transcarboxylation in propionic acid fermentation. *Proceedings of the National Academy of Sciences of the United States of America,* 46(1): 28-41.

Takeda, I., Stretch, C., Barnaby, P., Bhatnager, K., Rankin, K., Fu, H., Weljie, A., Jha, N. and Slupsky, C. (2009). Understanding the human salivary metabolome. *NMR in Biomedicine,* 22(6): 577-584.

Tedesco, F. (2008). Inherited complement deficiencies and bacterial infections. *Vaccine,* 26: I3-I8.

Tettelin, H., Saunders, N. J., Heidelberg, J., Jeffries, A. C., Nelson, K. E., Eisen, J. A., Ketchum, K. A., Hood, D. W., Peden, J. F. and Dodson, R. J. (2000). Complete genome sequence of Neisseria meningitidis serogroup B strain MC58. *Science,* 287(5459): 1809-1815.

Tlaskalová-Hogenová, H., Stepánková, R., Hudcovic, T., Tucková, L., Cukrowska, B., Lodinová-Zádníková, R., Kozáková, H., Rossmann, P., Bártová, J. and Sokol, D. (2004). Commensal bacteria (normal microflora), mucosal immunity and chronic inflammatory and autoimmune diseases. *Immunology letters,* 93(2): 97-108.

Tønjum, T., Garrity, G. M., Brenner, D., Krieg, N. and Staley, J. (2005). Class II. Betaproteobacteria class. nov. In: *Bergey's Manual® of Systematic Bacteriology*. 2nd ed. Springer, p. 774.

Trotter, C. L. and Greenwood, B. M. (2007). Meningococcal carriage in the African meningitis belt. *The Lancet infectious diseases,* 7(12): 797-803.

Turk, D. (1984). The pathogenicity of Haemophilus influenzae. *Journal of medical microbiology,* 18(1): 1-16.

Turner, S., Reid, E., Smith, H. and Cole, J. (2003). A novel cytochrome c peroxidase from Neisseria gonorrhoeae: a lipoprotein from a Gram-negative bacterium. *Biochemical Journal,* 373: 865-873.

Ulmer, J. B., Valley, U. and Rappuoli, R. (2006). Vaccine manufacturing: challenges and solutions. *Nature biotechnology,* 24(11): 1377-1383.

Upton, A. M. and McKinney, J. D. (2007). Role of the methylcitrate cycle in propionate metabolism and detoxification in Mycobacterium smegmatis. *Microbiology,* 153(12): 3973-3982.

Urwin, R., Holmes, E. C., Fox, A. J., Derrick, J. P. and Maiden, M. C. (2002). Phylogenetic evidence for frequent positive selection and recombination in the meningococcal surface antigen PorB. *Molecular biology and evolution,* 19(10): 1686-1694.

Vagenende, V., Yap, M. G. and Trout, B. L. (2009). Mechanisms of protein stabilization and prevention of protein aggregation by glycerol. *Biochemistry,* 48(46): 11084-11096.

Van Deuren, M., Brandtzaeg, P. and van der Meer, J. W. (2000). Update on meningococcal disease with emphasis on pathogenesis and clinical management. *Clinical microbiology reviews,* 13(1): 144-166.

van Duynhoven, Y. (1999). The epidemiology of Neisseria gonorrhoeae in Europe. *Microbes and infection/Institut Pasteur,* 1(6): 455-464.

Vedros, N. A., Hoke, C. and Chun, P. (1983). Neisseria macacae sp. nov., a new Neisseria species isolated from the oropharynges of rhesus monkeys (Macaca mulatta). *International Journal of Systematic Bacteriology,* 33(3): 515-520.

Vitovski, S. and Sayers, J. R. (2007). Relaxed cleavage specificity of an immunoglobulin A1 protease from Neisseria meningitidis. *Infection and immunity,* 75(6): 2875-2885.

Weinitschke, S., Denger, K., Cook, A. M. and Smits, T. H. M (2007). The DUF81 protein TauE in Cupriavidus necator H16, a sulfite exporter in the metabolism of C2 sulfonates. *Microbiology*, 153 (9): 3055-3060.

Weyand, N. J., Wertheimer, A. M., Hobbs, T. R., Sisko, J. L., Taku, N. A., Gregston, L. D., Clary, S., Higashi, D. L., Biais, N. and Brown, L. M. (2013). Neisseria infection of rhesus macaques as a model to study colonization, transmission, persistence, and horizontal gene transfer. *Proceedings of the National Academy of Sciences,* 110(8): 3059-3064.

Wimalasekera, R., Tebartz, F. and Scherer, G. F. (2011). Polyamines, polyamine oxidases and nitric oxide in development, abiotic and biotic stresses. *Plant Science,* 181(5): 593-603.

Wolever, T., Josse, R. G., Leiter, L. A. and Chiasson, J.-L. (1997). Time of day and glucose tolerance status affect serum short-chain fatty concentrations in humans. *Metabolism,* 46(7): 805-811.

Wolfgang, M., Park, H.-S., Hayes, S. F., Van Putten, J. P. and Koomey, M. (1998). Suppression of an absolute defect in type IV pilus biogenesis by loss-of-function mutations in pilT, a twitching motility gene in Neisseria gonorrhoeae. *Proceedings of the National Academy of Sciences,* 95(25): 14973-14978.

Wong, J. D. and Janda, J. M. (1992). Association of an important Neisseria species, Neisseria elongata subsp. nitroreducens, with bacteremia, endocarditis, and osteomyelitis. *Journal of clinical microbiology,* 30(3): 719-720.

Yagci, N., Artan, N., Çokgör, E. U., Randall, C. W. and Orhon, D. (2003). Metabolic model for acetate uptake by a mixed culture of phosphate‐and glycogen‐accumulating organisms under anaerobic conditions. *Biotechnology and bioengineering,* 84(3): 359-373.

Yang, F., Zeng, X., Ning, K., Liu, K.-L., Lo, C.-C., Wang, W., Chen, J., Wang, D., Huang, R. and Chang, X. (2011). Saliva microbiomes distinguish caries-active from healthy human populations. *The ISME Journal,* 6(1): 1-10.

Yazdankhah, S. P. and Caugant, D. A. (2004). Neisseria meningitidis: an overview of the carriage state. *Journal of medical microbiology,* 53(9): 821-832.

Yi, K., Rasmussen, A. W., Gudlavalleti, S. K., Stephens, D. S. and Stojiljkovic, I. (2004). Biofilm formation by Neisseria meningitidis. *Infection and immunity,* 72(10): 6132-6138.

Yi, K., Stephens, D. S. and Stojiljkovic, I. (2003). Development and evaluation of an improved mouse model of meningococcal colonization. *Infection and immunity,* 71(4): 1849-1855.